



**HAL**  
open science

# Immunomodulatory Properties of Galectin-9: Experimental and Translational Investigations

Thi Bao Tram Tran

► **To cite this version:**

Thi Bao Tram Tran. Immunomodulatory Properties of Galectin-9: Experimental and Translational Investigations. Cell Behavior [q-bio.CB]. Université Paris-Saclay, 2021. English. NNT : 2021UP-ASL081 . tel-04748758

**HAL Id: tel-04748758**

**<https://theses.hal.science/tel-04748758v1>**

Submitted on 22 Oct 2024

**HAL** is a multi-disciplinary open access archive for the deposit and dissemination of scientific research documents, whether they are published or not. The documents may come from teaching and research institutions in France or abroad, or from public or private research centers.

L'archive ouverte pluridisciplinaire **HAL**, est destinée au dépôt et à la diffusion de documents scientifiques de niveau recherche, publiés ou non, émanant des établissements d'enseignement et de recherche français ou étrangers, des laboratoires publics ou privés.

# Immunomodulatory properties of galectin-9: experimental and translational investigations

*Caractéristiques immunomodulatrices de la galectine-9: études  
expérimentales et translationnelles*

## Thèse de doctorat de l'université Paris-Saclay

École doctorale n° 582, Cancérologie: biologie – médecine – santé (CBMS)

Spécialité de doctorat : Sciences de la vie et de la santé

Graduate School : Life Sciences and Health. Référent : Faculté de médecine

Thèse préparée dans l'unité de recherche **Aspects métaboliques et systémiques de l'oncogénèse pour de nouvelles approches thérapeutiques (Université Paris-Saclay, CNRS, Institut Gustave Roussy)**, sous la direction de **Dr. Pierre BUSSON**, directeur de recherche

Thèse soutenue à Paris-Saclay, le 21 octobre 2021, par

**Thi Bao Tram TRAN**

## Composition du Jury

<b>Nathalie CHAPUT</b> Professeure, Université Paris-Saclay	Présidente
<b>Hélène DUTARTRE</b> Chargée de recherche, ENS Lyon	Rapporteur & Examinatrice
<b>Udo KONTNY</b> Professeur, Université d'Aix la Chapelle	Rapporteur & Examineur
<b>Olivier DELLIS</b> Maître de conférences, Université Paris-Saclay	Examineur
<b>Claire LHUILLIER</b> Research scientist, Sanofi – R&D	Examinatrice
<b>Pierre BUSSON</b> Directeur de recherche, Université Paris-Saclay	Directeur de thèse

## Acknowledgements

I would like to express my appreciation and gratitude to the members of my thesis examination board, for giving me a chance to present my work and evaluating it in an objective way. I would especially like to thank Prof. Udo Kontny and Dr. H el ene Dutartre for accepting to be the rapporteurs in the examination board. Your comments and suggestions helped me improve the manuscript and encouraged me to do my best in the final months of my thesis.

To my dearest francophones,

J'aimerais remercier toutes les personnes qui m'ont accompagn e depuis mes premiers jours   l'UMR 8126 jusqu'  ma soutenance   l'UMR 9018-METSY.

Je tiens   remercier mon directeur de th ese, Dr. Pierre Busson, qui m'a accueillie dans son  quipe et m'a donn e cette opportunit  de faire une th ese. Je te remercie pour la confiance, la patience et les encouragements au moments o  j'en avais besoin; la discipline quand il fallait me concentrer et des conseils   chaque fois que j'en cherchais un.

Je remercie particuli rement mon  quipe, avec qui je partage la routine au labo. Aurore et Nikiforos, qui m'ont appris le travail d' quipe, (chacun sa propre fa on, mais) vous  tiez toujours l  pour m'aider, quelque soit le probl me. J'ai beaucoup aim  notre coin   P.305 et les discussions o  je vous  couteais et rigolais plus que parler. Valentin, qui me mettait toujours un doute sur des r sultats jolis que j'avais attendus. Je te remercie pour l'esprit critique (et sceptique!) que tu m'as appris. Muriel, qui  tait toujours d bord e, soit par les r unions soit par les manips de Ficoll, mais qui lib rait imm diatement du temps   chaque fois que je lui posais une question. Et merci   Thierry, qui a relis ce manuscrit et m'a donn  beaucoup de suggestions pour l'am liorer. Je remercie  galement ceux qui nous ont rejoint pour une dur e assez courte mais qui ont  gay  notre  quipe: L etitia, Ludivine, Sarah, Nayeli, L a, Ana s, ... J'ai h te de vous inviter   ma th ese!

Je remercie mes amis-doctorants et mes coll gues dont j'ai eu la chance de faire connaissance. D'une mani re ou d'une autre, vous m'avez accueillie, accompagn e, confort e ou m'a

motivée, sans le savoir! Merci à chị Thái Hòa et Hồng Toàn, mes compatriotes qui me nourrissaient de temps en temps et qui se jouissaient avec moi autour un bon plat vietnamien. Merci à Florian, Amina, Kenza, Leslie, Fabi, Reynand, Alberto, Zhenrui, Yinxing qui sympathisaient bien à ma vie doctorante! À Aude, cô Anne, Seila, et Sokhon, qui m'accueillais pour les déjeuners, pour le bus qui partait tôt le matin au labo ou simplement pour des chit-chat dans les couloirs de IGR.

Je remercie également les membres de l'ancienne UMR 8126 et de la nouvelle UMR 9018. Je n'étais jamais seule quand j'avais besoin des conseils ou des aides. Vous m'avez donné la meilleure ambiance de travail où je me sentais être dans une famille. Chacun d'entre vous m'a inspiré à sa propre façon. Je tiens à remercier Dr. Joëlle Wiels, Dr. Marc Lipinski, Dr. Catherine Brenner, et Dr. Karim Benihoud, qui ont écouté à mes présentations au labo et qui m'ont donné beaucoup de conseils et suggestions constructives.

And to my friends from Vietnam, who are now in France or in any other parts of the world. I am grateful for your supports throughout the years. It was during those midnight calls, or those weekend walks, or the late-night talks that I got to understand more about myself and found out that I always had a friend to talk about anything that struggled me.

J'ai eu tellement de la chance que j'ai trouvé une deuxième famille en France. Je remercie à mes Tontons et Tatas pour des moments passés ensemble, pour les encouragements et le soutien persistants. Et à Bà, pour des petites histoires qui se répétaient de temps en temps mais finissaient toujours par me faire sourire et me conforter.

Lastly, I would like to thank my family for their love and support that give me strength in times of hardship. To my parents, and our little dog (which we call dearly Miss Cat!), I miss you all so much. But I am going to be home soon! To my sister and brother, words cannot say how much I am grateful to have you settled in Europe, so that I can have some place to go to in tough times (and get fed!). And to An, thank you for standing by me. Thương mọi người nhiều!

# Table of content

Acknowledgements.....	1
Table of content.....	3
List of Abbreviations .....	5
List of Figures and Tables.....	8
Chapter 1: Introduction to the "sugar code" .....	10
1.1.    General aspects of glycan biology.....	10
1.1.1.    Carbohydrates as a biological messenger.....	10
1.1.2.    The alphabet of the sugar code .....	11
1.1.3.    The many types of glycosylation.....	12
1.1.4. <i>N</i> -glycosylation.....	12
1.1.5. <i>O</i> -glycosylation.....	14
1.1.6.    Proteoglycans and glycosaminoglycans.....	16
1.1.7.    Decipher the sugar code: Lectins .....	16
1.1.8.    Glycome in health and disease .....	17
1.2.    General aspects of galectins .....	20
1.2.1.    Structure and specificity .....	20
1.2.2.    Distribution in tissue and cellular localization .....	22
1.2.3.    A review of galectin functions.....	24
Chapter 2: General aspects of T cell biology.....	27
2.1.    An overview of T cell subsets in the immune system.....	27
2.1.1.    Diversity of T cell subsets.....	27
2.1.2.    Identity of T cells: an interplay of cytokines, receptors and transcription factors .....	28
2.1.3.    Plasticity of T cell phenotype .....	33
2.2.    How T cells acquire effector phenotype.....	37
2.2.1.    TCR activation ignites series of T cell physiological changes .....	37
2.2.2.    Formation of the immunological synapse .....	39
2.2.3.    T cell exhaustion versus senescence.....	44
Chapter 3: General aspects of galectin-9.....	47
3.1.    Structure, expression, tissular and cellular distribution .....	47
3.1.1.    Structure of the galectin-9 proteins and transcripts .....	47
3.1.2.    Galectin-9 gene and its regulation.....	49

3.1.3.	Tissular and cellular localization .....	51
3.1.4.	Examples of functions provided by cell-associated gal-9 .....	52
3.1.5.	Summary of gal-9 functions in the immune system .....	53
3.1.6.	Overview of the membrane receptors of extra-cellular galectin-9 and their signaling pathways	54
3.2.	Galectin-9 and T cells .....	56
3.2.1.	Inhibitory effects of extra-cellular gal-9 on Th1 cells.....	56
3.2.2.	Inhibitory effects of extracellular gal-9 on CD8 <sup>+</sup> T cells .....	57
3.2.3.	Complex influence of extracellular gal-9 on regulatory T cells.....	58
3.2.4.	Indirect effects of extracellular gal-9 on Th2 cells .....	59
3.2.5.	Other aspects of galectin-9 interactions with T-cells.....	60
3.3.	Galectin-9 and B cells.....	61
3.4.	Galectin-9 and other effectors of the immune system distinct from T- and B-cells .....	62
3.4.1.	Eosinophils .....	62
3.4.2.	Neutrophils .....	62
3.4.3.	Basophils .....	63
3.4.4.	Natural Killer (NK) cells .....	63
3.4.5.	Monocytes / macrophages .....	63
3.4.6.	Dendritic cells.....	64
3.4.7.	Myeloid-derived Suppressor cells (MDSCs) .....	65
3.5.	Galectin-9 in non-tumoral pathologies.....	66
3.5.1.	Autoimmune diseases.....	66
3.5.2.	Viral infections .....	67
3.6.	Galectin-9 in cancer .....	69
3.6.1.	Galectin-9 and cancer: avoiding some pitfalls.....	69
3.6.2.	Overview and discussion of the anti-tumoral effects of gal-9.....	70
3.6.3.	Pro-tumoral effects of galectin-9.....	73
3.6.4.	Gal-9 in the context of tumor therapeutics .....	75
3.6.5.	Deregulation of gal-9 expression in a tumor context .....	76
<b>Results</b> .....		<b>78</b>
Article 1 .....		79
Article 2 .....		114
<b>Discussion and perspectives</b> .....		<b>126</b>
<b>Annex</b> .....		<b>133</b>
Summary.....		152
Bibliography .....		160

## List of Abbreviations

---

AHR	aryl hydrocarbon receptor
AIDS	acquired immunodeficiency syndrome
ALDH	aldehydedehydrogenase
AML	acute myeloid leukemia
AMPK	AMP-activated protein kinase
APC	antigen-presenting cell
BCL6	B-cell lymphoma 6 protein
BCR	B cell receptor
BTLA	B- and T-lymphocyte attenuator
CA19-9	carbohydrate antigen 19-9
CBS	carbohydrate binding site
CCRD	C-terminal carbohydrate recognition domain
CD	cluster of differentiation
CDG	Congenital disorders of glycosylation
CEA	carcinoembryonic antigen
Ceacam-1	carcino-embryonic antigen cell adhesion molecule 1
CIA	collagen-induced arthritis
CLIC	clathrin-independent carriers
CLL	chronic lymphocytic leukemia
CRD	carbohydrate recognition domain
c-SMAC	central supramolecular activation cluster
CTL	cytotoxic T lymphocyte
CTLA-4	cytotoxic T lymphocyte antigen-4
CXCR	CXC-chemokine receptor
DC	dendritic cells
d-SMAC	distal supramolecular activation cluster
EAE	autoimmune encephalomyelitis
EBV	Epstein-Barr virus
EDEM	ER degradation-enhancing $\alpha$ -mannosidase I-like
EOMES	eomesodermin
gal-9	galectin-9
GALNT	GalNAc transferase
GC	germinal center
GlcNAc	<i>N</i> -acetylglucosamine
GM-CSF	granulocyte macrophage-colony-stimulating factor
GPI	glycosylphosphatidylinositol
GSL	glycosphingolipids
HAVACR	hepatitis A virus cellular receptor

HBV	hepatitis B virus
HCC	hepatocellular carcinoma
HCV	hepatitis C virus
HGNC	HUGO (Human Genome Organization) Nomenclature Committee
HIV	human immunodeficiency virus
HMGB1	high mobility group protein B1
HNSCC	Head and neck squamous cell carcinomas
HSV1	Herpes Simplex virus 1
ICAM	intercellular adhesion molecule
ICOS	inducible T cell costimulatory
IFN	interferon
Ig	Immunoglobulin
IL	interleukin
IRF	interferon regulatory factor
IS	immunological synapse / immune synapse
ITAM	immunoreceptor tyrosine-based activation motif
ITIM	immunoreceptor tyrosine-based inhibitory motif
iTreg	induced regulatory T cell
ITSM	immunoreceptor tyrosine-based switch motif
KLRG	killer cell lectin-like receptor subfamily G member
KO	knockout
LAT	Linker for activation of T cells
LFA-1	Lymphocyte function-associated antigen 1
LCMV	Lymphocytic choriomeningitis virus
LEAD	systemic lupus erythematosus
LPS	lipopolysaccharides
MAP	mitogen-activated protein
MCP1	macrophage chemoattractant protein 1
MDSC	Myeloid-derived Suppressor cell
Mgat	<i>N</i> -acetylglucosaminyltransferase
MHC	major histocompatibility complex
MHCp	MHC-peptide complex
miR	microRNA
MTOC	microtubule organizing center
MTORC1	mammalian target of rapamycin complex 1
NCRD	N-terminal carbohydrate recognition domain
NK	Natural Killer cell
NPC	nasopharyngeal carcinoma
nTreg	natural regulatory T cell
OGA	<i>O</i> -GlcNAcase



OGT	<i>O</i> -GlcNAc transferase
OST	oligosaccharyltransferase
PAMP	pathogen-associated molecular pattern
PBMC	peripheral blood mononuclear cell
PD-1	programmed death-1
PD-L1	programmed death-ligand 1
PKC	protein kinase C
PMM2	phosphomannomutase 2
PNGase	peptide: <i>N</i> -glycanase
Poly I:C	polyinosinic:polycytidylic acid
PSA	prostate specific antigen
p-SMAC	peripheral supramolecular activation cluster
PtdSer	phosphatidyl-serine
ROR $\gamma$ t	retinoic acid-related orphan receptor $\gamma$ (thymus-specific)
SAP	serum amyloid P
SA- $\beta$ -Gal	senescence-associated- $\beta$ -galactosidase
SHP	Src homology 2 domain-containing tyrosine phosphatase
SLP	Src homology 2 domain-containing leukocyte protein
SMAC	supramolecular activation cluster
STAT	signal transducer and activator of transcription
Tc	cytotoxic T cell
TCR	T cell receptor
Tfh	follicular helper T cell
Th	helper T cell
TIGIT	T-cell immunoreceptor with Ig and ITIM domains
TIL	tumor-infiltrating lymphocyte
Tim-3	T cell immunoglobulin and mucin domain containing-3
TNF	tumor necrosis factor
Treg	regulatory T cell
WASp	Wiskott-Aldrich syndrome protein

# List of Figures and Tables

---

## List of Figures

Fig. 1	Representations of glucose	11
Fig. 2	Illustration of the equilibrium including the two anomeric forms of D-glucose	11
Fig. 3	The major types of glycosylation in human	13
Fig. 4	The main types of N-glycan	14
Fig. 5	Biosynthesis of N-linked glycosylated proteins	15
Fig. 6	Structures of O-GalNAc main cores.	17
Fig. 7	Six levels of regulation of affinity for binding of a glycan to a lectin	17
Fig. 8	The major groups of galectins and the interactions of galectin-glycans	23
Fig. 9	Expression, secretion, and functional diversification of galectins	26
Fig. 10	Key features of helper T cell subsets	29
Fig. 11	Key features of regulatory T cell subsets	31
Fig. 12	Structures of the T cell receptor complex	37
Fig. 13	Signaling cascade upon the activation of TCR	38
Fig. 14	Immune synapse formed during the interaction between T cell and an antigen-presenting cell (APC)	39
Fig. 15	Comparison between synapse formation in CD4+ T helper cells and cytotoxic T lymphocytes (CTLs)	40
Fig. 16	An illustration of the human galectin-9 NCRD–lactose complex	47
Fig. 17	Modulatory effects of galectin-9 on various populations of immune cells	54
Fig. 18	T cell immunoglobulin and mucin domain 3 (TIM-3), its ligands, and signaling adaptor proteins	55
Fig. 19	The glycosyltransferase GCNT2 replaces poly-LacNAc straight chains by multiple short branches of LacNAc units, which is known as the I-branching activity	61
Fig. 20	N-glycan structures present on naive, GC, and memory B cells	62
Fig. 21	The contribution of intracellular and extracellular tumor Gal-9 to the differentiation and expansion of MDSCs and the subsequent inhibition of T-cells.	66
Fig. 22	La galectine-9 provoque 2 effets en parallèle	153
Fig. 23	Schéma de la procédure expérimentale	154

Fig. 24	Regroupement des échantillons basé une liste de gène définie par la publication de Wong et al. (2015)	155
Fig. 25	Analyse statistique de quelques gènes présents dans la liste à la figure 24	156
Fig. 26	Analyse par cytométrie en flux sur l'expression de CXCR5, CD40 et FoxP3 des lymphocytes T traitées par la gal-9 NC ou la gal-9 M	157
Fig. 27	Modèle d'interaction entre lymphocytes B et T sous l'effet de la galectine-9, dans le contexte du microenvironnement des follicules secondaires	158
Fig. 28	Distribution de la concentration de la galectine-9 plasmatique selon les sites de la tumeur primaire ( <i>à gauche</i> ) ou le nombre de sites métastatiques ( <i>à droite</i> )	159

## List of Tables

Table 1	Common saccharides with their abbreviation and the symbol nomenclature	12
Table 2	Enzymes involved in the N-linked glycosylation.	16
Table 3	Enzymes involved in the synthesis of O-linked glycosylated proteins.	17
Table 4	Protein folds with lectin activity	18
Table 5	A summary of cytotoxic T cell subsets	32
Table 6	Characteristics of Gal-9 isoforms	49

# Introduction

# Chapter 1: Introduction to the "sugar code"

---

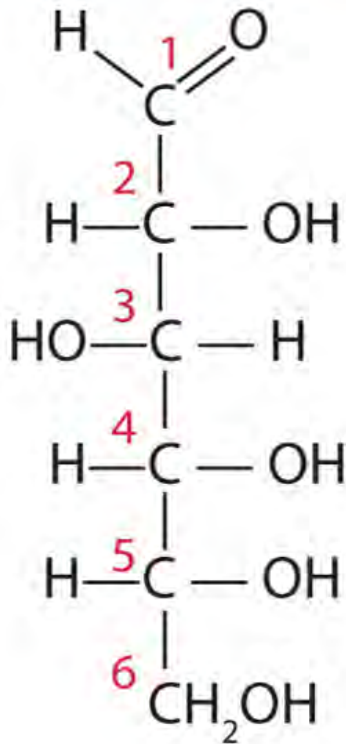
## 1.1. General aspects of glycan biology

### 1.1.1. Carbohydrates as a biological messenger

The discovery of DNA structure and later the Central Dogma enunciated by Francis Crick established the concept of sequential information in living organism (1). Whether it is a tree, a man or a woman, a wombat or a bee, its phenotype is the 'materialization' of sequences made from defined alphabets: proteins' peptide chains built from amino acids which themselves are products of the translation from the "letters" of nucleotides (2). In our days, we may be so familiar with this flow of translating while keeping biological information intact, usually referred to as the 'genetic code', but back in the time when this concept was first put forward, the complex process that follows the synthesis of proteins was yet to be discovered. And so, it is inevitable that the Central Dogma overlooked the post-translation modifications, in particular the glycosylation process (3). Attached to proteins or lipids at a high density and diversity, carbohydrates emerge as a powerful tool to convey information and influence at a certain extent the function of these biomolecules.

Carbohydrates can surpass the capacity of nucleotides or amino acids as a system of encoding information (2). First, from a variety of their structural units, carbohydrates can form many more isomers of dimers, thus oligomers, than nucleotides or amino acids permit. Imagine of two 6-carbon rings where each carbon is numbered from 1 to 6 (*Fig. 1*). If a bridge is to be drawn between the two, a linkage at the C2 of the first ring to the C2 of the second ring would give a different configuration compared to a combination of C2 and C3. This is what happens when a monosaccharide is joined with another to form a dimer. Although the glycosidic bond may appear as the same to equivalent hydroxyl groups available at each carbon of the anomeric center, the overall configuration is different for each pair of carbon that forms a linkage. In contrast to carbohydrates, only one dimer could result from a combination of two nucleotides or amino acids. Second, unlike nucleic acids and proteins whose messages are

**Fischer projection**



**Cyclic monosaccharide**



Fig. 1 **Representations of glucose.** Glucose can be represented in a linear form known as Fischer projection or in a cyclic form as a 6-carbon ring.

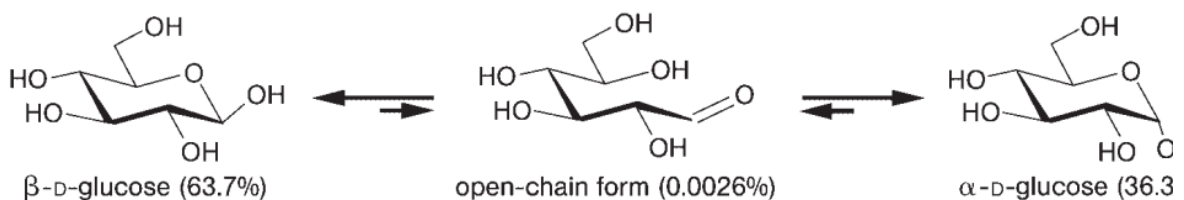


Fig.2 **Illustration of the equilibrium including the two anomeric forms of D- glucose.** The cyclic form results from a reaction between the OH group on the fifth carbon and with the aldehyde group. A solution of monosaccharides is an equilibrium mixture of open-chain form and cyclic form in variable ratios; in the case of D-glucose, the percentage of each in equilibrium is shown in the bottom line. *Adapted from (4).*

encoded in linear mode, carbohydrates can grow a chain of oligosaccharide or introduce branches to their structures. In addition to the variety of dimers formed, monosaccharides are open to having more than 1 hydroxyl group bridged to another monosaccharide through glycosidic bond (5). In other words, if we return to our carbon rings, when two contacts are formed at two carbons in a ring, and each of the added rings continue to make linkages in the same manner, a branched structure is generated. The capacity to either elongate the chain or make branches of carbohydrates gives rise to complex glycomes that vary not only among species but also between individuals. As highlighted by Hart (1992) and Cook (1995), glycans may provide us with a fundamental insight that opened the door "to one of the last great frontiers of biochemistry" (6,7).

### 1.1.2. The alphabet of the sugar code

The letters in the alphabet of the sugar code are monosaccharides. In the late 19<sup>th</sup> century, Emil Fischer introduced the classical chain structure of monosaccharide where he figured out how the  $(\text{H}_2\text{O})_n$  molecules were distributed over the carbon backbone, resulting in the general empirical formula  $\text{C}_x(\text{H}_2\text{O})_n$  with  $n$  an integer ranging from 3 to 9 (8). The structure is organized as a chain of chiral hydroxymethylen units; one end is a hydroxymethyl group while the other could be either an aldehyde group in aldoses, or an  $\alpha$ -hydroxy ketone group for ketoses (8). The simplest aldose is glyceraldehyde, whereas the ketose counterpart is dihydroxyacetone; both have 3 carbons in their structure, the only difference is the asymmetric (chiral) carbon atom in glyceraldehyde that dihydroxyacetone does not have. Apart from dihydroxyacetone, all monosaccharides have at least one asymmetric carbon atom, which enables the intramolecular reaction to join the 2 ends of a monosaccharide into a cyclic form. As demonstrated by the work of B. Tollens, a solution of monosaccharides is an equilibrium mixture of acyclic and cyclic form; the percentage of each depends on the sugar structure, though the cyclic structure is dominant in living organisms (*Fig.2*) (5). To date, about 250 types of monosaccharides have been isolated and identified; they are usually classified by the number of carbons in their structure: trioses are 3-carbon monosaccharides, tetraoses are 4-carbon sugars, and so on. Sugars with higher number of carbon are rarely found in nature; in fact, the monosaccharides occurring naturally are almost exclusively pentoses and hexoses (9). Therefore, these classes of monosaccharides are brought into focus in the scope of this














Monosaccharide	Abbreviation	Symbol
Arabinose	Ara	
Fructose	Fru	
Fucose	Fuc	
Galactose	Gal	
Galactosamine	GalN	
<i>N</i> -acetylgalactosamine	GalNAc	
Glucose	Glc	
Glucosamine	GlcN	
<i>N</i> -acetylglucosamine	GlcNAc	
Glucuronic acid	GlcA	
Mannose	Man	
Muramic acid	Mur	
Neuraminic acid	Neu	
Sialic acid	Sia	
Rhamnose	Rha	
Ribose	Rib	
Xylose	Xyl	

Table 1. **Common saccharides with their abbreviation and the symbol nomenclature.**

First put forward by Kornfeld and colleagues in 1978, the use of symbols for representation of vertebrate glycans rose to popular use and was eventually adopted in the first edition of the textbook *Essentials of Glycobiology*. The authors later took advantage of color, in 2005, to overcome the limitations and inconsistencies in representing the diversity of glycans. The symbol nomenclature has since been widely disseminated and accepted by the Consortium for Functional Glycomics as well as the scientific community (10). A complete version is available on the website *Glycopedia* (<https://www.glycopedia.eu/resources/a-picture-dictionary-of-monosaccharide-symbols/article/the-picture-dictionary>).



manuscript, as they take part in the process of encoding and conveying information in mammals.

These letters are nonsensical unless put together to make a word or a sentence; likewise, monosaccharides as single units do not convey much information to proteins and lipids until the process of glycosylation does the craftwork to create long, serving sugar chains called glycans. In line with the diversity and involvement of glycans in biological processes, the standardization in drawing their structure became essential. The use of symbols to represent monosaccharides -the letters in the sugar code – is now widely accepted and recommended in the scientific community (9,10). A table of common monosaccharides in mammals with their symbol is presented here for the reader's reference (*Table 1*).

### 1.1.3. The many types of glycosylation

In normal states, oligosaccharides (glycans) are usually attached to a scaffold through a covalent bond, which could be either a protein or a lipid, to form a glycoconjugate. Although free oligosaccharides have been reported in yeast strains to be generated from misfolded glycoproteins and peptide:*N*-glycanase (PNGase) activity, their presence in the cytoplasm of yeast and mammalian cells remains in low micromolar concentration and has little evidence of any physiological roles (12–15). Glycoconjugates, on the contrary, are rather abundant in the cell, as much as 5-10% of the cellular mass, and engaged in various biological processes (16). Glycoconjugates with lipid scaffolds include glycosphingolipids, which is typically present in the lipid bilayers of cellular membranes. Protein glycosylation includes many different types, each of them is defined by the characteristics of the glycans added, such as N-linked glycans, O-linked glycans, phosphorylated glycans, glycoaminoglycans and glycosylphosphatidylinositol (GPI) anchors to peptide backbones, as well as C-mannosylation of tryptophan residues (*Fig. 3*) (17,18).

As our study on galectin-9 focuses on its effects to T cell via protein interactions, we would discuss more in detail on protein glycosylation.

### 1.1.4. *N*-glycosylation

#### **Basic structure of *N*-linked glycans**

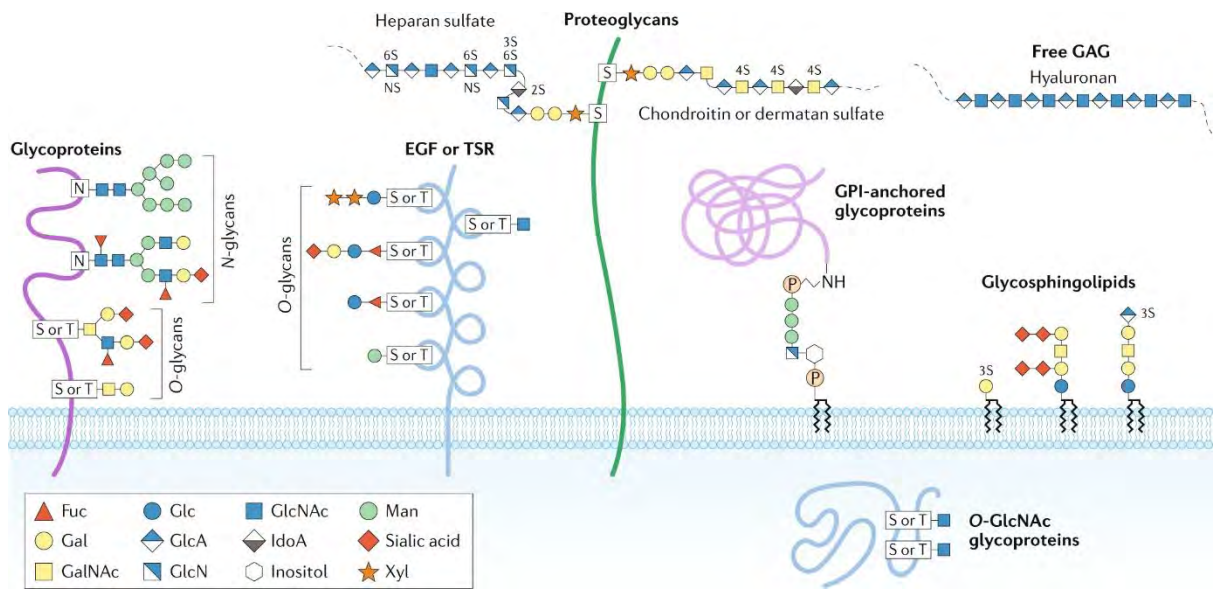


**Fig. 3 The major types of glycosylation in human.** *N*-linked and *O*-linked glycosylation are the most popular, where glycan chains are linked to nitrogen and oxygen atoms of amino acid residues, respectively. In general, *N*-glycans are branched and highly heterogeneous, consisting of a core glycan of two GlcNAc and three Man residues attached to the amino group of Asn (N) at the consensus glycosylation motif Asn-X-Ser/Thr (X could be any amino acid except for Pro). *O*-glycosylation consists of glycans bound to the hydroxyl groups of Ser (S) or Thr (T) residues. The initial sugar attached to the protein and the additional sugar structures added to the initial glycan can be used as the basis to subclassify *O*-glycans: (1) GalNAc is the initial glycan of mucin-type *O*-glycosylation; (2) *O*-linked fucose (Fuc) and *O*-linked Man often occur in specific protein domains, such as epidermal growth factor (EGF) repeats, thrombospondin type I repeats (TSR) or dystroglycan. Proteoglycans are defined by long glycosaminoglycan (GAG) chains consisting of a tetrasaccharide core GlcA – Gal – Gal – Xyl attached to the hydroxyl group of Ser at Ser-Gly-X-Gly amino acid motifs. A free form of GAGs is synthesized at the plasma membrane only by addition of GlcA and GlcNAc and not attached to protein cores, such as hyaluronan. Glycosylphosphatidylinositol (GPI)-anchored glycoproteins is another class of glycoconjugates that has a Man<sub>3</sub>-GlcN core attached to phosphoethanolamine; the GlcN residue is linked to phosphatidylinositol embedded in the cell membrane. Glycosphingolipids are a class of glycoconjugate with glycan attached to cellular membrane lipids. *Adapted from* (19).

*N*-linked glycans usually refer to proteins glycosylated by a  $\beta$ -1N-glycosidic bond that joins ***N*-acetylglucosamine (GlcNAc)** to an **asparagine (Asn)** residue, although other *N*-glycan linkages with other sugars have been reported in prokaryotes. In eukaryotes, the minimal amino acid sequence to form an *N*-glycan is Asn-X-Ser/Thr (serine/threonine), in which "X" is any amino acid except proline (Pro), while the sugar core is usually GlcNAc<sub>2</sub>Man<sub>3</sub>. A variety of monosaccharides can be added to this base, these additions give rise to three general types: (1) high-mannose *N*-glycan, in which only mannose (Man) residues extend the core; (2) complex, in which GlcNAc primes the extension of each arm with other sugars; (3) hybrid, in which Man extends the Man $\alpha$ 1-6 arm of the core and the other arm is elongated by one or two GlcNAcs (*Fig. 4*) (20).

### Synthesis of *N*-glycan

The biosynthesis of *N*-glycan is most complex in mammals, occurring in two phases and in two compartments, the endoplasmic reticulum (ER) and the Golgi apparatus (*Fig. 5*). The first phase is initiated in the cytoplasmic side of the ER, where a branched carbohydrate structure made from GlcNAc and Man is bound to dolichol phosphate (Dol-P). When flipped to face the ER lumen, the lipid-glycan enters the second phase where glycosidases and glycosyltransferases process their sugar moieties in a species-, cell type-, protein-, and even site-specific manner. In general, glycans are supplied with Man and Glc units to generate 14-sugar structures—**Glc<sub>3</sub>Man<sub>9</sub>GlcNAc<sub>2</sub>-P-P-Dol**. They are then transferred to **Asn** in the receptive Asn-X-Ser/Thr sequons of nascent proteins by the multisubunit enzyme **oligosaccharyltransferase (OST)**. As the protein folding continues, Glc residues are removed by  **$\alpha$ -glucosidases**, the terminal  $\alpha$ 1-2Man is subsequently removed from the central arm of GlcNAc<sub>2</sub>Man<sub>9</sub> by **ER  $\alpha$ -mannosidase I** before entering the *cis*-Golgi compartment. Most glycoproteins leave the ER carry *N*-glycans with either 8 or 9 Man residues, and if misfolded they are recognized and targeted for degradation by **ER degradation-enhancing  $\alpha$ -mannosidase I-like (EDEM)** proteins. Glycans move to the *cis* compartment of the Golgi apparatus if they are qualified at this quality-control checkpoint and enter the early processing steps with the trimming of  **$\alpha$ 1-2Man** residues by  **$\alpha$ 1-2 mannosidase I**. The resulting **GlcNAc<sub>2</sub>Man<sub>5</sub>** structures undergo sequential modifications in the *medial*-Golgi that generate hybrid and complex *N*-glycan. Some GlcNAc<sub>2</sub>Man<sub>5</sub> structures, however, can escape this process and enter maturation phase as high-mannose

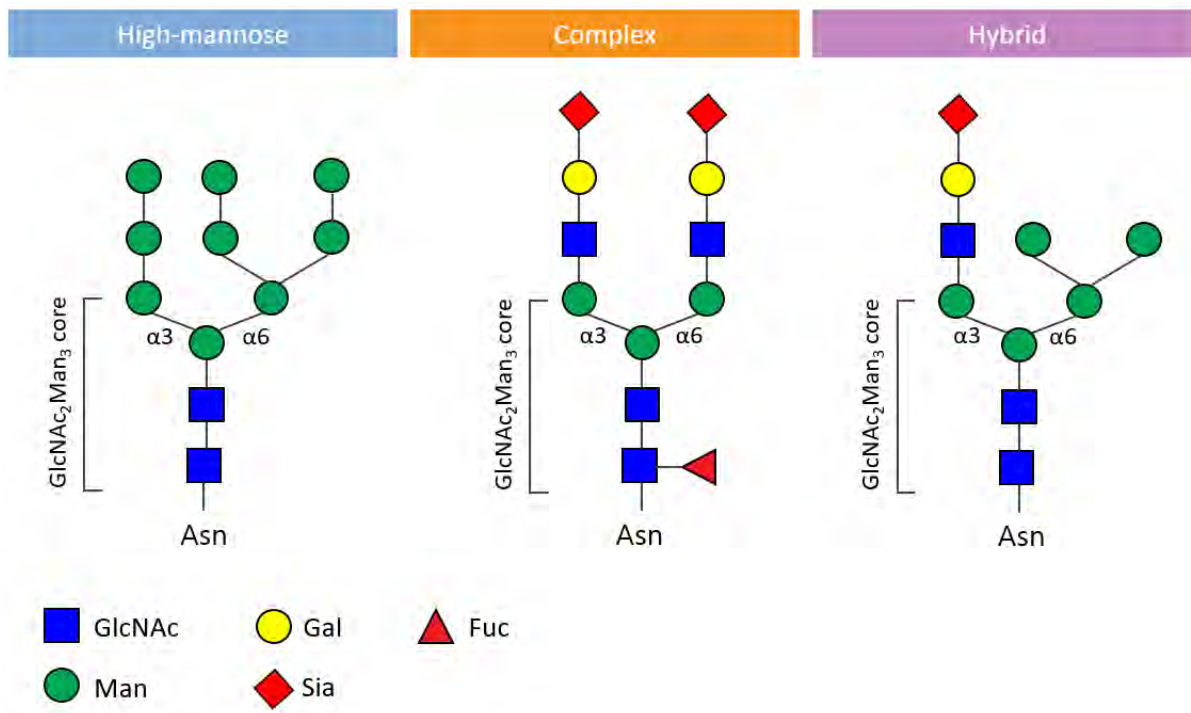


Fig. 4 **The main types of N-glycan.** N-glycan is formed by a linkage between GlcNAc with an Asn residue of protein, resulting in a  $\text{GlcNAc}_2\text{Man}_3$  core. Man residues of the core make a typical antenna where various sugars are added to build a more complex structure. High-mannose N-glycan has two arms extended by Man residues; complex N-glycan is characterized with extensions primed by GlcNAc then continued with other sugars; hybrid N-glycan is the combination of the two aforementioned types, with the  $\text{Man}\alpha 1-6$  arm extended by Man and the other initiated by one or two GlcNAc.

membrane or secreted glycoproteins carrying GlcNAc<sub>2</sub>Man<sub>5-9</sub> *N*-glycans. Others received a GlcNAc residue in the GlcNAc<sub>2</sub>Man<sub>5</sub> core through an ***N*-acetylglucosaminyltransferase** enzyme called **GnT-I (MGAT1)** in mammals). The action of GnT-1 is the prerequisite for the generation of complex and hybrid glycans; if Man residues of the GlcNAcMan<sub>5</sub>GlcNAc<sub>2</sub> glycan produced by GnT-I are subsequently cut off by an  $\alpha$ -mannosidase II, the glycan continues to be modified in medial-Golgi compartment, where various GnTs generate additional branches and matures as complex *N*-glycans. If not, the glycan passes on to maturation as a hybrid *N*-glycan. (20,21)

The maturation of *N*-glycans takes place in the *trans*-Golgi compartment, expanding the limited repertoire of hybrid and branched *N*-glycans to an extensive array of complex *N*-glycans. This process includes sugar addition to the core or elongation of branching GlcNAc residues and "capping" elongated branches. This "capping" reaction consists of adding sialic acids, fucose and galactose sugars, as well as sulfate to complex *N*-glycan branches, thus facilitating the contact of terminal sugars to lectins and antibodies. (20)

### 1.1.5. *O*-glycosylation

*O*-glycosylation of proteins occurs by linkages between sugar residues and functional hydroxyl groups on Ser and Thr, hence the term "*O*-linked". A good model of *O*-linked glycosylation is mucin, one of the main ingredients that gives mucus the gel-like form as we know it. Having a large number of Ser and Thr residues, mucin harbors *O*-glycans among which the cross-linking due to disulfide bonds promotes gelation (22). At a closer inspection, the *O*-glycosylation taking place in mucins is of GalNAc class; these glycans are initiated from a GalNAc attached to Ser or Thr residues. Other sugars including Man, Gal, Fuc and Glc can also serve as primer for *O*-glycosylation, but GalNAc and GlcNAc are the most common classes of *O*-linked glycan in humans (22).

Sharing the same biantennary structure as *N*-glycans, *O*-glycans are less branched but they are more diverse due to non-templated biosynthesis. GalNAc-linked glycans, for instance, have up to 6 major basic core structures: cores 1-4, terminal GalNAc(Tn) and sialyl-Tn antigens (19,22). Their synthesis is initiated by the polypeptide **GalNAc transferases (GALNTs)**, which have different specificity for amino acid motifs, adding complexity in terms of regulation to

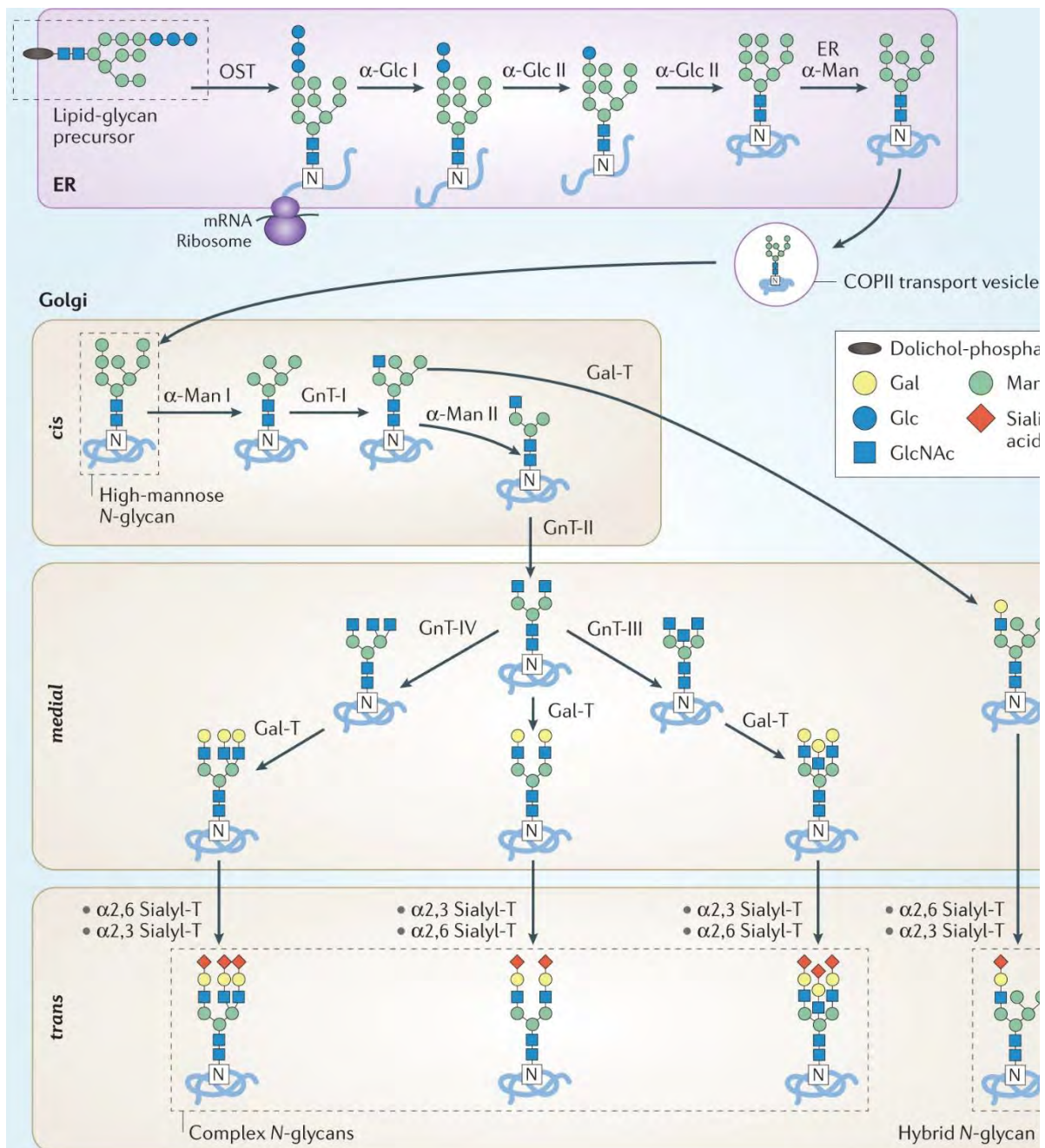


Fig. 5 **Biosynthesis of N-linked glycosylated proteins.** The first phase takes place in the endoplasmic reticulum and generates **Glc<sub>3</sub>Man<sub>9</sub>GlcNAc<sub>2</sub>-P-P-Dol** structures. These are then transferred to **Asn** in the receptive Asn-X-Ser/Thr sequons of nascent proteins by the multisubunit enzyme **oligosaccharyltransferase (OST)** at the beginning of the second phase, where glycan structures are elongated. Various steps of addition and removal are done by mannosidase and carbohydrate transferase enzymes, resulting in N-glycans of high-mannose, complex and hybrid type. The maturation of N-glycans takes place in the *trans*-Golgi compartment, adding sialic, fucose, galactose or sulfate to complex structure of these glycans. Adapted from (19).

how and where *O*-glycans are attached (19,22). As the protein moves through the *cis*-, *medial*- and *trans*-Golgi compartment, various glycosyltransferases expand the structure by adding Gal, GlcNAc, Sia, and in some instances Fuc (22). Unlike *N*-glycans, this model of glycosylation does not follow a stepwise procedure that interlaces addition and removal of sugars to the glycoconjugate. Instead, the glycopeptide *O*-glycan chains are initiated and then simply elongated, but the diversity of enzymes that take part in the process gives rise to an enormous set of carbohydrate structures (22). These glycans are abundant on extracellular and secreted as well as membrane glycoproteins, including mucins, human immunoglobulin A1 (IgA1), and blood groups (19).

GlcNAc-linked glycans, on the other hand, are not discovered until 1983, but the number of proteins found to be glycosylated with it has increased rapidly (23). There are many reasons for their late discovery, but it is generally due to the uniqueness of the *O*-GlcNAc model of glycosylation. Distinct from their fellow glycans, the GlcNAc moiety is not elongated from other sugars to form complex structures, and thus is not solid enough to pass through the ionization process in mass spectrometry without falling off the polypeptide (23). At the cellular level, this simple structure is subjected to multiple cycles of attachment and removal from its protein substrate. The dynamic cycling of *O*-GlcNAc in the life of a protein is regulated through ***O*-GlcNAc transferases (OGTs)** and ***O*-GlcNAcases (OGAs)**; these enzymes exist in different forms and levels in subcellular compartments. However, they all have the same rapid activity cycle and seem to play important roles in cellular functions, especially in cellular metabolism where *O*-GlcNAc may act as a sensor of nutrients available in the cell (19,23). Moreover, for some subsets of proteins, *O*-GlcNAc even competes with the phosphorylation process of Ser and Thr residues, adding complexity to the regulatory circuits (24). One example where this competition appears to be essential to the cellular functions is the phosphorylation of CTD repeat domain (YSPTSPS) of RNA polymerase II which has many *O*-GlcNAc clusters. After the initiation of the transcription, *O*-GlcNAc moieties are removed, and replaced by *O*-phosphate, which subsequently sets off the elongation of mRNA (23).

	Enzyme	HGNC nar
Synthesis of the Dolichol-Linked Precursor	Chitobiosyldiphosphodolichol beta-mannosyltransferase	ALG1
	Dol-P-Glc:Glc(2)Man(9)GlcNAc(2)-PP-Dol alpha-1,2-glucosyltransferase	ALG10
	GDP-Man:Man(3)GlcNAc(2)-PP-Dol alpha-1,2-mannosyltransferase	ALG11
	Dol-P-Man:Man(7)GlcNAc(2)-PP-Dol alpha-1,6-mannosyltransferase	ALG12
	UDP-N-acetylglucosamine transferase subunit ALG14 homolog	ALG14
	Alpha-1,3/1,6-mannosyltransferase ALG2	ALG2
	Dol-P-Man:Man(5)GlcNAc(2)-PP-Dol alpha-1,3-mannosyltransferase	ALG3
	Dolichyl-phosphate beta-glucosyltransferase	ALG5
	Dolichyl pyrophosphate Man9GlcNAc2 alpha-1,3-glucosyltransferase	ALG6
	Probable dolichyl pyrophosphate Glc1Man9GlcNAc2 alpha-1,3-glucosyltransferase	ALG8
	Alpha-1,2-mannosyltransferase ALG9	ALG9
	Dolichol kinase	DOLK
	Dolichyldiphosphatase 1	DOLPP1
	UDP-N-acetylglucosamine--dolichyl-phosphate N-acetylglucosaminophosphotransferase	DPAGT1
	Dolichol-phosphate mannosyltransferase	DPM
	Glutamine--fructose-6-phosphate aminotransferase [isomerizing] 1	GFPT1
	Mannosyl-oligosaccharide glucosidase	MOGS
	Mannose-P-dolichol utilization defect 1 protein	MPDU1
	Oligosaccharyltransferase	OST
	Phosphomannomutase 2	PMM2
	Protein RFT1 homolog	RFT1
Polyprenol reductase	SRD5A3	
UDP-glucose:glycoprotein glucosyltransferase 1	UGGT1	
UDP-glucose:glycoprotein glucosyltransferase 2	UGGT2	
Processing and maturation	Beta-1,4 N-acetylgalactosaminyltransferase 2	B4GALNT2
	Beta-1,4-galactosyltransferase 1	B4GALT1
	Beta-1,4-galactosyltransferase 7	B4GALT7
	Mannosyl-oligosaccharide 1,2-alpha-mannosidase IC	MAN1C1
	Alpha-mannosidase 2	MAN2A1
	Alpha-mannosidase 2x	MAN2A2
	Alpha-1,3-mannosyl-glycoprotein 2-beta-N-acetylglucosaminyltransferase	MGAT1
	Alpha-1,6-mannosyl-glycoprotein 2-beta-N-acetylglucosaminyltransferase	MGAT2
	Beta-1,4-mannosyl-glycoprotein 4-beta-N-acetylglucosaminyltransferase	MGAT3
	Alpha-1,3-mannosyl-glycoprotein 4-beta-N-acetylglucosaminyltransferase A	MGAT4A
	Alpha-1,3-mannosyl-glycoprotein 4-beta-N-acetylglucosaminyltransferase B	MGAT4B
Alpha-1,3-mannosyl-glycoprotein 4-beta-N-acetylglucosaminyltransferase C	MGAT4C	
Alpha-1,6-mannosylglycoprotein 6-beta-N-acetylglucosaminyltransferase A	MGAT5	
Alpha-1,6-mannosylglycoprotein 6-beta-N-acetylglucosaminyltransferase B	MGAT5B	
Capping reactions	Alpha-(1,6)-fucosyltransferase	FUT8
	Galactosylceramide sulfotransferase	GAL3ST1
	CMP-N-acetylneuramate-beta-galactosamide-alpha-2,3-sialyltransferase 1	ST3GAL1
	Beta-galactoside alpha-2,6-sialyltransferase 1	ST6GAL1

Table 2. **Enzymes involved in the N-linked glycosylation.**



### 1.1.6. Proteoglycans and glycosaminoglycans

Proteoglycans are glycoproteins in the extracellular matrix with a higher level of glycosylation. In addition to canonical *N*-glycans and *O*-glycans, proteins are bound with long sugar repeats via Ser residues at Ser-Gly-X-Gly amino acid motifs (25). These chains are called glycosaminoglycans, usually characterized with a substantial mass made from more than 80 sugars, comparing to the tail of 5-12 monosaccharides that forms *N*-glycans (26). The glycosaminoglycans are built from disaccharide repeats budding from GlcNAc or GalNAc, combined with anuronic acid (that is, glucuronic or iduronic acid) or galactose. They are the main blocks that make up the glycocalyx, or the "sugar coat" of the cell, which works as a reservoir for the sequestered growth factors and allows the maintenance of the cell membrane (26).

### 1.1.7. Decipher the sugar code: Lectins

Lectins are a class of carbohydrate-binding proteins, distinct from antibodies, enzymes and transport proteins for free mono-, di- and oligosaccharide. The separation of lectin from other categories is based on the nature of the interaction; the term "lectin" itself is defined as binding partners for glycoconjugate glycans (27,28). The reactivity of lectins to carbohydrate is established by more than 15 folding patterns (in animals) that form carbohydrate recognition domains (CRDs) (29). Each distinct fold is built from a common ancestral gene, yet the gene duplication and sequence diversification generate a set of proteins with same configuration of contact site but different specificity and affinity level for glycans (2,30). An overview of protein folds with examples of lectin and their associated ligands is presented in *Table 4*.

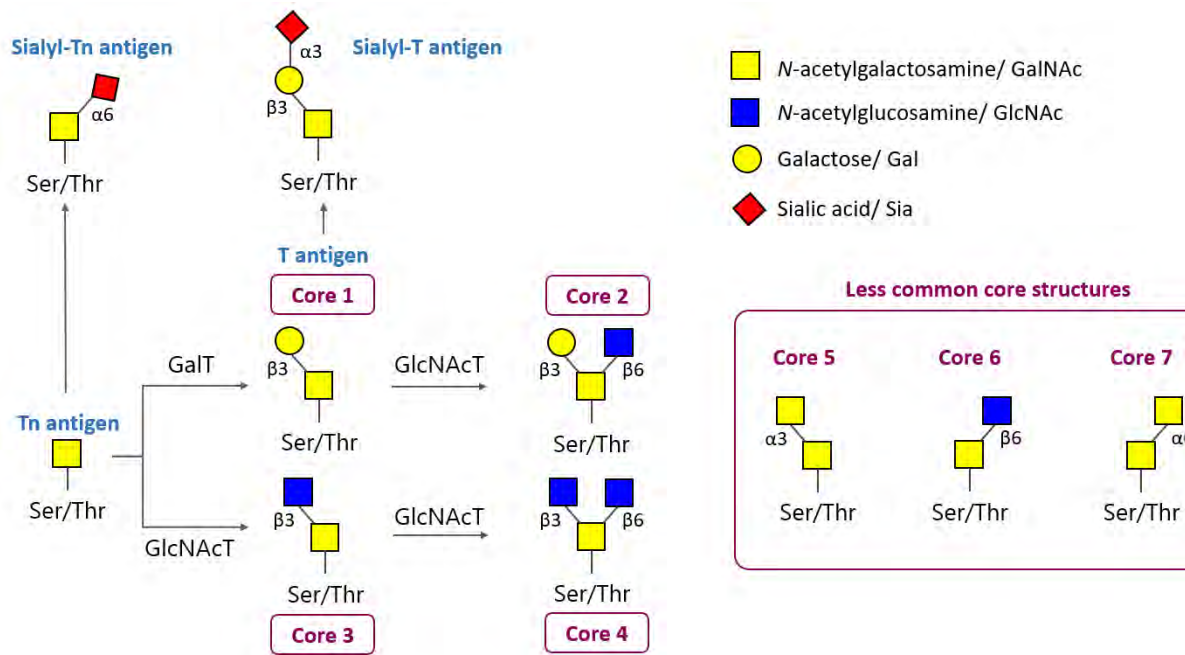


Fig. 6 Structures of O-GalNAc main cores.

Enzyme	HGNC name
Polypeptide N-acetylgalactosaminyltransferase	GALNT
Core 1 $\beta$ 1-3 galactosyltransferase 1	C1GALT1
Essential chaperone for T synthase	C1GALT1C1
Core 2 $\beta$ 1-6 N-acetylglucosaminyltransferase	GCNT1
Core 3 $\beta$ 1-3 N-acetylglucosaminyltransferase 6	B3GNT6
Core 2/4 $\beta$ 1-6 N-acetylglucosaminyltransferase 2	GCNT3
Elongation $\beta$ 1-3 N-acetylglucosaminyltransferase	B3GNT3
I branching $\beta$ 1-6 N-acetylglucosaminyltransferase	GCNT2
$\beta$ 1-3 galactosyltransferase	B3GALT5
Core 1 $\alpha$ 2-3 sialyltransferase	ST3GAL1, ST3GAL4
$\alpha$ 2-6 sialyltransferase	ST6GALNAC1 - 4
Core 1 3-O-sulfotransferase	GAL3ST4
$\alpha$ 1-2 Fucosyltransferase	FUT1, FUT2

Table 3. Enzymes involved in the synthesis of O-linked glycosylated proteins.

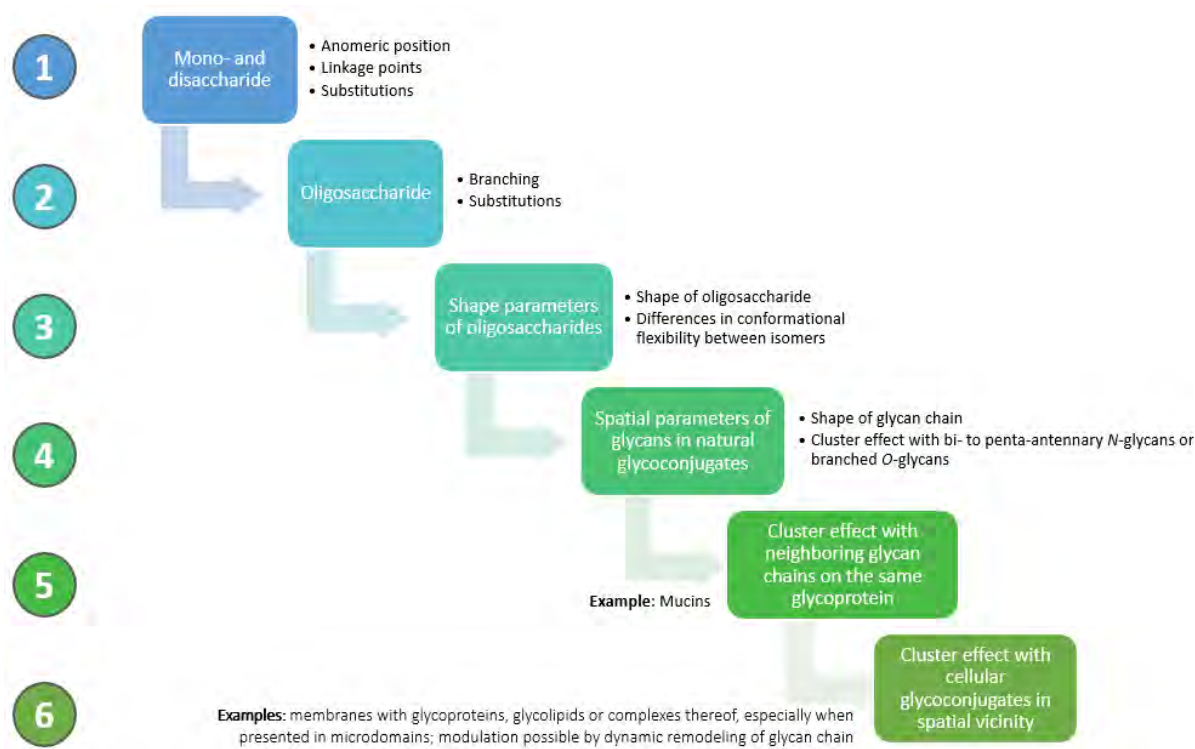


Fig. 7 **Six levels of regulation of affinity for binding of a glycan to a lectin.** Adapted from (29).

Evolving from simple structures such as mono- and disaccharide to complex chains of sugars, glycans provide many levels of affinity regulation for binding to lectins (29); these shape the parameters to turn a carbohydrate epitope into a privileged docking point for a lectin. From the numerous glycoconjugates of the glycocalyx, lectins are capable of selecting between non-cognate and cognate epitopes, therefore they target distinct receptors to fulfill specific functions (29). This functional pairing, associated to the structural diversity, make lectins the platform for reading and translating sugar-encoded information (30).

### 1.1.8. Glycome in health and disease

As we have well discussed in the previous parts, glycans are omnipresent in the cells and the extracellular matrix, incorporated in proteins and make up more complicated structures such as the "sugar coat". They require a complex and tangled system of enzymes and regulatory circuits for their synthesis, assembly, modification, remodeling and degradation (2). Indeed,

Type of fold	Example for lectin	Example for ligand
C-type	asialoglycoprotein receptor, collectins, selectins	Fuc, Gal, GalNAc, Man, heparin tetrasaccharide
I-type (Ig fold)	N-CAM, TIM-3, siglecs	Man <sub>6</sub> GlcNAc <sub>2</sub> , HNK-1 epitope, α2,3/6-sialylated glycans
P-type	mannose-6-phosphate receptors (MR) and proteins with MR homology domain (erlectin, OS-9)	Man-6-phosphate, Man <sub>5,6</sub> GlcNAc <sub>2</sub>
β-sandwich (jelly-roll)	<p><b>a) galectins</b></p> <p>b) calnexin, calreticulin</p> <p>c) ERGIC-53</p> <p>d) CRD of Fbs1 in SCF E3 ubiquitin ligase and peptide-<i>N</i>-glycanase</p> <p>e) pentraxins</p> <p>f) G-domains of the LNS family (laminin, agrin)</p>	<p><b>β-galactosides</b></p> <p>Glc<sub>1</sub>Man<sub>9</sub>GlcNAc<sub>2</sub></p> <p>Man<sub>7</sub>GlcNAc<sub>2</sub></p> <p>Man<sub>3</sub>GlcNAc<sub>2</sub>; mannopentaose</p> <p>glycosaminoglycans, MOβDG, 3-sulfated Gal, GalNAc and GlcA, Man-6-phosphate</p> <p>heparin</p>
β-trefoil	<p>a) fibroblast growth factors</p> <p>b) cystein-rich domain of C-type macrophage mannose receptor</p> <p>c) lectin domain in GalNAc-transferases involved in mucin-type O-glycosylation</p> <p>d) hemolytic lectin CEL-III of sea cucumber and lectin EW29 of earthworm</p>	<p>heparan sulfate</p> <p>GalNAc-4-sulfate in LacdiNAc</p> <p>GalNAc</p> <p>Gal</p>
β-propeller	<p>a) 4-bladed: tachylectin-3</p> <p>b) 5-bladed: tachylectin-2</p> <p>c) 6-bladed: tachylectin-1</p>	S-type lipopolysaccharide GlcNAc/ GalNAc KDO
β-prism I	secretory proteins zg16 p/b	not defined
β-prism II	pufferfish (fugu) lectin	Man
β-barrel with jelly-roll topology	tachylectin-4, eel ( <i>Anguilla anguilla</i> ) agglutinin, <i>Xenopus</i>	Fuc
fibrinogen-like domain	<p>a) Ficolins</p> <p>b) intelectins (mammalian, <i>Xenopus</i>)</p> <p>c) tachylectin-5</p> <p>d) slug (<i>Limax flavus</i>) lectin</p>	<p>GlcNAc</p> <p>Gal<sub>f</sub>, pentoses</p> <p><i>N</i>-acetylated sugars</p> <p>sialic acid</p>
link module	CD 44, TSG-6, LYVE-1, aggregating proteoglycans	hyaluronic acid
hevein-like domain	tachycytin and spider ( <i>Selenocosmia huwena</i> ) neurotoxin; cobra venom cardiotoxin	GalNAc; heparin-derived disaccharide
(β/α) <sub>8</sub> barrel (glycoside hydrolase family 18)	YKL-40 (human cartilage glycoprotein-39; chitinase-like lectin)	(GlcNAc) <sub>n</sub>
short consensus repeat (complement control protein module)	factor H (complement regulator)	glycosaminoglycans, sialic acid

Table 4. **Protein folds with lectin activity.** Adapted from (29).

the "glycosylation machinery" of the cell is estimated to occupy 1 to 3% of the human genome (31). The idea of studying the glycomic deviations from normal status is tempting, especially in pathologies relating to genetic mutations such as congenital disorders and cancers, or in immunology, where glycan patterns can be crucial to the distinction between self and non-self.

Congenital disorders of glycosylation (CDG) were first found in children with multi-system disorders, typically present with developmental delay, failure to thrive, hypotonia, neurologic abnormalities, hepatopathy and coagulopathy (32). These multi-systemic manifestations are due to defects in either a single glycosylation step or several pathways. Both could lead to altered activation, presentation, or transport of sugar precursors; altered expression and/or activity of glycosidases or glycosyltransferases, and altered expression and/or activity of proteins that control the glycosylation machinery or maintain the Golgi apparatus (21). These defects can be classified into 4 categories, depending on the type of glycosylation affected: 1- *N*-linked glycosylation, 2- *O*-linked glycosylation, 3- combined *N*- and *O*-linked/multiple glycosylation, and 4- lipid and glycosylphosphatidylinositol (GPI) anchor biosynthesis defects (32). Current treatment of CDGs aims at compensating the defects by a dietary supplementation. For instance, in MPI-CDG - one of the most common CDGs, the mutation in the gene ***MPI*** encoding for **Man-6-P isomerase** inhibits the interconversion of Man-6-P and fructose-6-phosphate, subsequently leads to a shortage of Man for glycosylation (33). Mannose dietary supplementation is thus an effective treatment for patients with MPI-CDG (34,35). Nevertheless, for other CDGs such a symptomatic treatment may not be sufficient and relevant. Patients with PMM2-CDG – the most common type of CDGs, for example, are struggled with defective phosphomannomutase 2 (PMM2) that abrogates the conversion of Man-6-phosphate to Man-1-phosphate. In turn, the synthesis of the lipid-bound precursor of *N*-glycans, Glc<sub>3</sub>Man<sub>9</sub>GlcNAc<sub>2</sub>-P-P-Dol, cannot occur and no compensation can be made through a dietary therapy (33,36). Novel strategies are recently developed, using pharmacological chaperones to stabilize defective, misfolded proteins that suffer from loss-of-function mutations in the gene PMM2 (37). Other CDGs might also benefit from this type of treatment, however most of them require new therapeutic approaches that are more personalized and based on the identification of relevant genetic mutations in each patient.

In cancer, aberrant glycosylation was first reported following SV-40 virus transformation of mouse fibroblasts in 1969 (38,39). Since then, the number of studies concerning fundamental changes in the glycosylation patterns of cell surface and secreted glycoproteins in malignant transformation and cancer progression has been increasing. Aberrant glycosylation actively promotes tumor progression by promoting cancer hallmarks, which comprehend proliferative signaling, resistance to cell death, invasion and metastasis, angiogenesis, inflammation and immune escape (40,41). In general, the modifications usually stem from abnormal regulations of glycosyltransferases, either through genetic mutations or epigenetic regulations, resulting in shorter *O*-glycans and more branched *N*-glycans (42). These alterations in glycan structure are also accompanied with changes in glycan sialylation and fucosylation, which in turn modify the nature of terminal epitopes at the glycan chains (42). Many *de novo* expression of specific glyco-epitopes have made way for diagnostic biomarkers to assess patient prognosis and responses to treatment. Examples of such glycoproteins include CEA (carcinoembryonic antigen), MUC1 (CA15-3/CA27.29), MUC16 (CA-125) and PSA (prostate specific antigen) (43–46). Recent studies have identified dysregulated **sialyltransferases** as associated with tumor pro-survival pathways or metastasis. These include **ST3GalIII**, **ST3GalIV**, which may give rise to elevated level of CA19-9 (carbohydrate antigen 19-9) in pancreatic, gastric, and colorectal cancers; **ST6GalII** is also upregulated in pancreatic and colon cancers (43,47–50). Another comprehensive study also reported **ST6GALNAC5** as the key gene mediating brain metastasis in breast cancer (51). With more studies shedding light on glycome profiles of cancer cells, aberrant glycosylation is becoming an integral part of recognized cancer hallmark traits.

Glycosylation is highly implicated in immune activities. First, immune receptors use glycan patterns to distinguish "non-self" structure present on the surface of microorganism, also known as pathogen-associated molecular pattern (PAMP). Beside the pathogen recognition, glycans are also involved in physiological processes of immune cells, regulating their development, differentiation and proliferation (52). In the scope of this work, as we would spend more time discussing on T cells reactions, a deeper insight on modification of glycosylation in T cell development phases would be helpful. Different glycosylation enzymes take part in shaping T cell receptors and therefore regulate the signaling that leads them to proliferation, differentiation or even suppression. For instance, receptors such as TCR, CD25, and CD4 have complex branched *N*-glycans that are catalyzed by **1,6-N-acetylglucosaminyl**

**transferase V (GnT-V)**, encoded by **MGAT5** (52–55). Alterations in GnT-V activity, as well as **alpha-mannosidase II ( $\alpha$ -MII)**, **N-acetylglucosaminyltransferase I (GnT-I, MGAT1)** and **II (GnT-II, MGAT2)**, lead to a compromised T cell homeostasis associated with autoimmune disorders in humans and mouse models (52). GnT-I-mediated glycosylation and *O*-GlcNAcylation through **OGT (*O*-GlcNAc transferase)** also play a role in regulating T cell development and self-renewal (56). Moreover, glycosylation may be modified following TCR activation and in turn decides T cell fate. Studies have found TCR activation associated with an increased  $\beta$ 1,6-GlcNAc branched *N*-glycosylation of CTLA-4, which enhances CTLA-4 retention at the T cell surface and thereby promotes immune tolerance (57). In reverse, a reduced *N*-glycosylation due to Thr17Ala polymorphism in human CTLA resulted in a limited CTLA-4 retention at the T cell surface (58). Similar to CTLA-4 study, others also found a correlation between the levels of complex branched N-glycans on PD-1 and PD-L1, and their abundance at the cell surface which marks T cell exhaustion (59).

## 1.2. General aspects of galectins

### 1.2.1. Structure and specificity

Formerly termed as S-type lectins due to their solubility, galectins are a family of lectins, capable of recognizing polysaccharides and glycans with  $\beta$ -galactoside bonds (60). They are widely present in multicellular organisms, sharing homologous **carbohydrate recognition domains (CRDs)** in their primary structure. The **CRDs** in galectins are encoded by a sequence that varies from 20 to 50% among different species, but they have a common pattern of folding that create a curved sandwich structure with two  $\beta$ -sheets facing each other: the convex F-sheet and the concave S-sheet (61). In a groove of the S-sheet is the “sugar pocket” that is usually referred to as **carbohydrate binding site (CBS)**. **CBS** interacts directly with disaccharide elements containing the  $\beta$ 1-4 or  $\beta$ 1-3 galactoside bond which is recognized within the target polysaccharide. The sequence of CRD consists of 130 amino acids; 8 of them are invariant and about a dozen are highly conserved. The invariant amino acids are His44, Asn46, Arg48, Val59, Asn61, Trp68, Glu71 and Arg73. Mutation of Trp68 to alanine or leucine

abolishes the interaction with  $\beta$ -galactoside (61). However, the interaction between CBS and  $\beta$ -galactoside alone results in low affinity binding. Additional interactions specific to each galectin stabilize these bonds and give them a greater specificity. On the one hand, galectin ligands interact with the amino acids of the CRD, which is distinct from the CBS. On the other hand, galectin ligands also interact with amino acids outside the CRD. This explains the fact that each of the galectins, while using the same fundamental mechanism of attachment, interacts with a specific spectrum of polysaccharide ligands. Within this spectrum specific to each galectin, there is a real gradation of affinity which may vary in function of the physico-chemical conditions, in particular the concentration of the galectins and their level of polymerization. Galectins might even reach an affinity comparable to that of an antibody for its antigen (62).

In addition to lectin-like interactions with the polysaccharide ligands that involve CRDs, galectins can bind to other types of ligands through protein-protein interactions. Ongoing studies tend to prove that these protein-protein interactions can modify the galectin conformation and consequently, the spectrum of their interactions with polysaccharide ligands. Protein-protein interactions of galectins were initially reported for the binding to cytosolic and nuclear components but recently they have also been observed for extracellular galectins (63). For instance, galectin-1 interacts with the  $\lambda 5$  region of pre-BCR during the stages of proliferation and differentiation of B cells (64). More recently, an interaction of galectin-9 with another lectin, dectin-1, has been reported on macrophages in a model of murine pancreatic carcinoma (65). In order to standardize their nomenclature, the first galectin discovered (electrolectin) was named galectin-1 (66). Its closest counterpart was named galectin-2, later rejoined by galectins 3 and 4 (67). The remaining members of this family were then numbered consecutively in order of discovery up to a current total of 15 galectins, of which 11 are found in human (68).

Based on their tertiary structure, galectins are divided into 3 groups: "**prototype**", "**chimera**" and "**tandem repeat**" (*Fig. 8*). The first group consists of galectins with only one CRD able to homodimerize. It includes galectins -1, -2, -5, -7, -10, -11, -13, -14 and -15. The second group consists of only one member, galectin-3. It also has only one CRD but this CRD is associated with an N-terminal collagenous domain allowing the formation of pentamers. Finally, the third



group is characterized by two CRDs connected by a polypeptide sequence ("binding" or "linker" peptide). It includes galectins -4, -6, -8, -9 and -12 (69). Under certain conditions, having two CRDs could enhance the signaling properties of these galectins (70). Indeed, these two covalently linked CRDs allow, at lower concentrations than for the prototype galectins, the formation of large multimers. They can take part in important processes, for example, the formation of structured and extended molecular networks on the surface of the plasma membranes which are called "lattices".

## 1.2.2. Distribution in tissue and cellular localization

### **Distribution on a systemic level**

Galectins are present in a wide range of tissues. Their expression profile can evolve within the same tissue depending on its stage of development, its degree of differentiation or its homeostatic state (71–73). Galectins -1, -3, -8 and -9 are the most ubiquitous. In humans, they are present in the bone marrow, endocrine glands, lymphatic organs, the placenta, and some of them are also found in the adipose tissue, the central nervous system, the reproductive and respiratory systems (74). In contrast, galectin-13 exhibits a more limited expression profile and is essentially found in the placenta. It is also known as placental protein-13 (PP13) (75).

In the circulation, their concentrations vary according to the galectin type, the patient, and the study. It is difficult to estimate the average concentration for each of them as the technique used may have an impact on the measurement (up to a factor of 50) (76). However, it is possible for the same technique to notice that some galectins, such as galectin-1, are abundant in the circulation while others, such as galectin-9, are poorly detected (77).

As mentioned previously, the galectin expression is modulated during different stages of development, cell differentiation as well as under certain physiological, even pathological, conditions. Several factors are involved in these expression changes. Oxidative stress, for example, mimicked by menadione, induces an increase in the expression of galectins -1, -3, -8 and -10, as well as a decrease in the expression of gal-9 (78). High-caloric diets cause changes in the expression of galectins -1, -3, -9 and -12 in the circulation, in adipocytes, or in macrophages located in visceral and subcutaneous adipose tissue (79). Modulation of galectin

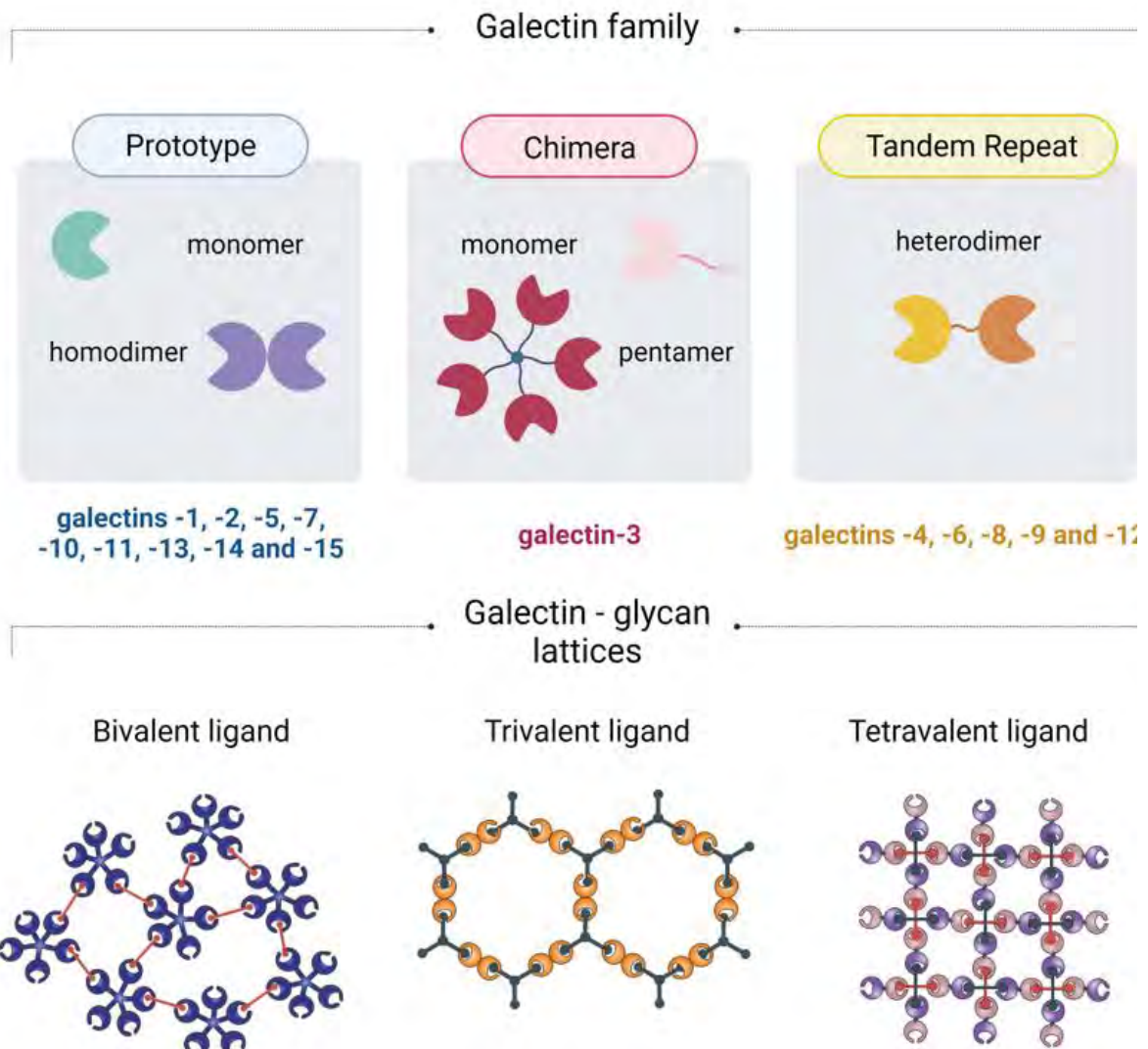


Fig. 8 **The major groups of galectins and the interactions of galectin-glycans.** Some examples of lattice structure resulted from interactions between galectins and multivalent glycans. From left to right: chimeric galectin combined with a bivalent glycan; prototypic galectin interacting with a trivalent glycan; galectin with tandem repeat binding to a tetravalent glycan. Lattices in reality can be a lot more complicated because they involve different types of glycans and probably different galectins.

expression is also involved in the regulation of inflammation. For example, gamma interferon is able to induce an increase in the expression of gal-9 (80). In the case of HTLV1 virus infections, a direct impact of the viral protein Tax has also been reported on the increased expression of gal-1 at the transcriptomic level (81).

Several studies on mouse models invalidating the expression of one of the galectins did not reveal a lethal phenotype associated with the absence of any of them. Rather, it seems that their absence is associated with a body difficulty to adapt to stressful situations. Thus, a decrease in the regeneration of muscle fibers is observed in gal-1 knockout mice (KO) (82). In gal-7 KO mice, a defective epithelial repair is observed, characterized in particular by a slowing of the healing process, as well as hyper-keratinization after exposure to UVB (83). Gal-3 KO mice, in contrast, exhibit intestinal protrusions which could be associated with a defective enterocyte differentiation. In fact, in the absence of gal-3, a defect in intracellular protein trafficking has been found (84).

### **Cellular localization of galectins**

At the cellular level, it is possible to distinguish three main types of galectin localizations: (1) intracellular with the presence of galectins in the cytoplasm or in the nucleus, (2) on the outer surface of the plasma membrane which generally results from an interaction with cell surface polysaccharides carried by glycoproteins or glycolipids (forming the glycocalyx), and (3) their possible presence in the extracellular medium (85).

The transport of galectins to the cell surface can be done through various types of pathways (60). Either they are associated with the polysaccharides formed in the post-Golgi vesicles and exposed to the surface of the cell when these vesicles are incorporated into the plasma membrane, or they are secreted into the extracellular environment by unconventional mechanisms that are still poorly understood and secondarily attach to cell surface polysaccharides (86). In this regard, galectins, in fact, lack a signal peptide necessary for the transport to the endoplasmic reticulum and secretion to the extracellular environment. Several studies have looked at these unconventional secretion pathways, describing the mechanisms for a handful of galectins (mainly gal-1 and -3) in particular contexts. It appears that direct

translocation could be a means of secretion. Gal-3 interacts with membrane lipids and spontaneously crosses the plasma membrane in living cell, as well as in protein-free membrane models (87). This phenomenon is also observed in models deficient in glycosylation functions, therefore it seems independent of interactions with carbohydrates (68,88). The other possible means of secretion are based on the release of vesicles carrying galectins (89). These may be microvesicles, the formation of which has been described for gal-1 after its accumulation under the plasma membrane. It can also be a release via exosomes or lysosomes into the extracellular medium (86). Little is known about how galectins enter the endosomal compartment. One possible route could be adsorption to damaged vesicles, a mechanism that will be explained shortly, in the next section, and which concerns the galectins (-1, -3, -8 and -9) (90). The latter could, after the vesicle repair, remain bound to them. However, this explanation is not satisfactory for the majority of cells which constitutively secrete galectins. Regarding the secretion via exosomes, my host team was the first to demonstrate such phenomenon for the transport of extracellular gal-9 (91,92). However, the mechanism of exosome formation has not been discovered until recently, in a study of galectin-3. This study reveals a direct interaction of the Tsg101 protein with a very conserved motif of gal-3 (P(S/T)AP). Tsg101 part of a protein complex involved in the formation of intraluminal vesicles in multivesicular bodies and interaction with this protein allows the recruitment of gal-3 into these intraluminal vesicles (93) .

### 1.2.3. A review of galectin functions

Due to their presence in the variety of cellular compartments, galectins perform an abundant and diverse range of functions. In general, the galectins inside cells will exert functions relating to cell growth, differentiation, survival, structure, polarization, and migration. The example of gal-3 gives an idea of the diversity of locations and functions that galectins can perform within cells. When present in the cytosol, gal-3 is able to interact with the KRAS GTPase, thereby modulate the intensity and duration of this signaling pathway (94,95). It also builds up around damaged vesicles and mediates the autophagic response (96,97). In addition, this galectin interacts with importin- $\alpha$  involved in the transit of biomolecules through nuclear pores (98). Once in the nucleus, gal-3 can be involved in the splicing of pre-messenger RNAs (99).

As mentioned previously, the contribution of galectins to the labeling, repair and recycling of damaged intracellular vesicles is a subject of study which has been particularly fruitful in the recent years. The initial impetus was done by the Philippe Sansonetti's team at the Pasteur Institute. This study focused on the penetration of bacteria of the Shigella type into macrophages or epithelial cells. They showed that phagosomes or vesicles carrying bacteria recruited cytosolic gal-3 by modifying the repertoire of the polysaccharides exposed on their external surface. It was then shown that the labeling of intracellular vesicles by galectins led to their change of destination towards autophagic compartments (100). As a result of this work, the same concepts were extended to all kinds of situations of cellular aggressiveness involving internal vesicles from the use of transfection agents for gene therapy to the toxic effects of protein aggregates in degenerative nervous diseases (101).

Each of the galectins interacting specifically with a subgroup of polysaccharides tends to create intermolecular bridges between glycoproteins and glycolipids on the cell surface. These phenomena are amplified by the tendency of galectins to form multimers and the bivalence of galectins in tandem, resulting in the redistribution of biomolecules at the surface of the plasma membrane. This explains why galectins are key players in "the lateral organization of the membrane". More specifically, they can induce an organization into networks of glycoproteins or glycolipids, which are often called "lattices". The formation of these lattices enclosing membrane receptors affects their ability to transmit signals inside the cell, either to amplify them or to mitigate them (102). These phenomena of modulation by galectins concern in particular the receptors for growth factors or cytokines, and the receptors for T cells or B cell antigen. In addition, galectins on the cell surface can lead to the coalescence of membrane microdomains rich in glycolipids (also called glycosphingolipids or GSL). Authors, and in particular the team of L. Johannes at the Curie Institute, have shown that this latter phenomenon could trigger major mechanical modifications involving the underlying cytoskeleton and result in a particular endocytosis called CLIC-type endocytosis (clathrin-independent carriers) (103). This phenomenon is characterized morphologically by the formation of deep membrane invaginations or endocytosis wells and biochemically by the participation of dynein. It could play a physiological role in the internalization of certain proteins of the plasma membrane. For example, according to the work of L. Johannes's team, gal-3 could play a major role in triggering CLIC-like endocytosis for  $\alpha 5/\beta 1$  integrin and for the

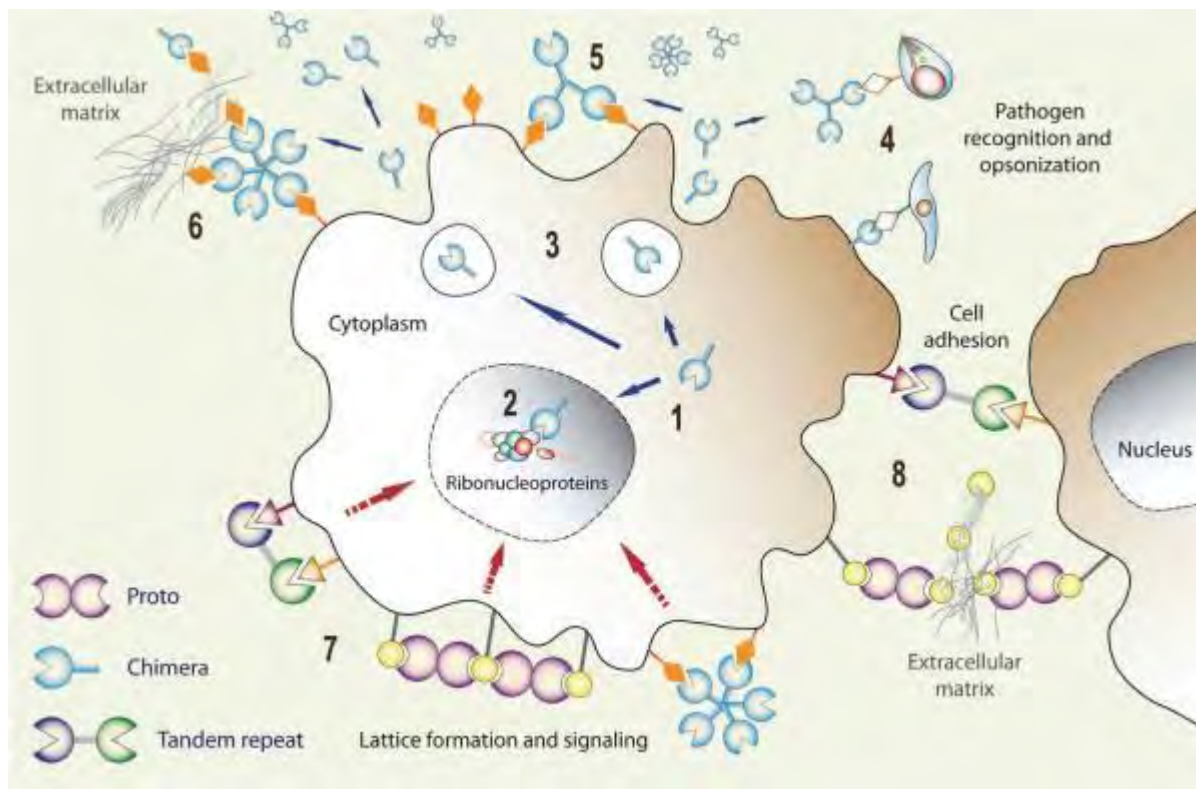


Fig. 9 **Expression, secretion, and functional diversification of galectins:** (1) Galectin transcripts are translated in the cytoplasm, and the proteins can be translocated into the nucleus (2) where they can associate with ribonucleoproteins *via* unconventional mechanism(s), galectins can be secreted to the extracellular space (3) where they can function as pattern recognition receptors for microbial glycans (4), bind to the host cell surface glycans (5), and cross-link them with ECM glycans (6) thereby, for example, promoting cell migration. Galectins can also cross-link cell surface glycans and induce clustering of microdomains and lattice formation at the cell surface (7) that can trigger signaling cascades, or cross-link neighboring cells (8) and promote cell-cell interactions/adhesion. *Figures and captions are adapted from (84).*

CD44 receptor. One of their hypotheses suggests that the observations on gal-3 are not at all accidental but correspond to a physiological process of endocytosis quite distinct from those used by the clathrin-coated vesicles or caveolae. They believe that other galectins are involved in similar processes. These ideas are summed up in the hypothesis term "glycolipid and lectin" (GL-lect) (103,104).

In addition to the functions performed inside or at the cell surface, galectins have many functions in the extracellular environment. Once secreted, the galectins will be able to interact with new partners and intervene in the regulation of other processes (105). They are notably involved in the assembly, organization and regulation of membrane receptors including receptors involved in the control of apoptosis. They also play a role in cell adhesion in the extracellular matrix. They can act locally but also at a distance, after passing through the bloodstream and in particular the regulation of the immune system, making them comparable to cytokines.

## Chapter 2: General aspects of T cell biology

---

### 2.1. An overview of T cell subsets in the immune system

#### 2.1.1. Diversity of T cell subsets

T cells are a major component that crafts specific responses of the adaptive immunity, while enabling an immune memory that can respond more vigorously to repeated exposures to the same pathogen. The life of a T cell begins when a T lymphocyte reaches maturation in the thymus and enters the circulation or populates the peripheral lymphoid organ: it is ready to encounter its first antigen. Until then, mature T lymphocytes are still naïve cells, they are incapable of elicit any kind of response against an infectious challenge. Upon interaction with an antigen, T cells are activated and undergo extensive changes in their phenotype - a process where T cells differentiate into various subsets of effector cells, each of them having a distinguishable functional capacity. As an immune reaction evolves, T cells may go through apoptosis or survive in a functionally quiescent or slowly cycling state for many years after the elimination of the antigen. Those surviving cells eventually become memory T lymphocytes; some of them, called central memory T cells, migrate to lymph nodes, ready to be reactivated and to respond rapidly if the antigen is reintroduced. Others, known as effector memory cells, reside in mucosal tissues or circulate in the blood; like central memory cells, they can mount rapid effector responses to eliminate the antigen once recruited to the site of infection.

In between the naïve and memory phase, T cells evolve through an activation and differentiation process that gives rise to a variety of effector subsets. In classic literature, activated T cells were classified into three categories: (1) the cytotoxic T lymphocytes (CTL) characterized by the CD8 expression and the direct killing of their target, (2) helper T lymphocytes, defined by the CD4 expression, which provide the immune system with chemical guidance to respond against danger, (3) a small group of T cells that do not express the usual  $\alpha$  and  $\beta$  chains of the T cell receptor (TCR). Instead, this minor lineage has its TCR formed by  $\gamma$  and  $\delta$  chains, hence the name  $\gamma\delta$  T cells. With time, new T cell subsets were identified with



distinct features and functions. Helper T cells, for instance, can be classified into as many as six functional phenotypes, including the classic helper 1 (Th1) and helper 2 (Th2). Likewise, CD8<sup>+</sup> T cells were found to have different patterns of cytokine expression, and some might even lack cytotoxicity.

### 2.1.2. Identity of T cells: an interplay of cytokines, receptors and transcription factors

The first classification method for T cells was based on their cytokine profile, as in the "Th1 – Th2" theory suggested by Coffman and Mossman (106,107). It was widely accepted until the recent decades during which our understanding of the phenotype differentiation grew rapidly. T-effector differentiation models suggest a three-step process. TCR signals first lead to activation and induce the expression of cytokine receptors (108). Signals from specific cytokine receptors then promote the expression of "master" transcription factors that are specific to each lineage. These transcription factors enable the expression of genes associated with a particular phenotype while inhibiting the differentiation into other T cell subsets. They also induce epigenetic changes that control gene accessibility and maintain the acquired phenotype in a cell-intrinsic manner (109). In the next sections, we will discuss in more details the signature molecules of each subset associated to their functions and that allow us to classify T cells.

#### Helper T cells

As mentioned previously, helper T cells can be ordered into at least six subsets, which belong to four general categories: (1) pro-inflammatory effectors, (2) regulatory of anti-inflammatory effectors, (3) effectors that promote B cell follicle development, (4) effectors that provide long-term memory.

- **Helper 1 and helper 2 T cells**

Th1 and Th2 are the best-documented subsets of the CD4<sup>+</sup> T cell lineage. Th1 differentiation is induced in infections by intracellular bacteria, fungi, and viruses. These infections lead to the release of IL-12, IL-18, interferon (IFN)- $\gamma$ , and type I interferons by innate immune cells such as dendritic cells (DC) and natural killer (NK) cells. In the activation process, signal of IFN- $\gamma$  activates signal transducer and activator of transcription 1 (STAT1), which initiates the

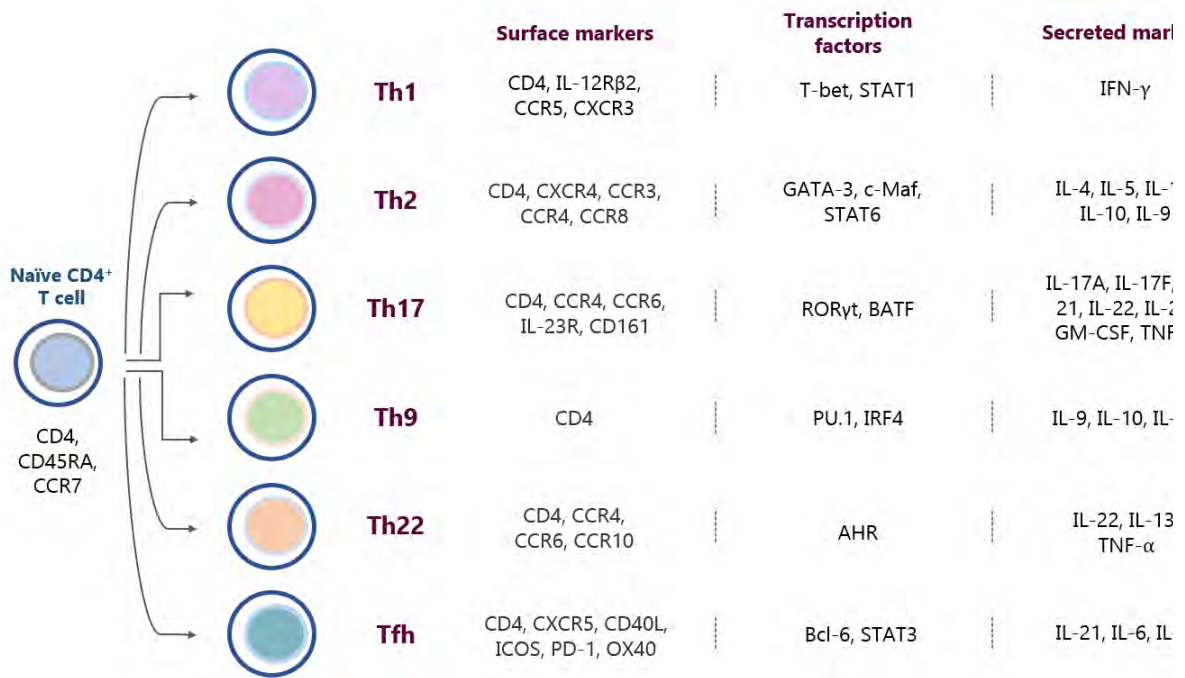


Fig 10. Key features of helper T cell subsets.

expression of the transcription factor T-bet. T-bet then drives the differentiation process towards Th1 phenotype, by promoting the production of IFN-  $\gamma$ , the signature molecule of Th1 cells, beside the granulocyte macrophage-colony-stimulating factor (GM-CSF), IL-2 and lymphotoxin (LT, tumor necrosis factor (TNF)-  $\alpha$ ). In turn, macrophages, NK, B and CD8<sup>+</sup> T cell are activated to attack the pathogen-infected cells. (109)

While T-bet is the "master" transcription factor of Th1, c-Maf and GATA-3 are the switch for Th2 differentiation process. In the absence of IFN-  $\gamma$ , IL-4 released by basophils, eosinophils, mast cells, or NK-T cells interact with IL-4 receptors – IL-4R – upon TCR activation and promote the production of c-Maf and GATA-3 through IL-4R/STAT6 signaling. C-Maf establishes Th2 phenotype by inhibiting IFN-  $\gamma$  production while pushing IL-4 release. Likewise, GATA-3 promotes the production of IL-5 and IL-13, which constitute the cytokine signature of Th2 cells with IL-4 (110). These cytokines activate the class switching process of B cell towards IgG2, IgE and IgA. High levels of IgE combined with IL-4 and IL-5 can recruit and activate eosinophils and mast cells to release inflammatory factors such as histamine, platelet-activating factor, prostaglandins and leukotrienes. Th2 responses are therefore usually associated with the protection against helminths, allergies, or other hyperresponsive airway conditions (109). Other cytokines that are also associated with Th2 responses are IL-10 and IL-9 (111,112).

- **Helper 17 T cells (Th17)**

In the early 2000s, many studies uncovered a new subset independent of Th1- or Th2-related transcription factors (113). The subset was later recognized as a distinct lineage characterized by the production of IL-17A and IL-17F (IL-17A/F), and subsequently named Th17, as opposed to Th1 and Th2, named following their order of identification. Th17 differentiation takes place in the absence of type I interferons, IFN-  $\gamma$  and IL-4; the signaling pathway that actively induces Th17 phenotype is yet to be elucidated. Nevertheless, IL-1 $\beta$ , IL-6, IL-23 and TGF- $\beta$  were reported to promote the polarization of T cells towards Th17, leading to the production of ROR $\gamma$ t as the main driver of Th17 phenotype (114,115). Beside IL-17A/F, Th17 cells also produce other cytokines such as IL-22, IL-26, GM-CSF, TNF- $\alpha$  - which allow them to strongly elicit inflammation - and IL-21, which promote plasma cell differentiation.

- **Helper 9 T cells (Th9)**

Although many T cells are known to secrete IL-9, in particular Th2, a specialized subset dedicated to producing IL-9 was officially recognized in 2008 (116). The mechanism of Th9 differentiation is not clear, but one study found TGF- $\beta$ -Smad2/4 as a signaling pathway that regulates IL-9 expression while another study revealed that initial CD4<sup>+</sup> T cells could be induced into Th9 cells under the TGF- $\beta$  and IL-4 conditions (117,118). As a transcription factor, PU.1 was identified as specific to Th9 (119,120); GATA-3 is also involved, but in an indirect manner by downregulating the level of FoxP3, the "master" regulator of regulatory T cells (121). In addition to IL-9, Th9 cells produce IL-21; this duo expression allows Th9 to participate in diverse immune responses. For instance, Th9 can take part in the protection from helminth and asthma by enabling enrichment of eosinophils and mast cells through IL-9 production, whereas their secretion of IL-21 promotes the differentiation of Th17 or activates NK cells to inhibit tumor growth (122,123).

- **Helper 22 T cells (Th22)**

Similar to Th9, Th22 was recognized as a distinct phenotype of T cells with expression of IL-22, a cytokine previously found to be associated with Th17. First described by Trifari *et al.* in 2009, Th22 cells are characterized by co-expression of the chemokine receptor CCR6 and the skin-homing receptors CCR4 and CCR10, beside the production of IL-22 and TNF- $\alpha$ , with aryl hydrocarbon receptor (AHR) as the key transcription factor (124). The functions of Th22 cells are difficult to be generalized; they are neither anti-inflammatory nor pro-inflammatory. However, Th22 cells have been described to enable epithelial innate immune responses (125), or synergize with IL-17 to induce pro-inflammatory cytokines in human bronchial epithelial cells (126).

- **Follicular helper T cells (Tfh)**

Follicular helper T cells were initially recognized as a distinct T cell subset that resides in secondary lymphoid tissues, with a key role of regulating the T-cell-dependent B cells response. Tfh cells are characterized by the expression of CXCR5 (CXC-chemokine receptor 5), which is also the receptor for chemokine homing to B-cell zone in the lymph nodes (127). In addition to CXCR5, Tfh cells also express ICOS (inducible T cell costimulatory), PD-1 (programmed death-1), CD200, BTLA (B- and T-lymphocyte attenuator), OX-40, and SAP (serum amyloid P). Upon activation and induction in the presence of IL-6, IL-12 and IL-21, Tfh

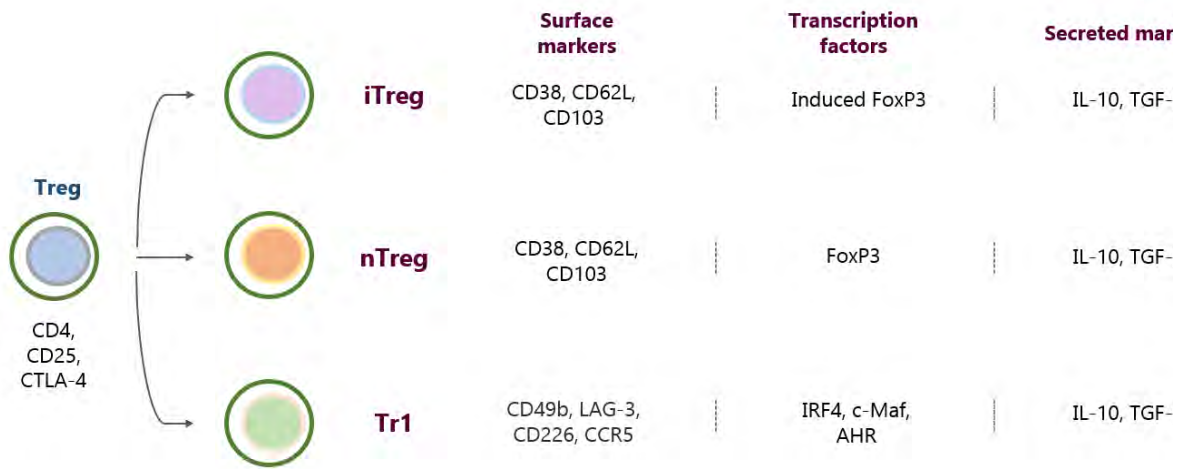


Fig. 11 Key features of regulatory T cell subsets

upregulate CXCR5, leading to the migration of ICOS and OX-40 to the interface between T cell and B cell areas in the lymph nodes. Here, Tfh interact with B cells through antigen presentation; B cells provide signals through ICOS-L and IL-6 while Tfh cells provide CD40L and IL-21, resulting in Ig class switching, affinity maturation and differentiation of B cells into plasma cells and memory B cells (128). The differentiation of Tfh cells is dependent on the transcription factor BCL6 (B cell lymphoma protein 6) (129); interestingly, BCL6 were found to be co-expressed with T-bet, GATA-3 or ROR $\gamma$ t in some studies, implying an incomplete separation between Tfh and other effector T cell subsets (109).

Recently, there is also reports on a subset of follicular T cells with suppressive function on immune responses, known as **follicular T regulatory cells (Tfr)**. Because of their FoxP3 expression, they were initially considered as a subset of specialized regulatory T cells that reside in the germinal center (GC) before recognized as a distinct subset. Tfr are characterized by the expression of FoxP3 along with Tfh typical markers – BCL6, CXCR5, ICOS and PD-1, with a production of IL-10 (130). Tfr are thought to restrict GC reaction by suppressing a number of Tfh and GC B cells (131,132). However, a few studies demonstrate that IL-10 from Tfr cells can increase either IgE specificity or promote B cell differentiation in the GC, in food allergy immune responses or acute infections with lymphocytic choriomeningitis virus (LCMV) respectively (133,134). A subset of circulating Tfr can also arise from thymus-derived Tregs or naïve FoxP3<sup>-</sup> cells in a PD-L1-dependent manner. The CXCR5<sup>-</sup>FoxP3<sup>+</sup> Tregs are activated upon interaction with dendritic cells; they subsequently enter the peripheral circulation to migrate into the B cell follicles of the secondary lymphoid tissues (130).

### **Regulatory T cells (Treg)**

Regulatory T cells are defined by their capacity to "soothe" inflammation by suppressing activities of pro-inflammatory cells. Although we usually refer to Treg as T cell with expression of CD25, IL-10 TGF- $\beta$ , and the transcription factor FoxP3, this latter is actually **natural Treg**, or **nTreg**, and is only one subset among several subpopulations of regulatory T cells. nTreg originates from thymus (135), and suppresses immune reactions either through contact-dependent mechanism where membrane-bound TGF- $\beta$  blocks T cell proliferation, or contact-independent mechanism which involves soluble TGF- $\beta$  and IL-10 (136). **Induced Tregs**, or **iTregs**, are induced to express FoxP3 in the periphery (137). They share other similar

Subset	Effector cytokines	Transcription factors	Surface markers	Cytotoxicity
Tc1	IFN- $\gamma$ , TNF- $\alpha$	T-bet, EOMES, STAT4	IL18R	✓
Tc2	IL-4, IL-5, IL-13	GATA-3, STAT6	CRTH2	✓
Tc9	IL-9	IRF4, STAT6	-	✗
Tc17	IL-17A, IL-17F, IL-21, IL-22	ROR $\gamma$ t, IRF4, STAT3	IL23R, CD38, CD86, CD101, CD161, CCR6, 4- 1BB <sup>low</sup>	✗
Tc22	IL-22, TNF- $\alpha$ , IL-2	AHR	-	✓

Table 5. **A summary of cytotoxic T cell subsets.** *Adapated from (138).*

characteristics with nTreg, in that they express CD25, CD38, CD62L, and CD103. Another major subpopulation of regulatory T cells is the **Tr1**, which lacks the expression of FoxP3 and does not necessarily express CD25, but produces IL-10 in response to stimulation (109,139). These cells are induced in the respiratory tract when they encounter an antigen in the presence of IL-10 and TGF- $\beta$  (109).

### Cytotoxic T cells

Cytotoxic T cells are typically considered as a uniform population of CD8<sup>+</sup> T cells that have cytotoxicity by producing an abundant amount of IFN- $\gamma$  and the protease granzyme B. The CD8<sup>+</sup> T cell population is, in fact, similar to their CD4<sup>+</sup> counterpart, in that it is composed of many distinct subsets. Some of them can be regarded as the equivalent to their CD4<sup>+</sup> counterparts in terms of function (140,141).

- **Tc1**

The typical cytotoxic T cells, known for their exceptional cytotoxic activities towards cells harboring intracellular pathogens, are called **Tc1**, according to the new classification of CD8<sup>+</sup> T cells. They are characterized by high levels of perforin, granzyme B, IFN- $\gamma$ , and tumor necrosis factor (TNF- $\alpha$ ), with an elevated expression of IL-18R on their surface (138,142). The differentiation of Tc1 cells involves several key transcription factors, namely STAT4, T-bet, and EOMES (eomesodermin). As STAT4 is the direct downstream signal transducer of IL-12 receptor, Tc1 phenotype can be induced under the signal of IL-12 (143), produced by antigen-presenting cells (APCs), such as macrophages and dendritic cells.

- **Unconventional CD8<sup>+</sup> T cells with cytotoxicity: Tc2 and Tc22**

Unconventional CD8<sup>+</sup> T cell subsets include cells with cytokine patterns that are similar to some helper T cell subsets. The differentiation of these newcomers does not pass through the same pathway as Tc1, they rather do not express EOMES or any of Tc1's master transcription factor; yet some of them still possess a certain level of cytotoxicity by the production of granzyme B and/or low level of IFN- $\gamma$ . **Tc2** and **Tc22**, for example, express high level of granzyme B and present robust cytotoxic activities, although only Tc2 cells were found to have an expression of IFN- $\gamma$ , at a diminished level. Similar to their CD4<sup>+</sup> counterparts, **Tc2** cells produce type II cytokines such as IL-4, IL-5, IL-13, mediated by the transcription factors GATA-3 and STAT6 (144,145). **Tc22** was also recognized as a distinct lineage specialized in the production of IL-



22, although this classification was controversial, mostly because Th17 and Tc17 cells also release IL-22 (146). The differentiation of Tc22 is also driven by TNF- $\alpha$  and the transcription factor AHR, as in Th22 cells; however, IL-6 was also found to take part in this process (147).

- CD8<sup>+</sup> T cells with reduced cytotoxicity: Tc17 and Tc9

**Tc17** cells, on the contrary, have a reduced cytotoxic activity demonstrated by a low expression of both granzyme B and IFN- $\gamma$  (148,149). The commitment of Tc17 involves IL-6 and TGF- $\beta$  as the main drivers, leading to the activation of STAT3 and ROR $\gamma$ t, which are also essential to the Th17 lineage (149). The last CD8<sup>+</sup> subset that lacks cytotoxicity is the **Tc9** cells, which is the corresponding phenotype of Th9. Recently identified, the function of these cells is still unclear, so is their poor production of granzyme B. However, studies have found STAT6 and IRF4 (interferon regulatory factor 4) to actively mediate Tc9 polarization under the combined actions of IL-4 and TGF- $\beta$  (150).

### 2.1.3. Plasticity of T cell phenotype

The differentiation of T cells may appear as roads diverging from a roundabout: the cells evolve in one direction until they reach the differentiation pathway that defines their effector function. But in the immune reaction "real life", the T cell response often shifts from predominant effector functions at the initial stage to predominant suppressive functions at later stages thus limiting the risk of collateral tissue damage. The immune system uses different strategies to maintain the balance between effector and regulatory T cells: it is either local induction of diverse T cell subtypes with distinct functional profiles or, inside a given T cell lineage, the switch from one to another differentiation program. This type of switch is achievable owing to the remarkable plasticity of T cell differentiation. More recently, this plasticity, which provides the immune system with the flexibility to respond to diverse conditions of infection, has been increasingly appreciated.

#### **Plasticity of CD4<sup>+</sup> T cells**

As discussed earlier, the interaction with a cognate antigen presented by APCs initiates the differentiation of CD4<sup>+</sup> T cells into a variety of effector subsets. The process is governed by the combination of cytokines present in the microenvironment and the strength of the interaction between the TCR and the APC (151). For a long time, these factors were thought to induce the

commitment of CD4<sup>+</sup> T cells to distinct effector lineages supported by stable programs of gene expression and specific cytokine sets. The commitment of T cells to a unique phenotype has been recently re-evaluated at the wake of closer inspections revealing the T cell plasticity through conversions among Th17, Treg, Tfh and even classical Th1-Th2 subsets.

- **Th1 and Th2 cells**

It is well documented that the commitment to either Th1 or Th2 phenotype is an irreversible program, in the sense that Th1 cells cannot be re-differentiated into Th2, and vice versa. Upon the recognition of a cognate antigen, signals of IL-12 and IFN- $\gamma$  from the surrounding environment guide naïve T cells into Th1 differentiation; T-bet is activated and becomes the master regulator initiating the production of IFN- $\gamma$ . Conversely, in the presence of IL-4, T cells differentiate towards Th2 phenotype under the regulation of GATA-3, resulting in the production of IL-4, IL-5, IL-13 and IL-10. The acquisition of either Th1 or Th2 effector function gets off to a good start, so that each feature of one phenotype represses the differentiation into the other while reinforcing the original fate of T cells. Not to mention T-bet and GATA-3, both IFN- $\gamma$  and IL-4 were shown to inhibit the expression of the alternative lineage while inducing stably imprinted epigenetic modifications to ensure the preservation of the cytokine profile is preserved during cellular divisions independently of the polarizing cues (152–155).

Nevertheless, Th1 cells can unconventionally acquire properties of the Th2 lineage in secondary of chronic immune responses. Notably, human memory Th1 cells have been reported with Th2 features such as being responsive to IL-4 stimulation and subsequently capable of IL-4 production without losing IFN- $\gamma$  expression upon TCR activation *in vitro* (156). Some human T cells co-express of lineage-defining factors T-bet and GATA-3 (157); an unexpected expression of IL-10 was also reported in Th1 in the peripheral blood. Although IL-12 could induce IL-10 expression in Th1 clones, T cells with IFN- $\gamma$ /IL-10 co-expression are present at low frequencies and are thought to respond selectively to chronic infections (158,159). Therefore, it is possible that Th1 cells can switch from a pro-inflammatory to a regulatory phenotype to prevent overshooting immune responses. It is still unclear if their phenotype or their IFN- $\gamma$  expression are stable throughout their proliferation upon chronic stimulation.

Unlike the well-documented acquisition of Th2 features in Th1 clones, human blood Th2 cells appear to be less flexible (156). A study in mice showed Th2 could produce IFN- $\gamma$ , in addition to IL-4, upon stimulation by IFN and IL-12 (160).

- **Instability of Th17 lineage**

Th17 cells were initially discovered as a CD4<sup>+</sup> T cell lineage with a differentiation program independent of T-bet and GATA-3 and characterized by the production of IL-17A and IL-17F. Effector functions of Th17 are driven by the transcription factor ROR $\gamma$ t as the master regulator; while the production of IL-17 is reinforced by ROR $\gamma$ t, it is repressed by both signature cytokines of Th1 and Th2 cells – IFN- $\gamma$  and IL-4 (113). Moreover, another cytokine, IL-27, which promotes Th1 differentiation by inducing T-bet and IL-12R $\beta$ 2, IL-27, also suppresses Th17 development (161). These findings support the notion that signals from Th1 and Th2 cells inhibit Th17 differentiation, and thereby confirming Th17 as a lineage distinct from Th1 and Th2 subsets.

However, under different environmental cues, Th17 cells can lose IL-17 expression or acquire features of other T cell phenotypes. For instance, in homeostatic or inflammatory conditions, Th17 cells are detected to have IFN- $\gamma$  production, implying a possible relationship with Th1 phenotype. Interestingly, cells polarized in Th17 phenotype may be converted to either Th1 or Th2 phenotype in the presence of IL-12 or IL-4 respectively, accompanied with a loss of IL-17A and IL-17F expressions if they are not exposed constantly to IL-6 and TGF- $\beta$  (162). In addition, the phenotype of Th17 itself could be either pathogenic or protective, depending on whether Th17 cells are able to limit host tissue damage by producing IL-10. In this notion, Th17 cells differentiating from IL-6 and TGF- $\beta$  can express IL-10 while addition of IL-23 suppresses this feature, giving rise to Th17 cells with only pro-inflammatory cytokines (163). Some Th17 cells are also identified as expressing FoxP3, the transcription factor of regulatory T cells. The role of TGF- $\beta$  in Th17 differentiation has been a subject of debate, because TGF- $\beta$  has been well-documented as an immunosuppressive cytokine; yet in the case ROR $\gamma$ t<sup>+</sup>FoxP3<sup>+</sup> T cells, the implication of TGF- $\beta$  is somewhat consistent. In fact, T cells with dual expression have been identified in both mouse and human (164). These cells are present in the early development stage of Th17 and in naïve T cells after exposure to TGF- $\beta$ . They are believed to represent an intermediate stage during commitment to an effector lineage Treg or Th17. A pro-inflammatory environment with IL-6, IL-21, IL-23 and low levels of TGF- $\beta$  supports a Th17

commitment by upregulating ROR $\gamma$ t while inhibiting FoxP3 expression and functions. Conversely, high concentrations of TGF- $\beta$  in the absence of pro-inflammatory cytokines support a Treg commitment through activation of FoxP3 (114). Furthermore, conversions between Th17 and Treg phenotype have been observed in similar environment profiles. Th17 cells can be converted from Treg cells after exposure to a proinflammatory cytokine environment. Similarly, polarization in high concentrations of TGF- $\beta$  with the presence of IL-6 gives rise to a FoxP3<sup>+</sup>IL17<sup>+</sup> T cell population; the circulating human FoxP3<sup>+</sup>IL-17<sup>+</sup> T cells are found with *in vitro* suppressive activity, but it is yet to be clear whether they are also capable of conventional Th17 functions (164,165). The reciprocal conversion of Treg from IL-17-expressing cells have not been reported, it is very likely that Treg phenotype is earlier than Th17 in the differentiation order.

- Flexibility of the Treg phenotype

Apart from conversion to Th17, redifferentiation of Tregs into other effector helper T cells have been reported. Notably, under stimulation by IL-12, FoxP3<sup>+</sup> Tregs could acquire expression of T-bet and IFN- $\gamma$ . They eventually become regulatory Th1 and are thought to be specialized to restrain Th1 responses (166). Moreover, while FoxP3<sup>+</sup>IL-17<sup>+</sup> T cells are reported with suppressive functions, IFN- $\gamma$ -producing Tregs have a reduced suppressive capacity (167). Interestingly, even though they function to inhibit cytotoxic T cells, Tregs in tumor-draining lymph nodes in mice and *in vitro* human blood can acquire cytotoxic features. In a malignant context, cytotoxic Tregs attack DC, NK and CD8<sup>+</sup> T cells with perforin and granzyme B, thereby suppress the tumor clearance property of these anti-tumoral cells (168–170).

Tregs can also be redifferentiated to a follicular helper T cell phenotype. In Peyer's patches, FoxP3<sup>+</sup> Treg cells can turn into Tfh cells through a loss of FoxP3 expression. They subsequently participate in GC formation and interact with B cells through CD40 (171). Remarkably, a study by Zheng *et al.* pointed out an enhanced formation of GC following an inactivation of IRF4 specifically in FoxP3<sup>+</sup> T cells (172). Although the inactivation of IRF4 resulted in fact of an increased production of Th2 cytokine, it is possible that a Tfh cell increase was missed because they were not in the scope of this work. Collectively, these observations suggest a potential involvement of IRF4 in restraining the reprogramming of Treg cells into Tfh phenotype.

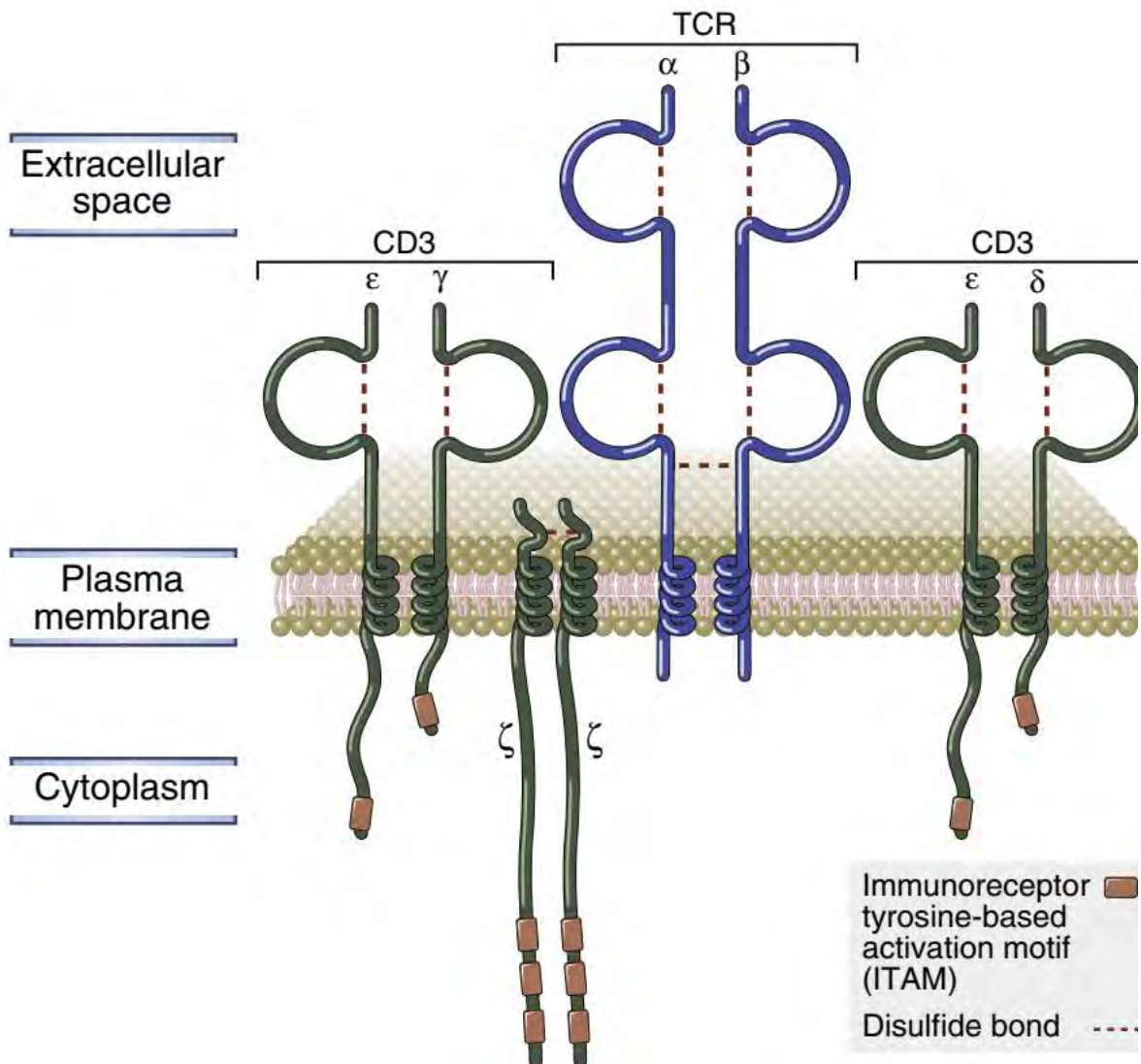


Fig. 12 **Structures of the T cell receptor complex.** T cell receptor is composed of two transmembrane polypeptide chains,  $\alpha$  and  $\beta$ , which are linked to each other through a disulfide bridge. Each of these chains has one N-terminal variable (V) domain, one constant (C) domain followed by a hydrophobic transmembrane region and a short cytoplasmic region. Because their cytoplasmic region is too short to have any intrinsic enzymatic activity, the TCR chains are closely associated with the CD3 proteins and  $\zeta$ -chains. In mammals, the complex contains 4 chains of CD3:  $\gamma$  and  $\epsilon$ ,  $\delta$  and another  $\epsilon$  form heterodimers, while two  $\zeta$ -chains make a homodimer. They contain many immunoreceptor tyrosine-based activation motifs, or ITAMs, in their cytoplasmic tails. *Adapted from (173).*

## 2.2. How T cells acquire effector phenotype

### 2.2.1. TCR activation ignites series of T cell physiological changes

The activation of T cell launches the differentiation phase that decides T cell's effector function. Precursors of T lymphocytes arise from stem cells in the bone marrow, they go through complex maturation stages in the thymus where they eventually become naïve T cells with functional antigen receptors. They subsequently enter the circulation to reach secondary lymphoid organs - that is, the spleen, the lymph nodes, the mucosal and cutaneous lymphoid tissues – ready to be activated. However, pathogens and infected cells do not penetrate the lymphoid organs; to be activated, T cells need an intermediary: the antigen-presenting cells (APCs). Any protein antigens that manage to cross the epithelial barriers are captured by antigen-presenting cells (dendritic cells or macrophages), even those that circulate in the blood might also get captured by dendritic cells in the blood or the spleen. With a capacity to migrate to T cell zones in the secondary lymphoid organs, these APCs stimulate T cells through two signals: the first is from the antigen's peptide that matches with the TCR while the second is via the costimulatory receptors of T cells, leading to cytokine secretion and expression of cytokine receptors. Then, the naïve T cell has become a functional effector T cell.

The recognition of antigen by the TCR complex is a complicated process, in the sense that it recruits various elements to initiate a series of signaling reactions that result in the transcription of specific genes and the acquisition of a specific effector function. Before we look into any of the biochemical mechanisms, we should understand the TCR complex structure (*Fig. 12*). T cell receptor is composed of two transmembrane polypeptide chains,  $\alpha$  and  $\beta$ , which are linked to each other through a disulfide bridge. Each of these chains has one N-terminal variable (V) domain, one constant (C) domain followed by a hydrophobic transmembrane region and a short cytoplasmic region (173). Because their cytoplasmic region is too short to have any intrinsic enzymatic activity, the TCR chains are closely associated with the CD3 proteins and  $\zeta$ -chains. In mammals, the complex contains 4 chains of CD3:  $\gamma$  and  $\epsilon$ ,  $\delta$  and another  $\epsilon$  form heterodimers, while two  $\zeta$ -chains make a homodimer. They contain many immunoreceptor tyrosine-based activation motifs, or ITAMs, in their cytoplasmic tails. The

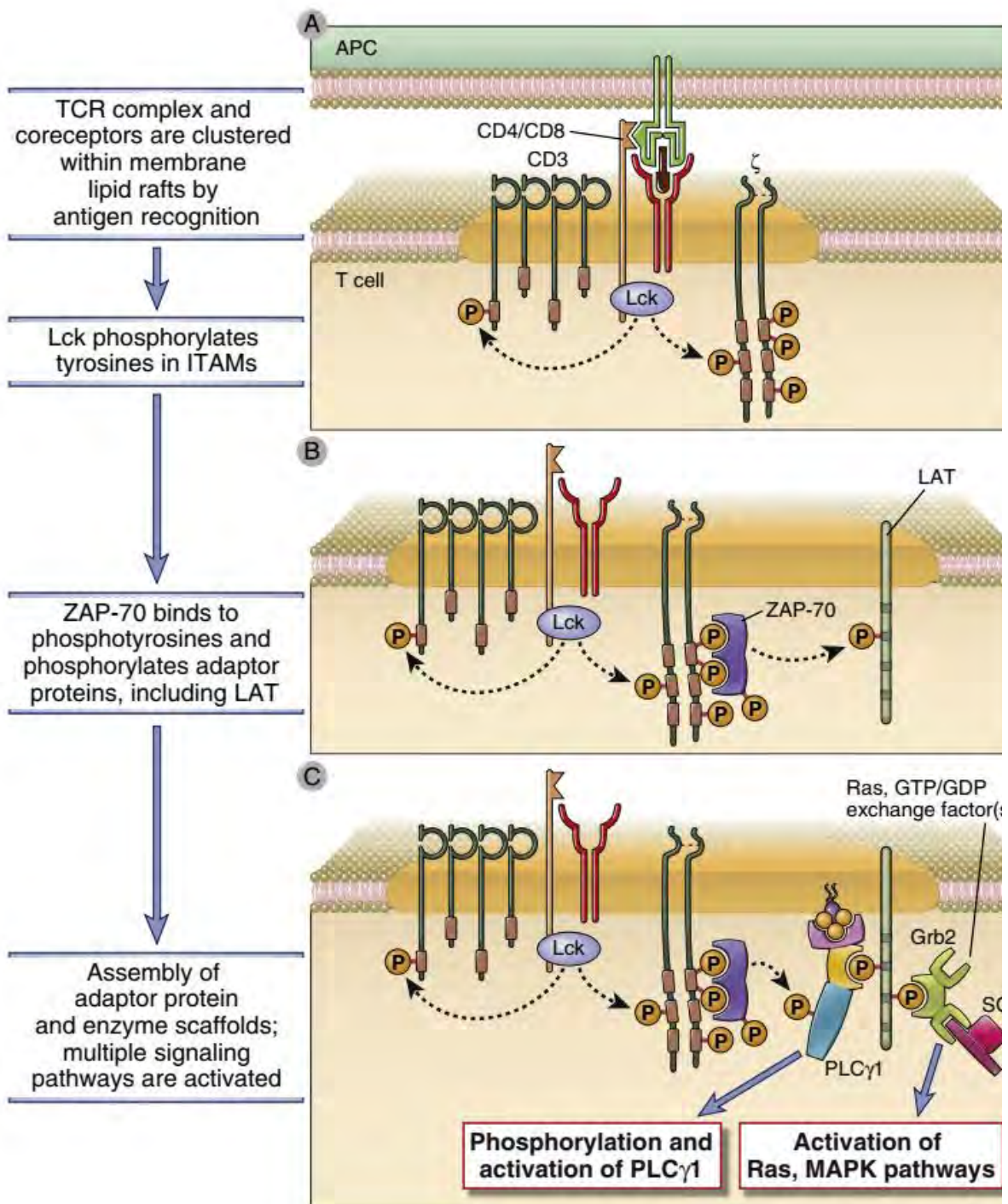


Fig. 13 Signaling cascade upon the activation of TCR. Adapted from (174).

ITAMs are docking sites for tyrosine kinase, an important messenger in signaling pathways (173,174).

Before any signaling reaction could take place, TCR needs to be activated through the recognition of an antigen. This task is performed by the V regions of the TCR  $\alpha$  and  $\beta$  chains, which recognize peptide fragment of protein antigen bound to the major histocompatibility complex, usually designated as MHC. Not just any MHC can work; first it must be the right class of MHC: CD4 molecules are restricted to class II MHC and CD8 molecules can only bind to class I MHC (175). In addition to CD3 and the  $\zeta$ -chains, TCR is also accompanied by either CD4 or CD8 molecules (each of which characterizes one of the two main lineages of T cells); these co-receptors strengthen the binding of T cells to APCs and facilitate signaling by the TCR complex for T cell activation. Each of these co-receptors bind selectively to the non-polymorphic domain of MHC as described previously, thus creating an MHC class restriction in the antigen recognition of TCR. Conversely, the polymorphic domain of MHC is the region where the antigen peptide is bound to and where the TCR comes into contact with the MHC-peptide complex; the TCR is therefore specific to the combination of antigenic peptide and polymorphic domain of MHC (173).

When a TCR finds its match, signals from multiple receptors are immediately integrated to initiate the TCR signaling cascade (*Fig. 13*). Earliest event is the conformational change of the TCR-CD3 complex under the prerequisite of TCR-CD3 clustering (176). The conformational change exposes a proline-rich sequence in CD3 $\epsilon$  that recruits the ubiquitously expressed adaptor protein Nck (177) and also activates TCR-CD3-associated Src kinases Lck and Fyn (178). The activated Lck and Fyn subsequently phosphorylate the ITAMs in the cytoplasmic tail of CD3's  $\zeta$ -chains; within seconds, these ITAMs recruit the tyrosine kinase ZAP-70 ( $\zeta$ -associated protein of 70 kD). As a result, ZAP-70 is functional and begins phosphorylating numerous cytoplasmic signaling molecules, initiating the signaling cascades (174,178). A key target of ZAP-70 phosphorylation is the membrane-anchored adaptor protein LAT (linker for the activation of T cells). Phosphorylated LAT brings a variety of downstream components of the TCR signaling pathways close to their upstream activators. Important targets of LAT include PLC $\gamma$ 1 (phospholipase C $\gamma$ 1) which activates subsequently the calcium- and PKC-mediated signaling pathways, and Ras, which is engaged in the MAP (mitogen-activated protein) kinase



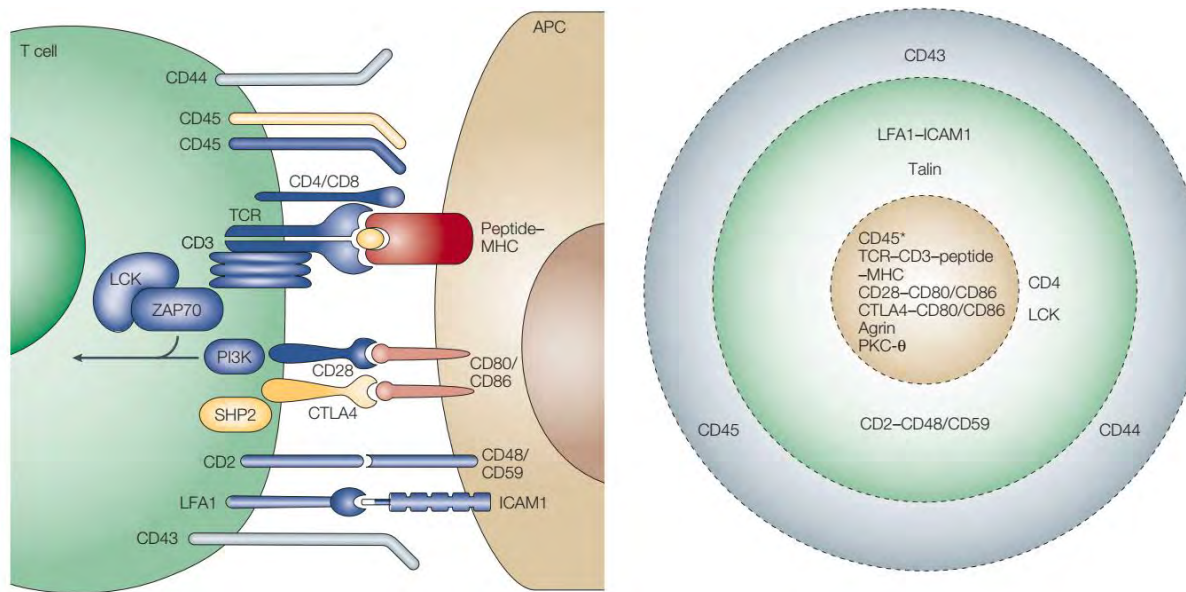


Fig. 14 **Immune synapse formed during the interaction between T cell and an antigen-presenting cell (APC).** **c-SMAC** (for central supramolecular activation cluster) is the center of the interaction interface, where TCR complex and co-stimulatory receptors are concentrated, allowing the activation signaling cascade to be launched. The binding of the T cell to the APC is enforced by the peripheral ring that surrounds the c-SMAC – the **p-SMAC** – where are gathered adhesion molecules such as LFA1 (lymphocyte function-associated antigen 1), ICAM-1 (intercellular adhesion molecule-1), and the cytoskeletal linker talin. The region distal to the synapse outside the p-SMAC, known as **d-SMAC**, is made of a radial lamellipodium enriched in F-actin; it is also where bulky molecules such as CD43 and CD45 are localized. *Adapted from (179)*

signaling pathways. Meanwhile, the adaptor protein Nck recruits F-actin to TCR through its interactions with WASp (Wiskott-Aldrich syndrome protein) and SLP-76 (Src homology 2 domain-containing leukocyte protein of 76 kD) (180). These activities contribute to the rearrangement of the actin cytoskeleton that leads to the transport of receptors, costimulators and intracellular signaling molecules to the contact site between T cell and APC (177,181,182). The cellular interface formed from this mobilization is called the immunological synapse (IS). As it plays a significant part in the activation state of the responding T cell and therefore influence its effector functions, we will discuss in more detail about this specialized structure.

### 2.2.2. Formation of the immunological synapse

#### Process and characteristics of the IS formation

When a TCR recognizes an MHC-peptide complex (MHCp), T cell forms an adhesion zone with the antigen-presenting surface where areas of close contact help the TCR complex sustain the interaction with MHCp; this is the beginning of an immunological synapse, or a supramolecular activation cluster (SMAC). If the TCR engagement exceeds a threshold rate and level, a ring of clustered TCRs is formed at the periphery of the nascent IS. Within seconds, the ring moves to the center of the contact area, concentrating TCR complexes with CD4 or CD8 coreceptors, receptors for costimulators (such as CD28), PKC- $\theta$  (protein kinase C- $\theta$ ), and adaptor proteins that are associated with the cytoplasmic tails of the transmembrane receptors (174,183). This portion of the synapse, called **c-SMAC** (for central supramolecular activation cluster), regulates both the TCR signaling and its degradation (184). Although the TCR signaling is initiated before the formation of the synapse, the IS provides a stable interface to overcome the problems of low affinity of TCR for MHCp and the limited number of MHC molecules displaying any peptide on an APC. At some point in the IS formation, the interaction between TCRs and MHC-peptide complexes stabilizes, they no longer dissociate and thus facilitate a longer and effective T cell signaling (174,183). The binding of the T cell to the APC is enforced by the peripheral ring that surrounds the c-SMAC – the **p-SMAC** – where are gathered adhesion molecules such as LFA1 (lymphocyte function-associated antigen 1), ICAM-1 (intercellular adhesion molecule-1), and the cytoskeletal linker talin. The region distal to the synapse outside the p-SMAC, known as **d-SMAC**, is made of a radial lamellipodium enriched in F-actin; it is also where bulky molecules such as CD43 and CD45 are localized (179,183,184).

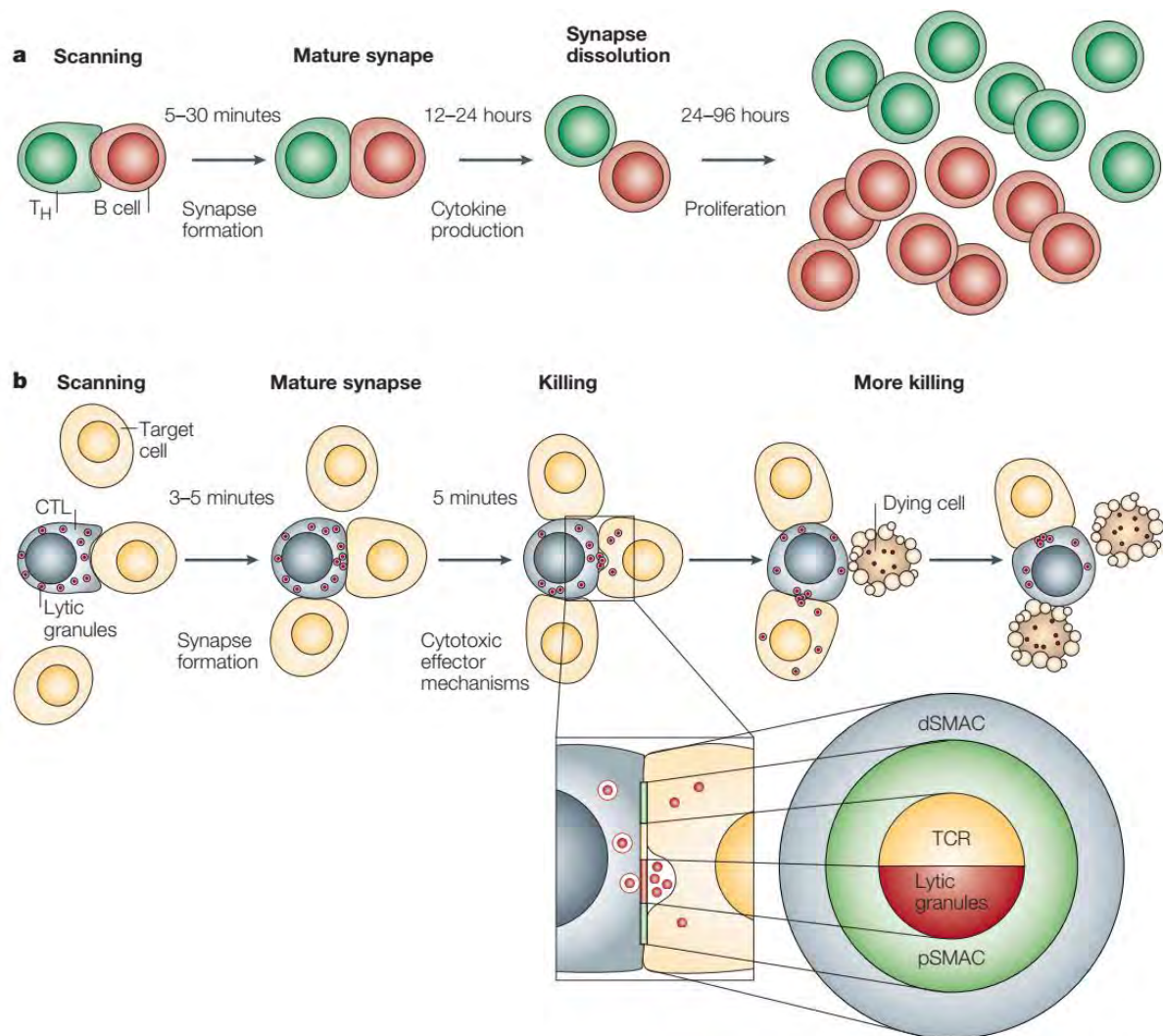


Fig. 15 **Comparison between synapse formation in CD4<sup>+</sup> T helper cells and cytotoxic T lymphocytes (CTLs).** **a)** CD4<sup>+</sup> effector T cells form one mature synapse with B cells within 5–30 minutes after initial cell contact. This synapse lasts many hours during which cytokine production and release occurs and requires continuous T-cell receptor (TCR) signals for maintenance. Eventually conjugates break apart and cells undergo several divisions. **b)** CTLs form a rather transient synapse with their target cells and deliver their lethal hit within a few minutes. Lytic granules are rapidly transported to a region within the central region of the supra-molecular activation complex (c-SMAC), which is devoid of TCRs. Whereas granule release takes place within minutes, target cell blebbing occurs within 20–30 minutes, during which cells can still be loosely attached to one another. *Figure and caption adapted from (179).*

The cytoskeletal rearrangements that enable the formation of the immunological synapse give rise to polarization of T cells towards the stimulatory APC (185). As first described by Kupfer *et al.*, upon the stimulation by B cell, the MTOC (microtubule organizing center) of T cell moved from the far side to a location underneath the synapse, closer to the antigen source; the same movement was reported by Monks *et al.* for the Golgi apparatus associated with MTOC (186,187). The polarization eventually reorients the secretory apparatus of T cells, ensuring the specific delivery of secretory granules and signals to APCs or targets. For instance, Th cells are able to deliver CD40L to B cells following the accumulation of these molecules at the immunological synapse. Similarly, Th cells activate dendritic cells through the delivery of IL-12 using the same mechanism (185,186).

But not all T cells have the same structure of immunological synapse. Although the synapses are organized according to the same principles for distinct T cell types, their patterns might vary from one subset to another. For instance, a discrete secretory domain was identified in the cytotoxic CD8<sup>+</sup> T cells, within the p-SMAC and next to the c-SMAC; other differences with the CD4<sup>+</sup> T cells were subtle, but notable: PKC- $\theta$  was also present at a significant level in p-SMAC, and signaling proteins at the contact site were asymmetric, concentrated at one side of the ring (188). Interestingly, a study on immune exhaustion in viral persistence demonstrated that PD-L1 of CD8<sup>+</sup> T cells was localized in the c-SMAC and stabilized the IS formation. This stabilization resulted in the impairment of the cell motility. Conversely, restoring T cell motility by PD-1-PD-L1 blockade enabled the recovery of T cell effector functions (189). On the other hand, it is noteworthy that CD4<sup>+</sup> T cells show different patterns of IS depending on the partner cell. Studies have indicated differences between CD4<sup>+</sup> T cell activation by dendritic cells and by B cells. While interactions with B cells induce the typical IS structure, with TCRs encircled by a ring of adhesion molecules, interactions with dendritic cells give rise to a multifocal synapse at the interface with T cells, that is, several clusters of TCRs surrounded by adhesion molecules (190). Of note, in terms of dynamic characteristics, regulatory T cells have been reported to form the most stable IS, beside CD4<sup>+</sup> T cells with a sedentary stability, and CD8<sup>+</sup> T cells with a motile meta-stable IS (191,192).

### **Regulation of the IS formation**

Not much is known about the cellular determinants that contribute to the diversity of IS patterns. From a biophysical standpoint, rearrangement of the actin skeleton is likely involved in the different interactions of T cell subsets with APCs. Certainly, it is the activation of the TCR and signaling molecules that initiates the F-actin dynamics driving the micron-scale changes of cell shape required for the IS formation; but the actin flow itself is necessary to sustain TCR signaling (193).

One cannot take place without the other. On the one hand, T cell activation initiates the signaling cascade that brings into play the molecules capable of modulating the cytoskeletal organization. In addition to the downstream signaling pathways of the TCR, the costimulatory receptor CD28 and the integrin LFA-1 participate in the activation of actin-regulatory proteins. While TCR activation leads to the activation of WASp by Nck, which orchestrates the polymerization of branched actin filaments (193), CD28 binding to CD80/86 can mediate robust F-actin polymerization (194). Also, LFA-1 binding activates SLP-76 to polymerize F-actin (193,195,196), not to mention the fact that they are all associated with the F-actin network.

On the other hand, studies have shown several aspects on how the F-actin network can control or mediate signaling events in T cell's immunological synapse. While the formation of IS requires the cytoskeletal rearrangements, the maintenance of T cells in quiescent state in the absence of antigen also needs a certain involvement of the actin cytoskeleton. Indeed, the oligomerization and clustering of the TCR, which increases the sensitivity of the T cells to antigens, is a regulated activity (197). In the absence of antigen, the cytoskeleton prevents the clustering of the TCR or downstream signaling intermediates such as LAT (198). Upon T cell activation, initial TCR-induced actin polymerization is required for cell spreading and IS formation. However, this observation, done in experimental systems, is not necessarily the same *in vivo*. In fact, initial interactions between T cells and APCs occur in the context of T cell migration which is dependent on actin network expansion and myosin contraction (199,200). Moreover, before the interaction is stable enough to establish an IS at the interface of T cell/APC, T cells scan for antigen through mobile synapse-like structures known as kinapses. Analogous to mature synapse in terms of protein segregation patterns, kinapses are not symmetrical until an antigen recognition activates T cell, converting them to a stable IS by altering the symmetry of the actomyosin network through PKC- $\theta$  signaling and WASp activity

(201). Meanwhile, microclusters of TCR and downstream signaling components are continuously formed in p-SMAC zone with early activities of tyrosine phosphorylation (202). Once the IS is stabilized, the actin network promotes the transport of these new microclusters to the center zone of the contact (the c-SMAC), where they get dephosphorylated, ubiquitinated and internalized to form IS-associated microvesicles (203). These activities make F-actin flow a molecular countdown for signal termination. Indeed, depolymerization of F-actin is shown to abrogate the generation of new microclusters in the cell periphery as well as the inward movement of existing microclusters to the c-SMAC. The seizure of microclusters in the cell also prolongs signaling lifetime in this context; the modulation at the level of microcluster dynamics thus provides a potential initiative to tune T cell responses over various antigenic signals (181) .

### **Glycans in the IS formation**

Glycosylation indirectly regulates the formation of the immunological synapse through the glycosylated signaling proteins. At the level of single proteins, sugars protect molecules in the synapse complexes from the protease activity during the signal transduction which may take up to several hours in class II APCs (204). For instance, CD8 has a globular head that binds to MHCp; this domain is tied to the T cell membrane by a polypeptide arm extended with four *O*-linked sugars (205). The sugars are thought to confer rigidity to the extended peptide while shielding it from proteases (206).

Another implication of glycosylation, and also its major role, is to provide the lectin-glycoprotein lattice. Multivalent interactions between endogenous lectins and glycosylated receptors profoundly influence molecular events in the formation of the IS such as receptor trafficking, bridging association with other glycoproteins, restricting receptor clustering and preventing receptor endocytosis. Many studies have been focusing on the glycosylation by the enzyme Mgat5 (*N*-acetylglucosaminyltransferase 5), which synthesizes  $\beta$ 1,6 *N*-glycan branching structure. Disrupting endogenous galectin-glycoproteins interactions, either by targeting the enzyme Mgat5 or by incubation of the cells with soluble sugars to compete with the galectin binding, results in the same phenotype of T cells with enhanced TCR mobility and TCR signaling (54,207–209). Also, this type of disruption has been reported to induce the recruitment of the CD4, Nck, SLP-76, WASp, and F-actin protein to the TCR in the absence of the TCR ligand (210). Of note, TCR signaling could stimulate the transcription of *N*-glycan-processing enzymes including alpha-mannosidase II and Mgat5 as a feedback loop (211). Consistently, enhancement of *N*-glycan branching in vivo by oral administration of GlcNAc restricts TCR signaling, inhibiting Th1 and Th17 responses (212). Therefore, branching of the receptor *N*-glycans on the cell surface by Mgat5 can tailor T cell responses by controlling their activation.

On the other side of the lectin-glycoprotein lattice, galectin-3 have been reported to dampen TCR clustering at sites of IS, thereby limiting TCR activation at basal conditions (213). In mouse models and human tumor-infiltrating lymphocytes, exogenous galectin-3 binds to TCR *N*-glycans and segregates it from CD8 molecules, leading to the loss of function of cytotoxic lymphocytes (214). Moreover, the interactions between galectin-3 and *N*-glycans on CTLA-4 (cytotoxic T lymphocyte antigen-4) could prevent this inhibitory receptor from endocytosis, thus allowing sustained inhibitory signals (215). Interestingly, intracellular galectin-3 is also found to promote TCR downregulation at the IS via interactions with regulatory proteins (216). Following a similar pattern, studies on galectin-1 reported an autocrine regulatory role of this glycan-binding protein that negatively controls TCR signaling (217). The roles of lectin-glycoprotein lattices in the context of T-cell activation turn out to be diverse and complicated, yet it is interesting to observe that both extra-cellular gal-3 and gal-1 can downregulate the TCR signaling.

### 2.2.3. T cell exhaustion versus senescence

#### **The two different states of dysfunction in T cells**

Senescence and exhaustion are the two dysfunctional states of T cells in a context of repeated antigen stimulation. Although they have many overlapping functions, exhausted and senescent T cells have distinguishable phenotypes and functions.

Exhaustion develops when there is a high antigenic load that eventually leads to a progressive loss of T cell function; if this high antigenic load persists, exhausted T cells are ultimately deleted. First described in the chronic infection with LCMV, T cell exhaustion typically refer to the lack of effector functions in CD8<sup>+</sup> T cells (218). Exhausted T cells are characterized with the expression of a panel of inhibitory receptors, including PD-1, CTLA-4 and Tim-3 (T cell immunoglobulin and mucin domain containing-3) (219,220). The loss of functions is described to occur in a hierarchical manner: first IL-12 production is compromised, then TNF production, and finally, at a severe stage of exhaustion, IFN- $\gamma$  itself (221). Although exhausted CD8<sup>+</sup> T cells are often associated with a defective cytotoxicity, recent study has suggested the defects to be of limited scale (222). Exhaustion also occurs in CD4<sup>+</sup> T cells; as they do not have cytotoxicity, the exhaustion is thought to limit the magnitude of effector T cell responses (223).

Unlike exhaustion, senescence is a loss of proliferative capacity following extensive replication due to the long exposure to a persisting antigen. Occurring in chronic infection and various types of cancers, T cell senescence is triggered by the telomere shortening or erosion and/or "damage signals", that is, oxidative stress, cell culture stress, DNA-damaging chemotherapeutic agents and mitogenic oncogenes. Interestingly, induction of senescence is also suggested to be a mechanism of suppressing naïve/effector T cells used by Tregs and tumor-derived Tregs (224–226). According to this concept, tumor cells and Tregs induce DNA damage responses in responder T cells, leading to the cell cycle arrest and eventually senescence in the latter (224,227).

In summary, exhaustion is related to excessive abundance of antigens whereas senescence is related to the time length of antigenic stimulation.

#### **Identification of exhausted and senescent T cells**



As mentioned before, exhausted T cells present a panel of inhibitory receptors that mark their loss of function. These receptors include PD-1, CTLA-4, Tim-3, LAG-3, BTLA, TIGIT (T-cell immunoreceptor with Ig and immunoreceptor tyrosine-based inhibitory motif domains), CD244 (also called the natural killer cell receptor 2B4) and the glycoprotein CD160; CD39 and the costimulatory molecules 4-1BB are also found to have a high expression in exhausted tumor-infiltrating CD8<sup>+</sup> T cells. Exhausted T cells are also characterized with an impaired cytotoxicity and cytokine production, notably IL-2, TNF and IFN- $\gamma$  (228). Various transcription factors take part in the development of T cell exhaustion. The major drivers of dysfunctional CD8<sup>+</sup> T cells in cancers include NFAT, the nuclear receptor Nr4a, HMG-box transcription factor TOX, and GATA-3 (229–232). Of note, exhausted CD8<sup>+</sup> T cells can be classified into progenitor or terminally exhausted T cells based on their profile of T-bet and EOMES expression. Because many studies have found EOMES replaces T-bet at a later stage of continuous antigenic stimulation, progenitor exhausted T cells are defined as T-bet<sup>high</sup>EOMES<sup>low</sup>PD-1<sup>int</sup> while terminally exhausted T cells are T-bet<sup>low</sup>EOMES<sup>high</sup>PD-1<sup>high</sup> (233,234).

Senescent cells are typically characterized with a dramatically reduced expression of costimulatory molecules CD27 and CD28. They also acquire the senescence-associated phenotype: high expression of SA- $\beta$ -Gal (senescence-associated- $\beta$ -galactosidase), surface markers Tim-3, CD57, CD45RA and KLRG-1 (killer cell lectin-like receptor subfamily G member 1), and a secretory profile that is rich in proinflammatory cytokines such as IL-2, IL-6, IL-8, TNF, IFN- $\gamma$  as well as in suppressive cytokines IL-10 and TGF- $\beta$  (224,225,235–237). In terms of effector function, senescent CD8<sup>+</sup> T cells have a reduced expression of granzyme B and are able of amplifying immune suppression (238,239). In addition to activity abrogation of key molecules involving in TCR signaling, T cell senescence is driven by an upregulation of cell cycle regulatory molecules p16, 121 and p53 which function to keep cells in a cell cycle arrest (227).

### **Immune synapse in dysfunctional T cells**

On a biophysical standpoint, the root of T cell exhaustion stems from the inability to form functional immune synapses with the target cells (240). In chronic lymphocytic leukemia (CLL), for example, healthy T cells is unable to form proper immune synapses upon their encounter with CLL-B cells. More specifically, there is a suppression of F-actin polymerization that prevent

key adhesion and signaling molecules from joining the nascent synapses (241). Similar observations have been reported in other cancer models, where defective actin polymerization prevent tumor-infiltrating lymphocytes (TILs) from attacking cancer cells (242). The different inhibitory receptors that characterize the exhaustion state may use the same strategy to trigger the functional loss of T cells. For instance, PD-1 antagonizes TCR signaling under many mechanisms. In regard to signaling pathways, PD-1 recruits SHP2 (Src homology 2 domain-containing tyrosine phosphatase 2) through its ITIM and ITSM (immunoreceptor tyrosine-based switch motif) inhibitory domains, which in turn prevents ZAP-70 phosphorylation and association with CD3 $\zeta$  at the TCR complex while blocking PKC- $\theta$  activation. Alternatively, at the site of IS, PD-1 form a microcluster with TCR; then, this formation interferes with TCR signaling and leads to T cell suppression (243). In chronic infections, persistent antigen load stabilizes the IS through the PD-1 engagement: T cells are paralyzed in the sense that they cannot be released from the contact site to interact with other targets (189).

The situation is different in the case of T cell senescence. Senescent T cells are typically defined by the loss of CD28 expression following an exposure to repeated antigen stimulations. On one hand, signals from the environment using the common  $\gamma$ -chain cytokines such as IL-2, IL-7 and IL15 could accelerate the loss of CD28 in CD8 T cells activated by the TCR (244,245). In addition, the presence of type I interferons in pro-inflammatory environment also drives an accumulation of CD8<sup>+</sup>CD28<sup>-</sup> and CD4<sup>+</sup>CD28<sup>-</sup> T cells in culture (246). On the other hand, it is possible that the loss of expression results from a dysfunctional IS formation. In a normal context, CD28 is co-located with TCR microclusters at early recognition of MHCp. When the IS matures, CD28 present at c-SMAC segregates away from the TCR and gets internalized to be degraded; a newly recycled CD28 is rapidly recruited to the contact site, recovering the same level of expression as before activation (247,248). During a chronic infection, as T cell activation is sustained, recruited CD28 molecules are maintained at the synapse instead of going into the turnover process (249). A sustained TCR activation and turnover thus gradually diminishes the CD28 expression by shutting down the generation of new CD28. And since CD28 is an activator of Akt, the loss of CD28 expression leads to signaling failure in processes regulated by the Akt pathway, the most significant being the loss of telomerase activity, which finally results in the cell cycle arrest and the particular phenotype of T cell senescence (250,251).

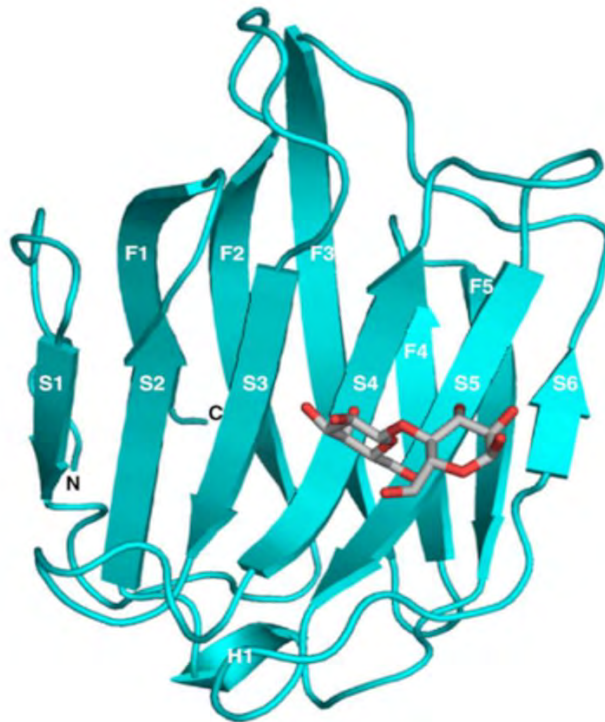


Fig. 16 **An illustration of the human galectin-9 NCRD-lactose complex.** The five (F1–F5) and six-stranded (S1–S6)  $\beta$ -sheets and one short helix (H1) are indicated by the letter-number code. The lactose molecule is shown as a rod model. *Figure and caption adapted from (252).*

## Chapter 3: General aspects of galectin-9

---

### 3.1. Structure, expression, tissular and cellular distribution

#### 3.1.1. Structure of the galectin-9 proteins and transcripts

Galectin-9 (gal-9) was initially isolated and identified in 1997 by two independent groups, (1) as a neo-antigen occurring in tissues from patients with Hodgkin lymphoma (253), and (2) simply as a new member of the galectin family, with a specific binding activity for the  $\beta$ -galactosyl disaccharidic group (254). Later on gal-9 has been described as a potent eosinophil chemoattractant but this has not been confirmed in subsequent investigations (255). Then gal-9 has devoted greater attention as a modulator of various biological functions, especially in the immune system, in physiological and pathological contexts for example in malignant diseases.

#### **Galectin-9 protein structure and interactions with glycans**

Gal-9 is a galectin of tandem repeat type, having two distinct CRDs joined by a linker peptide. Independent crystallographic studies by two Japanese groups published similar results on gal-9 structure (252,256). Each CRD consists of two  $\beta$ -sheets – the first with six (S1 to S6) and the other with five (F1 to F5) strands - closely packed in anti-parallel directions, forming a sandwich structure (*Fig. 16*). Although they share only 35% homology in their amino-acid sequence, there is little structural difference between the C-terminal CRD (CCRD, 149 aa) and the N-terminal CRD (NCRD, 148 aa), except for an  $\alpha$ -helix between F5 and S2 of the CCRD. However, the recognition of  $\beta$ -galactoside disaccharidic groups occurs at different site for each CRD. On the side of CCRD, the oligosaccharide group is bound to the concave site formed by S3 and S6 strands. On the NCRD side, S4 and S6 form a binding site where the  $\beta$ -galactoside group is inserted.

One characteristic feature of gal-9 among other galectins is its preferential binding for complex glycoconjugates, especially those containing poly-N-acetyl-lactosamines (poly-

LacNAc) carried by *N*- or *O*-glycans linked to glycoproteins or by glycolipids. This affinity is even greater for branched poly-LacNAcs (bi-, tri- or tetra-antennary). This relative selectivity for poly-LacNAcs is more marked for the NCRD than the CCRD (252,257). Typical oligosaccharide ligands of gal-9 are the Thomsen–Friedenreich antigen (disaccharide) and the Forssman antigen (pentasaccharide). The Forssman antigen is often bound to ceramide with which it forms a glycosphingolipid. It is sometimes carried by *O*-glycosylated glycoproteins. The affinities of the NCRD for the Forssman pentasaccharide has been reported to be higher in humans than in mice, which might result from differences in the amino acid sequence on the concave sides of the 2 NCRDs (252,258,259). Finally, it is worth to mention that Gal-9 binding to poly-LacNAc can be strongly impaired by some structural changes. One of these changes has been very well documented in B-cells. Transition from “linear poly-LacNAcs” (meaning with straight antenna) to I-branched forms (meaning with ramified antenna) strongly impairs gal-9 binding, especially on the CD45 molecule (260). We will come back to this point in subchapter 3.3 on gal-9 and B-cells.

### **Galectin-9 isoforms and derived products**

The transcript of full-length gal-9 consists of 11 exons; due to the alternative splicing process, exon 5 and 6 can be truncated, resulting in three splice variants frequently described in the literature with various length of the linker peptides: (1) gal-9L or gal-9FL (long), (2) gal-9M or gal-9 $\Delta$ 5 (medium), and (3) gal-9S or gal-9 $\Delta$ 5/6 (short) (261). Details on the molecular characteristics of gal-9L, M and S can be found in *Table 6*. So far very few functional differences between the three isoforms have been reported. We can mention differential effects on E-selectin expression and adhesion in LoVo colon carcinoma cells (262). The longer linker is thought to be more flexible and therefore capable of increasing gal-9 potency, especially in triggering T cell death, so that it can influence the lattice formation and glycan binding (263). In return, the linker peptide is the target of proteases like metalloproteinases, elastases and thrombin. The longer the linker, the more vulnerable it is to protease attacks, thus gal-9S is more stable than gal-9M, itself more stable than gal-9L. An artificial isoform of gal-9 which is completely devoid of linker peptide - often called gal-9NC - is highly stable and more active than the natural isoforms in most functional tests (264). The cleavage of the linker peptide is done mainly by the neutrophil elastase and MMP3. These proteases are highly expressed in inflamed tissues and/or sites of tissue remodeling (76,265).




Isoform	Structure	Length of linker peptide	Molecular weight (kDa)
Gal-9L	NH <sub>2</sub> —  —COOH	58	39.5
Gal-9M	NH <sub>2</sub> —  —COOH	26	35.9
Gal-9S	NH <sub>2</sub> —  —COOH	14	34.7

Table 6. **Characteristics of Gal-9 isoforms.** The three isoforms of gal-9 (L: long, M: medium, S: short) have linker peptides that vary in length. These linkers bridge the two carbohydrate recognition domains (CRD) that enable the binding to glycans.

There is evidence that after cleavage of the linker peptide, gal-9 is not homogeneously degraded. Padilla *et al.* have recently reported the detection of a truncated form of gal-9 in the plasma of patients suffering from AIDS (acquired immunodeficiency syndrome) at the acute phase, tuberculosis or both diseases. This fragment called TR-Gal9 in their paper seems to be somehow similar to the NCRD. The authors claim that high concentrations of this fragment in the plasma samples from recently infected AIDS patients is associated with a bad outcome (76,265).

Finally, it is worth to mention that in addition to the main isoforms, an exclusion of exon 10 from the mature mRNA of galectin-9 have been reported by several groups, notably in variants gal-9 $\Delta$ 10, gal-9 $\Delta$ 5/10 and gal-9 $\Delta$ 5/6/10 (266,267). While the lack of exon 5, either alone or in combination with exon 6, leads to a shorter linker peptide, the exclusion of exon 10 results in a prototype-like isoform of galectin-9 as the CCRD is cut off due to the premature stop codon with exon 11 generated from the created frameshift. Interestingly, these variants do not appear to be secreted, which suggests an intracellular role, although their precise function is yet to be elucidated (268).

### 3.1.2. Galectin-9 gene and its regulation

The aforementioned proteins and transcripts of galectin-9 are, in fact, products from the gene *LGALS9* (gene ID: 3965). This gene is located on chromosome 17, in its longer arm at 11.2 loci (the position is 17q11.2). In humans, two galectin-9-like coding genes have been found on the same chromosome but in the shorter arm, resembling to a duplication of the gal-9 gene. Their chromosomal position is thus 17p11.2. Although initially considered as pseudogenes (269), *LGAGL9B* and *LGALS9C* (gene IDs: 284194, 654346 respectively) are now recognized as true genes due to the good exon-intron structure. In fact, each of them encodes a predicted protein of the same size and highly similar to gal-9. However, they are rarely mentioned in the literature, except for studies relating to whole-exome sequencing and copy number variation analysis which show that they are actually transcribed (supplementary data from Broséus *et al.*) (270).

The expression of the gene *LGALS9* can be regulated by signals from the environment. Such regulation was first reported in the case of IFN- $\gamma$  in the paradigm context of autoimmune disease and chronic inflammation. Several studies found gal-9 expression to be stimulated by IFN- $\gamma$  in endothelial cells and fibroblasts (80,271), but it was the work of Zhu *et al.* (272) that put forward the idea of IFN- $\gamma$  inducing gal-9 expression as a way to disrupt the feedback loop that promoted experimental autoimmune encephalomyelitis (EAE). Given the correlation of Tim-3 mRNA expression with the activation of effector Th1 cells, the authors found gal-9 specifically bound to carbohydrate chains of Tim-3. The Tim-3/gal-9 eventually induced cell death in Th1 cells, in particular those that produced IFN- $\gamma$ . This finding might appear contradictory to the fact that IFN- $\gamma$  is highly expressed in patients with multiple sclerosis but also helps to explain why IFN- $\gamma$ -deficient mice develop profound EAE. Consistently, in HCV (hepatitis C virus) chronic infection, Mengshol *et al.* found IFN- $\gamma$  induced galectin-9 production in macrophages (273). The increase of gal-9 in turn leads to the production of pro-inflammatory cytokines while expanding Tregs in the presence of TGF- $\beta$  and inducing apoptosis of HCV-specific CTLs.

The recent work of Yang *et al.* highlights the role of IFN- $\beta$  in the regulation of gal-9 expression. In A375 human melanoma cells, the authors found that IFN- $\gamma$  only had modest effect as opposed to the strong upregulation of gal-9 by IFN- $\beta$ , at both protein and mRNA levels, while TNF- $\alpha$  had no effect (274). This is true in many cell lines including HCC (hepatocellular carcinoma), prostate cancer, pancreatic and lung cancers. Interestingly, IFN- $\beta$  induces gal-9 in lung carcinoma cells with wild type EGFR but not with mutant EGFR, suggesting that EGFR signaling may be involved in the upregulation of gal-9 expression. However, these cell lines with defective EGFR signaling are not affected when it comes to gal-9 secretion, which proves that gal-9 expression and secretion are independently regulated by IFNs. Similarly, in the monocytic cell line THP-1 and in primary macrophages which have a constitutive expression of gal-9, the secretion is still regulated by IFNs. These findings suggest that there is a concerted action of IFN- $\beta$  and IFN- $\gamma$  to upregulate gal-9 expression in APCs; when put in the context of gal-9 interaction with Tim-3, the secretion of gal-9 promoted by IFNs can dampen antitumoral T cell response by inducing cell death.



Another remarkable regulator of gal-9 is TGF- $\beta$ , as demonstrated by the work of Wu *et al.* (275). An amplified target of gal-9 that in turn re-enforces FoxP3 expression in iTreg cells, TGF- $\beta$  is also revealed to take part in a positive feed-forward loop: in the presence of TGF- $\beta$ , gal-9 is expressed as early as 12 hours after activation and its expression is sustained throughout the iTreg differentiation. The high levels of gal-9 mRNA and protein in iTregs, in comparison to nTregs or other T cell subsets, suggests that TGF- $\beta$  enhances gal-9 expression. We will get back on this study in the sub chapter 3.2.3 to discuss more on the immunological aspect.

Some PAMPs could be a stimulator of galectin-9 such as lipopolysaccharides (LPS) and the viral mimic polyinosinic:polycytidylic acid (poly I:C, a synthetic double-stranded RNA). In endothelial cells, poly I:C is efficient to induce gal-9 expression through TLR3, PI3K and IRF3 pathway, whereas gal-9 protein is undetectable during induction by LPS from *E. coli* (276). Conversely, in periodontal ligament derived cells, LPS upregulates the expression of gal-9 mRNA and protein (277).

At the level of transcription factors, the stimulation of gal-9 expression can involve many signaling pathways depending on the cell type and the regulator. For instance, the effect of IFN- $\gamma$  is mediated by HDAC3/PI3K/IRF3 in endothelial cells, whereas in fibroblasts, expression of gal-9 is upregulated via MAPK, PI3K and JAK/STAT (278). On the other hand, in the study by Wu *et al.*, TGF- $\beta$  reinforces gal-9 expression in a positive feed-forward loop through Smad3. The latter is found to interact with multiple binding sites in the *LGALS9* promoter in iTreg cells, but not in Th0 (275).

Lastly, non-physiological factors can enhance gal-9 expression. These include viruses and chemotherapy. Many viruses enhance gal-9 expression in infected cells for example the Epstein-Barr virus (279). We can also mention Hepatitis B and C viruses, influenza and dengue viruses (280). We will get more into details about the role of chemotherapy in the subchapter 3.6 on galectin-9 and cancers.

### 3.1.3. Tissular and cellular localization

Like other galectin family members such as galectin1, -3, -8 and -5, galectin-9 has a broad range of tissue distribution. It seems to be widely distributed in liver, small intestine, thymus, kidney, spleen, lung, cardiac and skeletal muscle, but barely detectable in reticulocyte and

brain (281,282). Moreover, the expression of galectin-9 is also developmentally regulated and is detected at high levels in the developing thymus and liver. At later stages of life gal-9 is weakly expressed in most tissues in basal conditions but its expression is often enhanced in the context of inflammation or immune response, especially in endothelial cells (283).

At the cellular level, galectin-9 can be detected in the cytoplasm and at the surface of the plasma membrane. It can shuttle between the plasma membrane and the Golgi apparatus (284). Sometimes, it is also detected in the nucleus (278,285). When making cell protein extracts, about 50% of the cell-associated galectin-9 can be recovered with soluble elements of the cytoplasm. Another fraction is co-purified with components of the cellular membrane network (286). Although there is no secretion signal in its sequence, gal-9 can be secreted to the extracellular medium by unconventional pathways. As shown by our group, a substantial fraction of gal-9 produced by various cell types is found in the extracellular space in association with exosomes or microvesicles (91,92). In addition, there is evidence of another pathway of gal-9 secretion which is independent of exosome release. It has been documented for a subset of CD4<sup>+</sup> T cells which display gal-9 molecules at their surface and release gal-9 in the extracellular space under a soluble form (287). So far the mechanism of this extracellular release has not been uncovered (a few hypotheses are provided in the general chapter on galectins).

#### 3.1.4. Examples of functions provided by cell-associated gal-9

Inside the cell, gal-9 has mainly functions related to the building and maintenance of cell architecture. At the cell surface, it plays a role in plasma membrane organization and signal transduction. This will be briefly summarized in this sub-chapter. Like other galectins, for example galectin-8, gal-9 is involved in the repair and recycling of intra-cellular damaged vesicles. In case of lysosomal damages induced by various agents for example pathogens or metformin, there is an abnormal exposure of intra-lumen glycans. This results in binding of galectins, including gal-9 which activates AMPK (AMP-activated protein kinase) which then inhibits m-TORC1 (mammalian target of rapamycin complex 1). One consequence of this signaling cascade is the activation of macro-autophagy which includes a process of lysosome repair (288,289).

Gal-9 also plays a role in the process of cell polarization. This has been investigated in MDCK (Madin-Darby Canine Kidney) cells. Knocking out gal-9 in these cells blocks their polarization. There is evidence that apical sorting of specific proteins and lipids requires a circuit based on gal-9 binding at the surface of the plasma membrane, preferentially on the Forssman glycosphingolipid, its internalization to the Golgi and recycling to the plasma membrane (284).

Regarding more specifically the function of gal-9 in the plasma membrane, investigations made on dendritic cells have shown a role in maintaining its rigidity. This involves the modulation of a small G-protein called Rac1 and of the sub-cortical organization of the actin cytoskeleton. In the absence of gal-9, for example in gal-9 KO mice, pathogen uptake by DC is impaired (290).

Signaling by some membrane receptors of the TNF-receptor family – namely 4-1BB (also called CD137 or TNFRSF9) and DR3 (also called TNFRSF25) requires an interaction with gal-9 at the cell surface (291,292). It seems that gal-9 contributes to the trimer organization of these receptors which is required for their signaling activity. For these receptors, the interaction with their cognate ligand (4-1BBL and TL1A, respectively) seems to be insufficient to achieve the trimer formation. Several questions remain pending: 1) which part of the gal-9 molecule interacts with 4-1BB and DR3; 2) whether the facilitation of their signal transduction would be made only by endogenous gal-9 produced by the same cell or by extracellular gal-9 released by other cells.

### 3.1.5. Summary of gal-9 functions in the immune system

The extracellular gal-9, bound to exosomes or released in soluble forms, can behave to some extent like a cytokine. Indeed, the gal-9 released by producer cells has the capacity to act on distant target cells. In whole organisms, essentially in mice, extracellular gal-9 has mainly immunosuppressive functions. This is well illustrated by studies on experimental viral infections, allografts and auto-immune diseases (subchapter 3.5.1). Investigations performed *in vitro* suggest that these immunosuppressive effects are predominant in the adaptive immune system and to a large extent mediated by the Tim-3 receptor. As explained in the next sections, Tim-3 stimulated by gal-9 delivers inhibitory signals in CD4<sup>+</sup> and CD8<sup>+</sup> conventional T cells and in plasma cells (see subchapters 3.2.1 and 3.4.1 to 4). Through its binding to CD44,

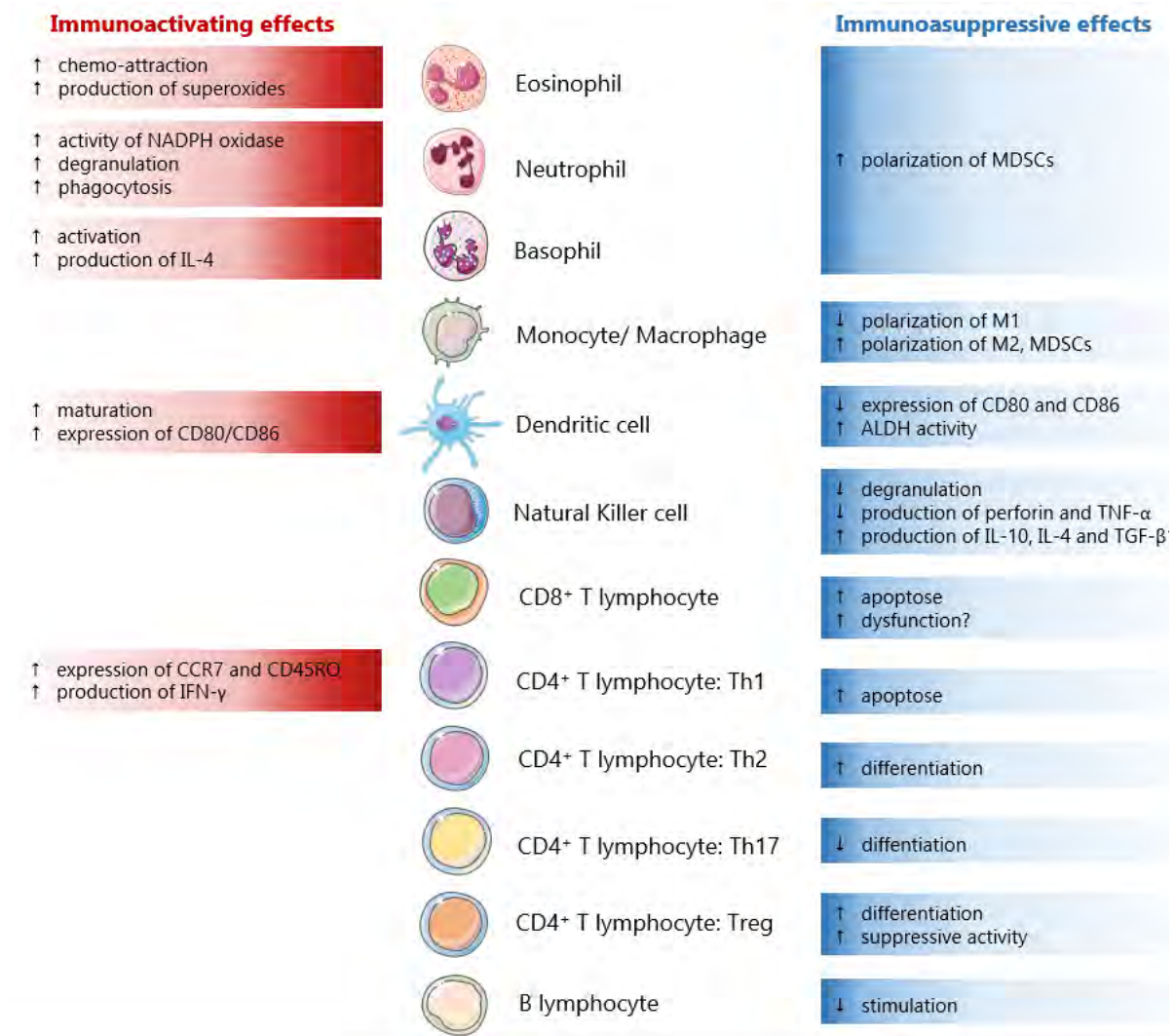


Fig. 17 **Modulatory effects of galectin-9 on various populations of immune cells.** Gal-9 has immunosuppressive effects in general. The immunoactivating effects are mainly on granulocyte lineages. *Adapted from the work of Claire Lhuillier.*

Gal-9 can also enhance the differentiation/expansion of iTregs induced by TGF- $\beta$  (3.2.3). However, this immunosuppressive activity of gal-9 in the adaptive immune system is not fully consistent. There is at least one exception represented by the elimination of tissue-resident Tim-3<sup>+</sup> Tregs (274,293). With regard to the innate immune system, the balance of immune suppressive and immune activating effects of gal-9 is even more complex. On the one hand, gal-9 impairs NK cell cytotoxicity, induces the M2 polarization of macrophages and represses CXCL9 production by DCs (subchapter 3.4). On the other hand, there are scattered observations about the stimulation of interferon- $\gamma$  or TNF- $\alpha$  production by macrophages or DCs treated *in vitro* with gal-9 (273,294). This inflammatory response resulting from gal-9 stimulation of the innate immune system might be required in some cases for a successful immune response.

### 3.1.6. Overview of the membrane receptors of extra-cellular galectin-9 and their signaling pathways

#### **Tim-3 as a membrane receptor for gal-9**

Tim-3 is the most studied membrane receptor of gal-9 also called HAVCR2 (for Hepatitis A virus cellular receptor). Structural details can be found in the Uniprot data base (<https://www.uniprot.org/uniprot/Q8TDQ0>). Tim-3 is a 301-aa type I transmembrane glycoprotein which belongs to the immunoglobulin super family. Tim-3 has an N-terminal extra-cellular domain (aa 22-202), a single trans membrane domain (aa 203-223) and a C-terminal intra-cytoplasmic domain (aa 224-301). The extra-cellular part includes a binding pocket for phosphatidyl-serine (PtdSer) upstream of a mucin domain with *O*- and *N*-glycosylation on Thr145 and Asn172 respectively. The intracellular tail has a conserved tyrosine-based signaling motif (295). In addition to gal-9, three ligands of Tim-3 have been identified: PtdSer, the carcino-embryonic antigen cell adhesion molecule 1 (Ceacam-1) and the high mobility group protein B1 (HMGB1). There is strong evidence that PtdSer, Ceacam-1 and HMGB1 bind to the same N-terminal binding pocket of Tim-3 in contrast with gal-9 which binds to the glycosylated segments of Tim-3 (*Fig. 18*) (295–298). In their initial landmark study on gal-9/Tim-3 interaction, Zhou *et al.* have shown that both CRDs of gal-9 are required for optimal binding to Tim-3 (272). Gal-9 is suspected to bridge Tim-3 molecules at the surface of the target cells by concomitant binding of the 2 CRDs. Strikingly all monoclonal antibodies

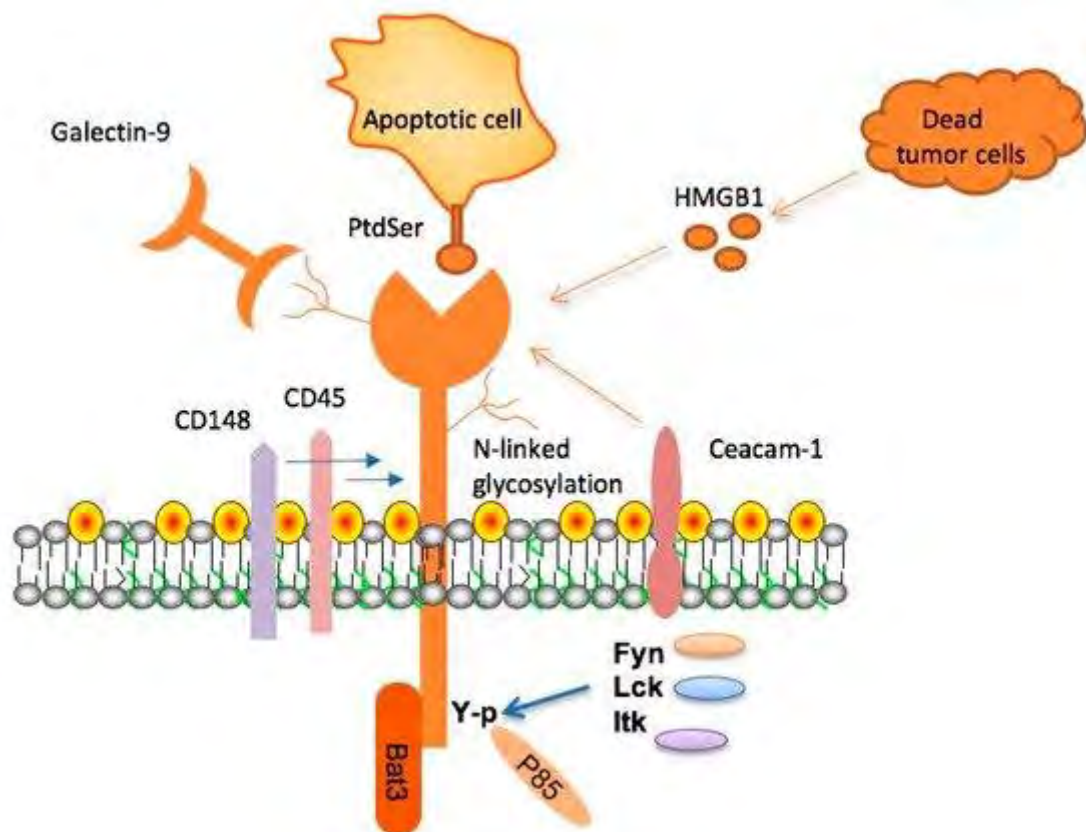


Fig. 18 **T cell immunoglobulin and mucin domain 3 (TIM-3), its ligands, and signaling adaptor proteins.** Four ligands—namely, galectin-9 (Gal-9), phosphatidylserine (PtdSer), high mobility group protein B1 (HMGB1), and carcinoembryonic antigen cell adhesion molecule 1 (Ceacam-1)—have been identified to bind to the variable immunoglobulin (IgV) domain of TIM-3. In terms of signaling, HLA-B associated transcript 3 (Bat-3) binds to the cytoplasmic tail of TIM-3 and inhibits TIM-3 function. Fyn, Lck, and Itk, three tyrosine kinases, bind and phosphorylate specific tyrosine residues within the cytoplasmic domain of TIM-3. The phosphorylated tyrosines within the cytoplasmic domain of TIM-3 can recruit other downstream signaling adaptors such as p85 adaptor protein. In addition, Gal-9 can mediate the formation of clusters containing TIM-3, CD45, and CD148. (294)

blocking Tim-3 with a functional efficacy blocks its interaction with PtdSer and Ceacam-1 but not with gal-9 (296). This applies to many anti-Tim-3 antibodies currently used in clinical trials like MGB453 (Novartis) (299). As explained in the subchapter 3.2, Tim-3 is a mediator of gal-9 induced cell death active on a fraction of CD4<sup>+</sup> and CD8<sup>+</sup> conventional T cells and a fraction of Tregs (Tim-3<sup>+</sup> Tregs often abundant in tumors) (274,293). The signaling pathways leading to cell death in these cells are not entirely known. Phosphorylation of the tyrosines 256 and 263 of the cytoplasmic tail of Tim-3 which induces the release of Bat3 seems to be a key step for the activation of cell death mechanisms (300). Another inhibitory mechanism investigated in CD8<sup>+</sup> T cells is based on the entry of Tim-3 in the immunological synapse upon gal-9 binding of its extra-cellular domain and subsequent attraction of the CD45 phosphatase in the synapse (301). As explained in subchapter 3.4, gal-9 binding of Tim-3 at the surface of NK cell impairs their cytotoxic activity. To our knowledge, the underlying signaling pathways have not been investigated. Same remarks can be done for gal-9 binding of Tim-3 at the surface of DCs which downregulates their production of CXCL9. Finally the gal-9 binding to Tim-3 at the surface of plasmocytes was reported to induce their apoptosis (302).

### **Membrane receptors distinct from Tim-3**

A very recent and important breakthrough for our understanding of the activity of the extracellular gal-9 in the immune system is its capacity to bind PD-1 at least at the surface of T cells and may be other cells (274). This publication shows that gal-9/PD-1 interaction is primarily mediated by the C-terminal CRD of gal-9 and the *N*-glycan linked to Asn116 of PD-1. One remarkable consequence of this binding is the formation of Tim-3/gal-9/PD-1 complexes at the surface of target cells. These complexes are included in larger molecular edifices of low solubility corresponding to galectin-glycoprotein lattices. Another functional consequence is that co-expressed PD-1 tends to protect Tim-3<sup>+</sup> T cells from cell death induced by gal-9 which might be explained by the Tim-3 sequestration in membrane lattices.

Dectin-1 has been identified as a gal-9 membrane receptor at the surface of human and murine macrophages (65). Also called C-type lectin domain family 7 member A, dectin-1 is a lectin with affinity for cell wall constituents from pathogenic bacteria and fungi. Daley *et al.* have shown that its interaction with gal-9 results in higher SYK phosphorylation and NF- $\kappa$ B activation with a subsequent increase in CD206 expression and IL-10 production. It is

noteworthy that gal-9 binding to dectin-1 is glycan-independent and probably does not involve the CCRD nor the NCRD (65).

At the end of this subchapter, we will briefly summarize the possible binding of extracellular gal-9 to a number of other membrane receptors. Some of them are widely - but not exclusively - expressed in the immune system. Gal-9 binding to CD44 has been observed in the context of iTregs (see subchapter 3.2) and basophils (subchapter 3.4). Gal-9 can also interact with CD44 at the surface of osteoblast with a contribution to their differentiation (303). CD45 binding has been shown for B cells (subchapter 3.3). Gal-9 binding to CD206 was reported for macrophages (subchapter 3.4). Gal-9 can bind the external part of the glucose transporter GLUT2. This interaction slows down the internalization of GLUT-2 (278). Finally, we can mention gal-9 interaction with the *O*-glycans of the protein disulfide isomerase (PDI) at the surface of the plasma membrane (283). When localized at the cell surface, PDI facilitates the cleavage of disulfide bonds. Again gal-9 binding tends to increase PDI retention at the surface of the plasma membrane. Gal-9 binding to PDI on T-cells potentiates HIV infection (304).

## 3.2. Galectin-9 and T cells

### 3.2.1. Inhibitory effects of extra-cellular gal-9 on Th1 cells

The first landmark publication which unveiled the contribution of gal-9 in the physiology of the immune system was mainly focused on the gal-9 interactions with Th1 lymphocytes. In 2005, Zhu *et al.* were the first to identify Tim-3 as a receptor of gal-9 and to demonstrate that Tim-3 stimulation by gal-9 at the surface of Th1 lymphocytes resulted in their apoptosis; their study was entirely based on murine models (Vijay Kuchroo's team in Boston) (272). *In vitro*, the apoptosis of Th1 cells was obtained at relatively high concentrations of recombinant gal-9, 250 to 500 nM. These authors presented gal-9 as a physiological brake facilitating the termination of the immune response: "the IFN- $\gamma$  that induces tissue inflammation also induces an inhibitory ligand (galectin-9) in the target tissue, which delete Th1 cells and thereby prevents protracted inflammation in target organs".

Although this study had a profound influence on most of the subsequent researches about gal-9 functions in the immune system, in humans as well as in mice, one conclusion of this



publication was not subsequently confirmed: the selectivity of apoptosis induction on Th1 cells. Nowadays, we now know that other T lymphocyte subpopulations are even more sensitive to apoptosis induction by the extracellular gal-9, notably the CD8 Tim-3<sup>+</sup> T lymphocytes (274). The bias of their initial conclusion can be explained by the research route followed by Vijay Kuchroo's team. Their initial aim was to identify a ligand for Tim-3 which was an orphan receptor at the time. They were indeed able to identify gal-9 as a Tim-3 ligand by biochemistry and mass spectrometry methods (272). In addition, at this time, Kuchroo's team focused on the selective expression of Tim-3 by CD4<sup>+</sup> T cells strongly polarized towards a Th1 phenotype. However, this expression is actually much more widespread both in the various T cell sub-populations and also in other cell types. There was already a suggestion that, although T-cell apoptosis was substantially reduced in Tim-3<sup>-/-</sup> transgenic mice, other gal-9 receptors were presumably active at the T-cell surface (272).

### 3.2.2. Inhibitory effects of extracellular gal-9 on CD8<sup>+</sup> T cells

Later on, several research teams have reported the inhibitory effects of gal-9 on CD8<sup>+</sup>T cells. These effects were first demonstrated in a murine allograft model in which exogenous gal-9 induced apoptosis of alloreactive cytotoxic T cells. Indeed, in contrast with naïve CD8<sup>+</sup> T cells, these alloreactive CD8<sup>+</sup> T cells expressed the Tim-3 receptor (305). A few years later, apoptosis induction of CD8<sup>+</sup> T cells expressing Tim-3 by extra-cellular gal-9 was confirmed in a murine model of infection by the Herpes Simplex virus 1 (HSV1) (306,307). Almost concomitantly, the inhibitory effects of gal-9 on CD8<sup>+</sup> Tim-3<sup>+</sup> T cells were also observed in a murine model of AML (acute myeloid leukemia): the C1498 leukemic cells proliferating in syngeneic C57BL/6 mice. The CD8<sup>+</sup> Tim3<sup>+</sup> T-cells also expressed PD1. Consistently, administration of anti-PD1 antibodies was more efficient against C1498 cells in gal-9-KO mice (308). Finally, a few months ago the inhibitory effects of gal-9 on CD8<sup>+</sup> T cells was reported in the murine model of colonic carcinoma MC38 (274) This paper will be extensively commented in the next sub-chapter about gal-9 and Tregs. We have much less information about the influence of gal-9 on CD8<sup>+</sup> T cells in humans. However, Mengshol *et al.* have reported apoptosis induction by extra-cellular gal-9 applied on HCV-specific CTL clones (273). The caspase 8 pathway was involved in this process. Similar observations have been reported for CTLs specific of the HBV (309) All

these publications have emphasized the role of the gal-9/Tim-3 pathways. However, we cannot exclude the contribution of other receptors to gal-9 influence on CD8<sup>+</sup> T cells.

### 3.2.3. Complex influence of extracellular gal-9 on regulatory T cells

During the years following the publication by Zhu *et al.* on gal-9 and Th1 cells (272), there was a series of studies which demonstrating the role of gal-9 in the differentiation and/or expansion of various types of Tregs. One of these first studies was based on a murine experimental model of auto-immune disease: the collagen-induced arthritis (CIA). Both wild-type and gal-9 KO mice were used in this study. The risk of CIA was increased in the absence of endogenous gal-9. Endogenous gal-9 and even more injected exogenous gal-9 were shown to suppress the differentiation of Th17 cells while promoting the regulatory T phenotype. *In vitro*, recombinant gal-9 increased Treg conversion of splenic T-cells in the presence of anti-CD28, TGF- $\beta$  and IL-2 (310). Later on, similar observations were reported in other murine models based on cutaneous allografts or concanavalin-A-induced hepatitis (311,312). In these publications, a contribution of Tim-3 to Treg expansion was often suggested but not demonstrated in a very convincing way. *In vitro* stimulation of human Treg differentiation and/or expansion by recombinant gal-9 in association with TGF- $\beta$ 1 was first reported in 2010 by Mengshol *et al.* in collaboration with our team (273). It was confirmed by several subsequent studies, often in the context of viral hepatitis for example by Ji *et al.* (313). N. Delhem *et al.*, in collaboration with our group, investigated other aspects of gal-9 influence on Tregs, in the context of nasopharyngeal carcinoma (NPC). Exosomes, derived from malignant NPC cells containing gal-9 and CCL-20 chemokine, induced the Treg chemotaxis and also the conversion of CD4<sup>+</sup>CD25<sup>-</sup> T cells into CD4<sup>+</sup>CD25<sup>+</sup>FoxP3<sup>+</sup> cells, with proven suppressive activity therefore identified as Tregs. These newly generated Tregs had a low level of Tim-3 expression. However, in this model, the contribution of gal-9 carried by tumor exosomes was suspected but not formally demonstrated in contrast with CCL20 for which specific neutralizing antibodies were used (314).

One of the first studies attempting to elucidate the molecular mechanisms of gal-9 effects on Tregs, done by K. Lv *et al.* in 2012, showed that extracellular gal-9 was promoting the activation of the Smad pathway triggered by the TGF- $\beta$  in murine CD4<sup>+</sup> T-cells, and especially the phosphorylation of Smad2/3 and their interaction with Smad4 (315). These data were

consolidated soon after by the observation that extracellular gal-9 could interact with CD44 and promoted the formation of a CD44-TGF $\beta$ -R1 complex resulting in enhanced activity of the Smad pathway, stimulation of the CNS1 enhancer upstream of the *FoxP3* gene and expression of the FoxP3 protein (275).

In summary, we can highlight three observations regarding gal-9 and Tregs. First, most of our knowledge was obtained in murine systems. Next, while there is ample evidence that extracellular gal-9 enhances Treg differentiation and/or expansion *in vivo*, when the same effects are investigated *in vitro*, it seems that gal-9 does not act by itself but rather in cooperation with other factors, especially TGF- $\beta$ . Finally, while there is convincing evidence that extracellular gal-9 can contribute to the conversion of peripheral T cells into iTregs, we do not know yet its impact on nTregs.

A major breakthrough of our understanding of the gal-9 and T-regs relationships has been made very recently thanks to the study of Yang *et al.* based on the MC38 (a colon adenocarcinoma cell line) murine tumor model (274). The authors found that by itself a systemic treatment with anti-gal-9 antibodies had only marginal effects on tumor growth while there was a remarkable synergy when they combined the anti-gal-9 with an antibody targeting GITR a molecule preferentially expressed at the surface of Tregs. Investigating why the therapeutic Treg depletion was so important in this setting, they found that endogenous gal-9 depleted not only intra-tumoral Tim3<sup>+</sup>CD8<sup>+</sup> T cells but also Tim3<sup>+</sup>CD25<sup>+</sup>FoxP3<sup>+</sup> Tregs. Therefore, the benefit of increasing the amount of intra-tumoral CD8<sup>+</sup> T cells under administration of the anti-gal-9 is apparent only with a concomitant depletion of Tim-3<sup>+</sup> intra-tumoral Tregs. In other words, the impact of gal-9 on Tregs is bidirectional at least in mice. Gal-9 enhances the differentiation and/or expansion of iTregs but it depletes a population of intra-tumoral Tregs which are Tim-3<sup>+</sup> and highly suppressive.

#### 3.2.4. Indirect effects of extracellular gal-9 on Th2 cells

To our knowledge, there are no direct effects of gal-9 on the differentiation and/or expansion of Th2 cells. However, Th2 cells might undergo indirect effects of gal-9 acting on cells of myeloid origin. For example, gal-9 was reported to bridge IgD to CD44 present at the surface of basophils, resulting in the secretion of cytokines involved in the Th2 response (316). In

metastatic melanomas, gal-9 promoted the Th2 polarization but precise description of the underlying mechanism was not reported (317).

### 3.2.5. Other aspects of galectin-9 interactions with T-cells

Several teams, including my host team, have used other novel approaches not covered by previous citations to investigate the effects of extracellular gal-9 on T cells.

Gooden *et al.* have treated resting human PBMCs (peripheral blood mononuclear cells) *in vitro* with low concentrations of gal-9. A wave of apoptosis was first triggered among the T cells, however, beyond the 3<sup>rd</sup> day, there was an expansion of the surviving T lymphocytes (318). These surviving and proliferating CD4<sup>+</sup> T lymphocytes were predominantly of the CD4<sup>+</sup> “central memory” phenotype, that is CCR7<sup>+</sup> CD45RO<sup>+</sup>. They were also strong producers of IFN- $\gamma$ . The authors claimed that they were Th1 cells but this was not formally demonstrated in the absence of sufficient data on transcription factors and cytokine production.

Investigations carried in my host team were based on the fact that even relatively low concentrations of recombinant gal-9 – around 30nM – induce apoptosis of T cells (both CD4<sup>+</sup> and CD8<sup>+</sup>), even in the absence of Th1 polarization and/or Tim-3 expression (319). With the initial aim to better understand the underlying mechanism of this apoptosis, my team chose to investigate the calcium mobilization induced in target T cells by extra-cellular gal-9 at a very early stage of their stimulation. Genetic ablation of the TCR $\beta$  chain or the CD3 $\zeta$  chain (in Jurkat cells) or blocking of the Lck tyrosine kinase (in fresh PBMCs) resulted in the loss of calcium mobilization without preventing the entry into apoptosis (319). The conclusion was that the induction of apoptosis by recombinant gal-9 was independent of calcium mobilization. One hypothesis was that early calcium mobilization was due to an unspecific TCR stimulation. Finally, it was speculated that for T-cells escaping apoptosis despite long term exposure to gal-9, long term low intensity stimulation of the TCR was one possible additional mechanism to acquire an immunosuppressive phenotype as reported in landmark publications (320,321).

Interestingly Florent Colomb *et al.* took over the hypothesis of our group that gal-9 might deliver unspecific stimulation of the TCR and they tested it in an HIV latency model (322). Given that gal-9 potentially reactivates latent HIV, the authors hypothesize that gal-9 might

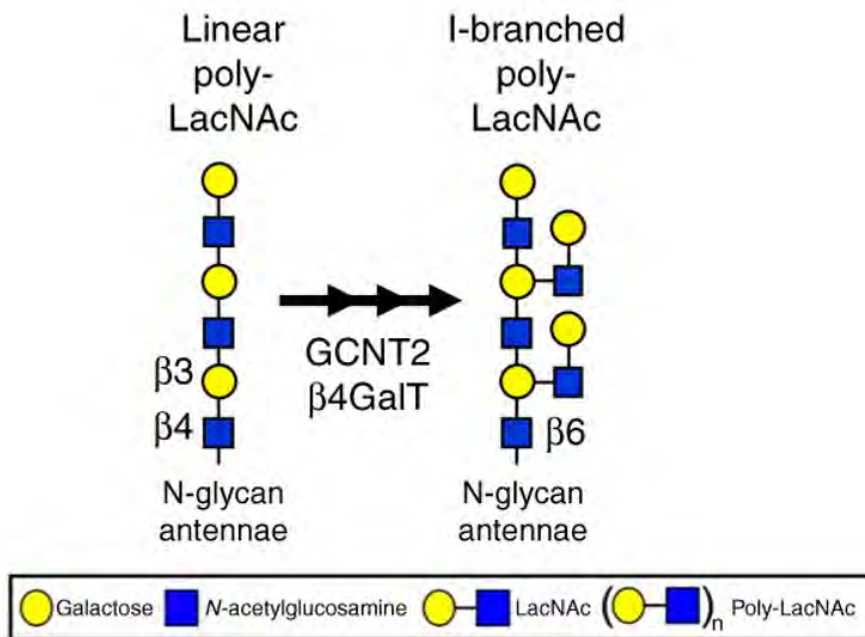


Fig. 19 The glycosyltransferase GCNT2 replaces poly-LacNAc straight chains by multiple short branches of LacNAc units, which is known as the I-branching activity. Adapted from (260)

regulated HIV transcriptional activity by inducing TCR signaling pathways. They observed a reduced gal-9-mediated viral reactivation due to Lck inhibition, whereas the phosphorylation of CD3 $\zeta$  chain was induced by gal-9. Furthermore, gal-9 also increased the phosphorylation of downstream signaling molecules, including ERK1/2 and CREB. Their conclusion was that gal-9 could be a therapeutic instrument for breaking HIV latency in its cellular reservoirs, not accessible to antiviral therapy. However, having in mind the potential immunosuppressive effects of gal-9, this might not be a good idea.

### 3.3. Galectin-9 and B cells

The main information regarding the effect of gal-9 on B cells comes from 2 studies published in 2018 (260,323). Cao *et al.* carefully described how gal-9 regulated BCR-induced signaling. It acted on the surface of cells by bringing together already existing IgM clusters, increasing the size and number of molecules per cluster. This reduced the mobility of IgMs on the cell surface and, together with the limitation of micro-cluster formation, adversely affected B cells activation by specific antigen. In addition, Giovanonne *et al.* showed that gal-9 also bound to the CD45 protein on the B cell surface, blocking calcium signaling and B cell activation by antigens. Remarkably, B cells are producers of gal-9 acting on themselves as an inhibitory factor. This inhibition was exerted in particular on naive and memory B cells. According to Giovanonne *et al.*, this inhibition was lifted at the level of the germinal centers due to a modification in the *N*-glycome of B cells. This modification is characterized by a switch towards glycans carrying branches of the I type at the cell surface, and in particular on the CD45 protein. In other words, linear poly-LacNAc straight chains tend to be replaced by multiple short branches of no more than 3 LacNAc units (*Fig. 19 and 20*). This structure had been initially described for the "adult I" blood group antigen. Indeed, glycans of this type have little affinity for gal-9. Their increased synthesis resulted from the increased expression of an enzyme called  $\beta$ 1-6 *N*-acetylglucosaminyl transferase (260).

Consistent with these mechanistic studies, it is known that gal-9 KO mice exhibit hyperproliferation of B cells leading to high antibody production, associated with an increase in the number of cells in the spleen, lymph nodes, thymus and Peyer's patches (324). This

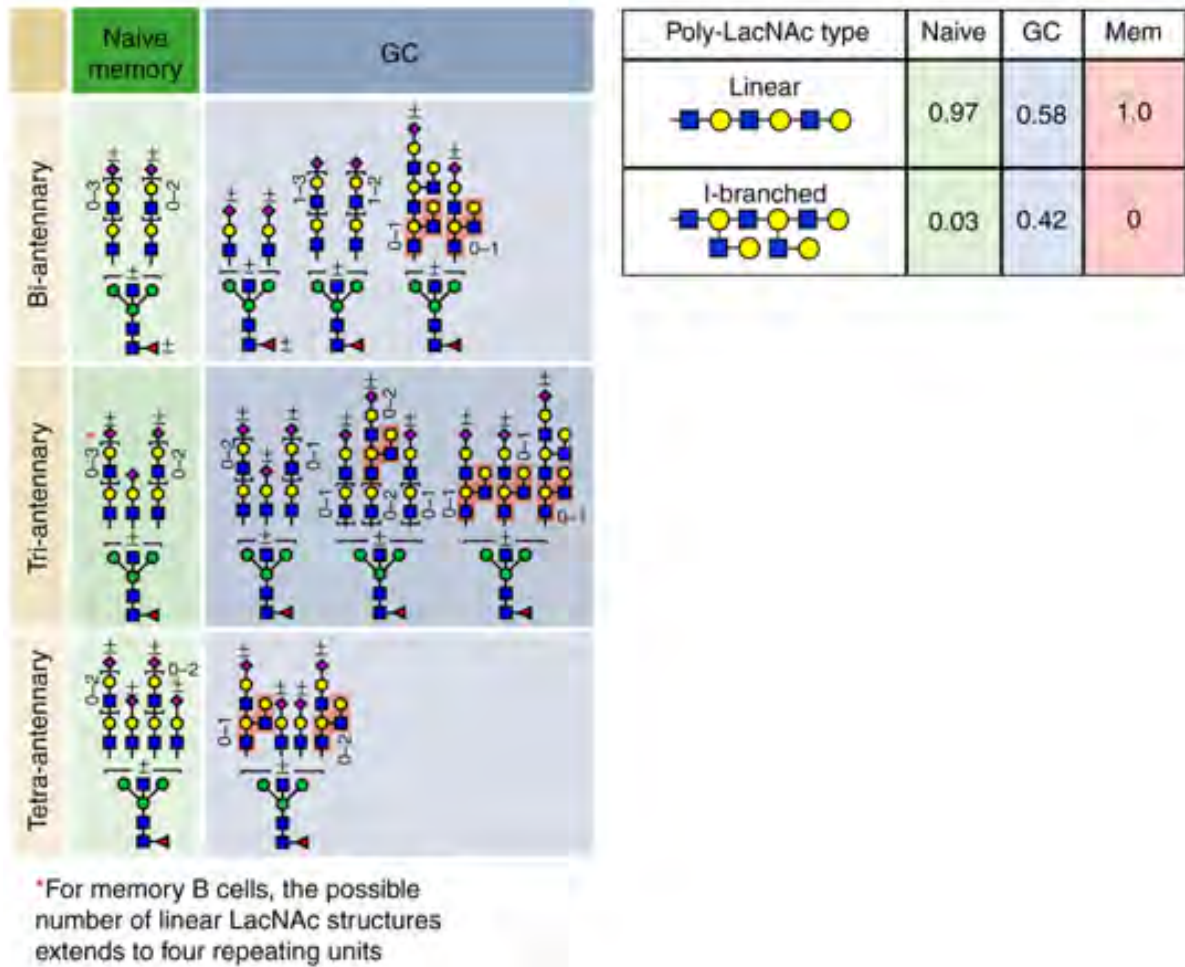


Fig. 20 **N-glycan structures present on naive, GC, and memory B cells.** (Left) Proposed N-glycan structures. Naive and memory B cells are depicted together due to similar N-glycomic features. I-branches are shaded red. A "+/-" signifies that the structure can be found with or without the indicated modification. Numbers indicate number of possible LacNAc units. (Right) Relative quantification of linear vs. I-branched poly-LacNAcs in naive, GC, and memory B cells. *Figure and caption adapted from (260)*

phenomenon could be implicated in the increased susceptibility of these mice to develop autoimmune diseases, such as rheumatoid arthritis (310).

More recently, a study by Chakraborty *et al.* suggested a dual function of galectin-9 towards B cells (325). In a context of gal-9 abundance in high endothelial venules, the authors demonstrated that gal-9 bridged B cells to endothelial cells, leading to a 2.5-fold increase in adhesion, while reducing by 40% the trans-endothelial migration level. RNA-seq analysis of B cells exposed to gal-9 revealed an increase in pathways that dampen cell activation and improve survival, yet the contrary was found for pathways regulating intracellular proteins, organelles and cytoskeleton dynamics. The induction of SLAMF7 gene by gal-9, in particular, suggested a promotion of SLAMF7-mediated inhibitory signals and cell survival, independent of BCR ligation. Together these results implied that gal-9 could bridge B cell to vascular endothelial cells while controlling B cell reactivity with anergic signals.

## 3.4. Galectin-9 and other effectors of the immune system distinct from T- and B-cells

### 3.4.1. Eosinophils

In one of the first publications about Gal-9, named by these authors Ecalectin, it was reported to be a chemoattractant for eosinophils, to improve their survival, and to stimulate their production of superoxides *in vitro* in a Tim-3–dependent manner (326). However, these effects of gal-9 on eosinophils have not been confirmed in subsequent publications, neither by the Hirashima group itself, nor by any other groups.

### 3.4.2. Neutrophils

Gal-9 induces degranulation and stimulates the NADPH oxidase activity of neutrophils. It has also been shown to be able to improve phagocytosis of bacteria of the genus *Pseudomonas Aeruginosa* by facilitating their opsonization (327).



### 3.4.3. Basophils

As already mentioned, Gal-9 is able to bind immunoglobulins of the IgD isotype at the surface of B cells to the CD44 protein present on the surface of basophils. It thus participates in the activation of basophils, leading to the production of IL-4, IL-5 and IL-13 and a subsequent increase in the Th2 response (316).

### 3.4.4. Natural Killer (NK) cells

Extracellular gal-9 functionally impairs natural killer cells in humans and mice as shown by Golden-Mason *et al.* (328). One of the clearest effects is a decrease in IFN- $\gamma$  production upon activation of NK by cytokines or infectious agents. In addition, there is a down-regulation of several genes involved in NK cell-mediated cytotoxicity pathways, for example a reduction in the expression of NCR1/NKp46, NCR3/NKp30, KIR3DL2, perforin 1. Consistently, gal-9 reduces NK cell efficiency in assays of cytotoxicity. In gal-9-KO mice, under viral infection, the number of NK cells producing IFN- $\gamma$  is greater than in WT mice. NK cells are known to express a substantial amount of Tim-3 at their surface at baseline and even more upon activation (329). However, for Golden-Mason *et al.*, gal-9 impairment of NK-cell functions was not blocked by anti-Tim-3 antibodies and not dependent on the level of Tim-3 expression, therefore probably mediated by another membrane receptor (328). Several groups have reported observations and experimental arguments suggesting that the Tim-3/gal-9 axis plays a role in the differentiation of special subsets of NK cells present in the placenta exhibiting immunosuppressive functions required for pregnancy maintenance and progress (330,331). Finally, we can mention a publication highlighting a chemotactic effect of extracellular gal-9 on NK cells which would be in part explained by the activation of the Rho/ROCK1 signaling pathway (332). The authors suggested a link with Tim-3 binding but this was not formally demonstrated. So far, to our knowledge, these data have not been confirmed by other publications.

### 3.4.5. Monocytes / macrophages

The ability of extracellular gal-9 to induce a polarization of macrophages towards an M2 phenotype to the detriment of an M1 phenotype has been reported in several experimental

models and clinical contexts. It is one major aspects of its immunosuppressive activity. Depending on the context, M2 polarization induced by extracellular gal-9 can involve distinct membrane receptors at the surface of macrophages. Zhang *et al.* have investigated the role of the Tim-3/gal-9 axis in the modulation of the phenotype of murine bone-marrow macrophages, stimulated by lipopolysaccharides. They have observed a biphasic effect with high gal-9 production, autocrine stimulation, M2 polarization on the short term (1h to 3h), and reduction of gal-9 expression and preferential M1 polarization on a longer term (up to 24h) (333). In a completely different context, using a mouse model of pancreatic carcinoma, Daley *et al.* have reported M2 polarization of macrophages resulting from gal-9 interaction with a surface protein called Dectin-1. As already mentioned in the subchapter 3.2, Dectin-1 is an innate immune receptor with crucial role for anti-fungal immunity. The SYK tyrosine-kinase is involved in its signaling (65). In this model, the invalidation of Dectin-1 is associated with a decrease in the infiltration by CD206<sup>+</sup> macrophages. Finally, a third study conducted in the context of melanoma has uncovered a direct interaction of gal-9 with CD206 at the surface of macrophages (which had already acquired an M2 phenotype). This interaction resulted in a greater release of FGF2, VEGF and MCP1 (macrophage chemoattractant protein 1) and a decrease in IP10 (CXCL10) secretion (334). Therefore, the interaction of gal-9 with CD206 was suspected to increase angiogenesis. The same study also suggested that gal-9 could favor the expansion of non-classical monocytes (CD14<sup>+</sup>CD16<sup>+</sup> or CD14<sup>-</sup>CD16<sup>+</sup>).

#### 3.4.6. Dendritic cells

Dendritic cells in the intestinal lining play a crucial role in building immune tolerance despite the many antigens present in the lumen of the digestive tract. It seems that gal-9 produced by intestinal cells plays a role in this phenomenon. Indeed, pre-exposure of dendritic cells to gal-9 decreases the expression of CD40 and CD80 in response to stimulation by the LPS (335). Gal-9 also induces an increase in ALDH (Aldehydedehydrogenase) activity in these cells (336). Paradoxically, another much older study showed that the addition of gal-9 to immature dendritic cells derived from cultured monocytes, participated in their differentiation and maturation, in particular by inducing an increase in the level of expression of CD80/86 receptors (337).

In the murine breast cancer model 4T1, intratumoral CD103<sup>+</sup> DCs were found to have a high expression of Tim-3. Administration of an antibody blocking Tim-3 interaction with gal-9 led to efficient tumor suppression. The authors demonstrated that this tumor suppression was due to higher CXCL9 production by CD103<sup>+</sup> DCs and enhanced granzyme B expression by CD8<sup>+</sup> T-cells. Interestingly, anti-gal-9 antibodies were equivalent to anti-Tim-3 in suppressing tumor growth and thought to follow the same mechanism (338).

### 3.4.7. Myeloid-derived Suppressor cells (MDSCs)

The MDSCs are known as heterogeneous CD11b<sup>+</sup> myeloid cells with potent suppressive activity on T cell responses. In mice, there are two categories of MDSCs : granulocytic (Ly-6G<sup>+</sup>) and monocytic (Ly-6C<sup>+</sup>) In a study conducted by Valérie Dardalhon *et al.*, the overexpression of gal-9 resulted in an expansion of CD11b<sup>+</sup> Ly-6G<sup>+</sup> cells and thereby an inhibition of immune responses (339). Moreover, ablation of the Tim-3 gene in Tim-3-KO mice restored normal amounts of CD11b<sup>+</sup> Ly-6G<sup>+</sup> cells and normal immune responses, despite the gal-9 overexpression. The expansion of CD11b<sup>+</sup> Ly-6C<sup>+</sup> MDSCs has been also shown in a murine model of myocarditis (340).

There is also evidence that gal-9 can induce the expansion of MDSCs in the human immune system. as shown by Zhang *et al.* (also involving some members of our group) (341). This study was based on the indirect co-culture of epithelial cells, with or without gal-9 production, and CD33<sup>+</sup> cells from PBMCs as target cells. Gal-9 was acting inside producing cells with induction of cytokine expression and release (especially IL-6 and IL-1-β). Gal-9 was also acting on the extracellular space penetrating in target cells and promoting their differentiation into CD33<sup>+</sup>CD11b<sup>+</sup>HLA-DR<sup>-</sup> MDSCs. At the molecular level, these processes are mainly supported by the degradation of the STING protein which is triggered by a direct interaction with galectin-9. (341)

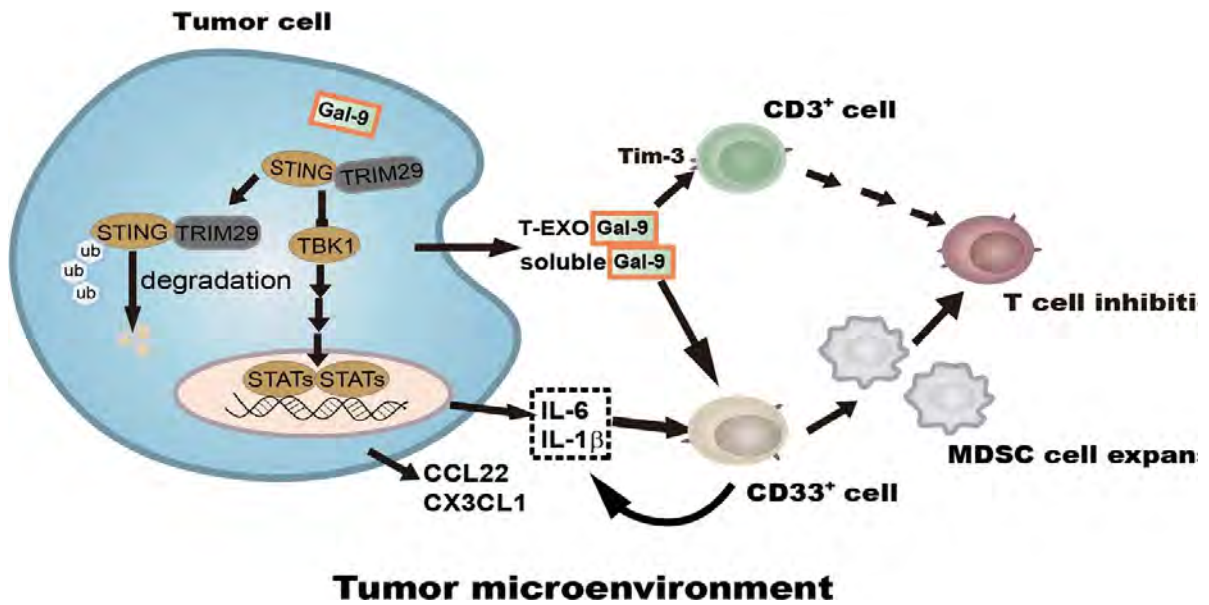


Fig. 21 **The contribution of intracellular and extracellular tumor Gal-9 to the differentiation and expansion of MDSCs and the subsequent inhibition of T-cells.**

Acceleration of STING degradation by Gal-9 inside tumor cells is one key step of this process.

(340)

## 3.5. Galectin-9 in non-tumoral pathologies

### 3.5.1. Autoimmune diseases

Several mouse models allow an exploration of the different contributions of gal-9 in the development of autoimmune diseases. For example, its immunoregulatory activity can be highlighted in KO-gal-9 mice, more sensitive to the induction of autoimmune diseases such as collagen-induced arthritis, a murine model of rheumatoid arthritis (310). Reciprocally, systemic administration of recombinant gal-9 (for example by the intraperitoneal route) limit the severity of the disease and can even prevent its appearance (310,342,343). This also applies to other autoimmune diseases. For example, researchers have reported the therapeutic potential of exogenous gal-9 in a murine model of systemic lupus erythematosus (LEAD). In humans, this disease is characterized by cellular and humoral immune responses directed against various tissues of the body (skin, kidneys, blood cells, lungs, etc.). The model developed on the murine strain MRL-lpr (lupus-prone; mutated in the Fas gene) exhibits this systemic autoimmunity. Systemic treatment with gal-9 reduces the severity of the clinical signs. To explain this outcome, the authors put forward a decrease in the production of autoantibodies due to substantial plasma cell apoptosis (302).

In other settings, the role of gal-9 in the physiopathology of autoimmune disorders is more difficult to understand. Indeed, gal-9 treatment could be beneficial, even in models where there is an increase in gal-9 production; for example, in murine asthma models, in which the amount of gal-9 was reported to be increased in the lung tissues (344–348). In this context, the beneficial effects of the administered gal-9 might result from its impact at the systemic level while remaining deleterious at the pulmonary level. This hypothesis would deserve in-depth studies. In human inflammatory diseases with an autoimmune component, we find the same complexity since in several cases an increase in gal-9 abundance is observed in inflamed tissues. For example, in patients with rheumatoid arthritis, the concentration of gal-9 tends to increase in the synovial fluid as well as in cells derived from the synovial tissue (fibroblasts, endothelial cells, macrophages, T and B cells) (342,349). In patients with LEAD there is also an increase in gal-9 concentration in PBMCs and plasma. In some pathologies, the level of gal-9

is even correlated with the severity of the disease (350,351). This is the case for atopic dermatitis, a condition in which the increased level of gal-9 is visible in the plasma of patients (352,353). In the latter pathology, as well as in some other autoimmune diseases, there is an accumulation of certain granulocytes, especially eosinophils (354). This observation is even more interesting since research has shown that gal-9 promotes citrullination (conversion of arginine to citrulline) of intracellular proteins in granulocytes (355). Indeed, this phenomenon has been mentioned several times as responsible for the production of autoantibodies by generating abnormally citrullinated proteins recognized as neo(auto)-antigens.

### 3.5.2. Viral infections

Many studies have focused on alterations of gal-9 production and functions in the context of numerous viral infections, either acute or chronic, localized or systemic, in humans as well as in animal models. Viral hepatitis related to HBV and HCV are probably the viral infections where the role of gal-9 has been most studied. Plasma gal-9 concentrations are increased in patients infected with HBV and HCV (285,356). This increase is also correlated with an expansion of Tregs and a decrease in the inflammatory response (309,357). In some ways, these effects are beneficial since they limit the damage caused by inflammation during infection, but they can also carry the risk of an insufficient immune response. It also appears that a high concentration of gal-9 in plasma increases the risk of progressing to chronic infection (358). One study even reports an even higher concentration of circulating gal-9 in HCV-infected patients who developed hepatocellular carcinoma (273).

There is also a marked increase in the concentration of circulating gal-9 during primary infection with HIV (359). This plasma gal-9 concentration is positively correlated with the patient's viremia. This has been confirmed by a recent study showing higher concentrations of plasma gal-9 for untreated AIDS patients from Philippines by comparison with healthy donors and tuberculosis patients free of AIDS (265). The authors were able to assess plasma concentrations for both full-length gal-9 and a truncated form roughly identical to the NCRD. This truncated form is generated mainly by the cleavage of the linker peptide (76). Plasma concentrations of both full length and truncated forms were increased in AIDS with

greater risk of death for the highest concentrations (265). More strikingly, even in the chronic phase of AIDS, the plasma concentration of gal-9, although lower than in the acute phase, remains higher than in healthy subjects. According to Tendon *et al.*, this remains true even after restoration of the circulating CD4<sup>+</sup> T cell level under tri-therapy (360). As mentioned in the subchapter 3.2 about gal-9 and T cells, HIV specialists are interested in gal-9 for other reasons. Several publications show that exogenous gal-9 can trigger the reversal of virus latency in vitro (361). This reactivation is thought to be due to a modulation of the viral gene transcription, dependent on the activation of the TCR, and involving the ERK1/2 kinases as well as the transcription factor CREB (322). This scenario is therefore different from those presented above, since reactivation does not a priori involve a decrease in the immune response, but a direct effect on the infected T cells. The persistence of HIV in latent form in certain cellular reservoirs represents a major obstacle to the complete eradication of the virus. Thus, treatment with gal-, in conjunction with anti-retroviral therapy, may be of benefit in the fight against infection. At least, that's what some researchers suggest, who also point to the inducing effect of gal-9 on the APOBEC3 protein (361). Indeed, this protein exerts a strong anti-retroviral effect by catalyzing single-stranded cytidine deamination reactions, inducing hypermutations which decrease the infectivity of the virus (361). However, the fact that gal-9 has a direct positive effect on the penetration of the virus into cells still free from infection, could represent a difficult obstacle to overcome in implementing this approach (304).

Increased plasma concentrations of gal-9 were also observed in acute viral infections, for example in the context of influenza. A study made on 43 influenza patients has shown a mean gal-9 plasmatic concentration about ten-fold greater than in healthy donors and 3-fold higher than in patients with pneumococcal infection (362). It is interesting to connect these clinical observations with the results of experiments made using a murine model of influenza A. In this model, inhibition of gal-9 improves the anti-viral response and even the vaccination process (363).

Gal-9 is also suspected to promote the reactivation of HSV1 in latently infected nerve cells. HSV-1 persists in the trigeminal ganglion and would be maintained in a latency phase, in particular thanks to the surveillance exercised by the CD8<sup>+</sup> T cells. Through apoptosis of CD8<sup>+</sup>

T cells, gal-9 could favor a reactivation of the virus (306,360).

On the other hand, in experimental HSV1 infections performed in mice, administration of gal-9 reduces inflammation as well as corneal scar lesions (307). This is probably due to the fact that, in this model, scar lesions result to a large extent from excessive activity of certain immune cells. The reduction of scar lesions would therefore not be due to the virus inactivation but rather to an attenuation of the inflammatory response.

In conclusion, enhanced production of gal-9 is often detected in the context of viral infections in the infected tissue as well as at the systemic level, with often greater concentrations of circulating gal-9. Gal-9 inflammatory effects seem to be often required at some stages of the immune response, but their excess may favor unwanted scar lesions. Reciprocally, the immune suppressive effects of gal-9 may compromise virus elimination and favor a lethal issue or the persistence of a chronic viral infection. Galectin-9 has also a role in some human bacterial infections, for example in tuberculosis, but this is beyond the scope of this bibliographical introduction (364).

## 3.6. Galectin-9 in cancer

### 3.6.1. Galectin-9 and cancer: avoiding some pitfalls

There is an abundant literature on the topic of galectin-9 and cancer, with initial publications dating back more than twenty years. However, this literature is confusing at first glance because the reader faces many data which seem to be contradictory. Sometimes there are clinical and experimental data which suggest that an abundant expression of gal-9 supports tumor aggressiveness and signals a poor prognosis. Sometimes, it is just the opposite. These apparent contradictions often arise for the same type of malignant disease for example melanomas (317,334,365,366). However, there are two important distinctions to be done to find a rationale in all publications on this topic. First, we must distinguish gal-9 produced by the malignant cells and that produced by the infiltrating or stromal cells. Next, it is important to differentiate cell-associated gal-9 (cytoplasmic, nuclear or at the surface of the plasma membrane) from extracellular gal-9.



Unfortunately, we rarely, if ever, have a direct measurement of the different amounts of gal-9 related to a malignant process: the total quantity produced by the malignant cells, the amounts of the cell-associated and extracellular gal-9, respectively. . We can merely estimate that the gal-9 detected by immunohistochemistry on tumor sections is an index of the cell-associated one while its concentration in the circulation, especially in the plasma, is an indication of the global extracellular gal-9 release.

A further degree of complexity may relate to the expression of the different isoforms of gal-9. As a reminder, gal-9 is expressed in three main isoforms: gal-9L, M and S. These differ in length, stability and activity. It is still unclear whether there are any functional differences between these three isoforms, other than greater stability for the short form. A more developed knowledge of these isoforms could help us to better understand whether gal-9 can have a positive or a negative contribution in tumor development.

Finally, we should note that in our experience, there is neither excellent antibody for the detection of gal-9 on tissue sections by IHC nor standardization of the detection methods. This can be an additional factor of confusion.

### 3.6.2. Overview and discussion of the anti-tumoral effects of gal-9

There are a number of reports dealing with various tumor types suggesting that abundance of intratumoral gal-9 assessed on histological sections is linked to a good prognosis. This is for example the conclusion of a meta-analysis based on 14 previous studies involving a total of 2326 patients (367). In the light of the reflections made in the previous subchapter, let us consider the case of cervix carcinomas in which a decrease in gal-9 expression at the tumor level correlates with a more severe histological grade of the disease according to a publication by Liang *et al.* (368). However, a puzzling point of this study, is the fact that the abundance of gal-9 is lower for carcinomas *in situ*, than for invasive low-grade carcinomas. This study does not take in account the immune-suppressive effects of extracellular gal-9. It is focused on intrinsic process occurring inside the malignant cells. It shows parallel decreases of E-cadherin and gal-9 expressions. Other studies report similar observations, without establishing a causal relationship between them. This is compatible with observations made for Head and Neck

carcinomas, where researchers have reported a low amount of gal-9 in tumoral tissues, while in the corresponding healthy tissues, they usually observe a very specific distribution of the protein at the level of the basement membrane. This suggests a link between the gal-9 expression and tissue differentiation (369). A complementary study reports in this same type of tumors a decrease in the expression of E-cadherin, by comparison with the basal and para-basal layers of the mucosa (370). The fact that this protein is involved in the maintenance of cell-cell bonds, is compatible with the idea of an increased metastatic potential associated to the decrease in gal-9 expression.

The idea that a low abundance of gal-9 in tumor tissue may promote the metastatic process is supported by several publications suggesting that the decrease in gal-9 expression increases the invasive potential of tumor cells. The best-known studies on this topic concern breast cancer. An often-cited study, published by Irie *et al.* in 2005, evaluated the abundance of gal-9 in sections of tumor tissue, for approximately 84 patients in a prospective series. The authors found an inverse correlation between the abundance of gal-9 and the frequency of metastatic relapses (371). In the same article, the authors compared MCF7 cells with strong or weak expression of gal-9. They observed a trend towards stronger aggregation for cells with high gal-9 expression both *in vitro* and in nude mouse tumors. Indeed, in the absence of gal-9 in these transplanted tumors, the malignant cells were divided into small islands within the stroma. However, breast cancer represents a good example of a situation where the pleomorphic and often divergent effects of gal-9 make it difficult to assess its overall impact on the tumor process, and, *a fortiori*, to use the abundance of gal-9 in tumor tissue as a prognostic factor. Indeed, a more recent study reports that, in breast cancers, gal-9/Tim-3 signaling on the surface of intratumoral dendritic cells inhibits their CXCL9 production, which leads to reduced activity of intratumoral CD8<sup>+</sup> T lymphocytes (372).

Other types of cancer present this complexity and this divergence between intrinsic anti-tumor effects inside the tumor cells ("cell-autonomous") and pro-tumor effects linked to the inhibition of effectors of the immune system in the tumor microenvironment. Thus, regarding melanoma, an often-cited study by Kageshita *et al.* (2002) tends to prove that intracellular gal-9 has an anti-metastatic effect, mainly on the basis of experiments performed *in vitro* (365). These authors report cell aggregation and apoptosis when melanoma cell lines are treated *in*

*in vitro* with recombinant gal-9. However apoptosis induction is significant only for high concentrations of recombinant gal-9 in the range of 300 nM which is beyond the physiological concentrations (same remark concerning a more recent publication on the same topic by Wiersma *et al.* 2012) (366). Clinically, Kageshita's study showed lower gal-9 abundance in malignant melanoma cells than in melanocytes from benign nevi, and a better prognosis for high gal-9 abundance in malignant cells on tumor tissue sections. A work carried out more recently on murine models – B16 melanoma and CT26 colonic carcinoma – gave results which go in the same direction: with supposed anti-metastatic effects of extracellular gal-9 *in vitro* (blocking of adhesion to the extracellular matrix), and *in vivo* – (decrease in pulmonary metastases resulting from intravenous injection of malignant cells) (373). Again, the concentrations of recombinant gal-9 used *in vitro* were very high.

In contrast, studies carried out on clinical specimens of metastatic melanoma have shown the following facts: a higher plasma gal-9 concentration in patients than in healthy controls, a worse outcome for patients with highest plasma concentrations and a stronger polarization of circulating lymphocytes towards a Th2 phenotype in these patients (317). In the patients with elevated plasma gal-9 concentration, gal-9 production is observed in malignant cells only at the tumor invasion front. This underlines the fact that the production of gal-9 may not have the same meaning depending on where it is generated. Thus, the expression of gal-9 by infiltrating DCs in metastatic melanomas was reported as predictive of a better response to adoptive transfer of T lymphocytes (374). In summary, in metastatic melanoma, the deleterious production of gal-9 is thought to come mainly from the malignant cells of the invasion front. This would explain, at least in part, the apparent contradiction between the study of Kageshita *et al.* and Wiermsa and those of Enninga *et al.* (317,334,365,366).

In lung cancer, a 2020 study found that high and low gal-9 concentrations in infiltrating and malignant cells, respectively, were associated with a poor prognosis (375). Finally, in the pancreatic carcinoma, it is also interesting to note that the increase in gal-9 expression is not constant during tumor development. Indeed, it appears to increase during stages II and III, before decreasing in stage IV of the disease (376).

*In vitro*, recombinant gal-9 was reported to induce selective cell death of colonic carcinoma cells bearing K-ras mutation. This cell death occurs in a context of “frustrated autophagy”

meaning that there is a blockade of the fusion of autophagosomes with lysosomes, autophagosome accumulation, swelling of lysosomes and cell death (377). Again, the gal-9 concentrations used in this study were well beyond physiological concentrations (300 nM).

Finally, we must point out the very specific case of some mesothelioma cells, where gal-9 binding at the surface of malignant cells impairs their proliferation and survival. In this context, gal-9 has no spontaneous antitumor effect. However, its binding at the cell surface by a monoclonal antibody specific for the CCRD (P4D2) induces reduced proliferation and even apoptosis in a fraction of 15 to 35% of the cells. This is observed when using either human or murine mesothelioma cell lines. No data are provided regarding fresh human mesothelioma cells. In contrast, another antibody specific for the NCRD (P1D9) does not have the same effect (378). It is not known whether similar phenomena can occur for other cell types either tumoral or not.

### 3.6.3. Pro-tumoral effects of galectin-9

As already mentioned in the previous sub-chapter, most pro-tumoral effects of gal-9 are related to its immunosuppressive effects. These effects have been first reported in human malignancies with a viral etiologic component, namely nasopharyngeal carcinoma involving latent EBV-infection and hepatocellular carcinoma associated to HBV or HCV (92,235). Later on, they were found in a wide range of malignancies unrelated to virus infection, including melanoma (as mentioned in the previous subchapter), pancreatic adenocarcinomas, renal and lung carcinomas, malignant gliomas, and head and neck carcinomas distinct from NPCs. In addition, there are two types of human malignancies where gal-9 has a direct oncogenic activity, in addition to its immunosuppressive action: acute myeloid leukemia and mesotheliomas.

As previously mentioned, in metastatic melanoma, intratumoral gal-9 is mainly produced by tumor cells located at the invasion front. High gal-9 concentration in the plasma is linked with a pejorative outcome. One pro-tumoral effect exerted by gal-9 in melanoma microenvironment is to favor the M2 polarization of macrophages. This modification results, at least in part, from a direct interaction of gal-9 with CD206 at the surface of the target macrophages. In addition, gal-9 induces Th2 polarization of T lymphocytes inside the tumor

microenvironment and at the systemic level (317,334).

The contribution of gal-9 to the development of pancreatic ductal adenocarcinoma (PDAC) has been mainly investigated by George Miller's team at the New York University. They have found that in pancreatic carcinomas, gal-9 is mainly derived from a particular variety of  $\gamma\delta$  T cells with suppressive activity. The same cells also express PD-L1 and thus significantly restrict the activation of  $\alpha\beta$  T cells (379). Again, tumor-associated macrophages are critical targets of gal-9 in PDAC. These publications related to PDAC have emphasized the interaction of gal-9 with Dectin-1 at the surface of tumor macrophages. This interaction induces M2 polarization, mediated at least in part by the activation of the SYK tyrosine kinase (65). In subjects with pancreatic carcinomas, the serum concentration of gal-9 is higher on average than in healthy subjects or subjects with benign lesions of the pancreas. In addition, a high level of concentration has a poor prognostic value in subjects with stage IV tumors (376).

In renal cell carcinoma, the high expression of galectin-9 is correlated to a lower rate of recurrence-free survival (380). According to Ohue *et al.*, in NSCLCs (non-small cell lung carcinomas), a strong expression of gal-9 by malignant cells is associated with a higher risk of pejorative outcome, in contrast to what is found for PD-L1 (381). In addition, J. Gao *et al.* have shown that subjects bearing NSCLCs have higher concentrations of plasma exosomes carrying the Tim-3 and gal-9 proteins than healthy donors, this being more marked for squamous cell carcinomas than for adenocarcinomas (382).

Gal-9 expression is frequently seen in malignant glioma cells while it is almost completely undetectable in normal brain cells. It is more abundant in stage IV than in stages III or II tumors. Usually there is a concomitant high expression of the Tim-3 receptor by infiltrating and peripheral CD4<sup>+</sup> and CD8<sup>+</sup> T lymphocytes (381,383–385).

With regard to HNSCCs, a strong expression of gal-9 by CD4<sup>+</sup> infiltrating lymphocytes has been reported for carcinoma of the oropharynx linked to HPV (386).

As previously mentioned, there is evidence that in AML (acute myeloid leukemia) gal-9 has a direct oncogenic contribution in addition to its immunosuppressive effect (387). In an elegant study, Kikushige *et al.* have shown that gal-9 secreted by mature leukemic cells engages the Tim-3 receptor at the surface of leukemic stem cells, and thus enhances their self-renewal.

This autocrine loop is one example of the indirect participation of mature leukemic cells in the mechanism of indefinite malignant proliferation (388). Nuclear translocation of  $\beta$ -catenin is one of the signaling mechanisms activated by gal-9 binding to Tim-3 at the surface of CD34<sup>+</sup> leukemic cells.

### 3.6.4. Gal-9 in the context of tumor therapeutics

#### Chemotherapy

Numerous publications have demonstrated an increase in the expression of gal-9 in tumor cells under the effect of the drugs used in chemotherapy. This effect was shown for a wide variety of malignancies and drugs. Yoon *et al.* have reported an increased expression of gal-9 in the MDA-MB-231 breast carcinoma cell line subjected to paclitaxel (10 nM), and to a lesser extent to doxorubicin and epirubicin (0.5  $\mu$ M) (389). This effect was not observed in the HS578T breast carcinoma cell line. The authors have investigated by IHC on breast tumor biopsies, collected before and after a neoadjuvant treatment in 13 patients. Gal-9 abundance was modified in 4 cases of basal-like tumors, with either an increased or a decreased expression (two cases each). These data are consistent with the fact that, in murine models of triple negative or luminal B breast carcinomas, there is a cooperative anti-tumor effect of anti-Tim-3 or anti-gal-9 antibodies, combined to paclitaxel (372). A more recent publication highlighted an increase in gal-9 expression under the influence of chemotherapy in cells derived from liver metastases of colorectal cancer without microsatellite instability (Jabbari, Kenerson *et al.* 2020) (390). Their experimental system was based on *ex vivo* cultures of sliced tumoroids which made it possible to maintain for 4 to 6 weeks a microenvironment similar to what exists in the tumor *in situ*. Single cell RNA-seq analyzes allow to distinguish two classes of tumors, according to the predominant phenotype of malignant epithelial cells, suggestive either of stem cells or enterocytes. In the second case, the application of Iritonecan or Oxaliplatin induced a strong expression of gal-9. Remarkably, the simultaneous application of a Tim-3 blocking antibody resulted in a synergistic anti-tumor effect.

#### Checkpoint inhibitors

There is evidence about gal-9 contribution to secondary and even primary resistance to immune checkpoint inhibitors mainly in the context of non-small cell lung carcinomas

(NSCLCs). Koyama *et al.* have investigated secondary resistance to anti-PD1 antibodies in two murine transgenic models of NSCLCs, based on inducible expression of either EGFR or a mutated form of K-ras (G12D) (391). Both models allowed investigations of lung tumors arising in immunocompetent animals. High expression of gal-9 was measured in malignant cells from K-ras-related tumors, where progression was observed after 8 to 10 weeks of treatment with anti-PD1 antibody. Consistently, better tumor responses were obtained under sequential treatment by anti-PD1, followed by anti-Tim-3 antibodies. In contrast, gal-9 was not involved in secondary resistance of EGFR-related tumors. They also investigated clinical human samples and reported about 4 times higher concentrations of gal-9, in pleural effusions of 2 lung carcinoma patients with secondary resistance to anti-PD1, by comparison with 4 patients not previously treated with anti-PD1 (Koyama, Akbay *et al.* 2016). Consistent observations were made in a cohort of 61 metastatic NSCLC patients by a group from Dijon (392). They analyzed various populations of circulating lymphoid and myeloid cells by flow cytometry (176 variables). They found that accumulation of lymphoid cells and monocytic MDSC (mMDSC) expressing, respectively, Tim-3 and galectin-9, was often concomitant of the resistance to PD-1 blockade, both for patients with primary or acquired secondary resistance. In addition, using PBMCs from patients, they were able to show that, *in vitro* treatment combining anti-PD1 and anti-Tim-3 antibodies induced interferon- $\gamma$  secretion by CD8<sup>+</sup> T cells, which was not the case with anti-PD1 or anti-Tim-3 used as single agents.

### **CAR-T cells**

Some experimental studies suggest that gal-9 produced by malignant cells may contribute to inhibit the antitumor effects of CAR-T-cells. For example, this has been reported in a study based on human pancreatic tumors xenografted in immunodeficient mice (393).

#### **3.6.5. Deregulation of gal-9 expression in a tumor context**

Data in the literature do not describe mutations or polymorphisms in the gal-9 gene associated with tumor development, as may be the case in rheumatoid arthritis (394). On the other hand, several studies have looked at the modification of the methylation profile of this gene and the expression of regulatory microRNAs. A comprehensive study looked at the analysis of the methylation profile of the gal-9 gene in melanoma cells. This study gives clues to understand

the origin of expressed gal-9, by separated observations of melanocytes and the various infiltrating cells (monocytes, CD4<sup>+</sup> and CD8<sup>+</sup> T lymphocytes, B lymphocytes and granulocytes). The authors have identified a relatively low level of methylation in leukocytes, unlike melanocytes, which exhibit a significant level of methylation in the promoter region (395). This phenomenon does not appear to be redundant from one tissue to another since studies conducted on colorectal cancers do not report changes in DNA methylation or in histones associated with the *LGALS9* gene (396). Informations relating to the deregulation of protein expression in this context, further describe a post-transcriptional regulation by microRNAs. One of the candidates put forward is miR-455-5p, whose production is significantly increased in tumor tissues, which at the same time show a significant reduction in gal-9. These data are currently only supported by *in vitro* tests on a tumor line of colonic origin, in which the recognition of the 3'UTR region (untranslated transcribed region) of the transcript by the miR has been verified (397). Another miR potentially involved in the regulation of gal-9 expression, miR-22, appears to be downregulated in hepatic carcinoma (398).

Of course, many of the functions performed by gal-9 depend on its ability to recognize specific polysaccharides. Even simple modifications of the glycans, caused by epigenetic alterations, for example which lead to the modification of glycosyltransferases expression or activity, can directly impact the sensitivity of cells to the signaling induced by gal-9 (399). However, there is no study yet reporting concrete examples of this type of modification related to gal-9, in a tumor context.



# Results

# Article 1

---

## 1. Introduction

During the years 2014-2016, studies had been carried out in our team regarding T-cell response of human T lymphocytes to *in vitro* treatment with recombinant gal-9. This topic was the subject of Claire Lhuillier's PhD thesis (319). This work was carried out in collaboration with Olivier Dellis, a renowned specialist in calcium flux, especially in immune cells (Inserm, Orsay, France). Experiments had been carried out both on cells of the Jurkat cell line and on T-cells of the peripheral blood from normal donors. The initial objective was to elucidate the mechanisms of the apoptosis induced by gal-9 in T lymphocytes. Initially Claire Lhuillier *et al.* demonstrated calcium mobilization triggered in less than one minute inside the T lymphocytes by the addition of recombinant gal-9 (it did not require the expression of Tim-3 at the plasma membrane). However, they quickly observed that this calcium mobilization was not necessary to trigger T-cell apoptosis. Indeed, the early calcium mobilization was abolished in Jurkat cells knocked-out for the tyrosine Lck or for various components of the CD3/TCR complex while a large fraction of these cells was still undergoing apoptosis under gal-9 treatment a few hours later exactly like wild-type cells. The same was true for peripheral T-cell challenged by recombinant gal-9 in presence of an Lck chemical inhibitor. However, even for wild-type Jurkat cells, not all the cells were entering apoptosis. Therefore, at the end of Claire Lhuillier's thesis, the following questions were remaining pending: 1) what is the long-term fate of T-cells challenged by gal-9 and resisting apoptosis; 2) does the activation of signaling pathways related to TCR activation by gal-9 results in some phenotypic conversion. In the following years, a partial response was given to the second question by Florent Colomb *et al.* They showed that addition of gal-9 to T-cells latently infected by HIV resulted in partial viral reactivation. This reactivation was antagonized by various signaling inhibitors including Lck, Erk and CREB inhibitors (322). Nevertheless, in 2018, at the beginning of my PhD thesis, the

phenotypic and functional characteristics of healthy T-cells surviving to gal-9 treatment were still poorly known.

In this first part of my thesis, the objective is to undertake this characterization using in as much as possible unbiased, largescale approaches like transcriptional profiling by RNAseq and multidimensional mass cytometry. My first approach was based on mass cytometry using a panel of 26 antibodies aiming at a broad scanning of major phenotypes and functions of T-cells. However, this panel did not contain any antibody related to follicular T-cells and this first series of CyTOF analysis was to some extent misleading. We got some clues about a relative expansion of Th2<sup>+</sup> CD4<sup>+</sup> cells following gal-9 treatment, but this was not confirmed when we resorted to Gata-3 staining by conventional cytometry (Gata-3 was not in the initial CyTOF panel). Fortunately, we were able to apply transcriptional profiling by RNA seq to T-cells surviving gal-9 challenge a few months later and thanks to multiple approaches of data analysis (I was able to profit from the first Covid-19 lock-down to learn R language). I was able to detect the transcriptional enhancement of several markers of follicular T-cells, especially CXCR5. Taking advantage of this result, we decided to come back to mass spectrometry with a new panel of 21 antibodies more focused on follicular T-cell markers. As explained in the manuscript, using these new tools, I was more successful and could confirm the induction of follicular T-cell markers resulting from gal-9 exposure.

## 2. Manuscript

## **Sustained exposure to extra-cellular galectin-9 promotes the differentiation of diverse CXCR5-positive follicular T-cells**

Thi-Bao-Tram Tran<sup>1</sup>, Aurore Gelin<sup>1</sup>, Valentin Baloche<sup>1</sup>, Philippe Rameau<sup>2</sup>, Cyril Catelain<sup>2</sup>, M'Boyba Khadija Diop<sup>3</sup>, Alexia Alfaro<sup>2</sup>, Muriel Gaudry<sup>4</sup>, Jiang Li<sup>5</sup>, Toshiro Niki<sup>6</sup>, Pierre Busson<sup>1</sup>

<sup>1</sup> CNRS, UMR 9018, Gustave Roussy and Université Paris-Saclay, 39 rue Camille Desmoulins, F-94805 Villejuif, France.

<sup>2</sup> Imaging and Flow Cytometry platform PFIC, Gustave Roussy, 39 rue Camille Desmoulins, F-94805 Villejuif, France.

<sup>3</sup> Plateforme de Bioinformatique, UMS AMMICA, Gustave Roussy, 39 rue Camille Desmoulins, F-94805 Villejuif, France.

(Plateforme d'évaluation préclinique, Gustave Roussy, 39 rue Camille Desmoulins, F-94805 Villejuif, France).

<sup>4</sup> Biologie des Leucémies de l'Enfant, Inserm, Gustave Roussy and Université Paris-Saclay, 39 rue Camille Desmoulins, F-94805 Villejuif, France.

<sup>5</sup> Department of Biotherapy, Sun Yat-sen University Cancer Center, Sun Yat-sen University, Guangzhou 510060, P. R. China

<sup>6</sup> Department of Immunology, Kagawa University, Kita-gun, Kagawa 7610793, Japan.

**Running Title:** Galectin-9 and follicular T-cells

**Key words:** Galectin-9, follicular T-cells

### **Contact**

Pierre Busson  
CNRS, UMR 9018, Gustave Roussy and Université Paris-Saclay  
39, rue Camille Desmoulins  
94 805 Villejuif, France  
Phone: +33 1 42 11 45 83 Fax: +33 1 42 11 52 45  
[Pierre.busson@gustaveroussy.fr](mailto:Pierre.busson@gustaveroussy.fr)

## Abstract

Prolonged exposure of T-cells to extra-cellular gal-9 is known to frequently occur in physiological and pathological conditions for example in the light zone of germinal centers inside secondary lymphoid organs. Its repercussions deserve further investigations. *In vitro*, exposure of activated T-cells to extra-cellular galectin-9 (gal-9) is known to induce partial cell death and various types of phenotypic conversions in surviving cells. We undertake a comprehensive and systematic investigation of these phenotypic modifications using T-cells derived from PBMCs treated with CD3/CD28 stimulation for 7 days with or without addition of recombinant gal-9. Gal-9-exposed and gal-9-naïve T-cells recovered at day 7 by magnetic sorting were then subjected to various comparative investigations including transcription profiling by RNAseq and multidimensional mass cytometry. Beside some phenotypic changes already reported in previous publications like a major decrease in CD8<sup>+</sup> cell subsets, one novel remarkable observation was the emergence of various phenotypes reminiscent of follicular (T<sub>f</sub>) T-cells. CXCR5 was the T<sub>f</sub> marker most consistently induced by initial gal-9 exposure. Its transcription was further increased by one additional gal-9 boost on isolated T-cells. Consistently, CXCR5 and CD40L were expressed at a higher level in splenic T-cells from wild type mice than from gal-9-KO transgenic mice. The CXCR5 T<sub>f</sub>-like T-cells resulting from gal-9 exposure *in vitro* were heterogeneous with a mix of CXCR5<sup>+</sup>/CD40L<sup>+</sup>/FoxP3<sup>-</sup>, CXCR5<sup>+</sup>/CD40L<sup>+</sup>/FoxP3<sup>-</sup> and CXCR5<sup>+</sup>/FoxP3<sup>+</sup>/CD40L<sup>-</sup>. Despite this phenotypic heterogeneity, gal-9-exposed- were more efficient than gal-9-naïve T-cells to protect B-cells from apoptosis. Gal-9 acting directly on B-cell was already known to increase the threshold of their activation in germinal center thus playing a role in the regulation of autoimmunity. Our data suggest another aspect of their action in germinal centers which is to enhance the differentiation of T<sub>f</sub> cells and thus to favor the maturation of B-cells targeting non-self-antigens.

## 1. Introduction

Galectins are a family of animal lectins sharing the capacity to bind  $\beta$ -galactosides contained in glycans carried by glycoproteins or glycolipids (Gooden, Wiersma et al. 2013, Johannes, Jacob et al. 2018). Their binding partners are inside the cells, at the cell surface or in the extra-cellular matrix. Each galectin contains one or two Carbohydrate Recognition Domains (CRD) which contain amino-acids directly involved in the interaction with the galactoside. Other amino-acids inside or outside the CRDs interact with distinct non-galactosidic parts of galectin partners. These additional interactions support the specificity of each galectin. Although devoid of signal sequences, several galectins can be released in the extra-cellular space by non-classical processes like membrane translocation or incorporation into secreted vesicles. Galectin-9 (gal-9) belongs to the category of "tandem repeats" galectins (John and Mishra 2016). Intra-cellular gal-9 has various functions, for example a role in the maintenance of cell polarity (Mishra, Grzybek et al. 2010, Mo, Costa et al. 2012). Extra-cellular gal-9 often behaves like a cytokine with multiple immunomodulatory functions. For example, it induces M2 polarization of macrophages through its interaction with 2 membrane receptors, Dectin-1 and CD206 (Daley, Mani et al. 2017, Enninga, Chatzopoulos et al. 2018). It impairs NK cell cytotoxicity and stimulates the expansion of MDSCs at least in part through its binding to the Tim-3 receptor (Dardalhon, Anderson et al. 2010, Golden-Mason, McMahan et al. 2013, Zhang, Huang et al. 2020). Gal-9 also affects B-cell functions. It antagonizes BCR signaling and B-cell activation (Cao, Alluqmani et al. 2018, Giovannone, Liang et al. 2018). Using murine cells, LK Smith *et al.* have shown that the inhibition of the BCR signaling by gal-9 can be achieved in different ways depending on the subtype of B-cells. For B-2 B cells, it is done by mediating the interaction between the IgM BCR and the negative co-receptors CD22 and CD45 while for B-1a, gal-9 bridges the BCR with the CD5 protein (Smith, Fawaz et al. 2021).

The impact of extra-cellular gal-9 on T-cells is complex and not fully elucidated. In cooperation with TGF- $\beta$ , gal-9 enhances the expansion and activity of induced T-regs (Seki, Oomizu et al. 2008, Mengshol, Golden-Mason et al. 2010, Wu, Thalhamer et al. 2014). On the other hand, gal-9 has a strong cytotoxic effect on T-regs expressing the Tim-3 receptor (Yang, Sun et al. 2021). The CD8<sup>+</sup> conventional T-cells are also negatively regulated by extra-

cellular gal-9. If they are in a state of exhaustion with Tim-3 expression, they can be pushed to cell death by extra-cellular gal-9 (Wang, He et al. 2007, Kang, Dutta et al. 2015) (Yang, Sun et al. 2021). Regarding CD4<sup>+</sup> T-cells, one of the first immunomodulatory effects of extra-cellular gal-9 to be reported in 2005 was the induction of cell death in murine Th1 T-cells expressing Tim-3 (Zhu, Anderson et al. 2005). Later on, gal-9 was shown by several groups - including ours - to be able to act on murine and human CD4<sup>+</sup> T-cells through membrane receptors independent of Tim-3, with effects like production of interferon  $\gamma$  or TNF- $\alpha$  and/or apoptosis (Su, Bi et al. 2011, Lhuillier, Barjon et al. 2015). Moreover, Gooden *et al.* have reported a biphasic response of CD4<sup>+</sup> cells when non-activated PBMCs were treated *in vitro* with recombinant gal-9. During the first 2 days, apoptosis was predominant whereas from day 3 and beyond, there was emergence and expansion of CD4<sup>+</sup> cells with some features reminiscent of Th1 central memory cells. The same phenotype shift was observed when gal-9-stimulation was applied on T-cells activated by CD3/CD28 stimulation (Gooden, Wiersma et al. 2013). This is consistent with one report from our group showing that extra-cellular recombinant gal-9 activates two pathways in peripheral T-cells. One pathway results in apoptosis and does not require calcium mobilization or TCR integrity. The other pathway results in early calcium mobilization and requires the integrity of the T-cell receptor/CD3 complex (Lhuillier, Barjon et al. 2015). The existence of this gal-9 TCR-related pathway was confirmed in a more recent publication (Colomb, Giron et al. 2019).

On the basis of these observations, using a combination of unbiased exploration modalities, we undertook a comprehensive characterization of T cell subpopulations surviving under sustained exposure to extra-cellular gal-9. We thought that this approach was likely to shed light on a number of physiological and pathological mechanisms. Indeed, while in most tissues Gal-9 is expressed at a low level at baseline, its expression is substantially increased in inflammatory conditions, especially in the presence of interferon  $\gamma$  and  $\beta$  (Yang, Sun et al. 2021). The light zone of germinal centers is a site of intense gal-9 expression with a major contribution of B-cells (Giovannone, Liang et al. 2018). There are also numerous pathological conditions where sustained high expression of gal-9 take place in damaged tissues, sometimes with high plasma concentrations, for several days, weeks or months. For example, high concentrations of plasma gal-9 have been recorded during acute viral infections like influenza, covid or the initial stage of AIDS (Kato, Ikeda et al. 2014,

Tandon, Chew et al. 2014, Bozorgmehr, Mashhour et al. 2021). High concentrations of gal-9 are also detected in the liver of patients with chronic viral hepatitis B or C (Mengshol, Golden-Mason et al. 2010, Barjon, Niki et al. 2012, Nebbia, Peppia et al. 2012). Production of gal-9 is also increased in various types of human malignancies like hepatocellular, pancreatic and nasopharyngeal carcinomas (Pioche-Durieu, Keryer et al. 2005, Li, Wu et al. 2012, Seifert, Reiche et al. 2020).

During the first stage of our study, our exploration of phenotypic changes induced by sustained exposure of T-cells to gal-9 showed a remarkable decline of the CD8<sup>+</sup> and a substantial expansion of the CD4<sup>+</sup> subpopulation. On the one hand, we made several findings consistent with previous reports like the emergence of a strong subset of CD4<sup>+</sup> FoxP3<sup>+</sup> CCR4<sup>+</sup> cells suggestive of induced T-regs. Besides, unexpectedly, we observed the emergence of a subset of cells with a phenotype highly suggestive of follicular T cells (T<sub>f</sub>). The physiological and functional relevance of these observations has been confirmed by 2 approaches: investigations on murine splenic T-cells showing a decrease in CXCR5 expression in transgenic mice KO for Gal-9 and the demonstration of enhanced survival of human B-cells co-cultured with T-cells previously exposed to gal-9.

## **2. Materials and Methods**

### **Blood donors**

PBMCs in the form of buffy coats from healthy adult donors were purchased from the "Etablissement Français du Sang" (blood transfusion provider) and used in fully anonymized form. Whenever possible, ampoules of viable cells were frozen for subsequent experiments based on cells from the same donor.

### **Activation and expansion of human T cells from peripheral blood with or without exposure to recombinant gal-9.**

Peripheral blood leucocytes from healthy donors were isolated using a Ficoll gradient separation then seeded in 6-well plates (5 X 10<sup>6</sup> cells per well in 4 ml culture medium) using RPMI 1640 medium (Gibco) supplemented with 10% fetal calf serum (FCS, Sigma-Aldrich),



antibiotics and non-essential amino acids (ThermoFisher Scientific). These leucocytes were immediately subjected to a procedure of T-cells activation and expansion lasting seven days (**Figure 1**). Starting from D1 they were stimulated with anti-CD3/CD28 antibodies (0.5 µg/ml each) starting from the beginning (D1). This stimulation was reinforced at D5 by addition of interleukin-2 (IL-2, 10 U/ml, Miltenyi). Simultaneously, a fraction of these leucocytes subjected to the above-mentioned T-cell expansion protocol were exposed to recombinant gal-9 NC (1.5 µg/ml or 45nM) from D1 to D7 yielding a sub-population of expanded T-cells identified as “exposed” to gal-9 (G9Expo-T-cells or GE-T-cells). The rest of the cells were subjected to the expansion protocol in the absence of gal-9 and were identified as gal-9 naïve (G9Naive-T-cells or GN-T-cells). In both cases expanded T cells were isolated at D7 from the leucocyte mix using a Pan T cell isolation kit (Miltenyi). These isolated G9Expo- or G9Naive-T-cells were either used immediately for various biochemical or molecular biology analyses or seeded for functional investigations in culture plates using 10% FBS RPMI in the absence of CD3/CD28 or IL-2 stimulations.

### **RNAseq analysis**

G9Expo- and G9Naive-T-cells (respectively GE- and GN-T cells) isolated by magnetic sorting at day 7 were further cultured for 6 hours in the presence or in the absence of recombinant gal-9 NC (15nM) resulting in 4 categories of experimental conditions: GES and GNS cells subjected to late gal-9 stimulation after magnetic sorting and GEU and GNU without late gal-9 stimulation. At the end of this 6h culture, cells were used for total RNA extraction using the TRI Reagent (MRC) according to the manufacturer's guide, with chloroform as the phase separator. RNA quantity and quality were assessed by spectrophotometry (Thermo Scientific Nanodrop 2000 microvolume spectrophotometer, RRID:SCR\_018042). RNA sequencing was performed by the Genomics Platform of Gustave Roussy Institute (UMS AMMICA – UMS 3655 CNRS, France). Data were processed by the Bioinformatics Platform of Gustave Roussy Institute. Each transcript was quantified using the software Salmon v. 0.14.1. Genes were annotated using Gencode v.33 Basic, with hg38 as the reference genome. Differentially expressed genes

(DEGs) were identified with DESeq2 v. 1.26.0. False discovery rate (FDR) threshold was set to 0.05; DEGs were clustered with GSEA 4.0.3 (Broad Institute) against MSigDB v. 7.1.

Additional clustering of RNA-Seq data regarding T cell phenotype was performed with DESeq2 v. 1.26.0. Raw read counts were stored in an *object class* with an associated *design* formula that expresses 2 variables used in modeling: condition (i.e., treatment with control medium or galectin-9 for example) and donor. Read counts were next subjected to a transformation using regularized logarithm (rlog) with specified *design* formula. Transformed counts of selected genes and conditions were extracted to generate mean-centered heatmap with R package pheatmap v. 1.0.12.

## **Antibodies**

Antibodies used for CyTOF analysis conventional flow cytometry on human cells are listed in the Supplementary Table 4 and Supplementary Table 7 respectively.

Antibodies used for the characterization of murine splenocytes are specified in the Supplementary Table 6.

## **CyTOF analysis**

### ***Staining procedure***

The CyTOF assay was performed following Fluidigm's instructions. For each condition,  $3 \times 10^6$  cells were stained with Cell-ID™ Cisplatin 5 mM (Fluidigm) for 5 min and quenched with DPBS/BSA (0.1%), using 5 times the volume of stained cells. After centrifugation, cells were resuspended in DPBS/BSA (0.1%) with a pre-mix cocktail of membrane antibodies, 1  $\mu$ l of each antibody for  $3 \times 10^6$  cells and incubated for 1h. After washing, cells were incubated for 1 hour at 4°C with 1 ml of cell intercalation solution, prepared with Cell-ID Intercalator-Ir 500  $\mu$ M (Iridium, Fluidigm) to reach the final concentration of 150 nM. Cells were later centrifuged with DPBS/BSA (0.1%) and pelleted, then resuspended with EQ Calibration Beads (Fluidigm) and in the end, cell events were acquired using the Helios system (Fluidigm).

### ***Data analysis***

Concatenated and normalized data were analyzed on Cytobank (Kotecha, Krutzik et al. 2010). Data were manually gated to remove dead cells, debris and non-singlet events. Data from each donor were separately subjected to viSNE analyses, each was performed on 21 parameters which were the antibodies used in the panel with equal event sampling selected. Fifteen to thirty thousand events per sample were selected, according to the lowest number of events available across all samples.

Expression profiles were further analyzed on events exported from Cytobank. For assessment of co-expression of CD4, CXCR5, CD40L, FoxP3, T cells were manually gated using FlowJo software.

## **Flow cytometry analysis**

### **Murine splenocyte activation**

Murine splenocytes were activated at the density of  $2 \times 10^6$  cells/ml. Cells were incubated with 5 nM (3.1 ng/ml) PMA (Sigma-Aldrich) and Ionomycin (Sigma-Aldrich) at 1 µg/ml for 6 hours at 37°C before cytokine staining. Brefeldin A (Biolegend) was added after 2 hours of activation, at 5 µg/ml.

### **Staining procedure**

Cells were washed with DPBS before the surface staining in DPBS containing 3% FBS. For experiments with murine spleen, an additional step with anti-CD16/CD32 (BD Biosciences) was performed to block Fc receptor. Cells were fixed with Fixation Buffer (Biolegend) and permeabilized with Intracellular Staining Permeabilization Wash Buffer (Biolegend) for cytokine staining after appropriate activation. Transcription factor staining was performed using True-Nuclear™ Transcription Factor Buffer Set (Biolegend). Data were acquired by LSR Fortessa II (BD Biosciences) and analyzed with Flowjo v. 10.5.3.

## **Animal care and experimentation**

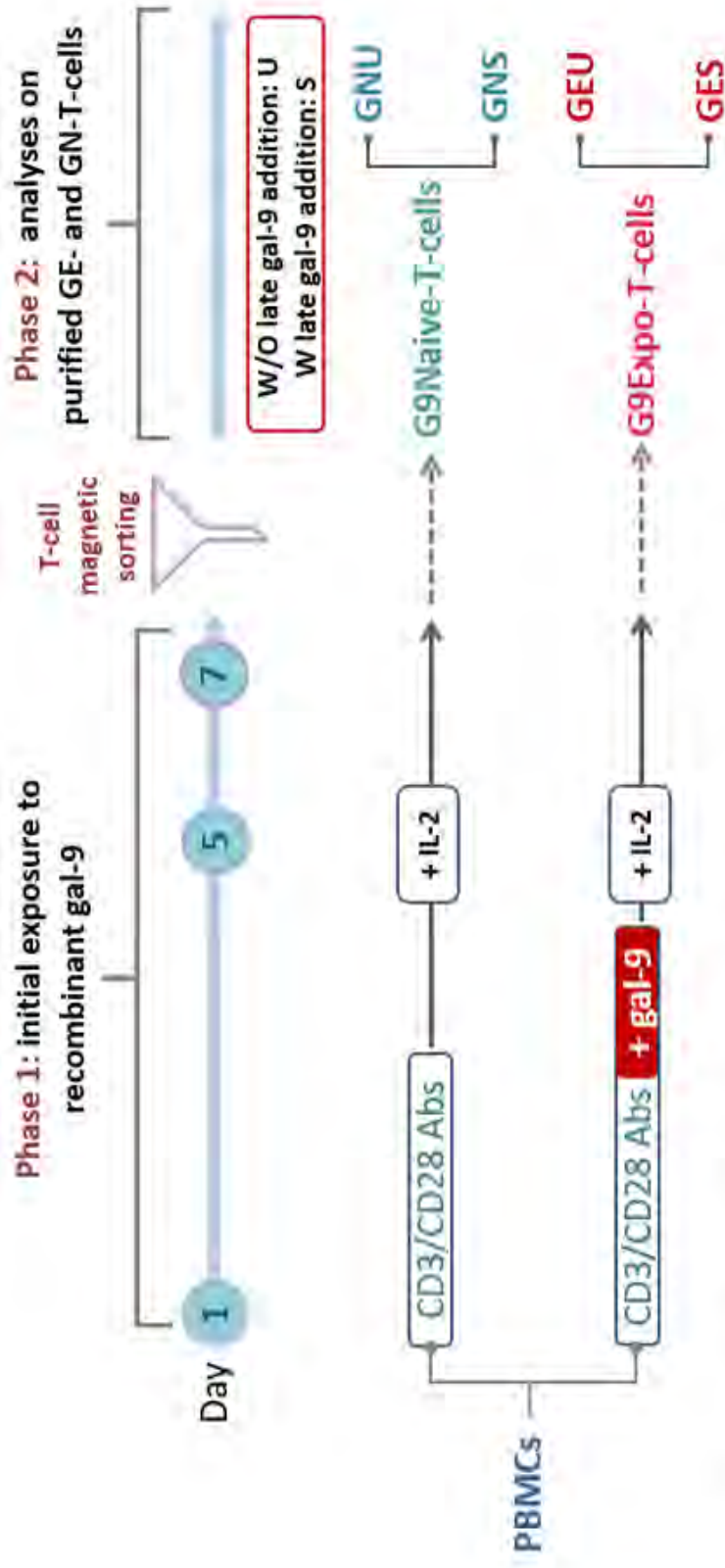


**Figure 1. Cartoon depicting the experimental system used to investigate the effects of T-cell exposure to high concentrations of extra-cellular gal-9.** During the first phase of the protocol, from day 1 to day 7, peripheral human T-cells from healthy donors are activated by CD3/CD28 stimulation in a context of co-culture with other types of leucocytes, with or without addition of recombinant gal-9NC (stable isoform - 45nM). Recombinant interleukin-2 is added at day 5 to extend T-cell proliferation. At day 7, T-cells are isolated from other PBMCs by negative magnetic sorting to enter the second phase of the protocol. These T-cells are called "gal-9-exposed" (G9Expo) or "gal-9-naive" (G9Naive) depending on whether or not they have been previously exposed to recombinant gal-9. They are then subjected to various types of investigations like RNA sequencing or flow cytometry, either directly or after a second stage of *in vitro* culture. This secondary culture is performed with or without addition of recombinant gal-9 NC (15nM), corresponding to the stimulated (S – GNS and GES) or unstimulated (U – GEU and GNU) conditions.

Animal procedures were performed according to protocols approved by the Ethics Committee for animal experimentation n°26 certified by the French ministry of agriculture (“Comité d’Ethique en Expérimentation Animale n°26”) (project number n°12147-201711081244492). Female C57BL6/JRi were purchased from Janvier Labs (France) and housed in the Gustave Roussy animal facility. The production and characterization of gal-9<sup>-/-</sup> C57BL6/JRj mice has already been reported (Seki, Oomizu et al. 2008). They were raised at the Gustave Roussy animal facility (Preclinical Research Platform - PFEP). Mice were used between 8 and 12 weeks of age. Overall, 100 mice were used for this study. Animal care was done as previously described: mice were housed in pathogen-free conditions in filter cap cages holding a maximum of 5 animals with irradiated aspen chip bedding and cotton fiber nesting material (Baloche, Riviere et al. 2021). They were maintained on a 12/12 light/dark cycle, with *ad libitum* UV-treated water and RM1 rodent diet. The animals were monitored every day for signs of pain, such as immobility or restlessness, reduction of drinking and food intake. The persistence of abnormal behaviors for more than one day led to the euthanasia of animals with suffering presumption. Prior to tissue collection, mice were sacrificed by cervical elongation. Otherwise, mice were euthanatized by carbon dioxide asphyxiation.

### **Co-culture of G9Expo- and G9Naive-T cells with Ramos cells**

Ramos cells cultured in RPMI 1640 medium (Gibco) supplemented with 10% fetal calf serum (FCS, Sigma-Aldrich) were collected and stained with CFSE (Sigma-Aldrich). Cells were incubated with CFSE at 2  $\mu$ M in DPBS (Gibco) for 20 minutes at 37°C, before another incubation with RPMI 1640 (Gibco) at the same temperature for 30 minutes to complete the final reactions of CFSE. Cells were then washed and co-cultured with G9Naive- or G9Expo- T cells on a ratio of  $1 \times 10^5$  cells per  $2 \times 10^5$  T cells, in 3 ml of RPMI 1640 medium supplemented with 5% FCS. After about 6 hours of culture in the rich medium, cells at each experimental condition were transferred to the low serum medium with 0.5% FCS and treated or not with gal-9 M at 1  $\mu$ g/ml.

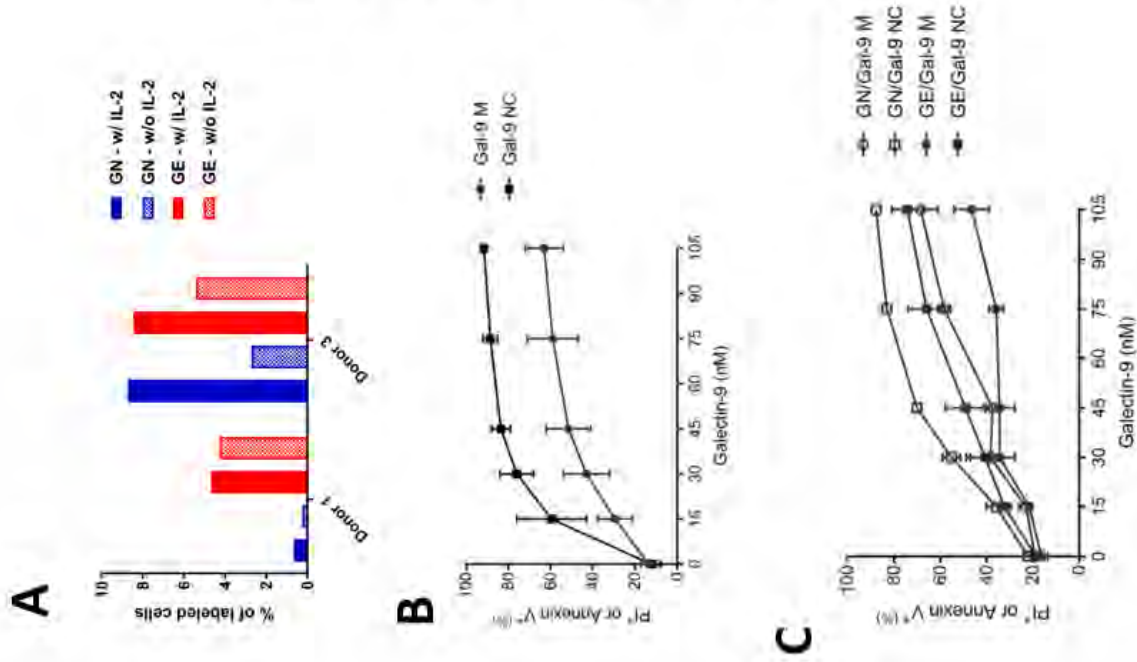


**Figure 2. Greater proliferative potential and resistance to gal-9-related cell death in T-cells following prior exposure to recombinant gal-9.** **A)** Gal-9-naive (G9Naive) and gal-9-exposed (G9Expo) T-cells were isolated by magnetic sorting and cultured *in vitro* for 4 days with or without addition of recombinant interleukin-2 (IL-2 10 U/ml). Then cell proliferation was assessed by incorporation of fluorescent EdU. In the absence of recombinant IL-2, there was an excess of proliferation for G9Expo-T-cells from both donors 1 and 3. In the presence of IL-2, this excess of proliferation was observed only for donor 3. **B)** T-cells isolated from PBMCs from 2 donors (1 and 3) by magnetic sorting at day 1 were subjected to gal-9 stimulation for 24 hours using the recombinant M and NC isoforms at increasing concentrations. Apoptosis (Annexin V) and /or cell death (Propidium iodide) was then assayed by flow cytometry. The maximal percentage of apoptosis (AnV pos. plus PI pos.) was 60% and 90% for gal-9M and gal-9NC, respectively. The IC50 were 12nM and 17nM, respectively. **C)** Assessment of the impact of gal-9 M and NC on G9Naive- and G9Expo-T-cells from the same 2 donors (24h exposure following magnetic separation). For G9Naive-T-cells the maximal percentages of apoptosis were almost identical to those of Fig. 2B. In contrast, there was a substantial reduction of the percentage of apoptosis for G9Expo-T-cells, especially in the presence of gal-9 M (from 60% to 40%).

## **Proliferation Assay**

Cell proliferation was assessed either by using dye dilution that allows tracing multiple generations of labeled cells, or by measuring *neo*-DNA synthesis. Both methods required acquisition of fluorescent signal by LSR Fortessa II. For generation tracking, cells were stained with CellTrace™ Far Red dye (Life Technologies, ThermoFisher Scientific) at the density of  $10^6$  cells/ml, following instructions from the manufacturer. Labeled cells were then cultured in appropriate conditions and collected 4 days after the start of treatment to acquire data. For neo-DNA synthesis, cells were labeled on the day of data acquisition (i.e, at the end of treatment). EdU (5-ethynyl-2'-deoxyuridine - Life Technologies, ThermoFisher Scientific) was added to cell culture at 20  $\mu$ M. Cells were then incubated in appropriate culture condition for 2 hours before being collected for revelation based on click chemistry. Detection of EdU was finally done through LSR Fortessa II.

## **Histology and immunohistochemistry**

Spleen tissues were collected from wild-type and *gal-9<sup>-/-</sup>* C57BL6/JRj mice and fixed in 4% paraformaldehyde solution in phosphate buffered saline (PBS). After fixation in 4% PFA, paraffin-embedded tissues were cut into 4 $\mu$ m thick sections. At least one section per tissue sample was stained with hematoxylin-eosin-saffranin (HES) for quality control. For CD40-L detection, slides were incubated with a specific rabbit monoclonal antibody (1:500) (Novus Cat# NBP2-66756). Primary antibody binding was revealed with the Rabbit PowerVision Kit (UltraVision 614 Technologies) and the DAB PowerVision kit (ImmunoVisionTechnologies Co.). All antibody applications were performed with a Bond RX automated Leica Slide Stainer. Image acquisition was performed with a Virtual Slide microscope VS120-SL (Olympus, Tokyo, Japan), 20X 621 air objective (0.75 NA, 345 nm/pixel).

## **Statistical Analysis**

Statistical analyses were performed using Graphpad Prism v. 7.04.

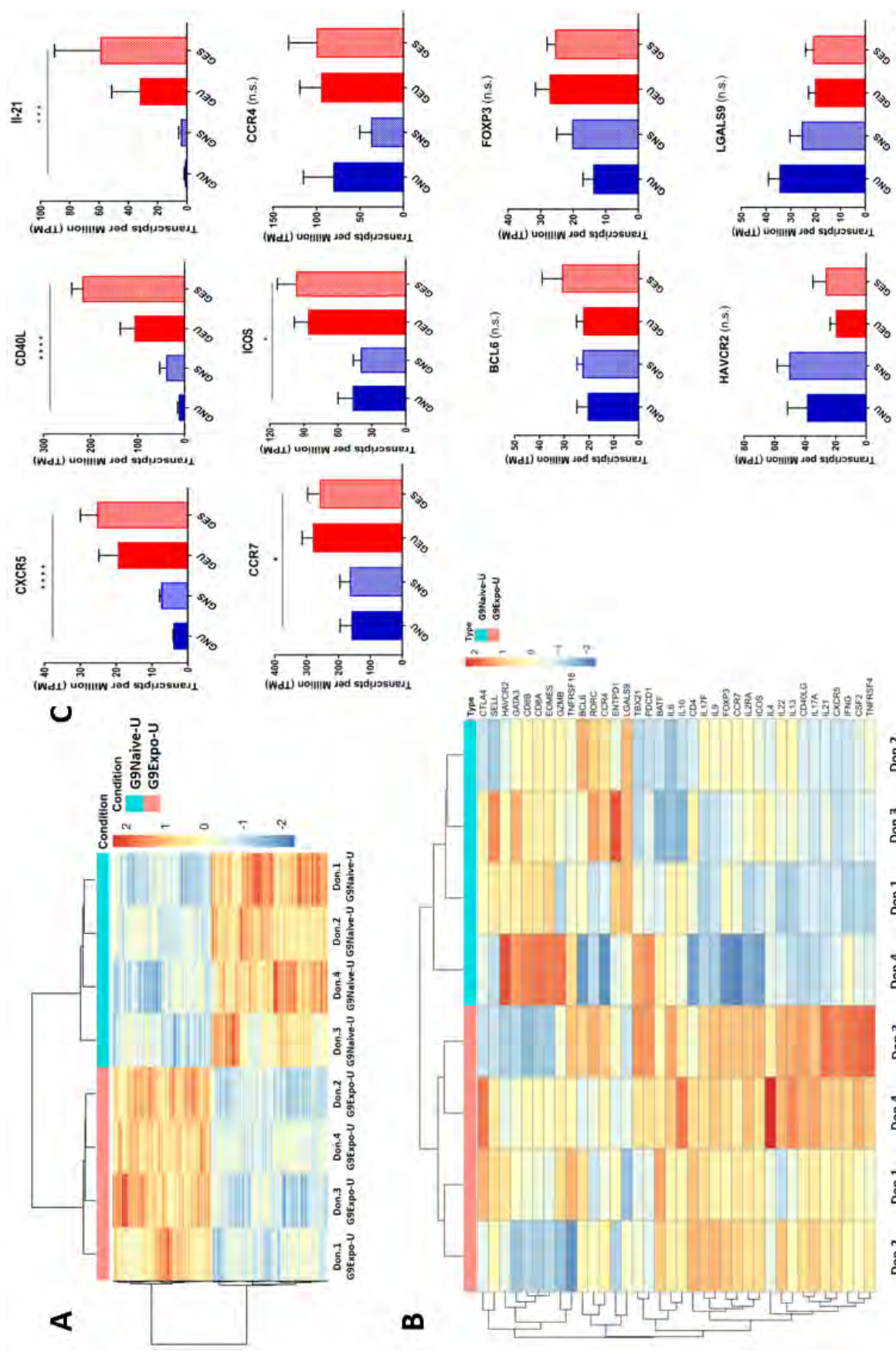


**Figure 3**



## 3. Results

### 3.1 Characteristics of the experimental system used to investigate the influence of recombinant gal-9 on human T-cells *in vitro*

The influence of extra-cellular gal-9 on the proliferation and differentiation of human peripheral T-cells was investigated using the experimental system summarized in **Figure 1**. Its aim was to expose proliferating human T-cells to high concentrations of gal-9 for 7 days in a context of co-culture with other leucocytes. At day 1 of this protocol whole PBMCs from healthy donors were treated with a combination of CD3/CD28 antibodies in the presence or in the absence of recombinant gal-9 NC, an artificial isoform of gal-9 which has a greater stability in cell culture conditions than the natural isoforms. Activation and proliferation of T cells was revived at day 5 by addition of IL-2. Several biological parameters were monitored during gal-9 exposure (1<sup>st</sup> phase of the protocol summarized in **Figure 1**). Since extra-cellular gal-9 can be released by various types of leucocytes including T-cells and monocytes, the overall concentration of gal-9 was checked in the culture medium of PBMCs cultured with or without addition of recombinant gal-9-NC. As shown in **Supplementary Figure 1A**, the overall concentration of gal-9 was at least 20 times greater for experimental conditions which included addition of recombinant gal-9. At day 7, all CD3<sup>+</sup> T-cells were separated from other types of PBMCs by untouched magnetic sorting and then used for various types of investigations. T-cells recovered by magnetic sorting following recombinant gal-9 exposure were called G9Expo-T-cells ("gal-9-exposed") whereas T-cells without previous exposure to recombinant gal-9 were called G9Naive-T-cells ("gal-9-naïve"). As shown in **Supplementary Table 2** and **Supplementary Figure 1B**, the ratio of total PBMCs and T-cells recovered at day 7 to the initial number of PBMCs seeded at day 1 was consistently about twice higher in the absence than in the presence of recombinant gal-9. This is probably explained by cytotoxic effects during the first two days of the treatment by recombinant gal-9.

**Figure 3. Impact of recombinant gal-9 on the transcriptome of human T-cells. A)** Heatmap of overall differential transcription between gal-9-naive (G9Naive-U) and gal-9-exposed (G9Expo-U) human T-cells. Gal-9 exposure was made prior to T-cell separation without late secondary addition of gal-9. Donors (don) of PBMCs are numbered from 1 to 4. The heatmap was generated using the DESeq2 software with correction of the donor effect. **B)** Heatmap of G9Naive-U/G9Expo-U differential transcription in connection with T-cell biology. Made with the same software as in A) on the basis of a list provided by Wong MT *et al.* (Cell Rep., 2015). **C)** Modifications of expression of some selected genes in T-cells W or W/O initial exposure to gal-9 and W or W/O late addition of gal-9 after magnetic separation. Mean values from 4 donors. G9Naive-U or GNU: no addition of gal-9. GNS: addition of gal-9 only after magnetic separation of T-cells. G9Expo-U or GEU : initial exposure to gal-9 without late addition. GES : initial exposure plus late addition.

### **3.2 Greater proliferative potential and resistance to gal-9-related cell death in T-cells following prior exposure to recombinant gal-9**

We then investigated EdU incorporation in T-cells after the magnetic sorting following 4 days of *in vitro* culture with or without addition of recombinant interleukin-2. Strikingly, we found that incorporation of EdU was higher in G9Expo- compared to G9Naive-T-cells (GE- and GN-T cells respectively). This excess of EdU incorporation was more consistent in the absence of recombinant IL-2 (**Figure 2** and **Supplementary Figure 2**). Our conclusion was that during the first stage of the experiment, a higher rate of T-cell death was resulting from initial exposure to recombinant gal-9. In contrast, after magnetic sorting and weaning of CD3/CD28 stimulation, a higher EdU incorporation and T cell proliferation rate was retained for G9Expo-T cells. In the next step, we hypothesized that GE-cells might acquire a greater capacity to resist gal-9-induced cell death. To address this point, G9Expo- and G9Naive-T-cells were challenged with increasing concentrations of either gal-9 NC or the M-isoform of WT gal-9. For each concentration of gal-9, the percentage of apoptotic and/or dead cells was assessed by flow cytometry. The same test was performed on T-cells separated from fresh PBMCs at D1. As expected G9Expo-T-Cells were significantly more resistant to the challenges by gal-9 NC and gal-9 M when compared to G9Naive-T-cells or to T-cells isolated from fresh PBMCs at D1 (**Figure 2B and C**). Overall, these findings suggested that most T-cells surviving under gal-9 exposure acquired some heritable characteristics including a higher level of resistance to gal-9 in comparison to T-cells not exposed to recombinant gal-9.

### **3.3 Recombinant gal-9 up-regulates transcripts of follicular T-cell markers**

To investigate the impact of gal-9 exposure on the assortment of peripheral T-cell sub-populations, we performed a comparative transcriptome analysis of GE- and GN-T-cells by bulk RNA-seq for 4 donors (**Figure 3**). More precisely, GE- and GN-T-cells isolated by magnetic sorting at D7 were subjected to a short secondary culture for 6h. This was made either in plain culture medium (G9Expo-U and G9Naive-U) or in medium containing recombinant gal-9NC (15 nM) G9Expo-S and G9Naive-S (for more details see the cartoon in (**Figure1**)).

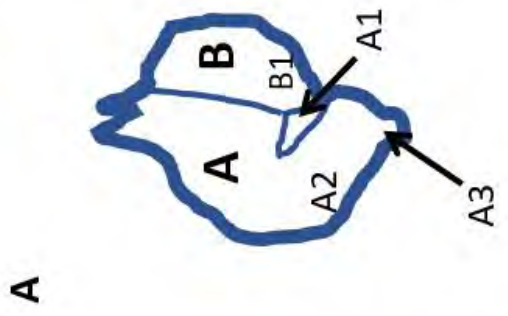
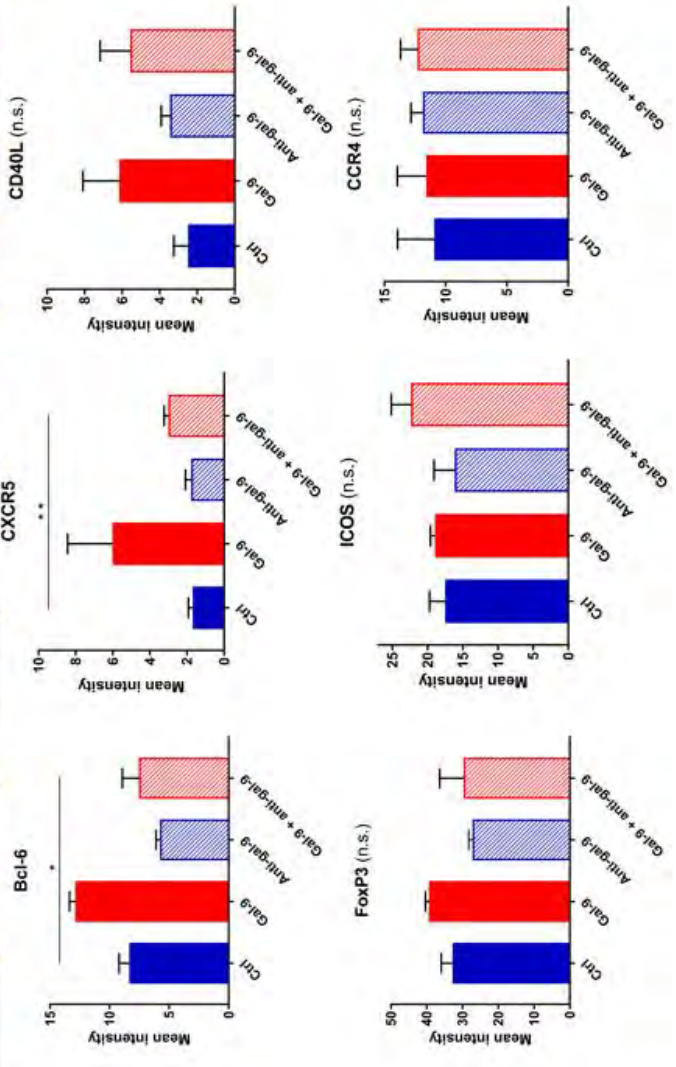
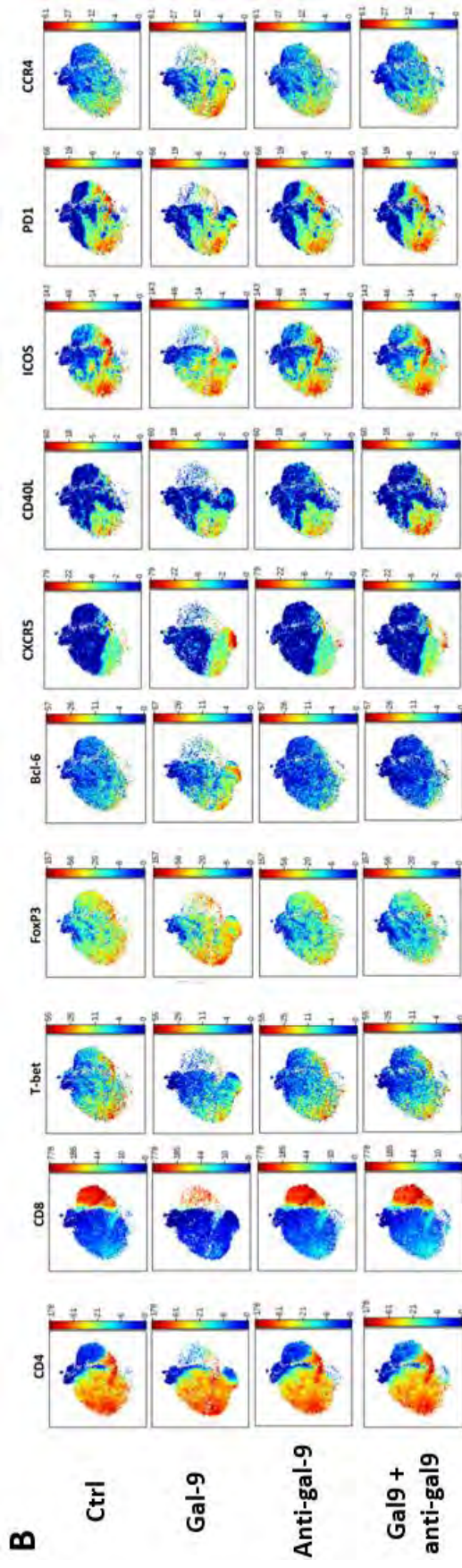


**Figure 4**

In the first step of our transcriptome study, we focused our efforts on the comparison of G9Expo-U and G9Naive-U cells, in other words, T-cells exposed or not exposed to gal-9 in the first phase of the experiment and not subjected to any stimulation by gal-9 after magnetic separation. A list of differentially expressed (DE) genes between GE- and GN-T-cells was generated using the DESeq2 package in R. It was validated in the heat map displayed in **Figure 3A** with a clear separation of GEU and GNU transcriptomes for cells of all 4 donors included in this analysis. This same list was subjected to enrichment analysis using the GSEA software on MSigDB (Subramanian, Tamayo et al. 2005, Liberzon, Subramanian et al. 2011). This resulted in a set of about 100 enrichment plots matching genes with differential expression between GE and GN T cells. A list of the 30 plots ranking with the highest enrichment score is provided in **Supplementary Table 3**. A majority of these plots – thirteen - were related to the biology of CD4<sup>+</sup> T-cells with three of them gathering genes known to be more abundant in T-regs by comparison with T-convs. Two plots were related to CD8<sup>+</sup> T-cells. Eleven were connected to immune cells distinct from T-cells including five in connection with B-cell biology. Four plots were about other cell types not related to the immune system. To achieve a more precise approach being closer to our own experimental system, we resorted to a list of 32 genes related to T-cell biology inspired from Wong et al. (2015) (Wong, Chen et al. 2015). This list was used for differential analysis of G9Expo-U and G9Naive-U data using the DESeq2 software with elimination of the donor effect. This resulted in the heatmap of **Figure 3B**. The most striking differences were recorded for a cluster of genes including *CD40LG* (i.e., *CD154*), *IL-17A*, *IL-21*, *CXCR5*, *IFN- $\gamma$* , *CSF2*. In a distinct cluster, *BATF* also exhibited strong differential expression. Three of these markers – *CXCR5*, *CD40LG* and *IL-21* and - were suggestive of a phenotype of follicular helper T-cells (Tfh) while *IL17A* was suggestive of a Th17 differentiation.

Outside of this cluster, following gal-9 exposure, we noted a greater amount of mRNAs for miscellaneous genes suspected to be influenced by extra-cellular gal-9. We can mention *ICOS* (because of its connection with the Tfh phenotype) plus *FoxP3*, *BATF* and *CCR7* involved in Treg, Th17 and memory T cell differentiation, respectively.

**Figure 4. Multidimensional mass cytometry of human T-cells subjected or not to gal-9 exposure. A)** Schematisation of t-SNE plots for manual annotation. **B)** t-SNE plots of selected markers detected on isolated T-cells from donor 5 (similar data for donors 6 and 7 are shown in Supplementary Figure 3). These cells have been subjected to 4 experimental conditions prior to magnetic separation : 1) activated T-cells among PBMCs without addition of recombinant gal-9 (Ctrl); 2) activated T-cells among PBMCs with addition of gal-9 (Gal-9); 3) activated T-cells with addition of an anti-gal-9 antibody (Mouse anti-Galectin-9 B-T33, Origene) (Anti-gal-9); 4) activated T-cells with addition of recombinant gal-9 plus the anti-gal-9 antibody (Gal-9 + anti-gal-9). Strikingly for every marker, all three control plots have a fairly homogenous pattern whereas a distinct pattern is consistently observed for conditions with gal-9 exposure. Two major components are designated A and B, essentially matching CD4<sup>+</sup> and CD8<sup>+</sup> subpopulations. Among the CD4<sup>+</sup> cells, the A1 subset is enriched in PD1<sup>+</sup> and ICOS<sup>+</sup> cells. It is not subjected to significant changes through the various experimental conditions. At baseline, the A2 subset seems to combine strong expressions of T-bet and FoxP3, in addition to ICOS and PD1. B1 designates a subset of CD8<sup>+</sup> cells which like A2 seems to combine the expression of T-bet and FoxP3. Gal-9 exposure results in a dramatic reduction of the whole CD8<sup>+</sup> component. It has a profound effect on the A2 subset changing the T-bet/FoxP3 balance in favor of FoxP3 with a concomitant increase in CCR4 expression in the same subset. The most spectacular change induced by gal-9 exposure is the emergence of the A3 subset combining CD4, T-bet, FoxP3, BCL-6, CXCR5, CD40-L, ICOS, PD1 and CCR4. **C)** Comparison of mean MFI values for Tfh markers detected on T-cells from 3 donors tested in the 4 experimental conditions mentioned in 4B.

In the second step of our transcriptome study, we took in account two additional experimental conditions resulting from the late addition of recombinant gal-9 after T-cell magnetic separation. **Figure 3C** shows that this late gal-9 stimulation had almost no effects on GNaive-T-cells for the expression of *CXCR5*, *CD40LG*, *IL-21*, *ICOS* and *BCL-6*. In contrast, this secondary addition of gal-9 was acting as a boost on GExpo-T-cells with a strong enhancement of the expression of *CXCR5*, *CD40L*, *IL-21* and to a lesser extent *ICOS* and *BCL-6* mRNAs. This suggests that gal-9 has, at least to some extent, a direct role in the induction of these genes related to Tf differentiation. On the other hand, the expressions of *FoxP3* and *CCR4* were not significantly enhanced by the late gal-9 boost.

### **3.4 Multidimensional mass cytometry demonstrates the upregulation of follicular T-cell markers under gal-9 exposure**

Impressed by the strong increase in *CXCR5*, *CD40L* and *IL21* transcription resulting from gal-9 exposure, we decided to investigate the impact of gal-9 at the cellular level using multidimensional mass cytometry with special attention to molecular markers related to the various subsets of follicular T-cells. Overall, we used a panel of 21 T-cell markers (Supplementary Table 3). PBMCs from three healthy donors were subjected to gal-9 exposure in the presence or in the absence of a gal-9 neutralizing antibody (mouse Mo Ab clone B-T33, AM32427AF-N Origene). Practically, we had four experimental conditions: PBMCs exposed to recombinant gal-9 by itself and three control conditions: PBMCs with no additives, PBMCs with recombinant gal-9 plus the neutralizing antibody and PBMCs with the neutralizing antibody by itself. T-cells of each condition were subjected to mass cytometry immediately after their magnetic separation (Donor 5, **Figure 4**) (Donors 6 and 7, **Supplementary Figure 2**). As shown on the t-SNE plots in **Figure 4A and B**, the patterns of T-cell distribution were fairly homogenous for all 3 control conditions in sharp contrast with the redistribution of several subsets resulting from gal-9 exposure. The most obvious modifications were a dramatic reduction of the CD8<sup>+</sup> population combined to a relative expansion of the CD4<sup>+</sup> population. Inside the CD4<sup>+</sup> component, there was a subpopulation undergoing reciprocal modifications: a reduction of T-bet expression combined to the enhancement of FoxP3, CCR4 and to a lesser extent CXCR5 and BCL6 expression. The most striking modification resulting from gal-9 exposure was seen at the bottom of the CD4 zone looking like an appendix identified by a

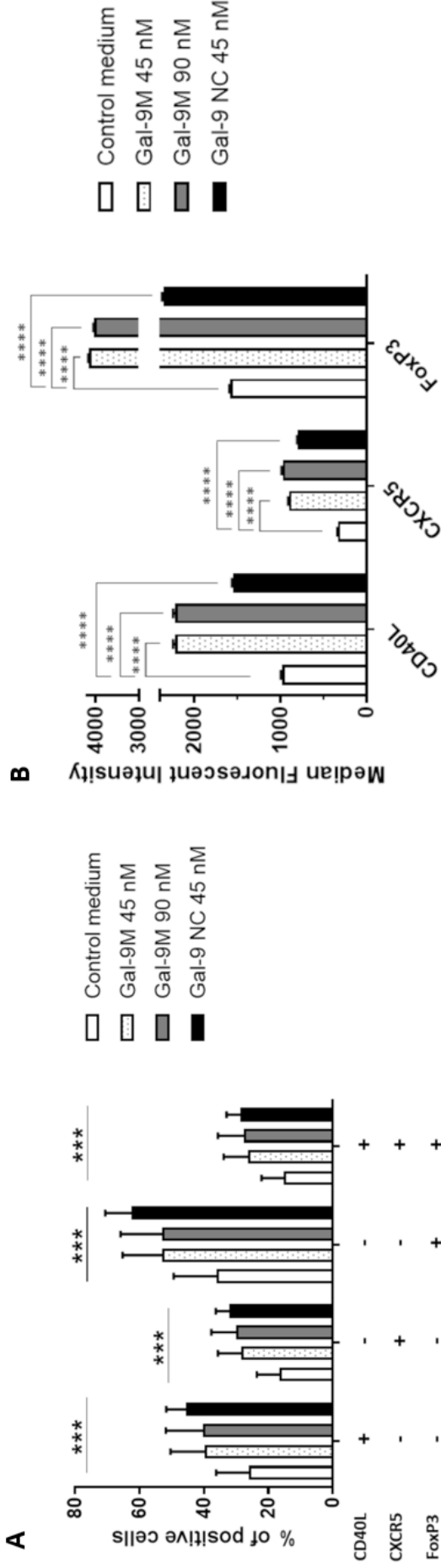


**Figure 5. Expression of CD40L, CXCR5, and FoxP3 in CD4<sup>+</sup> T cells after 7 days of treatment with gal-9 M or gal-9 NC.** Subjected to the same experimental procedure as in the mass cytometry assay, T cells from donors 8, 9 and 10 were magnetically sorted after 7 days of treatment with either gal-9 M (45 nM or 90 nM) or gal-9 NC (45 nM). CD40L, CXCR5, FoxP3 expression were analyzed among CD4<sup>+</sup> T cells of the sorted population. **A**) Percentage of CD4<sup>+</sup> T cells having expression of CD40L, CXCR5, FoxP3 or co-expression of these markers. Statistical significance was found by two-way ANOVA with  $p$ -value = 0.0005 in comparison of the 4 experimental conditions. **B**) Median fluorescent intensity (MFI) of CD40L, CXCR5 and FoxP3 expression in CD4<sup>+</sup> T cells. Pairwise comparison of MFI was performed by multiple  $t$ -test between control condition and each of gal-9 treatment. All comparisons have  $p$ -value < 0.000000001.



strong increase in CXCR5 expression. Other markers were affected in the same zone but with more heterogenous patterns. The CXCR5-positive subset was partially overlapped by other Tf markers (Bcl-6, CD40L, ICOS and PD1) and by T-reg markers (FoxP3, CCR4). Statistics based on the analysis of T-cells from 3 donors showed a significant overall increase in mean fluorescence following gal-9 exposure for Bcl-6 and CXCR5 but not CD40L, FoxP3 and CCR4 (**Figure 4C**). The robust stimulation of CXCR5 expression under gal-9 exposure was thus confirmed. At this point, we were wondering to what extent CXCR5 was co-expressed with other markers especially CD40L and FoxP3. According to previous publications, CD40L and FoxP3 are supposed to be mutually exclusive in follicular T-cells, being associated respectively with helper and regulator follicular T-cells (Ramiscal and Vinuesa 2013). Therefore, we looked at the distribution of FoxP3 and CD40L among CXCR5<sup>+</sup> cells for gal-9-treated cells of the 4 donors (**Supplementary Table 5**). We found the following trend: a majority of CXCR5<sup>+</sup> cells being FoxP3<sup>+</sup>; the same was true for CXCR5<sup>+</sup>CD40L<sup>+</sup> cells.

### **3.5 Up-regulation of follicular T-cell markers under exposure to a natural isoform of gal-9 (gal-9-M)**

A complementary experiment involving three additional donors was set up to confirm previous data. A recombinant protein representative of a natural isoform of gal-9, namely gal-9M, was used in addition to the artificial gal-9NC. Comparative assessment of CD40L and CXCR5 was made by conventional cytometry on G9Expo- and G9Naive-T-cells. Detection of FoxP3 was included in the same experiment. As shown in Figure 5, the up-regulation of CXCR5, CD40L and FoxP3 was confirmed with both gal-9NC and gal-9M, the latter being even more potent than the artificial isoform when fluorescence intensity was taken into account. Co-expression of CD40-L, CXCR5 and FoxP3 in a substantial number of cells was also confirmed.

### **3.6 Reduced expression of CXCR5 and CD40L in splenic T-cells from gal-9-KO transgenic mice**

Production of gal-9 is known to be abundant in germinal centers and we were wondering whether the induction of follicular markers on human T-cells exposed to recombinant gal-9 could reflect a physiological contribution of natural gal-9 to the follicular T-cell differentiation inside germinal centers. To address this question, we chose to investigate the expression of follicular markers in splenocytes from gal-9-KO transgenic mice with comparison with wild-type mice. As shown in **Figure 6**, a reduction of CXCR5 expression was detected by flow cytometry on splenic T-cells derived from gal-9-KO mice. Comparative assessment of CD40L expression was made by immuno-histo-chemistry on spleen sections from WT and gal-9-KO mice. CD40L staining was consistently less intense for gal-9-KO mice especially at the periphery of germinal centers, suggesting its lower expression in pre-Tfh cells (Ramiscal and Vinuesa 2013).

### **3.7 Prior exposure of human T-cells to recombinant gal-9 increases their capacity to rescue B-cells from apoptosis**

Knowing that extra-cellular gal-9 was able to contribute to the acquisition of Tfh markers by human and murine T-cells, it was important to investigate the acquisition of functional properties consistent with the Tfh phenotype. We knew that interactions with Tfh cells are essential to rescue from apoptosis centrocytic B-cells undergoing selection in the light zone of the germinal centers. Therefore we investigated whether G9Expo-T-cells were able to provide a protection to neighboring B-cells in a challenging environment. As a model of human germinal center B-cell, we used Ramos 266 cells which are lymphoma B cells of germinal center origin known to be responsive to the CD40L (Lederman, Yellin et al. 1994). Ramos B-cells were labelled with CFSE and pre-incubated overnight with G9Expo- or GNaive-T-cells and then transferred to a pro-apoptotic environment, with only 0.5% fetal calf serum. Knowing that gal-9 is abundant in the light zone of the germinal center, this pro-apoptotic medium was supplemented with recombinant gal-9M (30nM). As shown in **Figure 8**, B-cell survival was enhanced when they were co-cultured with G9Expo-T-cells.

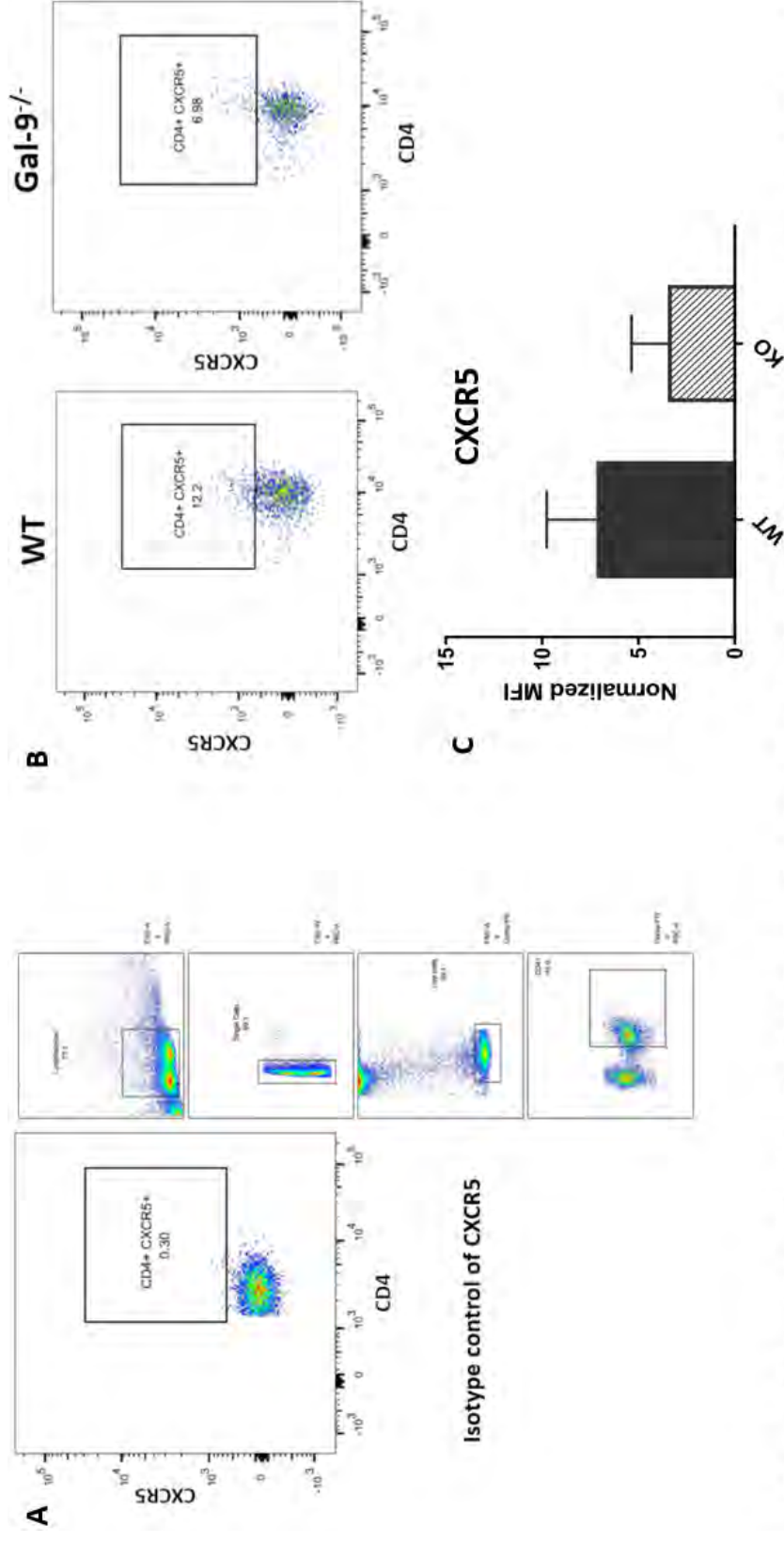


**Figure 6. Expression of CXCR5 in CD4<sup>+</sup> T cells of wild-type and *gal-9*<sup>-/-</sup> C57BL6/JRj mice.** Splenocytes from wild-type and *gal-9*<sup>-/-</sup> C57BL6/JRj mice were collected and stained with anti-CD4 and anti-CXCR5 antibodies. Dead cells were removed by gating on propidium iodide-negative events. **A**) Gating ancestry of CXCR5 isotype control. **B**) CXCR5<sup>+</sup> population in CD4<sup>+</sup> splenocytes. WT: wild-type mouse. *gal-9*<sup>-/-</sup> : *gal-9*-knock-out mouse. **C**) Normalized median of fluorescence intensity of CXCR5 was calculated by the ratio of MFI of stained sample on MFI of isotype control. Mean values from 3 pairs of mice. MFI: median of fluorescence intensity. WT: wild-type mice. KO: *gal-9*-knock-out mice.

## Discussion

Several previous studies have reported that a fraction of T-cells was able to resist cell death induced by extra-cellular gal-9 but until now their phenotypes and functional characteristics have not been systematically investigated. Previous studies have shed light on two peculiar T-cell subsets surviving gal-9 exposure. A majority of authors have focused their attention on gal-9 contribution to the expansion of induced T-regs in murine and human experimental systems (Seki, Oomizu et al. 2008, Mengshol, Golden-Mason et al. 2010, Lv, Zhang et al. 2013, Wu, Thalhamer et al. 2014). On the other hand, one group has reported the capacity of recombinant gal-9, in combination with CD3/CD28 stimulation, to favor the expansion of Th1 cells presenting a central memory phenotype (Gooden, Wiersma et al. 2013). In this context, our aim was to achieve a more comprehensive and systematic investigation of human T-cells expanding under sustained gal-9 exposure. Using RNAseq analysis and multidimensional flow cytometry, we were able to confirm several aspects of T-cell phenotypic conversions resulting from gal-9 exposure which were consistent with previous reports. In this category, we can mention the reduction of the CD8<sup>+</sup> and relative expansion of the CD4<sup>+</sup> subpopulations, the expansion of FoxP3<sup>+</sup> CCR4<sup>+</sup> cells and a clue in favor of the expansion of central memory T-cells based on the increase in CCR7 transcription following gal-9-exposure. In contrast despite a large amount of mRNAs encoding the BATF transcription factor in T-cells exposed to gal-9, we found no expression of Th17 markers by mass cytometry analysis, which is consistent with previous reports (Seki, Oomizu et al. 2008, Oomizu, Arikawa et al. 2012).

The main finding of this paper is the first report that exposure to extra-cellular gal-9 induces the emergence of diverse follicular T-cell subsets sharing a strong expression of CXCR5, a type of effect which has not been known until now. In a broad sense, follicular T-cells are T-cells homing in secondary lymphoid organs and contribute to the regulation of the B-cell immune response (Ramiscal and Vinuesa 2013, Stebegg, Kumar et al. 2018, Nakagawa and Calado 2021). Pre-Tfh (or pre-follicular helper T-cells) are initially primed by CD28 co-stimulation which is followed by *de novo* expression of Bcl-6 resulting in loss of CCR7 and acquisition of CXCR5 and ICOS expression of the plasma membrane. These pre-Tfh cells have sufficient

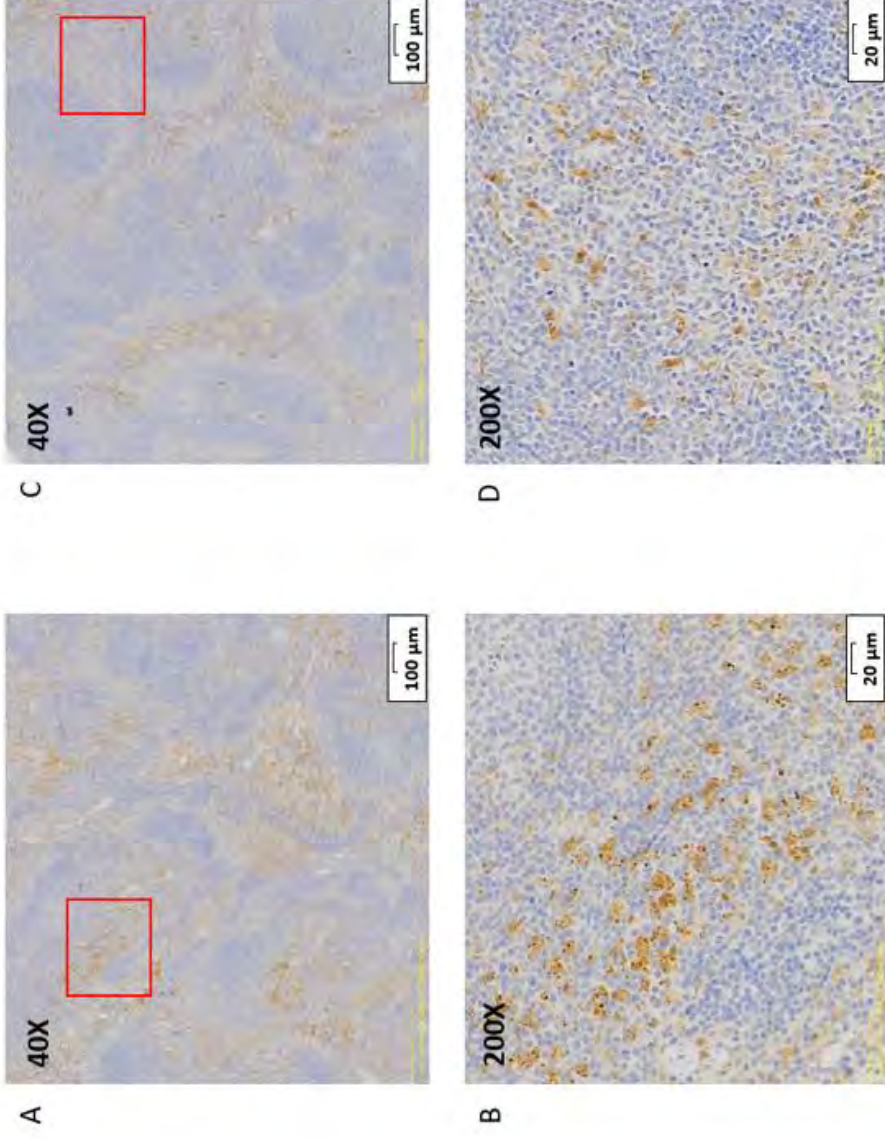
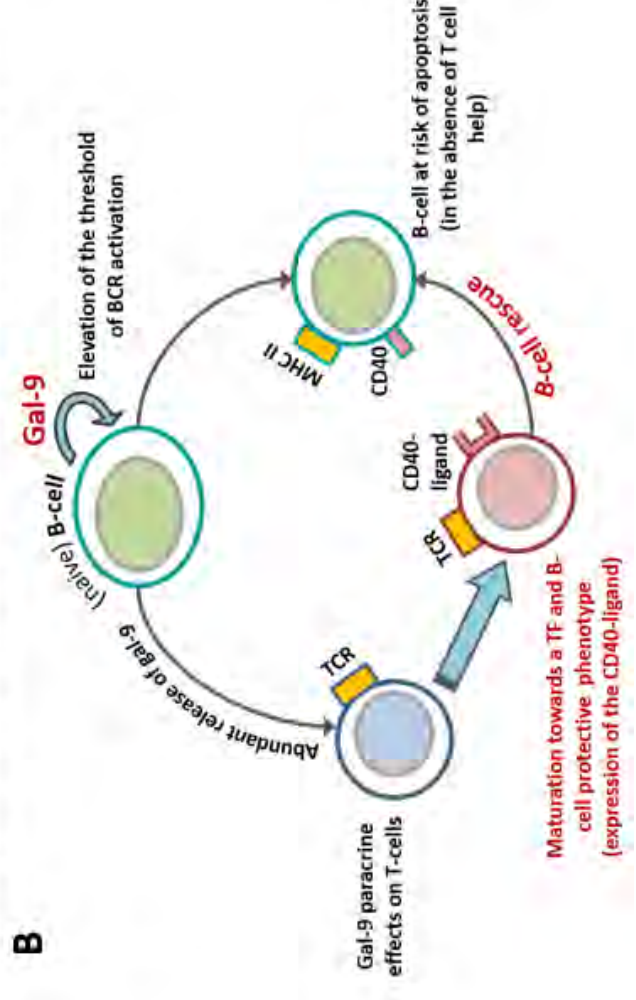
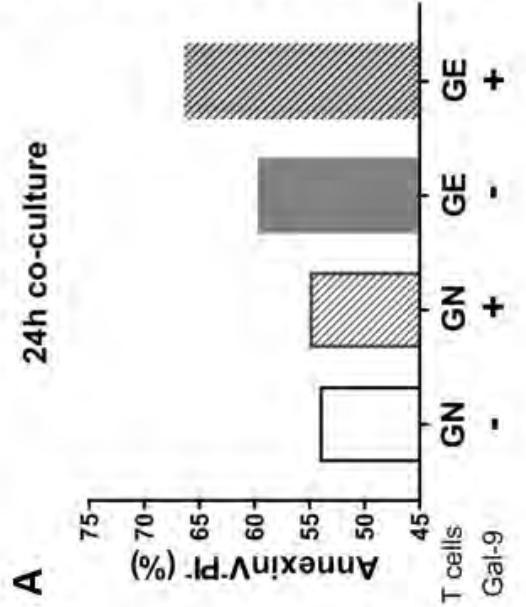


**Figure 7. Detection of CD40L by immunohistochemistry on spleen tissue section from wild-type and *gal-9*-KO C57BL6/JRj mice.** Staining was performed with a monoclonal antibody reacting with murine CD40L and counterstained with hematoxylin. **A and B)** wild-type spleen tissue at magnification 40x (A) and 200x (B). **C and D)** *gal-9*<sup>-/-</sup> spleen tissue at magnification 40x (C) and 200x (D). In most fields, CD40L staining was less intense for *gal-9*-KO than for WT mice, especially at the periphery of the germinal center.

equipment to participate to the extra-follicular antibody response through their interaction with B-cells at the border of B- and T-cell zones. Pre-Tfh cells become mature Tfh when they enter the light zone of the germinal center and acquire expression of PD-1 and IL-21. They can provide a survival signal to centrocytes, in other words B-cells which have mutated their Ig V-region. The CD40 ligand (CD40L) plays a key role in the delivery of this survival signal by Tfh as well as pre-Tfh. Inside the germinal center and beside Tfh cells Tfr or T follicular regulatory cells are CXCR5<sup>hi</sup>/ PD1<sup>hi</sup>/FoxP3<sup>+</sup> cells which can dampen antibody production. They can derive from natural T-regs or naïve T-cells. They usually express Bcl-6 but not CD40L (Ramiscal and Vinuesa 2013). In our study, among CXCR5<sup>+</sup> cells resulting from gal-9 exposure, we have observed subsets which seem to match with typical pre-Tfh and Tfh cells namely those which were CXCR5<sup>+</sup>/CD40L<sup>+</sup>/Foxp3<sup>-</sup>. On the other hand, cells which were CXCR5<sup>+</sup>/FoxP3<sup>+</sup>/CD40L<sup>+</sup> seem to match well with Tfr. The detection of cells with co-expression of CXCR5, FoxP3 and CD40L is puzzling. Additional investigation will be required to confirm the existence of this follicular T-cell subset. Despite the heterogeneity of the CXCR5<sup>+</sup> subset following gal-9 exposure, it is noteworthy that we could observe a greater protection against B-cell apoptosis when making co-cultures with G9Expo- than with G9Naive-T-cells. This suggests that to a large extent, the up-regulation of follicular T-cell markers is linked to a greater capacity of T-cell help in the corresponding cellular subsets.

Our observations about the up-regulation of Tf markers especially CXCR5 after exposure to gal-9 is in apparent contradiction with two previous reports stating that gal-9 antagonizes Tf differentiation (Zhuo, Zhang et al. 2017, Zhang, Li et al. 2021). For Zhuo *et al.* this claim is based on experiments showing a decrease of IL-21 production in CD4<sup>+</sup> peripheral T-cells (Zhuo, Zhang et al. 2017). However, the direct effects of recombinant gal-9 (30 nM, 48h) in these experiments are extremely weak. A greater effect is reported in the same publication using a Tim-3 blocking agent. However, this is not convincing since it is now well known that Tim-3 has other ligands distinct from gal-9 like HMGB1 or phosphatidyl-serine (Chiba, Baghdadi et al. 2012, Sabatos-Peyton, Nevin et al. 2018). For Zhang *et al.* the claim is based only on small differences in the counts of CD4<sup>+</sup>CXCR5<sup>+</sup> cells in pulmonary lymph nodes of WT and gal-9-KO mice (Zhang, Li et al. 2021) .

**Figure 8. Protective role of G9Expo-T cells towards B cells.** T cells collected from the primary culture made with or without gal-9 exposure were co-cultured with Ramos cells at the ratio 2:1. Ramos cells had been labeled with 2  $\mu$ M CFSE before being resuspended in culture medium with or without T cells. Cells were collected after 24 hours of co-culture and stained with Annexin V and propidium iodide. **A)** Surviving cells were gated on CFSE positive cells to evaluate Annexin V-PI frequency. A higher survival rate was observed when Ramos cells were co-cultured with G9Expo-T cells, even in the condition supplemented with gal-9 M 1 $\mu$ g/ml. GN: Gal-9-Naive T cells. GE: Gal-9-Exposed T cells. PI: propidium iodide. **B)** A model of interaction between T and B cells under the influence of gal-9 in the micro-environment of secondary follicles. Naïve B cells are known to produce a large amount of gal-9. Gal-9 is known to be abundant in the mantle zone and light zone of the germinal centers. Extra-cellular gal-9 in one way increases the threshold of BCR activation. Meanwhile, gal-9 enhances maturation of T-cells towards a follicular phenotype. These T-cells acquire the capacity to protect B-cells from apoptosis resulting from solitary BCR-activation, i.e. not concomitant of MHC II-TCR interaction. TCR: T cell receptor. MHC II: major histocompatibility class II.



One may wonder to what extent endogenous gal-9 might have effects similar to recombinant gal-9 on follicular T-cell differentiation. We have no evidence of such activity in the *in vitro* experimental setting based on human PBMCs. No changes in the expression of follicular markers were recorded in the presence of gal-9 neutralizing antibodies by comparison with the control condition. Fortunately the reduction of CXCR5 by splenic T-cells from gal-9-KO mice is a strong argument in favor of the contribution of endogenous mammalian gal-9, at some point, in the differentiation of follicular T-cells. Another potential limitation of our study is the extensive use of one artificial isoform of gal-9, gal-9NC. However, gal-9NC has been reported several times as having the same properties as the wild-type isoforms except that it is more stable and less prone to proteolytic digestion by enzymes like elastase (Nishi, Itoh et al. 2005, Gooden, Wiersma et al. 2013). This is beneficial for the reproducibility of the experiments made with PBMCs from various donors. In addition, the main effects produced by gal-9NC in G9Expo-T-cells were confirmed using the recombinant natural isoform gal-9M) **(Figure 5)**.

Another possible pitfall is due to the fact that the initial exposure of T-cells to recombinant gal-9 was done in the context of whole PBMCs, meaning that the phenotypic changes observed in G9Expo-T-cells could have resulted from indirect effects for example induction of cytokines released by monocytes. Interestingly, as shown in **Figure 3B** the expression of messenger RNAs related to the follicular phenotype – CXCR5, CD40-L, IL-21 – is further enhanced in purified G9Expo-T-cells under a boost of recombinant gal-9. This suggests that gal-9 is directly involved in these transcriptional modifications.



This study was not focused primarily on the mechanisms underlying the emergence of Tf-like cells. However, our data provide some clues on this topic. There is evidence that the phenotypic changes observed in T-cells exposed to gal-9 *in vitro* result from a combination of depleting and inducing effects. Depleting effects are shown by the dramatic reduction of CD8<sup>+</sup> T-cells demonstrated by mass spectrometry. On the other hand, we need to postulate inducing effects to account for the emergence of Tf-like cells under gal-9 exposure. At this point, we can only speculate about the membrane receptors bound by extra-cellular gal-9 and the activated signaling pathways. Tim-3 was probably not involved since mass cytometry analysis showed a dramatic reduction of Tim-3 positive cells following gal-9 exposure. We can consider a contribution of many other membrane receptors of gal-9 like components of the TCR, CD45 and CD44. This subject will deserve a full new cycle of investigations. The same remark applies to the signaling pathways involved in these phenotypic changes. According to previous publications from our group and other groups, one might consider a possible activation of the TCR pathway involving calcium mobilization and phosphorylation of the Lck tyrosine-kinase, a point that will deserve further investigation (Lhuillier, Barjon et al. 2015, Colomb, Giron et al. 2019).

Finally, it is interesting to consider our study in connection with a series of recent publications dealing with the role of gal-9 in the regulation of antibody production inside secondary follicular organs. These publications have been focused on the direct effects of gal-9 on the membrane of B-cells (Cao, Alluqmani et al. 2018, Giovannone, Liang et al. 2018, Smith, Fawaz et al. 2021). They demonstrate that extra-cellular gal-9 binds to the BCR and raises its threshold of activation for example by bridging the IgM BCR with the negative co-receptors CD22 and CD45 in B-2 B cells. Experiments performed on gal-9-KO mice demonstrate that these regulations are very important to prevent autoimmune reactions. On the other hand, our findings seem to reveal another aspect of gal-9 functions in secondary follicular organs (see the cartoon of **Figure 8B**). In addition to its role to prevent the production of auto-antibodies, one of its functions might be to facilitate the differentiation of follicular T-cells and consequently T-cell help to the maturation of “non-detrimental” B-cells which are poised to produce antibodies directed to non-self-antigens.

## Acknowledgments

This work was supported by the Bristol-Myers-Squibb Foundation for Research on Immunology (grant number: 1709-04-040) and the French Institut National du Cancer (INCa, grant n° 2017-031). TBTT was the recipient of a fellowship from the French Ministry of Research. This project was supported by grant "Taxe d'apprentissage Gustave Roussy-2018 and 2019-THTR".

We thank Karim Benihoud and Muriel David for helpful discussions.

## Author contributions.....

## Competing interest statement

PB is involved in a collaborative project about monoclonal antibodies neutralizing extra-cellular galectin-9 in collaboration with HiFiBiO-Therapeutics. Otherwise, the authors declare no potential conflicts of interest.

## Figure legends

**Figure 1. Cartoon depicting the experimental system used to investigate the effects of T-cell exposure to high concentrations of extra-cellular gal-9.** During the first phase of the protocol, from day 1 to day 7, peripheral human T-cells from healthy donors are activated by CD3/CD28 stimulation in a context of co-culture with other types of leucocytes, with or without addition of recombinant gal-9NC (stable isoform - 45nM). Recombinant interleukin-2 is added at day 5 to extend T-cell proliferation. At day 7, T-cells are isolated from other PBMCs by negative magnetic sorting to enter the second phase of the protocol. These T-cells are called "gal-9-exposed" (G9Expo) or "gal-9-naive" (G9Naive) depending on whether or not they have been previously exposed to recombinant gal-9. They are then subjected to various types of investigations like RNA sequencing or flow cytometry, either directly or after a second stage of *in vitro* culture.

This secondary culture is performed with or without addition of recombinant gal-9 NC (15nM), corresponding to the stimulated (S – GNS and GES) or unstimulated (U – GEU and GNU) conditions.

**Figure 2. Greater proliferative potential and resistance to gal-9-related cell death in T-cells following prior exposure to recombinant gal-9. A)** Gal-9-naive (G9Naive) and gal-9-exposed (G9Expo) T-cells were isolated by magnetic sorting and cultured *in vitro* for 4 days with or without addition of recombinant interleukin-2 (IL-2 10 UI/ml). Then cell proliferation was assessed by incorporation of fluorescent EdU. In the absence of recombinant IL-2, there was an excess of proliferation for G9Expo-T-cells from both donors 1 and 3. In the presence of IL-2, this excess of proliferation was observed only for donor 3. **B)** T-cells isolated from PBMCs from 2 donors (1 and 3) by magnetic sorting at day 1 were subjected to gal-9 stimulation for 24 hours using the recombinant M and NC isoforms at increasing concentrations. Apoptosis (Annexin V) and /or cell death (Propidium Iodide) was then assayed by flow cytometry. The maximal percentage of apoptosis (AnV pos. plus PI pos.) was 60% and 90% for gal-9M and gal-9NC, respectively. The IC50 were 12nM and 17nM, respectively. **C)** Assessment of the impact of gal-9 M and NC on G9Naive- and G9Expo-T-cells from the same 2 donors (24h exposure following magnetic separation). For G9Naive-T-cells the maximal percentages of apoptosis were almost identical to those of Fig. 2B. In contrast, there was a substantial reduction of the percentage of apoptosis for G9Expo-T-cells, especially in the presence of gal-9 M (from 60% to 40%).

**Figure 3. Impact of recombinant gal-9 on the transcriptome of human T-cells. A)** Heatmap of overall differential transcription between gal-9-naive (G9Naive-U) and gal-9-exposed (G9Expo-U) human T-cells. Gal-9 exposure was made prior to T-cell separation without late secondary addition of gal-9. Donors (don) of PBMCs are numbered from 1 to 4. The heatmap was generated using the DESeq2 software with correction of the donor effect. **B)** Heatmap of G9Naive-U/G9Expo-U differential transcription in connection with T-cell biology. Made with the same software as in A) on the basis of a list provided by Wong MT et al. (Cell Rep., 2015). **C)** Modifications of expression of some selected genes in T-cells W or W/O initial exposure to gal-9 and W or W/O late addition of gal-9 after magnetic separation. Mean values from 4

donors. G9Naive-U or GNU: no addition of gal-9. GNS: addition of gal-9 only after magnetic separation of T-cells. G9Expo-U or GEU: initial exposure to gal-9 without late addition. GES: initial exposure plus late addition.

**Figure 4. Multidimensional mass cytometry of human T-cells subjected or not to gal-9 exposure. A)** Schematisation of t-SNE plots for manual annotation. **B)** t-SNE plots of selected markers detected on isolated T-cells from donor 5 (similar data for donors 6 and 7 are shown in Supplementary Figure 3). These cells have been subjected to 4 experimental conditions prior to magnetic separation : 1) activated T-cells among PBMCs without addition of recombinant gal-9 (Ctrl); 2) activated T-cells among PBMCs with addition of gal-9 (Gal-9); 3) activated T-cells with addition of an anti-gal-9 antibody (Mouse anti-Galectin-9 B-T33, Origene) (Anti-gal-9); 4) activated T-cells with addition of recombinant gal-9 plus the anti-gal-9 antibody (Gal-9 + anti-gal-9). Strikingly for every marker, all three control plots have a fairly homogenous pattern whereas a distinct pattern is consistently observed for conditions with gal-9 exposure. Two major components are designated A and B, essentially matching CD4<sup>+</sup> and CD8<sup>+</sup> sub-populations. Among the CD4<sup>+</sup> cells, the A1 subset is enriched in PD1<sup>+</sup> and ICOS<sup>+</sup> cells. It is not subjected to significant changes through the various experimental conditions. At baseline, the A2 subset seems to combine strong expressions of T-bet and FoxP3, in addition to ICOS and PD1. B1 designates a subset of CD8<sup>+</sup> cells which like A2 seems to combine the expression of T-bet and FoxP3. Gal-9 exposure results in a dramatic reduction of the whole CD8<sup>+</sup> component. It has a profound effect on the A2 subset changing the T-bet/FoxP3 balance in favor of FoxP3 with a concomitant increase in CCR4 expression in the same subset. The most spectacular change induced by gal-9 exposure is the emergence of the A3 subset combining CD4, T-bet, FoxP3, BCL-6, CXCR5, CD40-L, ICOS, PD1 and CCR4. **C)** Comparison of mean MFI values for Tfh markers detected on T-cells from 3 donors tested in the 4 experimental conditions mentioned in 4B.

**Figure 5. Expression of CD40L, CXCR5, and FoxP3 in CD4<sup>+</sup> T cells after 7 days of treatment by gal-9 M or gal-9 NC.** Subjected to the same experimental procedure as in the mass cytometry assay, T cells from donors 8, 9 and 10 were magnetically sorted after 7 days of treatment with either gal-9 M (45 nM or 90 nM) or gal-9 NC (45 nM). CD40L, CXCR5, FoxP3

expression were analyzed among CD4<sup>+</sup> T cells of the sorted population. **A)** Percentage of CD4<sup>+</sup> T cells having expression of CD40L, CXCR5, FoxP3 or co-expression of these markers. Statistical significance was found by two-way ANOVA with  $p$ -value = 0.0005 in comparison of the 4 experimental conditions. **B)** Median fluorescent intensity (MFI) of CD40L, CXCR5 and FoxP3 expression in CD4<sup>+</sup> T cells. Pairwise comparison of MFI was performed by multiple  $t$ -test between control condition and each of gal-9 treatment. All comparisons have  $p$ -value < 0.00000001.

**Figure 6. Expression of CXCR5 in CD4<sup>+</sup> T cells of wild-type and *gal-9*<sup>-/-</sup> C57BL6/JRj mice.** Splenocytes from wild-type and *gal-9*<sup>-/-</sup> C57BL6/JRj mice were collected and stained with anti-CD4 and anti-CXCR5 antibodies. Dead cells were removed by gating on propidium iodide-negative events. **A)** Gating ancestry of CXCR5 isotype control. **B)** CXCR5<sup>+</sup> population in CD4<sup>+</sup> splenocytes. WT: wild-type mouse. *gal-9*<sup>-/-</sup>: gal-9-knock-out mouse. **C)** Normalized median of fluorescence intensity of CXCR5 was calculated by the ratio of MFI of stained sample on MFI of isotype control. Mean values from 3 pairs of mice. MFI: median of fluorescence intensity. WT: wild-type mice. KO: gal-9-knock-out mice.

**Figure 7. Detection of CD40L by immunohistochemistry on spleen tissue section from wild-type and gal-9-KO C57BL6/JRj mice.** Staining was performed with a monoclonal antibody reacting with murine CD40L and counterstained with hematoxylin. A and B) wild-type spleen tissue at magnification 40x (A) and 200x (B). C and D) *gal-9*<sup>-/-</sup> spleen tissue at magnification 40x (C) and 200x (D). In most fields, CD40L staining was less intense for *gal-9*-KO than for WT mice, especially at the periphery of the germinal center.

**Figure 8. Protective role of G9Expo-T cells towards B cells.** T cells collected from the primary culture made with or without gal-9 exposure were co-cultured with Ramos cells at the ratio 2:1. Ramos cells had been labeled with 2  $\mu$ M CFSE before being resuspended in culture medium with or without T cells. Cells were collected after 24 hours of co-culture and stained with Annexin V and propidium iodide. **A)** Surviving cells were gated on CFSE positive cells to evaluate Annexin V-PI<sup>-</sup> frequency. A higher survival rate was observed when Ramos

cells were co-cultured with G9Expo-T cells, even in the condition supplemented with gal-9 M 1µg/ml. GN: Gal-9-Naïve T cells. GE: Gal-9-Exposed T cells. PI: propidium iodide. **B)** A model of interaction between T and B cells under the influence of gal-9 in the micro-environment of secondary follicles. Naïve B cells are known to produce a large amount of gal-9. Gal-9 is known to be abundant in the mantle zone and light zone of the germinal centers. Extra-cellular gal-9 in one way increases the threshold of BCR activation. Meanwhile, gal-9 enhances maturation of T-cells towards a follicular phenotype. These T-cells acquire the capacity to protect B-cells from apoptosis resulting from solitary BCR-activation, i.e. not concomitant of MHC II-TCR interaction. TCR: T cell receptor. MHC II: major histocompatibility class II.

## Supplementary materials

**Supplementary Table 1:** Origins of PBMCs used for various modalities of investigation.

**Supplementary Table 2:** recapitulation of cell counts for human PBMCs subjected to *in vitro* activation with or without concomitant exposure to recombinant gal-9. D7/D1 ratio: quotient of the number of PBMCs collected on D7 by the number seeded on D1. Percentage of live cells among PBMCs collected on D7. Number of T-cells recovered after magnetic sorting of D7-PBMCs.

**Supplementary Table 3:** List of 30 enrichment plots from GSEA with best matching of differentially expressed genes between G9Expo- and G9Naive-T-cells.

**Supplementary Table 4:** Characteristics of the 21 metal-labeled antibodies used for mass cytometry analysis of G9Expo- and G9Naive-T-cells.

**Supplementary Table 5:** Frequency of FoxP3<sup>+</sup> and CD40L<sup>+</sup> positive cells among CD4<sup>+</sup>CXCR5<sup>+</sup> cells in 4 experimental conditions (gal-9 exposure and 3 control conditions).

Supplementary Table 1. Origins of PBMCs used for various modalities of investigation

	EdU incorporation	Bulk RNAseq		CytoTOF	Cytometry
Initial gal-9 exposure	+	+	+	+	+
Late gal-9 addition	-	-	+	-	
Names of exp conditions	G9NaiveU and G9ExpoU	G9NaiveU and G9ExpoU	G9NaiveS and G9ExpoS	G9NaiveU and G9ExpoU	
Donor 1	X	X	X		
Donor 2		X	X		
Donor 3	X	X	X		
Donor 4		X	X		
Donor 5				X	
Donor 6				X	
Donor 7				X	
Donor 8					X
Donor 9					X
Donor 10					X

Supplementary Table 2. Cell counts for PBMCs and T-cells recovered after 7 days of primary culture with or without gal-9 exposure

Experiments # (donor #)	PBMC W/O gal-9			PBMC W gal-9		
	D7/D1 cell number ratio	% live cells at D7	live T-cells recovered at D7	D7/D1 cell number ratio	% live cells at D7	live T-cells recovered at D7
Donor 1	1.023958	0.78	27870000	0.518889	0.49	13200000
Donor 2	0.858463	0.83	17465000	0.540597	0.53	15610000
Donor 3	0.832222	0.91	13510000	0.346667	0.56	10255000
Donor 4	1.062	0.83	25560000	0.417	0.68	21060000

**Supplementary Table 6:** List of antibodies used to characterize splenocytes of wild-type and gal-9<sup>-/-</sup> C57BL6/JRj mice.

**Supplementary Table 7:** List of antibodies used for conventional flow cytometry on human T cells.

**Supplementary Figure 1:** Evolution of gal-9 concentrations and cell count during the primary culture of PBMCs. **A)** Supernatants of cell culture were collected at day 1, 2, 5 and 7, then measured by ELISA assay to determine the concentration of gal-9. Mean values from 3 donors. CM: culture with control medium. Gal-9: culture with gal-9 45 nM. Anti-Gal-9: culture with anti-gal-9 antibody at 5 IU/ml. Anti-Gal-9 + Gal-9: culture with anti-gal-9 at 5 IU/ml at gal-9 at 45 nM. **B)** Ratio of PBMC counts at day 7 on total counts of cells seeded at the start of primary culture. Mean values from 4 donors (Supplementary Table 2). Analysis for significant difference was performed with Kruskal-Wallis test.

**Supplementary Figure 2:** Proliferation of gal-9-naïve and gal-9-exposed T cells (GN-T and GE-T respectively). After 7 days of primary culture with or without gal-9, GN-T and GE-T were isolated by magnetic sorting and labeled with CellTrace™ Far Red dye, then subjected to a secondary *in vitro* culture for 4 days with or without addition of recombinant interleukin-2 (IL-2, 10 UI/ml). At the end of secondary culture, cells were collected and labeled with 5-ethynyl-2'-deoxyuridine (EdU) and analyzed with flow cytometer. Fluorescent intensity of CellTrace was gated in 3 level (P1, P2, P3) with P3 being the youngest generation of T cell. **A)** CellTrace labeling of cells from donor 1. **B)** CellTrace labeling of cells from donor 3. **C)** EdU labeling of cells from donor 1. **D)** EdU labeling of cells from donor 3.

**Supplementary Figure 3:** t-SNE plots of selected markers detected on isolated T cells from donor 6 and donor 7. For both donors, the CD8<sup>+</sup> component is dramatically reduced under gal-9 exposure. The CD4<sup>+</sup> subset designated as A1 (PD1<sup>+</sup>, ICOS<sup>+</sup>) in the legend of figure 4 is not detected for these donors. Another CD4<sup>+</sup> subset designated as A2 (T-bet<sup>+</sup>, FoxP3<sup>+</sup>, PD1<sup>+</sup>, ICOS<sup>+</sup>) seems to be detected for donor 7 but not donor 6. Even in donor 6, the impact of gal-9 exposure on this subset is discreet. On the other hand, a subset similar to the A3 subset of donor 5 is recorded for donors 6 and 7 with the same essential characteristics: induction by gal-9 exposure and positivity for Bcl-6, CXCR5 and CD40-L.



Supplementary Table 3. List of 30 enrichment plots from GSEA with best matching of differentially expressed genes between G9Expo- and G9Naive-T-cells

Gene set name	SIZE	ES	NES	NOM p-val	FDR q-val	FWER p-val	RANK AT MAX	LEADING EDGE
GSE21670_UNTREATED_VS_IL6_TREATED_STAT3_KO_CD4_TCELL_DN	196	0.660259	3.060873	0	0	0	3012	tags=55%, list=14%, signal=64%
GSE22886_UNSTIM_VS_IL2_STIM_NKCELL_DN	200	0.629271	2.934044	0	0	0	5076	tags=65%, list=24%, signal=84%
GSE37532_TREG_VS_TCONV_CD4_TCELL_FROM_LN_UP	199	0.627402	2.9137	0	0	0	3765	tags=54%, list=18%, signal=65%
GSE45739_NRAS_KO_VS_WT_UNSTIM_CD4_TCELL_UP	197	0.617782	2.907723	0	0	0	2928	tags=52%, list=14%, signal=59%
GSE6674_ANTI_IJM_VS_ANTI_IJM_AND_CPG_STIM_BCELL_DN	198	0.610791	2.846054	0	0	0	3373	tags=52%, list=16%, signal=61%
GSE22886_UNSTIM_VS_IL15_STIM_NKCELL_DN	200	0.608372	2.844832	0	0	0	3982	tags=55%, list=19%, signal=66%
GSE2770_IL12_AND_TGFB_ACT_VS_ACT_CD4_TCELL_6H_DN	197	0.602405	2.806762	0	0	0	3845	tags=51%, list=18%, signal=62%
GSE6674_ANTI_IJM_VS_CPG_STIM_BCELL_DN	198	0.602847	2.804638	0	0	0	3339	tags=49%, list=16%, signal=58%
GSE28726_NAIVE_VS_ACTIVATED_VA24NEG_NKCELL_UP	200	0.59357	2.786653	0	0	0	3548	tags=51%, list=17%, signal=60%
GSE24634_TREG_VS_TCONV_POST_DAY3_IL4_CONVERSION_UP	199	0.598145	2.780119	0	0	0	5915	tags=61%, list=28%, signal=84%
GSE32986_UNSTIM_VS_GMCSF_AND_CURDLAN_LOWDOSE_STIM_DC_UP	199	0.592972	2.767923	0	0	0	3614	tags=49%, list=17%, signal=59%
GSE21927_SPLEEN_C57BL6_VS_E14_TUMOR_BALBC_MONOCYTES_DN	199	0.599646	2.756748	0	0	0	5128	tags=59%, list=24%, signal=77%
GSE24634_TREG_VS_TCONV_POST_DAYS_IL4_CONVERSION_UP	200	0.589874	2.740934	0	0	0	4872	tags=56%, list=23%, signal=72%
GSE21360_SECONDARY_VS_TERTIARY_MEMORY_CD8_TCELL_UP	200	0.588598	2.734395	0	0	0	5756	tags=58%, list=27%, signal=79%
GSE45739_NRAS_KO_VS_WT_ACD3_ACD28_STIM_CD4_TCELL_UP	195	0.587802	2.732486	0	0	0	2934	tags=47%, list=14%, signal=54%
GSE46606_UNSTIM_VS_CD40L_IL2_IL5_DAY3_STIMULATED_BCELL_DN	197	0.587583	2.726394	0	0	0	3798	tags=51%, list=18%, signal=62%
GSE23114_PERITONEAL_CAVITY_B1A_BCELL_VS_SPLEEN_BCELL_DN	200	0.573459	2.692929	0	0	0	4138	tags=48%, list=19%, signal=58%
GSE17974_0H_VS_4H_IN_VITRO_ACT_CD4_TCELL_DN	197	0.574701	2.679784	0	0	0	2900	tags=41%, list=14%, signal=47%
GSE36476_CTRL_VS_TSST_ACT_16H_MEMORY_CD4_TCELL_OLD_DN	200	0.567736	2.665826	0	0	0	3973	tags=48%, list=19%, signal=58%
GSE23321_EFFECTOR_MEMORY_VS_NAIVE_CD8_TCELL_DN	195	0.572572	2.661127	0	0	0	3971	tags=51%, list=19%, signal=62%
GSE46606_UNSTIM_VS_CD40L_IL2_IL5_DAY1_STIMULATED_BCELL_DN	196	0.57162	2.64289	0	0	0	4947	tags=57%, list=23%, signal=73%
GSE17974_CTRL_VS_ACT_IL4_AND_ANTIL_IL12_12H_CD4_TCELL_DN	198	0.565934	2.628674	0	0	0	3611	tags=42%, list=17%, signal=50%
GSE22432_MULTIPOTENT_VS_COMMON_DC_PROGENITOR_UNTREATED_UP	200	0.566102	2.619179	0	0	0	5207	tags=57%, list=24%, signal=74%
GSE37532_TREG_VS_TCONV_PPARG_KO_CD4_TCELL_FROM_LN_DN	199	0.568541	2.614713	0	0	0	3262	tags=44%, list=15%, signal=52%
GSE22611_NOD2_TRANSDUCED_VS_CTRL_HEK293T_STIMULATED_WITH_MDP_2H_DN	186	0.564311	2.614326	0	0	0	2924	tags=40%, list=14%, signal=46%
GSE5679_CTRL_VS_RARA_AGONIST_AM580_TREATED_DC_UP	200	0.558709	2.612869	0	0	0	4077	tags=45%, list=19%, signal=46%
GSE21670_STAT3_KO_VS_WT_CD4_TCELL_DN	197	0.558634	2.603294	0	0	0	2133	tags=42%, list=10%, signal=54%
GSE36476_CTRL_VS_TSST_ACT_16H_MEMORY_CD4_TCELL_YOUNG_DN	200	0.559742	2.588553	0	0	0	3503	tags=47%, list=16%, signal=56%
GSE21927_BALBC_VS_C57BL6_MONOCYTE_TUMOR_UP	198	0.555247	2.584418	0	0	0	4589	tags=48%, list=21%, signal=61%
GSE43863_TH1_VS_LY6C_INT_CXCR5POS_MEMORY_CD4_TCELL_UP	198	0.559339	2.583708	0	0	0	3486	tags=46%, list=16%, signal=54%

Supplementary Table 4. Characteristics of the 21 metal-labelled antibodies used for mass cytometry analysis of G9Expo- and G9Naive-T-cells

Identifier	Specificity	Mass and tags	Clone	Source
3141004B	Anti-Human CD49d	141Pr	9F10	Fluidigm
3143023A	Anti-Human NFAT1	143Nd	D43B1	Fluidigm
3145001B	Anti-Human CD4	145Nd	RPA-T4	Fluidigm
3146001B	Anti-Human CD8	146Nd	RPA-T8	Fluidigm
3148019C	Anti-Cross CD278/ICOS	148Nd	C398.4A	Fluidigm
3149001B	Anti-Human CD45RO	149Sm	UCHL1	Fluidigm
3150023B	Anti-Human CD134/OX40	150Nd	ACT35	Fluidigm
3152017B	Anti-Human CD95/Fas	152Sm	DX2	Fluidigm
3153008B	Anti-Human TIM-3	153Eu	F38-2E2	Fluidigm
3155009B	Anti-Human CD279/PD-1	155Gd	MBSA43	Fluidigm
3160004B	Anti-Human CD39	160Gd	EH12.2H7	Fluidigm
3161014C	Anti-Human T-bet	161Dy	4B10	Fluidigm
3162024A	Anti-Human FoxP3	162Dy	A1	Fluidigm
3163012B	Anti-Human/Mouse Bcl-6	163Dy	K112-91	Fluidigm
3164029C	Anti-Human CXCR5	164Dy	RF8B2	Fluidigm
3168006C	Anti-Human CD154/CD40L	168Er	24-31	Fluidigm
3169003B	Anti-Human CD25	169Tm	11C3C65	Fluidigm
3170010B	Anti-Human CD45RA	170Er	HI100	Fluidigm
3173015B	Anti-Human CD137/4-1BB	173Yb	2A3	Fluidigm
3175035A	Anti-Human CD194/CCR4	175Lu	L291H4	Fluidigm
3176004B	Anti-Human CD127/IL-7Ra	176Yb	4B4-1	Fluidigm

Supplementary Table 5. Frequency of FoxP3<sup>+</sup> and CD40L<sup>+</sup> positive cells among CD4<sup>+</sup>CXCR5<sup>+</sup> cells in 4 experimental conditions (gal-9 exposure and 3 control conditions)

	CD4 <sup>+</sup> CXCR5 <sup>+</sup> FoxP3 <sup>+</sup>			CD4 <sup>+</sup> CXCR5 <sup>+</sup> FoxP3 <sup>-</sup>			CD4 <sup>+</sup> CXCR5 <sup>+</sup> CD40L <sup>+</sup> FoxP3 <sup>+</sup>			CD4 <sup>+</sup> CXCR5 <sup>+</sup> CD40L <sup>+</sup> FoxP3 <sup>-</sup>		
	Donor 5	Donor 6	Donor 7	Donor 5	Donor 6	Donor 7	Donor 5	Donor 6	Donor 7	Donor 5	Donor 6	Donor 7
<b>Ctrl</b>	1.03	5.45	6.12	1.29	1.42	1.52	0.32	0.76	1.11	0.33	0.08	0.15
<b>Gal-9</b>	7.8	18.6	16.5	7.7	4.8	5	2.58	9.38	6.87	1.38	1.42	1.28
<b>Anti-Gal-9</b>	0.94	4.29	5.39	1.58	2.21	2.53	0.33	1.8	1.32	0.49	0.5	0.32
<b>Anti-Gal-9 + Gal-9</b>	1.13	11	11.8	3.9	1.7	4.1	0.53	3.74	4.76	1.97	0.32	1

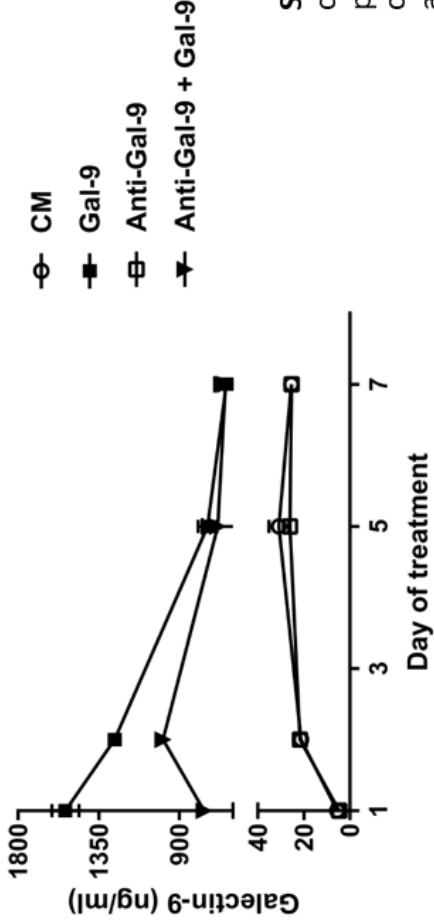
Supplementary Table 6. List of antibodies used to characterize splenocytes of wild-type and *gal-9<sup>-/-</sup>* C57BL6/JRj mice

Identifier	Specificity	Fluorescence	Source
106509	Anti-mouse CD154	APC	Biolegend
400911	Armenian Hamster IgG Isotype Ctrl Antibody	APC	Biolegend
145515	Anti-mouse CD185 (CXCR5)	PE/Cyanine7	Biolegend
400617	Rat IgG2b, $\kappa$ Isotype Ctrl Antibody	PE/Cyanine7	Biolegend
124611	APC anti-mouse CD40	APC	Biolegend
400511	Rat IgG2a, $\kappa$ Isotype Ctrl Antibody	APC	Biolegend
101613	Anti-mouse CD23	PE/Cyanine7	Biolegend
400254	Mouse IgG2a, $\kappa$ Isotype Ctrl Antibody	PE/Cyanine7	Biolegend
100405	Anti-mouse CD4	FITC	Biolegend
400605	Rat IgG2b, $\kappa$ Isotype Ctrl Antibody	FITC	Biolegend
152403	anti-mouse CD19 Antibody	FITC	Biolegend
400505	Rat IgG2a, $\kappa$ Isotype Ctrl Antibody	FITC	Biolegend
145511	Anti-mouse CD185 (CXCR5)	Brilliant Violet 421™	Biolegend
400639	Rat IgG2b, $\kappa$ Isotype Ctrl	Brilliant Violet 421™	Biolegend
553142	Purified Rat Anti-Mouse CD16/CD32 (Mouse BD Fc Block™)		BD Biosciences

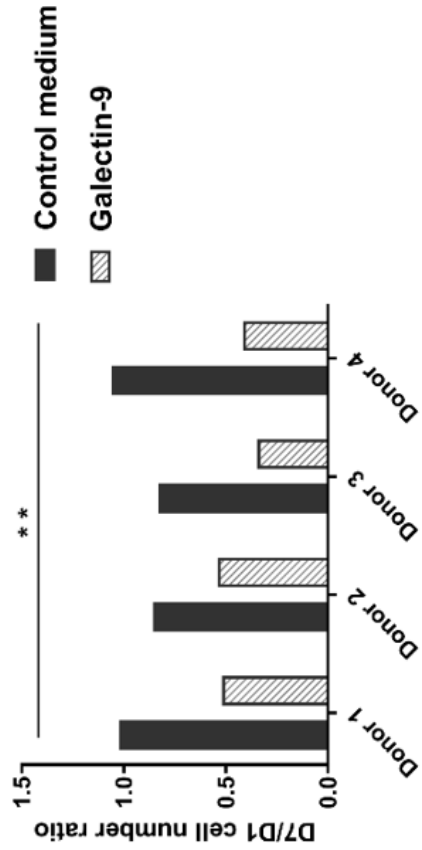
Supplementary Table 7. List of antibodies used for conventional flow cytometry on human T cells

Identifier	Specificity	Fluorescence	Source
356935	Anti-human CD185 (CXCR5)	Brilliant Violet 785™	Biologend
310837	Anti-human CD154	Brilliant Violet 711™	Biologend
300538	Anti-human CD4	FITC	Biologend
560046	Anti-Human FoxP3	PE	BD Biosciences
400169	Mouse IgG1, κ Isotype Ctrl	Brilliant Violet 785™	Biologend
400109	Mouse IgG1, κ Isotype Ctrl (FC)	FITC	Biologend
400167	Mouse IgG1, κ Isotype Ctrl	Brilliant Violet 711™	Biologend
400139	Mouse IgG1, κ Isotype Ctrl	PE	Biologend

### A Evolution of gal-9 concentrations

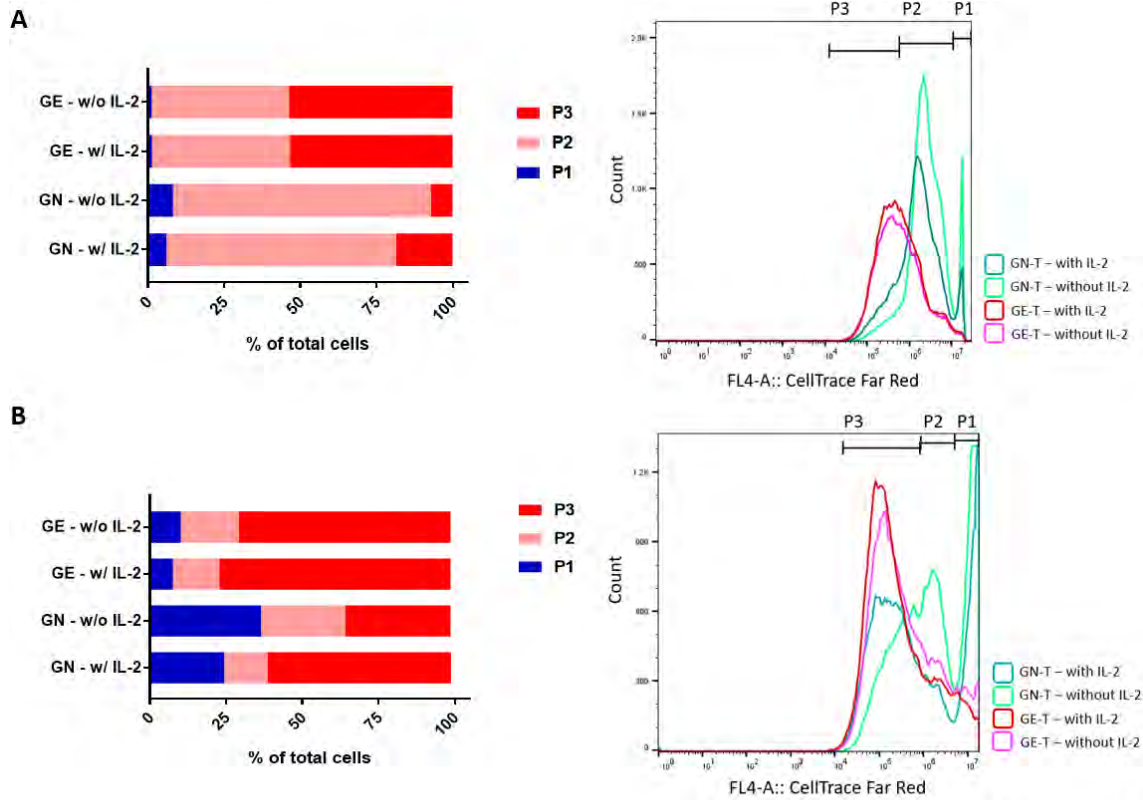


### B T cell recovery

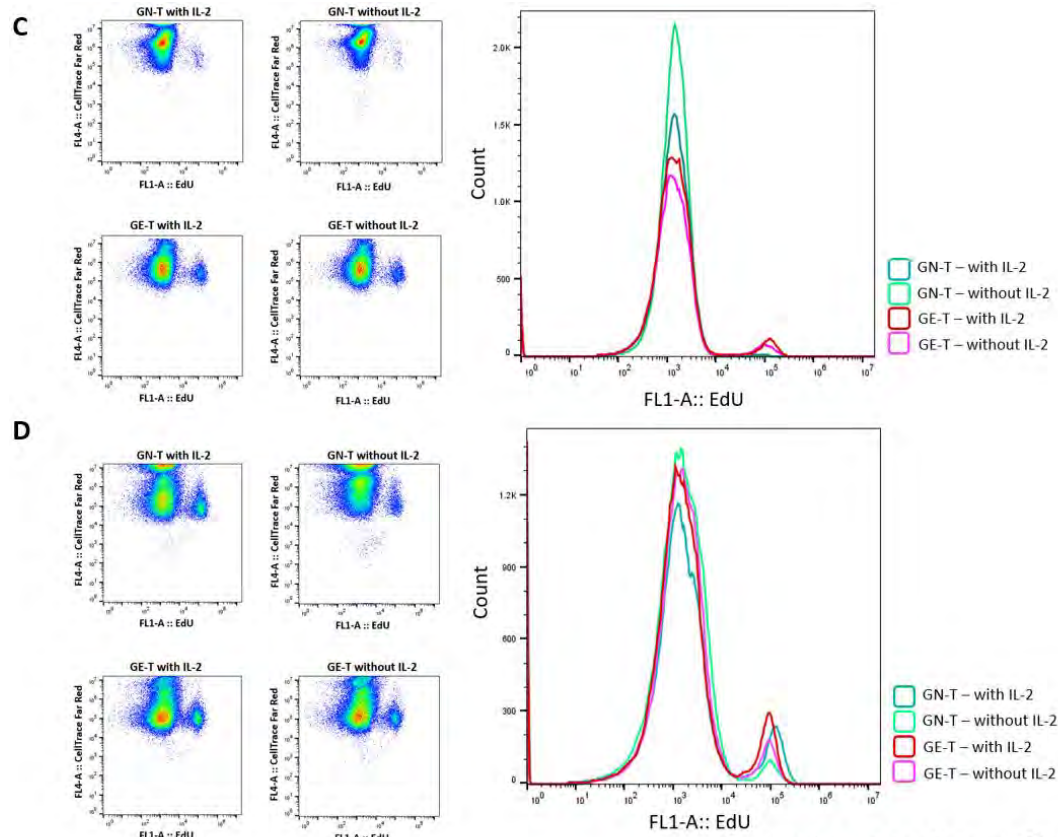


**Supplementary Figure 1.** Evolution of gal-9 concentrations and cell count during the primary culture of PBMCs. **A)** Supernatants of cell culture were collected at day 1, 2, 5 and 7, then measured by ELISA assay to determine the concentration of gal-9. Mean values from 3 donors. CM: culture with control medium. Gal-9: culture with gal-9 45 nM. Anti-Gal-9: culture with anti-gal-9 antibody at 5 IU/ml. Anti-Gal-9 + Gal-9: culture with anti-gal-9 at 5 IU/ml at gal-9 at 45 nM. **B)** Ratio of PBMC counts at day 7 on total counts of cells seeded at the start of primary culture. Mean values from 4 donors (Supplementary Table 2). Analysis for significant difference was performed with Kruskal-Wallis test.

## Supplementary figure 1

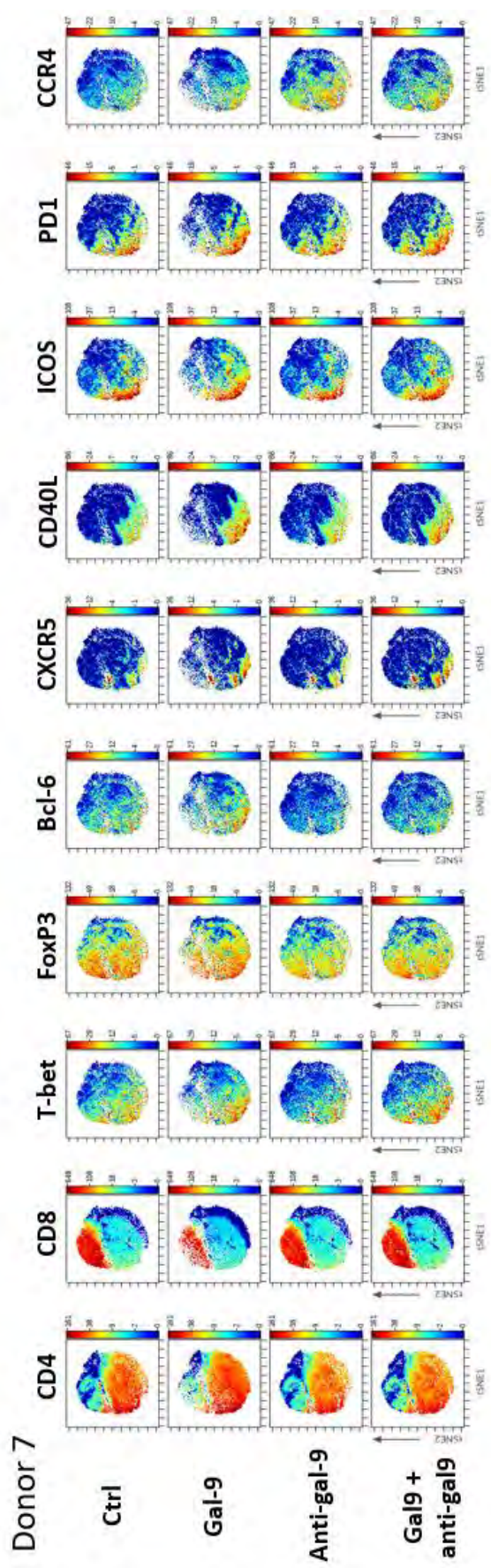
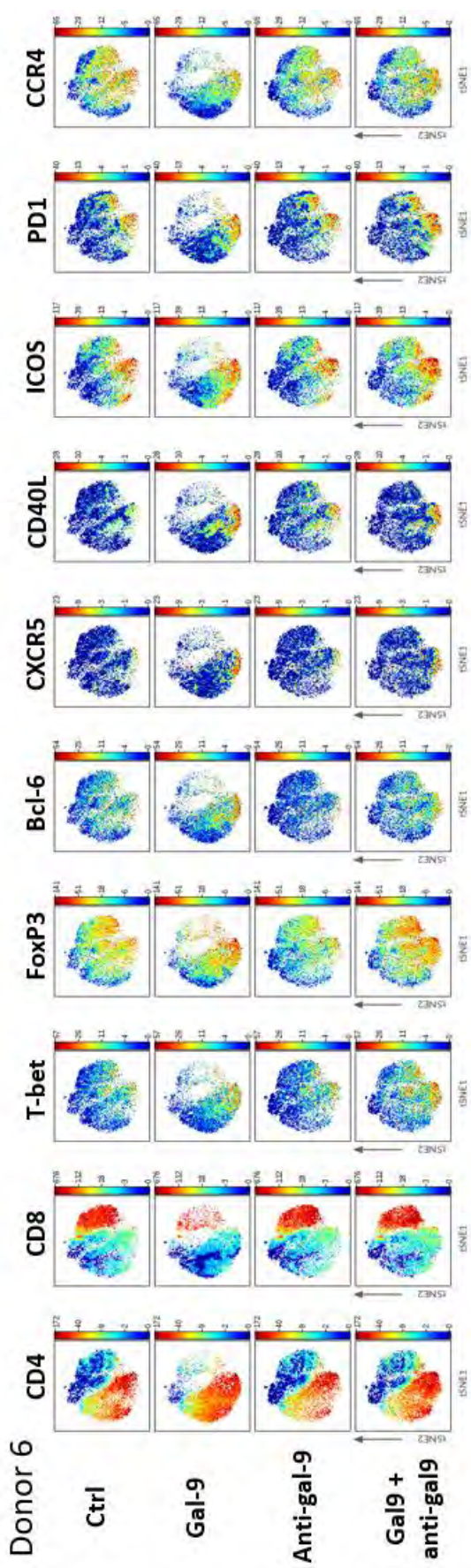


Supplementary figure 2



Supplementary figure 2

**Supplementary Figure 2. Proliferation of gal-9-naïve and gal-9-exposed T cells (GN-T and GE-T respectively).** After 7 days of primary culture with or without gal-9, GN-T and GE-T were isolated by magnetic sorting and labeled with CellTrace™ Far Red dye, then subjected to a secondary *in vitro* culture for 4 days with or without addition of recombinant interleukin-2 (IL-2, 10 UI/ml). At the end of secondary culture, cells were collected and labeled with 5-ethynyl-2'-deoxyuridine (EdU) and analyzed with flow cytometer. Fluorescent intensity of CellTrace was gated in 3 level (P1, P2, P3) with P3 being the youngest generation of T cell. **A)** CellTrace labeling of cells from donor 1. **B)** CellTrace labeling of cells from donor 3. **C)** EdU labeling of cells from donor 1. **D)** EdU labeling of cells from donor 3.





**Supplementary Figure 3. t-SNE plots of selected markers detected on isolated T cells from donor 6 and donor 7.** For both donors, the CD8<sup>+</sup> component is dramatically reduced under gal-9 exposure. The CD4<sup>+</sup> subset designated as A1 (PD1<sup>+</sup>, ICOS<sup>+</sup>) in the legend of figure 4 is not detected for these donors. Another CD4<sup>+</sup> subset designated as A2 (T-bet<sup>+</sup>, FoxP3<sup>+</sup>, PD1<sup>+</sup>, ICOS<sup>+</sup>) seems to be detected for donor 7 but not donor 6. Even in donor 6, the impact of gal-9 exposure on this subset is discreet. On the other hand, a subset similar to the A3 subset of donor 5 is recorded for donors 6 and 7 with the same essential characteristics: induction by gal-9 exposure and positivity for Bcl-6, CXCR5 and CD40-L.

## References

- Baloche, V., J. Riviere, T. B. T. Tran, A. Gelin, O. Bawa, N. Signolle, M. B. K. Diop, P. Dessen, S. Beq, M. David and P. Busson (2021). "Serial transplantation unmasks galectin-9 contribution to tumor immune escape in the MB49 murine model." *Sci Rep* **11**(1): 5227.
- Barjon, C., T. Niki, B. Vérillaud, P. Opolon, P. Bedossa, M. Hirashima, S. Blanchin, M. Wassef, H. R. Rosen and A.-S. Jimenez (2012). "A novel monoclonal antibody for detection of galectin-9 in tissue sections: application to human tissues infected by oncogenic viruses." *Infect Agent Cancer* **7**(1): 16.
- Bozorgmehr, N., S. Mashhour, E. Perez Rosero, L. Xu, S. Shahbaz, W. Sligl, M. Osman, D. J. Kutsogiannis, E. MacIntyre, C. R. O'Neil and S. Elahi (2021). "Galectin-9, a Player in Cytokine Release Syndrome and a Surrogate Diagnostic Biomarker in SARS-CoV-2 Infection." *mBio* **12**(3).
- Cao, A., N. Alluqmani, F. H. M. Buhari, L. Wasim, L. K. Smith, A. T. Quaile, M. Shannon, Z. Hakim, H. Furmli, D. M. Owen, A. Savchenko and B. Treanor (2018). "Galectin-9 binds IgM-BCR to regulate B cell signaling." *Nature communications* **9**(1): 3288.
- Chiba, S., M. Baghdadi, H. Akiba, H. Yoshiyama, I. Kinoshita, H. Dosaka-Akita, Y. Fujioka, Y. Ohba, J. V. Gorman, J. D. Colgan, M. Hirashima, T. Uede, A. Takaoka, H. Yagita and M. Jinushi (2012). "Tumor-infiltrating DCs suppress nucleic acid-mediated innate immune responses through interactions between the receptor TIM-3 and the alarmin HMGB1." *Nature immunology* **13**(9): 832-842.
- Colomb, F., L. B. Giron, T. A. Premeaux, B. I. Mitchell, T. Niki, E. Papasavvas, L. J. Montaner, L. C. Ndhlovu and M. Abdel-Mohsen (2019). "Galectin-9 Mediates HIV Transcription by Inducing TCR-Dependent ERK Signaling." *Frontiers in immunology* **10**: 267.
- Colomb, F., L. B. Giron, T. A. Premeaux, B. I. Mitchell, T. Niki, E. Papasavvas, L. J. Montaner, L. C. Ndhlovu and M. Abdel-Mohsen (2019). "Galectin-9 Mediates HIV Transcription by Inducing TCR-Dependent ERK Signaling." *Front Immunol* **10**: 267.
- Daley, D., V. R. Mani, N. Mohan, N. Akkad, A. Ochi, D. W. Heindel, K. B. Lee, C. P. Zambirinis, G. S. B. Pandian, S. Savadkar, A. Torres-Hernandez, S. Nayak, D. Wang, M. Hundeyin, B. Diskin, B. Aykut, G. Werba, R. M. Barilla, R. Rodriguez, S. Chang, L. Gardner, L. K. Mahal, B. Ueberheide and G. Miller (2017). "Dectin 1 activation on macrophages by galectin 9 promotes pancreatic carcinoma and peritumoral immune tolerance." *Nature medicine* **23**(5): 556-567.
- Dardalhon, V., A. C. Anderson, J. Karman, L. Apetoh, R. Chandwaskar, D. H. Lee, M. Cornejo, N. Nishi, A. Yamauchi, F. J. Quintana, R. A. Sobel, M. Hirashima and V. K. Kuchroo (2010). "Tim-3/galectin-9 pathway: regulation of Th1 immunity through promotion of CD11b+Ly-6G+ myeloid cells." *Journal of immunology* **185**(3): 1383-1392.
- Enninga, E. A. L., K. Chatzopoulos, J. T. Butterfield, S. L. Sutor, A. A. Leontovich, W. K. Nevala, T. J. Flotte and S. N. Markovic (2018). "CD206-positive myeloid cells bind galectin-9 and promote a tumor-supportive microenvironment." *J Pathol* **245**(4): 468-477.
- Giovannone, N., J. Liang, A. Antonopoulos, J. Geddes Sweeney, S. L. King, S. M. Pochebit, N. Bhattacharyya, G. S. Lee, A. Dell, H. R. Widlund, S. M. Haslam and C. J. Dimitroff (2018). "Galectin-9 suppresses B cell receptor signaling and is regulated by I-branching of N-glycans." *Nature communications* **9**(1): 3287.
- Golden-Mason, L., R. H. McMahan, M. Strong, R. Reisdorph, S. Mahaffey, B. E. Palmer, L. Cheng, C. Kulesza, M. Hirashima, T. Niki and H. R. Rosen (2013). "Galectin-9 functionally impairs natural killer cells in humans and mice." *Journal of virology* **87**(9): 4835-4845.
- Gooden, M. J., V. R. Wiersma, D. F. Samplonius, J. Gerssen, R. J. van Ginkel, H. W. Nijman, M. Hirashima, T. Niki, P. Eggleton, W. Helfrich and E. Bremer (2013). "Galectin-9 activates and expands human T-helper 1 cells." *PLoS One* **8**(5): e65616.
- Johannes, L., R. Jacob and H. Leffler (2018). "Galectins at a glance." *Journal of cell science* **131**(9).
- John, S. and R. Mishra (2016). "Galectin-9: From cell biology to complex disease dynamics." *J Biosci* **41**(3): 507-534.

Kang, C. W., A. Dutta, L. Y. Chang, J. Mahalingam, Y. C. Lin, J. M. Chiang, C. Y. Hsu, C. T. Huang, W. T. Su, Y. Y. Chu and C. Y. Lin (2015). "Apoptosis of tumor infiltrating effector TIM-3+CD8+ T cells in colon cancer." *Sci Rep* **5**: 15659.

Katoh, S., M. Ikeda, H. Shimizu, K. Mouri, Y. Obase, Y. Kobashi, K. Fukushima, M. Hirashima and M. Oka (2014). "Increased levels of plasma galectin-9 in patients with influenza virus infection." *Tohoku J Exp Med* **232**(4): 263-267.

Kotecha, N., P. O. Krutzik and J. M. Irish (2010). "Web-based analysis and publication of flow cytometry experiments." *Curr Protoc Cytom* **Chapter 10**: Unit10.17.

Lederman, S., M. J. Yellin, A. M. Cleary, A. Pernis, G. Inghirami, L. E. Cohn, L. R. Covey, J. J. Lee, P. Rothman and L. Chess (1994). "T-BAM/CD40-L on helper T lymphocytes augments lymphokine-induced B cell Ig isotype switch recombination and rescues B cells from programmed cell death." *J Immunol* **152**(5): 2163-2171.

Lhuillier, C., C. Barjon, T. Niki, A. Gelin, F. Praz, O. Morales, S. Souquere, M. Hirashima, M. Wei and O. Dellis (2015). "Impact of Exogenous Galectin-9 on Human T Cells CONTRIBUTION OF THE T CELL RECEPTOR COMPLEX TO ANTIGEN-INDEPENDENT ACTIVATION BUT NOT TO APOPTOSIS INDUCTION." *Journal of Biological Chemistry* **290**(27): 16797-16811.

Li, H., K. Wu, K. Tao, L. Chen, Q. Zheng, X. Lu, J. Liu, L. Shi, C. Liu, G. Wang and W. Zou (2012). "Tim-3/galectin-9 signaling pathway mediates T cell dysfunction and predicts poor prognosis in patients with HBV-associated hepatocellular carcinoma." *Hepatology*.

Liberzon, A., A. Subramanian, R. Pinchback, H. Thorvaldsdóttir, P. Tamayo and J. P. Mesirov (2011). "Molecular signatures database (MSigDB) 3.0." *Bioinformatics* **27**(12): 1739-1740.

Lv, K., Y. Zhang, M. Zhang, M. Zhong and Q. Suo (2013). "Galectin-9 promotes TGF-beta1-dependent induction of regulatory T cells via the TGF-beta/Smad signaling pathway." *Mol Med Rep* **7**(1): 205-210.

Mengshol, J. A., L. Golden-Mason, T. Arikawa, M. Smith, T. Niki, R. McWilliams, J. A. Randall, R. McMahan, M. A. Zimmerman and M. Rangachari (2010). "A crucial role for Kupffer cell-derived galectin-9 in regulation of T cell immunity in hepatitis C infection." *PLoS One* **5**(3): e9504.

Mishra, R., M. Grzybek, T. Niki, M. Hirashima and K. Simons (2010). "Galectin-9 trafficking regulates apical-basal polarity in Madin-Darby canine kidney epithelial cells." *Proceedings of the National Academy of Sciences of the United States of America* **107**(41): 17633-17638.

Mo, D., S. A. Costa, G. Ihrke, R. T. Youker, N. Pastor-Soler, R. P. Hughey and O. A. Weisz (2012). "Sialylation of N-linked glycans mediates apical delivery of endolyn in MDCK cells via a galectin-9-dependent mechanism." *Mol Biol Cell* **23**(18): 3636-3646.

Nakagawa, R. and D. P. Calado (2021). "Positive Selection in the Light Zone of Germinal Centers." *Front Immunol* **12**: 661678.

Nebbia, G., D. Peppia, A. Schurich, P. Khanna, H. D. Singh, Y. Cheng, W. Rosenberg, G. Dusheiko, R. Gilson, J. Chinaleong, P. Kennedy and M. K. Maini (2012). "Upregulation of the tim-3/galectin-9 pathway of T cell exhaustion in chronic hepatitis B virus infection." *PLoS One* **7**(10): e47648.

Nishi, N., A. Itoh, A. Fujiyama, N. Yoshida, S. Araya, M. Hirashima, H. Shoji and T. Nakamura (2005). "Development of highly stable galectins: truncation of the linker peptide confers protease-resistance on tandem-repeat type galectins." *FEBS Lett* **579**(10): 2058-2064.

Oomizu, S., T. Arikawa, T. Niki, T. Kadowaki, M. Ueno, N. Nishi, A. Yamauchi and M. Hirashima (2012). "Galectin-9 suppresses Th17 cell development in an IL-2-dependent but Tim-3-independent manner." *Clinical immunology*.

Pioche-Durieu, C., C. Keryer, S. Souquere, J. Bosq, W. Faigle, D. Loew, M. Hirashima, N. Nishi, J. Middeldorp and P. Busson (2005). "In nasopharyngeal carcinoma cells, Epstein-Barr virus LMP1 interacts with galectin 9 in membrane raft elements resistant to simvastatin." *J Virol* **79**(21): 13326-13337.

Ramiscal, R. R. and C. G. Vinuesa (2013). "T-cell subsets in the germinal center." *Immunol Rev* **252**(1): 146-155.

Sabatos-Peyton, C. A., J. Nevin, A. Brock, J. D. Venable, D. J. Tan, N. Kassam, F. Xu, J. Taraszka, L. Wesemann, T. Pertel, N. Acharya, M. Klapholz, Y. Etminan, X. Jiang, Y. H. Huang, R. S. Blumberg, V. K.

Kuchroo and A. C. Anderson (2018). "Blockade of Tim-3 binding to phosphatidylserine and CEACAM1 is a shared feature of anti-Tim-3 antibodies that have functional efficacy." Oncoimmunology **7**(2): e1385690.

Seifert, A. M., C. Reiche, M. Heiduk, A. Tannert, A. C. Meinecke, S. Baier, J. von Renesse, C. Kahlert, M. Distler, T. Welsch, C. Reissfelder, D. E. Aust, G. Miller, J. Weitz and L. Seifert (2020). "Detection of pancreatic ductal adenocarcinoma with galectin-9 serum levels." Oncogene **39**(15): 3102-3113.

Seki, M., S. Oomizu, K. M. Sakata, A. Sakata, T. Arikawa, K. Watanabe, K. Ito, K. Takeshita, T. Niki, N. Saita, N. Nishi, A. Yamauchi, S. Katoh, A. Matsukawa, V. Kuchroo and M. Hirashima (2008). "Galectin-9 suppresses the generation of Th17, promotes the induction of regulatory T cells, and regulates experimental autoimmune arthritis." Clin Immunol **127**(1): 78-88.

Smith, L. K., K. Fawaz and B. Treanor (2021). "Galectin-9 regulates the threshold of B cell activation and autoimmunity." Elife **10**.

Stebegg, M., S. D. Kumar, A. Silva-Cayetano, V. R. Fonseca, M. A. Linterman and L. Graca (2018). "Regulation of the Germinal Center Response." Front Immunol **9**: 2469.

Su, E. W., S. Bi and L. P. Kane (2011). "Galectin-9 regulates T helper cell function independently of Tim-3." Glycobiology **21**(10): 1258-1265.

Subramanian, A., P. Tamayo, V. K. Mootha, S. Mukherjee, B. L. Ebert, M. A. Gillette, A. Paulovich, S. L. Pomeroy, T. R. Golub, E. S. Lander and J. P. Mesirov (2005). "Gene set enrichment analysis: A knowledge-based approach for interpreting genome-wide expression profiles." Proceedings of the National Academy of Sciences **102**(43): 15545-15550.

Tandon, R., G. M. Chew, M. M. Byron, P. Borrow, T. Niki, M. Hirashima, J. D. Barbour, P. J. Norris, M. C. Lanteri, J. N. Martin, S. G. Deeks and L. C. Ndhlovu (2014). "Galectin-9 is rapidly released during acute HIV-1 infection and remains sustained at high levels despite viral suppression even in elite controllers." AIDS research and human retroviruses **30**(7): 654-664.

Wang, F., W. He, H. Zhou, J. Yuan, K. Wu, L. Xu and Z. K. Chen (2007). "The Tim-3 ligand galectin-9 negatively regulates CD8+ alloreactive T cell and prolongs survival of skin graft." Cellular immunology **250**(1-2): 68-74.

Wong, M. T., J. Chen, S. Narayanan, W. Lin, R. Anicete, H. T. Kiaang, M. A. De Lafaille, M. Poidinger and E. W. Newell (2015). "Mapping the Diversity of Follicular Helper T Cells in Human Blood and Tonsils Using High-Dimensional Mass Cytometry Analysis." Cell Rep **11**(11): 1822-1833.

Wu, C., T. Thalhamer, R. F. Franca, S. Xiao, C. Wang, C. Hotta, C. Zhu, M. Hirashima, A. C. Anderson and V. K. Kuchroo (2014). "Galectin-9-CD44 Interaction Enhances Stability and Function of Adaptive Regulatory T Cells." Immunity.

Yang, R., L. Sun, C. F. Li, Y. H. Wang, J. Yao, H. Li, M. Yan, W. C. Chang, J. M. Hsu, J. H. Cha, J. L. Hsu, C. W. Chou, X. Sun, Y. Deng, C. K. Chou, D. Yu and M. C. Hung (2021). "Galectin-9 interacts with PD-1 and TIM-3 to regulate T cell death and is a target for cancer immunotherapy." Nat Commun **12**(1): 832.

Zhang, C. X., D. J. Huang, V. Baloch, L. Zhang, J. X. Xu, B. W. Li, X. R. Zhao, J. He, H. Q. Mai, Q. Y. Chen, X. S. Zhang, P. Busson, J. Cui and J. Li (2020). "Galectin-9 promotes a suppressive microenvironment in human cancer by enhancing STING degradation." Oncogenesis **9**(7): 65.

Zhang, N., X. Li, J. Wang, J. Wang, N. Li, Y. Wei, H. Tian and Y. Ji (2021). "Galectin-9 regulates follicular helper T cells to inhibit humoral autoimmunity-induced pulmonary fibrosis." Biochem Biophys Res Commun **534**: 99-106.

Zhu, C., A. C. Anderson, A. Schubart, H. Xiong, J. Imitola, S. J. Khoury, X. X. Zheng, T. B. Strom and V. K. Kuchroo (2005). "The Tim-3 ligand galectin-9 negatively regulates T helper type 1 immunity." Nat Immunol **6**(12): 1245-1252.

Zhuo, Y., Y. F. Zhang, H. J. Wu, L. Qin, Y. P. Wang, A. M. Liu and X. H. Wang (2017). "Interaction between Galectin-9/TIM-3 pathway and follicular helper CD4(+) T cells contributes to viral persistence in chronic hepatitis C." Biomed Pharmacother **94**: 386-393.

## Article 2

---

### 1. Introduction

In 2020, during the third year of my PhD thesis, my host research team entered into a new five-year contract. We have integrated a new research unit moving from CNRS UMR 8126 (head Dr J. Wiels) to CNRS UMR 9018 (head Dr C. Brenner). Our team has welcomed new members. Three clinicians specialized in Head and Neck tumors, two surgeons (Dr P. Gorphe, Dr I. Breuskin) and one medical oncologist (Dr C. Even) have become associated members of our research team. These organizational changes gave us the opportunity to launch translational research projects related to gal-9. Currently one major concern of our clinician colleagues is to better understand and better predict primary or secondary resistances to the inhibitors of negative immune checkpoints (abbreviated in "Immune Checkpoint Inhibitors" or ICIs). Currently most ICIs are therapeutic antibodies blocking the PD1 or PD-L1 proteins. For example, Nivolumab or Pembrolizumab blocks the PD1 protein at the surface of immune cells, especially T-cells and NK-cells. Most Head and Neck malignancies treated in Gustave Roussy like in other French cancer centers are squamous cell carcinomas (abbreviated in HNSCCs). Most of them are related with tobacco and/or alcohol abuse. A fraction of them (about 20%) have a viral etiology, especially squamous cell carcinomas of the tonsils or oropharynx latently infected by HPV (human papilloma virus). As for other human solid tumors, anti-PD1 and to a lesser extent anti-PD-L1 antibodies give objective tumor responses in about 20% of the cases, often with sustained tumor remission or stabilization. However, it is important to understand why about 80% of HNSCCs are not responsive to the ICIs which are currently available and why most tumors initially sensitive to these agents will eventually resume progression after some months or years. One escape mechanism which is often suspected is the contribution of so-called soluble ICIs for example soluble HLA-G and some extra-cellular galectins like gal-3 or gal-9. Our ultimate goal is to identify patients bearing HNSCCs for whom tumor immune escape is mainly supported by extra-cellular gal-3 or gal-9 resulting in primary or secondary

resistances to current ICIs. We thought that the first step in this direction was to make a systematic assessment of the abundance of gal-3 and gal-9 in a series of patients bearing advanced HNSCCs with blood collection made just before starting the second line treatment. This has been done in collaboration with Dr C. Even who gave us access to the TopNivo cohort. There was a double rationale to focus our investigations on plasma galectins instead of making detection by IHC on tumor fragments. First, due to tumor heterogeneity the plasma concentrations may better reflect the overall abundance of gal-3 or gal-9 production than staining intensity of a tumor fragment. Next, in terms of immune suppression, soluble ICIs are expected to act not only in the tumor microenvironment but also at a systemic level.

## 2. Manuscript

# Plasma levels of cleaved forms of galectin-9 in the context of Head and Neck carcinomas: correlation with clinical and biological characteristics

*Thi Bao Tram Tran<sup>1&</sup>, Aurore Gelin<sup>1&</sup>, Matthieu Texier<sup>2</sup>, Léa Zimmerman<sup>1</sup>, Anne Aupérin<sup>2</sup>, Joël Guigay<sup>3</sup>, Florence Garic<sup>4</sup>, Muriel David<sup>5</sup>, Toshiro Niki<sup>6</sup>, Pierre Busson<sup>1&</sup>, Caroline Even<sup>7&</sup>*

<sup>1</sup> CNRS, UMR 9018, Gustave Roussy and Université Paris-Saclay, 39 rue Camille Desmoulins, F-94805 Villejuif, France.

<sup>2</sup> Service d'Epidémiologie et de Biostatistiques, Gustave Roussy and université Paris-Saclay, 39, rue Camille Desmoulins, F-94805, Villejuif, France

<sup>3</sup> Centre Antoine Lacassagne, Nice.

<sup>4</sup> Unicancer, Le Kremlin-Bicêtre

<sup>5</sup> HiFiBiO Therapeutics, Paris

<sup>6</sup> Department of Immunology, Kagawa University, Kita-gun, Kagawa 7610793, Japan.

<sup>7</sup> Service de cancérologie cervico-faciale, Gustave Roussy and université Paris-Saclay, 39, rue Camille Desmoulins, F-94805, Villejuif, France

& Equal contributions

## Abstract

Extra-cellular galectin-9 (gal-9) is suspected to act as a soluble negative immune checkpoint in various types of human malignancies, including Head and Neck squamous cell carcinomas (HNSCC). Its immune suppressive effects probably extend at the systemic level beyond the limits of the tumor microenvironment. Therefore, there is a need to investigate the status of gal-9 in the plasma of HNSCC patients. Previous studies carried out mainly in the context of infectious diseases have led to distinguish two forms of plasma gal-9: full-length and cleaved gal-9 proteins. Using appropriate ELISA systems, these two forms of plasma gal-9 have been investigated in a prospective series of 90 patients with relapsed and/or metastatic HNSCCs. Plasma galectin-1 and -3 were concomitantly assayed in order to better assess the specificity of our findings regarding gal-9. We report that full-length gal-9 was undetectable in most plasma samples and at best detected at very low concentrations. In contrast cleaved gal-9 was detected in all samples with significantly higher concentrations for patients whose primary tumor was derived from the hypopharynx and those with multiple metastatic sites. We found no similar correlations for gal-1 and gal-3. In a number of publications, papilloma virus-negative HNPCCs are considered as a single homogeneous entity. However, high plasma concentrations of cleaved gal-9 are preferentially detected in patients bearing hypopharyngeal carcinomas. This is a reminder that even among HPV-negative HNSCCs host-tumor interactions might have specific features which are dependent on the anatomical site of the primary tumor.



## Introduction

Most malignant tumors of the upper aero-digestive tract or “Head and Neck” tumors are squamous cell carcinomas (HNSCCs). They represent the 6th leading cause of cancer worldwide with an overall incidence of 650 000 new cases per year (Leemans, Braakhuis et al. 2011). In most cases, the main etiological factors are alcohol and tobacco abuse. However a fraction of them are related to infection by oncogenic viruses, notably HPV for a fraction of oropharyngeal carcinomas. There is a strong tendency in clinical and biological studies to fit the large set of HNPCCs into only two categories: HPV-positive or HPV-negative (Cillo, Kürten et al. 2020, Mito, Takahashi et al. 2021). However, one should keep in mind the dissymmetry of these two categories. Most HPV-positive HNSCCs arise from the epithelium of the oropharynx while the anatomic origins of HPV-negative HNSCCs are much more diverse including the oral cavity, the larynx and the hypopharynx. Despite the similarity of oncogenic factors, the diversity of the cells of origin probably has some influences on the phenotypes of the malignant cells as well as on host-tumor relationships. Surgery and/or concomitant chemoradiotherapy are still the standard of care for HNSCCs regardless of their viral or non-viral etiology. However, HPV-positive HNSCCs have a better prognosis than HPV-negative HNSCCs. Despite aggressive treatments, more than 50% of HPV-negative HNSCCs will relapse in the next 2 years.

Like for other human malignancies, immunotherapy, especially immune checkpoint inhibitors (ICIs) targeting the PD1/PD-L1 axis, has brought major practical and conceptual changes for the management of HNSCCs. Immunotherapy can achieve durable responses for patients previously regarded as incurable. Therefore, it provides compelling evidence that the immune system can have powerful anti-tumor effects even for advanced lesions. However, only 20% of the patients with relapsed or metastatic lesions benefit from immunotherapy and it remain difficult to predict which patients will benefit from this therapeutic modality (Borel, Jung et al. 2020, Clarke, Eriksen et al. 2021). So far, most of the investigations carried out to identify predictive biomarkers of the response to immunotherapy have been performed on tumor fragments, often fragments of the primary tumor. The most reliable tumor markers indicative of a good response to anti-PD1 antibodies is PD-L1 expression by at least a fraction of malignant cells or infiltrating cells, tumor mutational burden and abundance of CD8+ T-cells among infiltrating cells (Napolitano, Schipilliti et al. 2019). Still, there is a need to achieve better immune responses in a greater number of patients.

The prevalence of alternative checkpoint inhibitors is one mechanism suspected to support primary or secondary resistance to ICIs. There is growing evidence that tumor immune escape can be

promoted by biomolecules released in the extra-cellular space. sHLA, sPD-L1 or sPDL2 are well-known examples of such immune suppressive agents with the capacity to diffuse in biological fluids including peripheral blood (Botticelli, Zizzari et al. 2021, Kluckova, Durmanova et al. 2021). Some galectins, especially gal-9 (galectin-9) and to a lesser gal-1 (galectin-1) and gal-3 (galectin-3), can behave in the same way (Mereiter, Balmaña et al. 2019). Although devoid of signal sequences, they can be secreted in the extra-cellular space by non-conventional pathways, for example by translocation through the plasma membrane or in association with extra-cellular vesicles (Keryer-Bibens, Pioche-Durieu et al. 2006). Once in the extra-cellular space they behave like cytokines with predominant immunosuppressive activity (Ochieng, Furtak et al. 2002, Ruvolo 2016, Gordon-Alonso, Hirsch et al. 2017, Orozco, Martinez-Bosch et al. 2018, Nambiar, Aguilera et al. 2019, Baloch, Riviere et al. 2021).

In this context, we believe that it is important to determine the status of extra-cellular gal-9 in the plasma of patients bearing HNSCCs. So far, plasma gal-9 has been mainly investigated in studies dealing with infectious diseases. For example, elevated concentrations of plasma gal-9 were reported for influenza and covid 19, as well as active tuberculosis (Kato, Ikeda et al. 2014, Shete, Bichare et al. 2020, Bai, Furushima et al. 2021, Bozorgmehr, Mashhoury et al. 2021). Elevated concentrations were also reported in AIDS patients with very high levels at the acute phase and persistent mild excess even after restoration of the CD4 cell count under anti-viral therapy (Tandon, Chew et al. 2014).

Studies on plasma gal-9 in infectious diseases have stimulated methodological progress with one of us being at the forefront in refining ELISA detection. There are three isoforms of gal-9 which contain two CRD (carbohydrate recognition domains) linked by a stretch of amino-acids called the linker peptide. The only difference between these three isoforms is the length of the linker peptide with short, medium and long size for gal-9-S, -M and -L, respectively. The linker peptide of each isoform is vulnerable to cleavage by various proteases including elastase (Niki, Fujita et al. 2018). T. Niki et al. have shown that the bulk of plasma gal-9 is under the form of cleaved products corresponding to the N- or C-terminal CRD of the three isoforms (Niki, Fujita et al. 2018). In addition, they have developed specific combinations of antibodies for selective detection of intact gal-9 (FL-gal-9) and selective detection of the N-terminal product (Tr-gal-9) (Padilla, Niki et al. 2020, Bai, Furushima et al. 2021). Finally they have shown that the gal-9 ELISA kit manufactured by R&D system and widely used in the scientific and medical community mainly detect gal-9 cleaved products and tend to overreact with these products (Niki, Fujita et al. 2018).

With these physiopathological and molecular data in mind, we undertook to simultaneously assess plasma concentrations of FL-gal-9 and Tr-gal-9 in a prospective series of patients with relapsed and/or metastatic HNSCCs. This was made as an ancillary study of the TopNivo trial (NCT03226756). In addition, we assayed plasma gal-1 and gal-3 in the same series of patients to better appreciate the relevance and specificity of plasma gal-9 distribution in various tumoral conditions. Highest mean concentrations of plasma cleaved gal-9 were found in patients with hypopharyngeal primary tumor and patients with more than one metastatic site.

## Materials and Methods

### Patients and healthy controls

TopNivo is a safety study of Nivolumab in patients with recurrent and/or metastatic platinum-refractory HNSCCs. Nivolumab injections were given every 2 weeks, up to 12 cycles (1 cycle = 28 days). A total of 351 patients have been enrolled. For 90 of these patients, EDTA blood samples (about 9 ml) were collected prior to the onset of Nivolumab (at baseline). For each blood sample, about 4ml of plasma have been stored in 3 aliquots. Galectin-9 (gal-9) and galectin-3 (gal-3) concentrations have been assessed for all samples (baseline and post-treatment).

Plasma samples were also collected from 5 anonymous healthy donors purchased from Zenbio (NC, USA) (3M and 2F) (ages comprised between 19 and 65).

### Assays for plasma gal-9

Three types of ELISA were used to assay plasma gal-9. One assay was selective of human FL-gal-9 isoforms, using the combination of one monoclonal antibody reacting with the gal-9 N-terminal portion (9S2-3) and a rabbit polyclonal directed against its C-terminal portion (Mengshol, Golden-Mason et al. 2010). Normal concentrations of plasma FL-gal-9 from healthy donors are below 500 pg/ml (Padilla, Niki et al. 2020, Bai, Furushima et al. 2021). Another assay has been designed to react both with FL-gal-9 and the cleaved N-terminal product of gal-9; it uses the combination of 9S2-3 and ECA8 (MBL, Nagoya, Japan), both reacting with the N-terminal part of human gal-9 isoforms. Normal concentrations for this assay are below 1000 pg/ml (Padilla, Niki et al. 2020, Bai, Furushima et al. 2021). In addition we used the Quantikine ELISA kit from R&D system (reference DGal90) which was shown to have no selectivity for FL-gal-9 and to overreact with Tr-gal-9 (Niki, Fujita et al. 2018). For

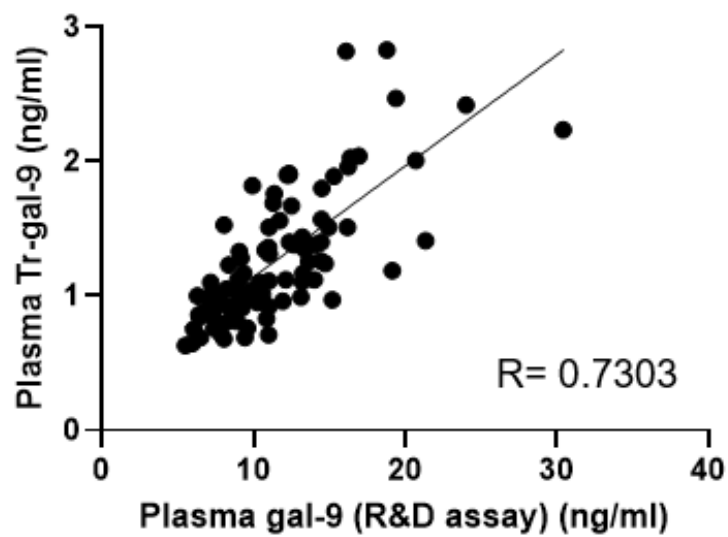


**Figure 1. Correlations of plasma gal-9 concentrations assayed with two ELISA systems.** X-axis : concentrations values obtained using the Quantikine ELISA kit from R&D system (DGal90). Y-axis : values obtained with an assay based on 2 monoclonal antibodies targeting the N-terminal portion of human gal-9. Pearson coefficient : R= 0.730

this assay, normal concentrations are below 10 ng/ml (Niki, Fujita et al. 2018). All assays were done in duplicate.

### **Assays for plasma gal-1 and -3**

Plasma gal-1 and -3 were assayed using appropriate Quantikine ELISA kits from R&D system as recommended by the manufacturer (references DGal10 and 30). All assays were done in duplicate.

## **Results**

### **Low abundance of FL-gal-9 in plasma samples from HNSCCs**

The mean concentration of plasma FL-gal-9 for the 5 healthy donors was 363 pg/ml which is consistent with previous reports (Padilla, Niki et al. 2020, Bai, Furushima et al. 2021). For the 90 HNSCCs patients, the mean concentration of FL-gal-9 was even lower at 165 pg/ml. FL gal-9 was undetectable for 2 out of 5 healthy donors and 27 out of 90 HNSCC patients.

### **Variable concentrations of Tr-gal-9**

The mean concentration of plasma Tr-gal-9 was 962 pg/ml +/- 375 for healthy donors. Again this is consistent with previous reports (Padilla, Niki et al. 2020, Bai, Furushima et al. 2021). For the 90 HNSCCs patients, it was 1275 pg/ml +/- 485. A good correlation was observed with gal-9 concentrations obtained using the Quantikine ELISA from R&D System (see **Fig. 1** – Pearson coefficient:  $R=0.730$ ). Concentration values obtained with the R&D assay were about 10 times greater than those obtained using the Tr-gal-9 assay. These observations are consistent with the notion that the Quantikine R&D ELISA mainly assesses cleaved forms of gal-9 while having a data amplifying effect (Niki, Fujita et al. 2018). Wide variations of gal-9 concentrations were recorded with 38 patients displaying normal values (below 10 ng/ml), 48 with concentrations between 10 and 20ng/ml, and 4 patients with concentrations above 20ng/ml. As shown in **Fig. 2** and **Fig. 3**, higher plasma gal-9 concentrations were found for hypopharynx primary tumors by comparison with HPV-negative oropharyngeal tumors and for patients with multiple metastatic sites by comparison with non-metastatic subjects.

### **Distribution of plasma gal-1 and -3**

Concentrations of plasma gal-1 and -3 were determined for the 90 HNSCC patients. We found only weak correlations with the distribution of plasma Tr-gal-9 (Pearson coefficients were 0.268 and 0.278 respectively) (**Fig. 4**). We found no statistically significant relationships between the concentration of

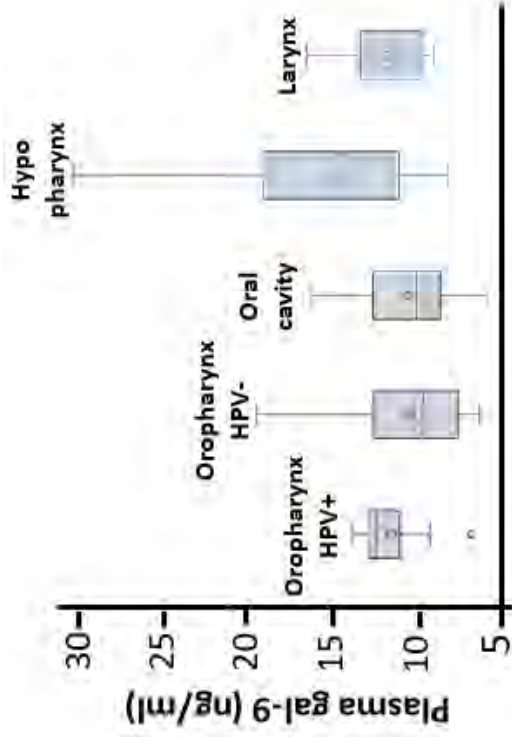


**Figure 2. Distribution of plasma gal-9 concentrations depending on the site of the primary tumor in HNSCC patients.** Statistical analysis according to the Kruskal-Wallis test :  $p = 0.0174$ . Pairwise comparisons show significant differences only between two groups: HPV-negative oropharyngeal and hypopharyngeal tumors.

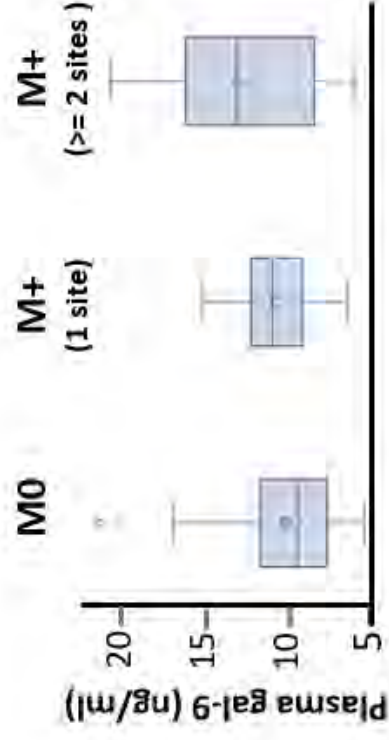


**Figure 3. Distribution of plasma gal-9 concentrations according to the number of metastatic sites in HNSCC patients.** M0: absence of any detectable metastatic site; M+ (1 site) ; only one metastatic site; M+ (>=2 sites) : two or more metastatic sites. Statistical analysis according to the Kruskal-Wallis test :  $p = 0.0274$ . Pairwise comparisons show significant differences only between the M0 and M+ (>=2 sites) groups.

plasma galectin-3 and the hypopharyngeal site of the primary tumor or the existence of several metastatic sites (Fig. 5 and 6).

## Discussion

The main results of this study can be summarized like this: plasma gal-9 concentration was higher for HNSCC patients having several metastatic sites and when the primary tumor was derived from the hypopharynx. Interestingly, this is not the case for gal-3, meaning that we are not just looking at nonspecific inflammatory changes affecting all galectins.

This must be related to previous publications about possible contributions of gal-9 to the immune escape in HNSCCs. Several years ago, our group has reported the abundant production of gal-9 by malignant cells from nasopharyngeal carcinoma (NPC) and its systemic diffusion in association with tumor exosomes (Klibi, Niki et al. 2009). However, no NPC were included in our present series. More recently, using tissue microarrays, Liu et al. have reported a positive correlation between the abundance of gal-9 in the tumor microenvironment and the presence of T-regs (FoxP3<sup>+</sup>) and M2 macrophages (Liu, Wu et al. 2018). Chang et al. have recently reported that high expression of pyruvate kinase M2 in HNSCCs promotes tumor progression and immune escape. One downstream mechanism of this immune suppression seems to be the up-regulation of gal-9 transcription resulting from lactate accumulation in malignant cells (Chang, Xu et al. 2021). On a broader perspective, there is growing evidence that gal-9 can be involved in primary or secondary resistance to immune checkpoint inhibitors in various types of malignancies (Koyama, Akbay et al. 2016, Limagne, Richard et al. 2019).

Regarding gal-3, other publications suggest that it can also contribute to tumor immune escape and could even be a therapeutic target in HNSCCs (Coppock, Mills et al. 2021, Curti, Koguchi et al. 2021). Curti et al. have reported a phase I dose escalation study of a combination of pembrolizumab (anti-PD1 antibody) and belapectin, a small molecule inhibiting galectin-3. This was done for a few patients with advanced melanomas or HNSCC ([NCT02575404](https://clinicaltrials.gov/ct2/show/study/NCT02575404)). Objective responses were obtained for 2 out of 6 HNSCC patients. Obviously, we need to wait for data of the phase II and III trials. Because Belapectin is a small molecule, it might act on both extracellular and intracellular gal-3.

There is a good rationale to investigate galectins and other soluble negative immune checkpoints in the blood. First they are expected to be active at the systemic level as well as inside the tumor. Next, spatial tumor heterogeneity is a major obstacle for the accuracy of potential

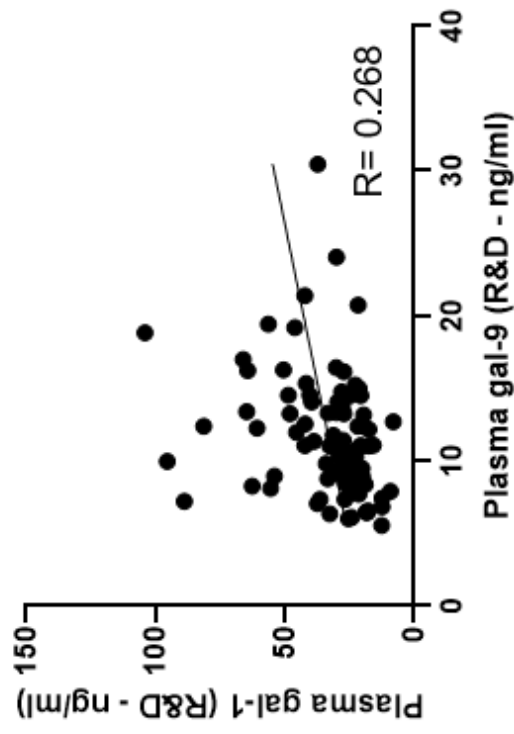


**Figure 4. Correlations of plasma gal-1 and -9 using R&D ELISA systems.** Quantikine ELISA kits from R&D system (DGal10 and 90). Pearson coefficient :  $R = 0.268$

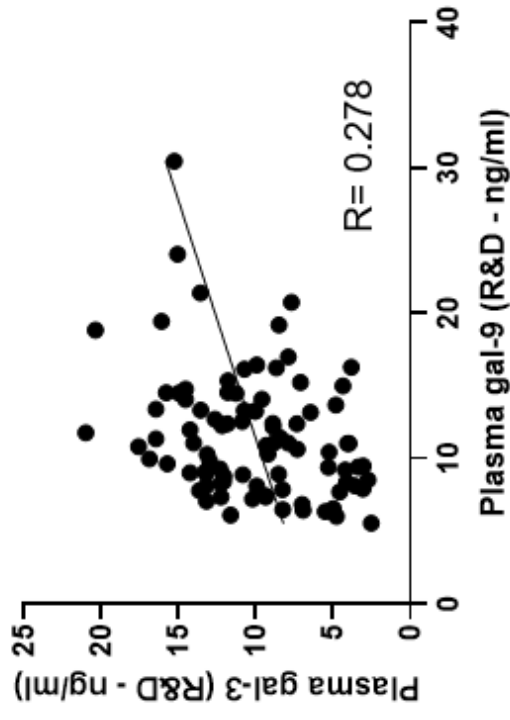


**Figure 5. Correlations of plasma gal-3 and -9 using R&D ELISA systems.** Quantikine ELISA kits from R&D system (DGal30 and 90). Pearson coefficient :  $R = 0.278$



predictive markers derived from investigations performed on tumor fragments. Another limitation of these markers is that they are not easily used in longitudinal monitoring because it is generally difficult to make iterative tumor biopsies. Therefore, it is important to investigate the immune status of the HNSCC patients at the systemic level, especially by investigation of non-invasive markers detectable in the peripheral blood, hoping to get a synthetic assessment of the anti-tumor potential of the immune system with the possibility of a follow-up of these markers at various stages of the treatment (Duchemann, Remon et al. 2020).

One of our future aims will be to monitor plasma galectin-9 concentration in HNSCC patients at various stages of the treatment and tumor evolution, for example at the initiation of immunotherapy and at disease progression in case of initial objective tumor responses. Another aim will be to seek correlations between high gal-9 concentrations and the plasma cytokine landscape and the plasma metabolome.

## References

- Bai, G., D. Furushima, T. Niki, T. Matsuba, Y. Maeda, A. Takahashi, T. Hattori and Y. Ashino (2021). "High Levels of the Cleaved Form of Galectin-9 and Osteopontin in the Plasma Are Associated with Inflammatory Markers That Reflect the Severity of COVID-19 Pneumonia." *Int J Mol Sci* **22**(9).
- Baloche, V., J. Riviere, T. B. T. Tran, A. Gelin, O. Bawa, N. Signolle, M. B. K. Diop, P. Dessen, S. Beq, M. David and P. Busson (2021). "Serial transplantation unmasks galectin-9 contribution to tumor immune escape in the MB49 murine model." *Sci Rep* **11**(1): 5227.
- Borel, C., A. C. Jung and M. Burgy (2020). "Immunotherapy Breakthroughs in the Treatment of Recurrent or Metastatic Head and Neck Squamous Cell Carcinoma." *Cancers (Basel)* **12**(9).
- Botticelli, A., I. G. Zizzari, S. Scagnoli, G. Pomati, L. Strigari, A. Cirillo, B. Cerbelli, A. Di Filippo, C. Napoletano, F. Scirocchi, A. Rughetti, M. Nuti, S. Mezi and P. Marchetti (2021). "The Role of Soluble LAG3 and Soluble Immune Checkpoints Profile in Advanced Head and Neck Cancer: A Pilot Study." *J Pers Med* **11**(7).
- Bozorgmehr, N., S. Mashhour, E. Perez Rosero, L. Xu, S. Shahbaz, W. Sligl, M. Osman, D. J. Kutsogiannis, E. MacIntyre, C. R. O'Neil and S. Elahi (2021). "Galectin-9, a Player in Cytokine Release Syndrome and a Surrogate Diagnostic Biomarker in SARS-CoV-2 Infection." *mBio* **12**(3).
- Chang, H., Q. Xu, J. Li, M. Li, Z. Zhang, H. Ma and X. Yang (2021). "Lactate secreted by PKM2 upregulation promotes Galectin-9-mediated immunosuppression via inhibiting NF- $\kappa$ B pathway in HNSCC." *Cell Death Dis* **12**(8): 725.
- Cillo, A. R., C. H. L. Kürten, T. Tabib, Z. Qi, S. Onkar, T. Wang, A. Liu, U. Duvvuri, S. Kim, R. J. Soose, S. Oesterreich, W. Chen, R. Lafyatis, T. C. Bruno, R. L. Ferris and D. A. A. Vignali (2020). "Immune Landscape of Viral- and Carcinogen-Driven Head and Neck Cancer." *Immunity* **52**(1): 183-199.e189.
- Clarke, E., J. G. Eriksen and S. Barrett (2021). "The effects of PD-1/PD-L1 checkpoint inhibitors on recurrent/metastatic head and neck squamous cell carcinoma: a critical review of the literature and meta-analysis." *Acta Oncol*: 1-9.

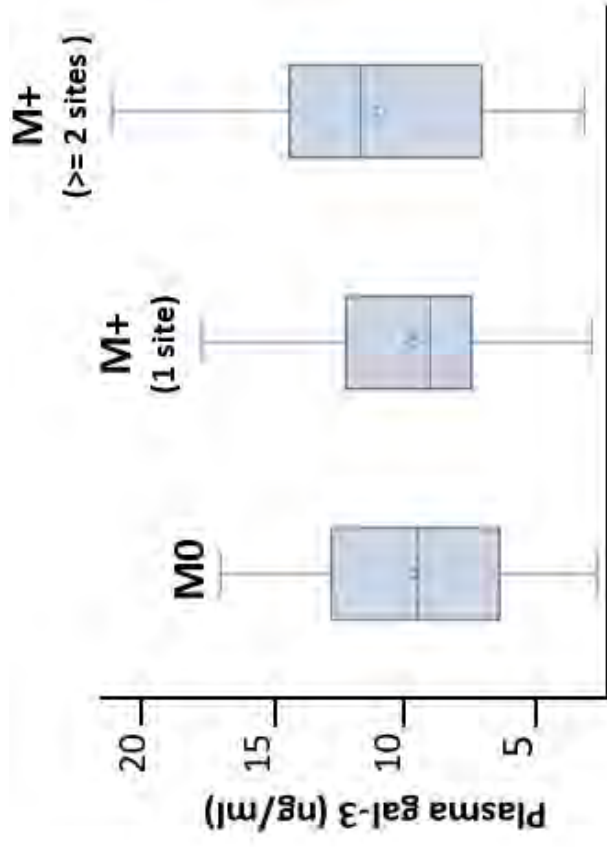


**Figure 7. Distribution of plasma gal-3 concentrations according to the number of metastatic sites in HNSCC patients.** M0: absence of any detectable metastatic site; M+ (1 site) : only one metastatic site; M+ (>=2 sites) : two or more metastatic sites. Statistical analysis according to the Kruskal-Wallis test :  $p = 0.508$

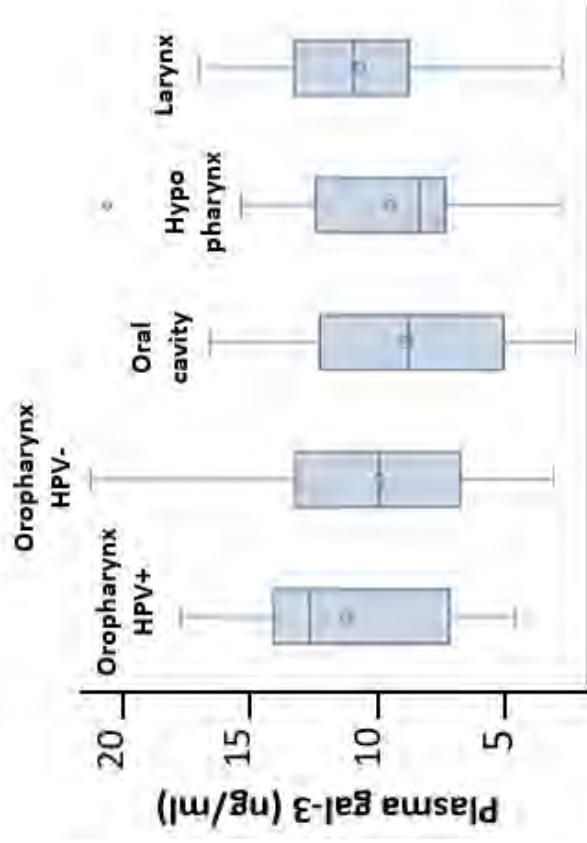


**Figure 6. Distribution of plasma gal-3 concentrations depending on the site of the primary tumor in HNSCC patients.** Statistical analysis according to the Kruskal-Wallis test :  $p = 0.611$

Coppock, J. D., A. M. Mills and E. B. Stelow (2021). "Galectin-3 Expression in High-Risk HPV-Positive and Negative Head & Neck Squamous Cell Carcinomas and Regional Lymph Node Metastases." Head Neck Pathol **15**(1): 163-168.

Curti, B. D., Y. Koguchi, R. S. Leidner, A. S. Rolig, E. R. Sturgill, Z. Sun, Y. Wu, V. Rajamanickam, B. Bernard, I. Hilgart-Martiszus, C. B. Fountain, G. Morris, N. Iwamoto, T. Shimada, S. Chang, P. G. Traber, E. Zomer, J. R. Horton, H. Shlevin and W. L. Redmond (2021). "Enhancing clinical and immunological effects of anti-PD-1 with belapectin, a galectin-3 inhibitor." J Immunother Cancer **9**(4).

Duchemann, B., J. Remon, M. Naigeon, L. Mezquita, R. Ferrara, L. Cassard, J. M. Jouniaux, L. Boselli, J. Grivel, E. Auclin, A. Desnoyer, B. Besse and N. Chaput (2020). "Integrating Circulating Biomarkers in the Immune Checkpoint Inhibitor Treatment in Lung Cancer." Cancers (Basel) **12**(12).

Gordon-Alonso, M., T. Hirsch, C. Wildmann and P. van der Bruggen (2017). "Galectin-3 captures interferon-gamma in the tumor matrix reducing chemokine gradient production and T-cell tumor infiltration." Nat Commun **8**(1): 793.

Katoh, S., M. Ikeda, H. Shimizu, K. Mouri, Y. Obase, Y. Kobashi, K. Fukushima, M. Hirashima and M. Oka (2014). "Increased levels of plasma galectin-9 in patients with influenza virus infection." Tohoku J Exp Med **232**(4): 263-267.

Keryer-Bibens, C., C. Pioche-Durieu, C. Villemant, S. Souquere, N. Nishi, M. Hirashima, J. Middeldorp and P. Busson (2006). "Exosomes released by EBV-infected nasopharyngeal carcinoma cells convey the viral latent membrane protein 1 and the immunomodulatory protein galectin 9." BMC Cancer **6**: 283.

Klibi, J., T. Niki, A. Riedel, C. Pioche-Durieu, S. Souquere, E. Rubinstein, S. Le Moulec, J. Guigay, M. Hirashima and F. Guemira (2009). "Blood diffusion and Th1-suppressive effects of galectin-9-containing exosomes released by Epstein-Barr virus-infected nasopharyngeal carcinoma cells." Blood **113**(9): 1957-1966.

Kluckova, K., V. Durmanova and M. Bucova (2021). "Soluble HLA-G, its diagnostic and prognostic value and potential target molecule for future therapy in cancer." Bratisl Lek Listy **122**(9): 60-617.

Koyama, S., E. A. Akbay, Y. Y. Li, G. S. Herter-Sprie, K. A. Buczkowski, W. G. Richards, L. Gandhi, A. J. Redig, S. J. Rodig, H. Asahina, R. E. Jones, M. M. Kulkarni, M. Kuraguchi, S. Palakurthi, P. E. Fecci, B. E. Johnson, P. A. Janne, J. A. Engelman, S. P. Gangadharan, D. B. Costa, G. J. Freeman, R. Bueno, F. S. Hodi, G. Dranoff, K. K. Wong and P. S. Hammersman (2016). "Adaptive resistance to therapeutic PD-1 blockade is associated with upregulation of alternative immune checkpoints." Nat Commun **7**: 10501.

Leemans, C. R., B. J. Braakhuis and R. H. Brakenhoff (2011). "The molecular biology of head and neck cancer." Nat Rev Cancer **11**(1): 9-22.

Limagne, E., C. Richard, M. Thibaudin, J. D. Fumet, C. Truntzer, A. Lagrange, L. Favier, B. Coudert and F. Ghiringhelli (2019). "Tim-3/galectin-9 pathway and mMDSC control primary and secondary resistances to PD-1 blockade in lung cancer patients." Oncoimmunology **8**(4): e1564505.

Liu, J. F., L. Wu, L. L. Yang, W. W. Deng, L. Mao, H. Wu, W. F. Zhang and Z. J. Sun (2018). "Blockade of TIM3 relieves immunosuppression through reducing regulatory T cells in head and neck cancer." J Exp Clin Cancer Res **37**(1): 44.

Mengshol, J. A., L. Golden-Mason, T. Arikawa, M. Smith, T. Niki, R. McWilliams, J. A. Randall, R. McMahan, M. A. Zimmerman and M. Rangachari (2010). "A crucial role for Kupffer cell-derived galectin-9 in regulation of T cell immunity in hepatitis C infection." PLoS One **5**(3): e9504.

Mereiter, S., M. Balmaña, D. Campos, J. Gomes and C. A. Reis (2019). "Glycosylation in the Era of Cancer-Targeted Therapy: Where Are We Heading?" Cancer Cell **36**(1): 6-16.

Mito, I., H. Takahashi, R. Kawabata-Iwakawa, S. Ida, H. Tada and K. Chikamatsu (2021). "Comprehensive analysis of immune cell enrichment in the tumor microenvironment of head and neck squamous cell carcinoma." Sci Rep **11**(1): 16134.

Nambiar, D. K., T. Aguilera, H. Cao, S. Kwok, C. Kong, J. Bloomstein, Z. Wang, V. S. Rangan, D. Jiang, R. von Eyben, R. Liang, S. Agarwal, A. D. Colevas, A. Korman, C. T. Allen, R. Uppaluri, A. C. Koong, A. Giaccia and Q. T. Le (2019). "Galectin-1-driven T cell exclusion in the tumor endothelium promotes immunotherapy resistance." J Clin Invest **129**(12): 5553-5567.

Napolitano, M., F. M. Schipilliti, L. Trudu and F. Bertolini (2019). "Immunotherapy in head and neck cancer: The great challenge of patient selection." *Crit Rev Oncol Hematol* **144**: 102829.

Niki, T., K. Fujita, H. Rosen, M. Hirashima, T. Masaki, T. Hattori and K. Hoshino (2018). "Plasma Galectin-9 Concentrations in Normal and Diseased Condition." *Cell Physiol Biochem* **50**(5): 1856-1868.

Ochieng, J., V. Furtak and P. Lukyanov (2002). "Extracellular functions of galectin-3." *Glycoconj J* **19**(7-9): 527-535.

Orozco, C. A., N. Martinez-Bosch, P. E. Guerrero, J. Vinaixa, T. Dalotto-Moreno, M. Iglesias, M. Moreno, M. Djurec, F. Poirier, H. J. Gabius, M. E. Fernandez-Zapico, R. F. Hwang, C. Guerra, G. A. Rabinovich and P. Navarro (2018). "Targeting galectin-1 inhibits pancreatic cancer progression by modulating tumor-stroma crosstalk." *Proc Natl Acad Sci U S A* **115**(16): E3769-e3778.

Padilla, S. T., T. Niki, D. Furushima, G. Bai, H. Chagan-Yasutan, E. F. Telan, R. J. Tactacan-Abrenica, Y. Maeda, R. Solante and T. Hattori (2020). "Plasma Levels of a Cleaved Form of Galectin-9 Are the Most Sensitive Biomarkers of Acquired Immune Deficiency Syndrome and Tuberculosis Coinfection." *Biomolecules* **10**(11).

Ruvolo, P. P. (2016). "Galectin 3 as a guardian of the tumor microenvironment." *Biochim Biophys Acta* **1863**(3): 427-437.

Shete, A., S. Bichare, V. Pujari, R. Virkar, M. Thakar, M. Ghate, S. Patil, A. Vyakarnam, R. Gangakhedkar, G. Bai, T. Niki and T. Hattori (2020). "Elevated Levels of Galectin-9 but Not Osteopontin in HIV and Tuberculosis Infections Indicate Their Roles in Detecting MTB Infection in HIV Infected Individuals." *Front Microbiol* **11**: 1685.

Tandon, R., G. M. Chew, M. M. Byron, P. Borrow, T. Niki, M. Hirashima, J. D. Barbour, P. J. Norris, M. C. Lanteri, J. N. Martin, S. G. Deeks and L. C. Ndhlovu (2014). "Galectin-9 is rapidly released during acute HIV-1 infection and remains sustained at high levels despite viral suppression even in elite controllers." *AIDS research and human retroviruses* **30**(7): 654-664.

# Discussion and perspectives

## Preamble

The discussion chapter of this thesis will be structured in two main parts: one relating to my manuscript number 1 and the other relating to manuscript number 2. These two parts will be followed by a very brief conclusion.

## Part 1: comments on manuscript n°1

---

The main finding of this manuscript is the induction of CXCR5 expression in human peripheral T-cells by exposure to recombinant gal-9. Remarkably, this T-cell response is enhanced, at least at the transcriptional level, when T-cells previously exposed to recombinant gal-9 among PBMCs and isolated by magnetic sorting are subjected to a boost of gal-9 stimulation. This means that the enhancement of CXCR5 transcription is at least in part due to a direct effect of gal-9 on T-cells. In the weeks to come, it will be very important to check whether this “boosting” effect is also observed by flow cytometry at the protein level.

One open question is which type of membrane receptor are contacted by recombinant gal-9 at the surface of target T-cells and which signaling pathways are activated downstream of these receptors. There is strong evidence that this effect is not mediated by Tim-3 since we observed a dramatic reduction in Tim-3 expression in T-cells exposed to gal-9 for 7 days (G9Expo-T-cells). Therefore, the boosting effect of late gal-9 stimulation following magnetic sorting of the T-cells is probably mediated by a receptor distinct from Tim-3. CD45 and CD44 are known to interact with extra-cellular gal-9 at the surface of various types of leucocytes (260,275). One may wonder whether they are involved in the up-regulation of CXCR5. A specific experimental program would be required to deal with this hypothesis. On the other hand, we and others have shown that proteins of the CD3/TCR complex and signaling kinases acting downstream of this complex like Lck, ERK1/2 and CREB are required for some effects of

extra-cellular gal-9 inside target T-cells: for example, calcium mobilization, IL-2 secretion or transcription activation of the latent HIV genome (Claire Lhuillier - J Biol Chem 2015; Florent Colomb Frontiers in Immunology). We do not know the exact mechanism of this mimicry of TCR activation, for example whether it results from a direct contact of gal-9 with proteins of the CD3/TCR complex. Nevertheless, we believe that it would be very interesting to know whether inhibition of lck using interfering RNAs or chemical inhibitors can block the up-regulation of CXCR5 resulting from the late boost of gal-9.

Most results presented in this manuscript were obtained from in vitro experiments using recombinant gal-9. Therefore, to get some insight on the physiological relevance of our findings, it was very important to perform additional investigations on an intact organism. We were able to compare the expression of CXCR5 and CD40L by splenic T-cells from wild type C57BL/6 mice and syngenic mice knocked-out for gal-9. We found a modest but consistent reduction of CXCR5 expression in cells from gal-9-KO mice. This is very encouraging but not sufficient. We may hope to find a greater difference if we compare WT and KO mice taken a few days after artificial immunization for example with ovalbumin. If the role of gal-9 in the up-regulation of CXCR5 expressed by T-cells is confirmed, it will be interesting to use this model to investigate the interplay between the already known factors of CXCR5 regulation and gal-9. It is known that CXCR5 expression by T-cells is determined at least in part by prior stimulation of CD28, by expression of Bcl6 and by contact with B-cells at the T/B interface around germinal centers (400,401). It would be interesting to know at which stage gal-9 interfere with the up-regulation of CXCR5., for example to determine whether gal-9 acts upstream or downstream of Bcl6. Unfortunately, so far, we have been in trouble to detect Bcl6 on tissue sections of murine spleens.

The heterogeneity of follicular T-cell markers expressed by CXCR5-positive T-cells exposed to recombinant gal-9 is well demonstrated by mass cytometry analysis. The cells co-expressing CXCR5 and FoxP3 are especially abundant. Their phenotype is suggestive of regulatory follicular T-cells (Tfr). Moreover, the detection of some CXCR5<sup>+</sup> cells with co-expression of CD40L and FoxP3 seems to be in contradiction with previous publications stating that these two markers are mutually exclusive (402). At this stage, we do not know whether the abundance of CXCR5/FoxP3 T-cells and of some CXCR5<sup>+</sup>/CD40L<sup>+</sup>/FoxP3<sup>+</sup> is an artifact due to

artificial experimental conditions. One way to address this question might be to investigate co-expression of CXCR5, CD40L and FoxP3 in murine splenic T-cells.

Despite the heterogeneity of CXCR5<sup>+</sup> cells resulting from gal-9 exposure, we have evidence that they have functional properties consistent with a follicular helper phenotype, namely a protective effect against apoptosis of B-cells. We acknowledge that this is the weakest part of our manuscript in its present form. This part needs to be strengthened. We plan the following complementary experiments based either on Ramos cells or on other experimental systems. With regards to the protection of Ramos cells, we will use G9Expo-T-cells with CXCR5 expression reinforced by a late gal-9 boost. Instead to use low serum to make Ramos cells prone to apoptosis we will use anti-IgM stimulation mimicking BCR activation as previously reported for this cell line (403). One drawback of this system is the possibility of alloreactions of T-cells against Ramos cells which are not HLA-matched. Another possible approach might be a co-culture assay using T and B cells from the same healthy donors with stimulation by staphylococcal enterotoxin B and subsequent assay of secreted IgG (404).



## Part 2: comments on article n°2

---

For the moment, the study reported in the manuscript number 2 is essentially descriptive with a relatively limited scope. The main results can be summarized like this: higher concentrations of plasma gal-9 products were observed for the patients having several metastatic sites and when the primary tumor was derived from the hypopharynx. Interestingly, this is not the case for gal-3 and probably gal-1, meaning that we are not just looking at nonspecific inflammatory changes affecting all galectins. In the weeks and months to come we hope to be able to go further. First, we need more information regarding the prognostic value of a high gal-9 concentrations. In collaboration with Matthieu Texier (Gustave Roussy Dpt of Epidemiology and Biostatistics), we have not found any relationship between the initial concentration of gal-9 products and progression-free survival (PFS). However, it is necessary to complete the analysis in order to investigate a correlation between gal-9 concentration and the initial response to Nivolumab. We will also look for correlations between gal-9 concentrations and the plasma cytokine landscape. We have some clues that patients with high concentrations of plasma gal-9 also have high concentrations of plasma cytokines CCL1, CCL27, IL-27 and CXCL9. Work is in progress to confirm this observation on a larger series of patients.

Interestingly, several studies are in progress on tumor fragments from the patients of the same cohort in the frame of the TopNivo consortium. These studies include bulk RNAseq and multiplex immunohistochemistry oriented towards the detection of lymphoid and myeloid markers (respectively in Eric Tartour's lab in Paris and Ellen Van Obberghen's lab in Nice). In a distinct future publication, it will be interesting to see whether some characteristics of the tumor microenvironment match some of our observations on plasma gal-9 products and related circulating biomolecules. For example, whether gal-9 mRNAs are more abundant in fragments from carcinomas of the hypopharynx. Or whether T-regs, M2 macrophages or MDSCs are more abundant for patients with high concentrations of plasma gal-9 products.

A remarkable, recent publication dealing with multiple myeloma reports that detection of gal-9 in malignant cells indicates a poor prognosis only when there is concomitant expression of PD-L1 (405). Therefore, it will be interesting to investigate concomitant expression of gal-9

and PD-L1 in the tumor microenvironment of HNSCCs and may be to make simultaneous assays of plasma gal-9 and soluble PD-L1 for these patients.

We may also expect additional information when it will be possible to make longitudinal monitoring. Recently, my host team has obtained interesting preliminary results for patients whose tumor was initially sensitive to anti-PD1 treatment but finally escaped. For several of these patients there was a substantial rise of gal-9 concentration concomitant to tumor progression.

## Conclusion of the two parts of the discussion

---

Extra-cellular gal-9 can behave like a cytokine whose effects are mainly immunosuppressive. In some malignant and infectious diseases, the inappropriate production of gal-9 contributes to disease progression. However, the results presented in the manuscript number 1 strongly suggest that extracellular gal-9 can play a role in the optimization of the cooperation between T and B lymphocytes and therefore in the optimization of the immune response. We meet here a general characteristic of the homeostasis of the immune system. Most of its cellular and molecular effectors have bidirectional effects with very complex mechanisms of compensation and self-limitation. The possible therapeutic benefit of their inhibition or stimulation is highly dependent on the physiological or pathological context.

# Annex



OPEN

## Serial transplantation unmasks galectin-9 contribution to tumor immune escape in the MB49 murine model

Valentin Baloché<sup>1</sup>, Julie Rivière<sup>2</sup>, Thi Bao Tram Tran<sup>1</sup>, Aurore Gelin<sup>1</sup>, Olivia Bawa<sup>3</sup>, Nicolas Signolle<sup>3</sup>, M'Boyba Khadija Diop<sup>4</sup>, Philippe Dessen<sup>4</sup>, Stéphanie Beq<sup>5</sup>, Muriel David<sup>5</sup> & Pierre Busson<sup>1</sup>✉

Mechanisms of tumor immune escape are quite diverse and require specific approaches for their exploration in syngeneic tumor models. In several human malignancies, galectin-9 (gal-9) is suspected to contribute to the immune escape. However, in contrast with what has been done for the infiltrating cells, the contribution of gal-9 produced by malignant cells has never been demonstrated in an animal model. Therefore, we derived isogenic clones—either positive or negative for gal-9—from the MB49 murine bladder carcinoma cell line. A progressive and consistent reduction of tumor growth was observed when gal-9-KO cells were subjected to serial transplantations into syngeneic mice. In contrast, tumor growth was unaffected during parallel serial transplantations into nude mice, thus linking tumor inhibition to the enhancement of the immune response against gal-9-KO tumors. This stronger immune response was at least in part explained by changing patterns of response to interferon- $\gamma$ . One consistent change was a more abundant production of CXCL10, a major inflammatory factor whose production is often induced by interferon- $\gamma$ . Overall, these observations demonstrate for the first time that serial transplantation into syngeneic mice can be a valuable experimental approach for the exploration of novel mechanisms of tumor immune escape.

Galectins are a family of mammalian lectins sharing the capacity to bind  $\beta$ -galactoside bonds contained in glycans carried by glycolipids or glycoproteins<sup>1</sup>. Each galectin selectively binds a specific range of glycans which can be located inside the cells, at the cell surface or in the extra-cellular matrix. Several galectins can be released in the extra-cellular medium by non-classical secretory pathways and behave like intercellular messengers. Galectin-9 (gal-9) plays a major role in the physiology of the immune system<sup>2</sup>. When secreted in the extra-cellular medium, it behaves somehow like a cytokine with mainly immunosuppressive effects. However, it has a broader range of potential surface receptors than most *bona fide* cytokines. Its effects are dependent on multiple surface glycoproteins or glycolipids containing  $\beta$ -galactoside bonds, for example Tim-3 (on T-cells) and Dectin-1 (on macrophages)<sup>3,4</sup>. In physiological conditions, gal-9 is expressed at a low level in most tissues and organs. Its production is enhanced under inflammatory conditions. This occurs in epithelial and endothelial cells, under stimulation by interferon- $\gamma$ <sup>4</sup>.

Several years ago, our group was the first to show the contribution of gal-9 to immune suppression in the micro- and macro-environment of a human malignancy, namely nasopharyngeal carcinoma, a tumor which is almost constantly associated with the Epstein-Barr virus (EBV)<sup>5</sup>. Since this publication, the contribution of gal-9 to immune evasion has been reported in a number of other malignancies as diverse as lung, breast and pancreatic carcinomas, melanomas and acute myeloid leukemias<sup>3,6-9</sup>. In vitro and in animal models, the immunosuppressive effects of gal-9 result from the inhibition of both the innate and adaptive immune responses<sup>10</sup>. Regarding innate immunity, gal-9 inhibits NK cell cytotoxicity while enhancing the activity of MDSCs<sup>11-13</sup>. Regarding

<sup>1</sup>CNRS, UMR 9018, Gustave Roussy and Université Paris-Saclay, 39 Rue Camille Desmoulins, F-94805 Villejuif, France. <sup>2</sup>Inserm, U1170, Gustave Roussy, 39 Rue Camille Desmoulins, F-94805 Villejuif, France. <sup>3</sup>Plateforme de pathologie expérimentale et translationnelle, UMS AMMICA, Gustave Roussy, 39 Rue Camille Desmoulins, F-94805 Villejuif, France. <sup>4</sup>Plateforme de Bioinformatique, UMS AMMICA, Gustave Roussy, 39 Rue Camille Desmoulins, F-94805 Villejuif, France. <sup>5</sup>HiFiBio Therapeutics, Pépinière Paris Santé Cochin, 29 Rue du Faubourg Saint-Jacques, F-75014 Paris, France. ✉email: Pierre.Busson@gustaveroussy.fr

adaptive immunity, it is known to induce cell death of CD4<sup>+</sup> Th1 and Th17 cells and exhaustion of CD8<sup>+</sup> cells while enhancing the expansion and activity of suppressive cells like iTregs<sup>4,14–17</sup>. Despite multiple observations supporting the contribution of extracellular gal-9 to tumor immune escape, there are still many unknowns and controversies about the overall contribution of gal-9 to the malignant process. Difficulties and sometimes confusion in this research area are, in our view, due to two main causes: (1) cells producing gal-9 in the tumor microenvironment are quite diverse depending on the type of malignancies; (2) there is a suspicion that cell-associated gal-9—inside malignant cells or at their surface—can have anti-metastatic effects. This hypothesis is mainly supported by observations from a prospective cohort of breast carcinoma patients where the abundance of gal-9 in tumor tissue sections is inversely correlated to the risk of metastatic relapse<sup>18</sup>. On the other hand, elevated concentrations of plasma or serum gal-9 are consistently associated with a more severe prognosis in various types of malignancies, including pancreatic carcinomas, metastatic melanomas and renal carcinomas<sup>6,19,20</sup>.

In humans as well as in animal models, tumor gal-9 is often produced both by malignant cells and by infiltrating cells of lymphoid or myeloid origin<sup>3,21</sup>. So far, to our knowledge, there is no murine tumor model designed to assess the immunosuppressive effect of gal-9 produced by the malignant cells themselves separately from gal-9 released by the infiltrating cells. To address this need, we used a gene editing approach to create isogenic gal-9-positive and gal-9-negative clones derived from the murine bladder carcinoma cell line MB49. The MB49 line was chosen for 2 reasons: (1) it has a substantial baseline expression of gal-9; (2) it is known to trigger a robust although ineffective immune response in C57BL/6 syngeneic mice<sup>22–24</sup>. Using this approach, we could demonstrate that gal-9 gene ablation makes MB49 cells much more sensitive to the anti-tumor immune response. However, the emergence of this immune response was progressive, requiring at least 3 serial passages and growth cycles on syngeneic mice to reach full efficiency and blockade of tumor growth. To elucidate the mechanisms of the immune response promoted by gal-9 gene ablation, we combined detection of infiltrating leucocytes by IHC, assessment of the diversity of the stromal T-cell repertoire, differential RNAseq of gal-9-KO and WT tumors and intra-tumoral cytokine detection at successive cycles of tumor growth. One of the main changes occurring prior to the blockade of tumor growth was a broad increase in transcription of genes encoding proteins involved in tumor cell response to interferon- $\gamma$ . Consistently, in vitro, the production of CXCL10 induced by exogenous interferon- $\gamma$  was more abundant in gal-9-KO cells than in control clones. *A contrario*, a poor response of gal-9-positive malignant cells to interferon- $\gamma$  might be one mechanism supporting the immune escape of wild-type MB49 tumors.

## Results

### Genetic ablation of the gal-9 gene in the MB49 cells and in vitro characterization of the gal-9-KO and control clones.

In order to explore the contribution of gal-9 produced by malignant cells to tumor immune escape, we selected the MB49 murine tumor model. MB49 cells originated from a bladder carcinoma and are compatible with C57BL/6 mice. They are known for generating hot tumors in syngeneic mice and to trigger relatively strong although inefficient primarily CD8 cytolytic adaptive immune response<sup>22–24</sup>. They are also known to be responsive to immune-checkpoint inhibitors. MB49 cells were shown to have constitutive, permanent expression of gal-9. The *Lgals9* gene was invalidated in clones derived from MB49 cells using the CRISPR/Cas9 strategy (Supplementary Figure S1A). This procedure resulted in three clones knocked-out for gal-9 (gal-9-KO clones: # 175, 345, 377) and 2 control clones (WT-Ctrl clones: # 116 and 376) which had undergone the same transfection and cloning process but had retained an intact *Lgals9* gene and gal-9 expression similar to the parental MB49 cells (Supplementary Figure S1B,C). We first observed that cell proliferation in vitro was not affected in gal-9-KO clones by comparison with WT-Ctrl clones and parental MB49 (Supplementary Figure S2). Comparative RNAseq analysis of gal-9-KO and control MB49 cells propagated in vitro resulted in two important observations: (1) the absence of a gene subset with a distinct pattern of expression in gal-9-KO by comparison with WT-Ctrl clones; (2) the absence of distinct transcriptional alterations for genes predicted to be vulnerable to off-target effects in gal-9-KO by comparison with WT-Ctrl clones (Supplementary Figures S3 and S4). Finally, we found no influence of gal-9 silencing on the expression of other galectins: gal-1, -3 and -8 (Supplementary Figure S5).

### A serial tumor transplantation assay unmasks the immune restriction of tumor growth for gal-9-KO MB49 cells.

Moving from in vitro to in vivo experiments, the next step of our study was to investigate the growth of tumors resulting from subcutaneous injections of gal-9-KO or control MB49 cells. However, we often faced technical concerns regarding the mode of injections of these cells: either early skin ulcerations resulting from superficial injections or unwanted infiltration of underlying organs when making deeper injections. This prompted us to set up tumor growth assays based on subcutaneous implantation of small tumor fragments. Cell injection was the method retained for the first passage allowing collection of tumor fragments for subsequent passages. This approach based on the implantation of small tumor fragments was successful in reducing the incidence of tumor ulcerations or tumor infiltrations in underlying organs. In addition, from multiple preliminary experiments like the one depicted in Fig. 1, progressively emerged the evidence that tumor growth of gal-9-KO clones was undergoing a progressive decline after several passages on syngeneic mice (C57BL/6 N) when using small tumor fragments in serial transplantations. This experimental sequence was thereafter designated as “serial tumor transplantation assay”. Using a variant of the protocol used for Fig. 1, we designed a larger experiment involving all 3 gal-9-KO clones along with the two WT-Ctrl clones and parental MB49 cells, with concomitant transplantation on immune-competent syngeneic (C57BL/6 N) and immune-deficient mice (Supplementary Figure S6). As shown in Fig. 2A, a progressive reduction of tumor growth was observed for gal-9-KO clones through successive passages. This reduction was hardly visible at the 2nd cycle of tumor growth, but stronger at the 3rd cycle although not statistically significant. At the 4th cycle, it was even

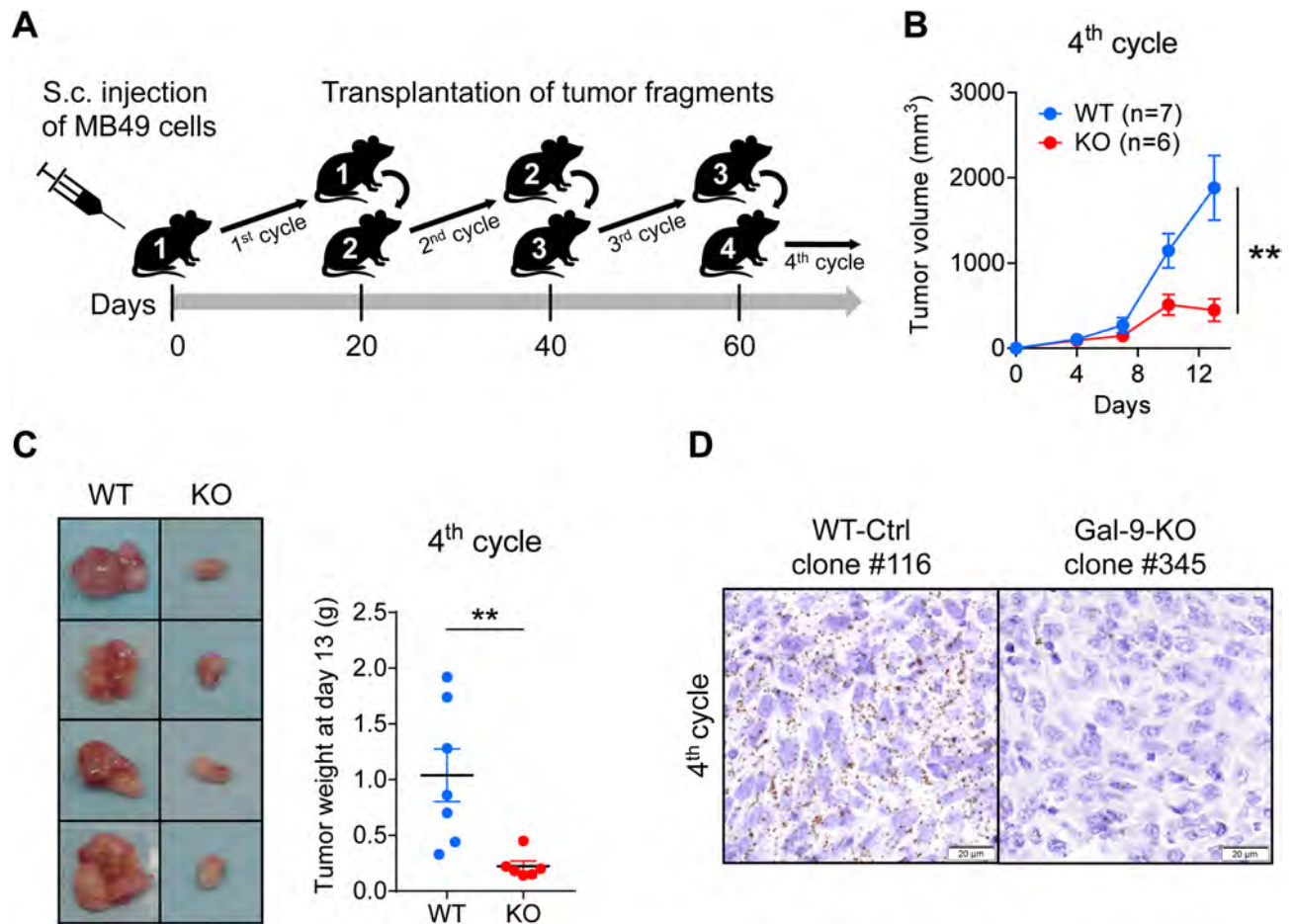
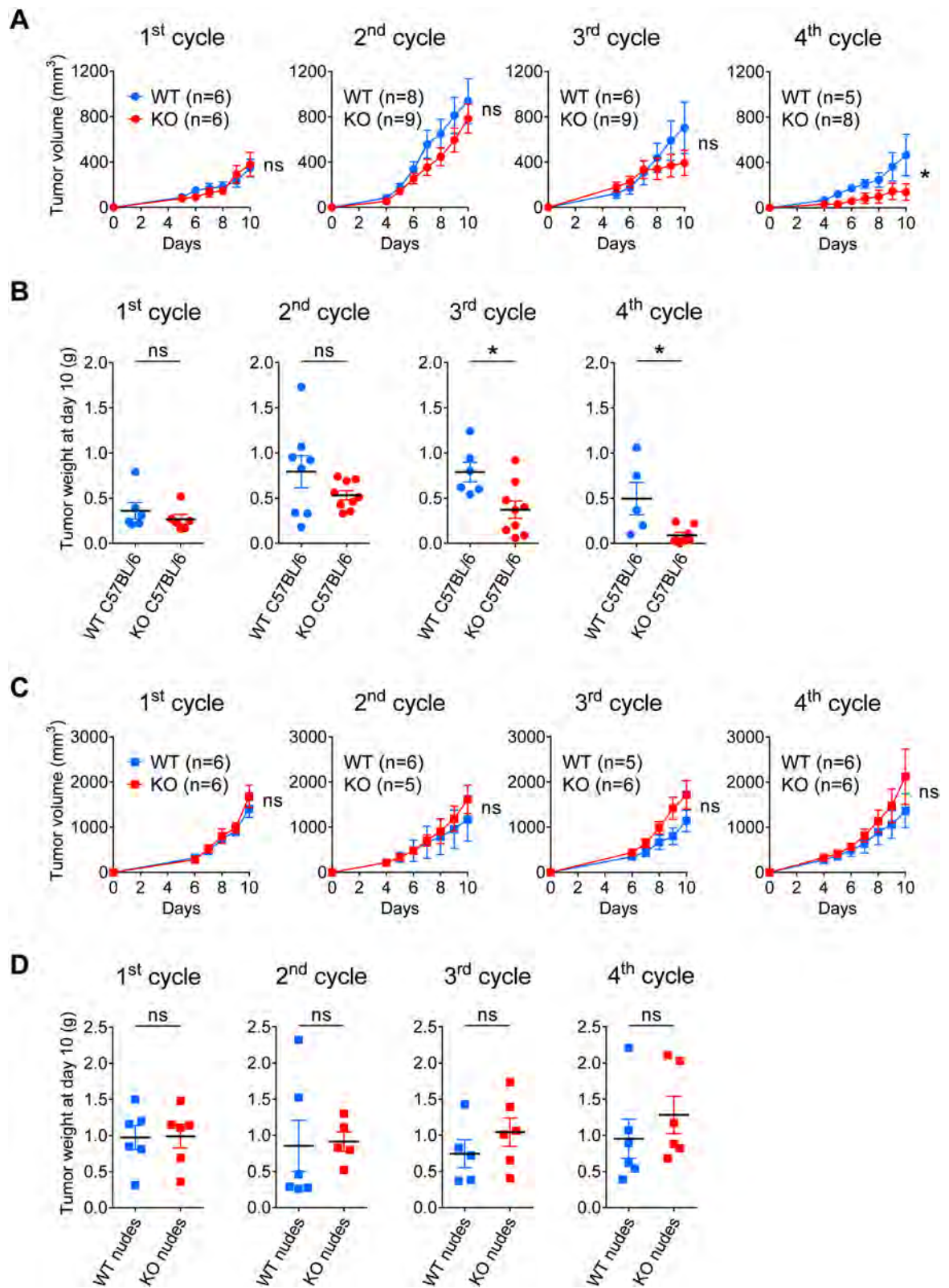


**Figure 1.** Pilot serial tumor transplantation assay using MB49 cells and isogenic clones in syngeneic mice (C57BL/6 N). (A) Cartoon depicting the main steps of the assay. The MB49 parental cell line (n = 3), the WT-Ctrl clone #116 (n = 4), the gal-9-KO clones #345 (n = 2) and #377 (n = 4), were subcutaneously injected into C57BL/6 female mice (opening the 1st cycle of tumor growth involving mice n°1). Twenty days later, tumors were collected and cut into small fragments. For each mouse donor, a small aggregate of tumor fragments (100 mg) was then subcutaneously transplanted into a single recipient mouse (2nd cycle involving mice n°2). This operation was repeated twice (opening the 3rd and 4th cycles of tumor growth involving mice n°3 and n°4 respectively). (B) Comparison of tumor growth curves for WT and KO tumors during the 4th cycle (mean volumes  $\pm$  SEM). WT tumors include tumors derived from the parental cells (MB49) and the WT-Ctrl clone #116. Significant differences in tumor volumes were recorded at day 13 (Mann–Whitney test). (C) Collection and comparative inspection of WT and gal-9-KO tumors at the completion of the 4th cycle of tumor growth. *Left panel:* visualization of selected representative tumors (Ctrl clone #116 and KO clone #377). The growth of gal-9-KO tumors was drastically reduced. Only small necrotic tumors were recovered. *Right panel:* graph showing a comparison of tumor weights for all mice of the 2 groups (7 and 6 mice respectively, Mann–Whitney test). (D) RNAscope detection of gal-9 transcripts in WT and KO tumor sections at the completion of the 4th cycle of tumor growth. Several WT and KO tumors were fixed in paraformaldehyde and paraffin-embedded. Then, tumor sections were subjected to in situ hybridization of gal-9 mRNA using the RNAscope method according to the manufacturer instructions (ACD—Biotechne). In tumors derived from parental and WT-Ctrl cells, numerous dots corresponding to gal-9 transcripts were detected in the vast majority of the cells. On the contrary, in gal-9-KO tumors, gal-9 RNA dots were much less abundant and restricted to some isolated cells (likely infiltrating immune cells or endothelial cells from the recipient mice).

more marked and statistically significant (individual growth curves are visible in Supplementary Figure S7A,B). Data based on tumor growth curves were confirmed by weight measurements of tumors excised following mouse euthanasia at the completion of each cycle, every 10 days. As shown in panel B of Fig. 2, the relative decline of tumor growth for gal-9-KO clones transplanted on syngeneic mice was statistically significant at cycle 3 and even more dramatic at cycle 4. Beyond cycle 4, we made two additional graft cycles involving all control tumors (n = 5) along with remaining gal-9-KO tumors (those weighting more than 90 mg at the completion of the 4th cycle, n = 3). At these next steps, all but one gal-9-KO tumor (from clone #345) stopped growing whereas all control tumors (from parental cells and control clones) still grew at a rapid path (Supplementary Figure S7C). Since gal-9-KO and WT MB49 cells had the same growth properties in vitro, our observations suggested that the progressive growth reduction of gal-9-KO tumors was related to a more efficient immune response in syngeneic





◀ **Figure 2.** Serial tumor transplantation assays of MB49 cells and isogenic clones using immunocompetent or immunodeficient mice. **(A)** Comparison of tumor growth curves for WT and KO tumors at each cycle (mean volumes  $\pm$  SEM). WT tumors include tumors derived from the parental cells (MB49) and the 2 WT-Ctrl clones # 116 and 376. For the 1st cycle of tumor growth, cells from the MB49 parental cell line ( $n = 3$ ), WT-Ctrl clones # 116 ( $n = 3$ ), 376 ( $n = 3$ ) and gal-9-KO clones # 175 ( $n = 3$ ), 345 ( $n = 3$ ) and 377 ( $n = 3$ ), were subcutaneously injected into C57BL/6N female mice. Subsequent passages were done using subcutaneous inoculation of aggregated tumor fragments (70 mg). In most cases, tumor fragments collected from one animal were inoculated in a single recipient mouse. Thus, we had 2 or 3 tumor lineages for each clone and for MB49 parental cells. Comparison of WT and KO groups were performed at the last point of each cycle and subjected to Mann–Whitney tests. As in the pilot experiment, the serial transplantations into syngeneic mice led to a progressive decrease in tumor volume for gal-9-KO tumors compared to WT-Ctrl and parental MB49-derived tumors. **(B)** Comparison of the tumor weights when mice were sacrificed at the completion of each cycle each ten days. The differences between the two groups were significant from the 3rd cycle (Mann–Whitney test). **(C and D)** The same experimental scheme was carried out in parallel using nude mice. In the context of these immunodeficient mice, there was no growth reduction during serial transplantation for gal-9-KO-derived tumors, as compared to WT-derived tumors (a slight, though non-significant, increase was actually observed). These observations highlight the contribution of the adaptive immune response to the reduction of gal-9-KO tumor growth.

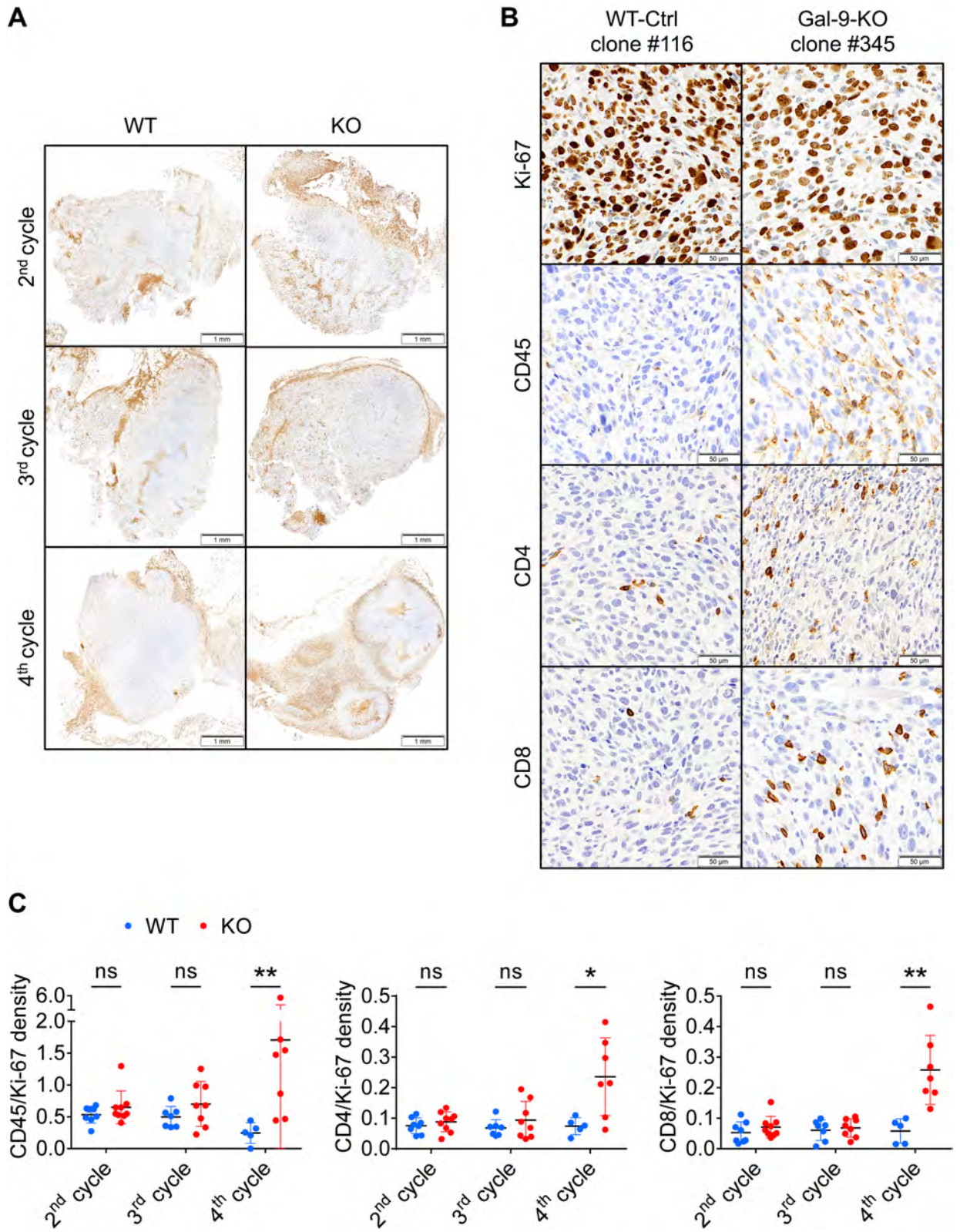
mice. We suspected that the progressive reduction of tumor growth for gal-9-KO clones was related to some improvement in the anti-tumor immune response. To confirm this hypothesis, in parallel with the previously presented experiments, we performed serial tumor growth assays on athymic (nude) mice comparing the 3 gal-9-KO clones, the 2 WT-Ctrl clones and the parental MB49. As shown in Fig. 2C,D, in the context of athymic mice, tumors derived from the gal-9-KO clones did not undergo progressive growth reduction. On the contrary, they had a tendency to grow even faster than the WT cells at cycles 3 and 4 (individual growth curves are visible in Supplementary Figures S7D,E).

### T-cells are involved in the enhancement of the immune response resulting from gal-9 invalidation in MB49 cells.

Because athymic mice are characterized by a complete absence of T-cell ontogenesis, these results suggested that the tumor growth reduction of the gal-9-KO clones was dependent on T-cells. To strengthen this hypothesis, we used immunohistochemistry to investigate T-cell infiltration of WT and gal-9-KO tumors grown on syngeneic mice. Tumor sections made at cycle 2, 3 and 4 were processed using antibodies reacting with Ki-67, CD45, CD4 and CD8. For each marker, density staining was quantified by digital imaging. Upon visual examination, we made two main observations. First, we noted that the bulk of leucocytes (CD45<sup>+</sup>), including T-cells (CD4<sup>+</sup> and CD8<sup>+</sup>), were concentrated at the periphery of tumor nodules. Their abundance in these areas was identical for KO and WT tumors at all cycles of tumor growth (Fig. 3A). In contrast, leucocytes were quite rare inside the tumor nodules except for gal-9-KO tumors at cycle 4 for which a substantial number of CD45<sup>+</sup>, CD4<sup>+</sup> and CD8<sup>+</sup> leucocytes were visible inside the nodules (Fig. 3B). This was confirmed by digital assessment of the 4 markers (Ki-67, CD45<sup>+</sup>, CD4<sup>+</sup> and CD8<sup>+</sup>) as shown by the histograms of Fig. 3C. The density of Ki-67 staining was used to normalize the density of the other markers. At cycles 2 and 3, densities of CD45, CD4 and CD8 staining inside the nodules were almost identical for KO and WT tumors. On the other hand, at cycle 4, staining densities of these 3 markers were much higher for KO than WT tumors. Overall, our conclusion was that T-cell infiltration of tumor nodules was specific for gal-9-KO tumors. However, this infiltration was detectable only at cycle 4, therefore at a late stage of the anti-tumor immune response, when tumor growth was already strongly impaired (5/8 KO tumors were of minimal size, weighing less than 70 mg). These observations suggested that, upstream of T-cells infiltration, some immune-related events were occurring in a different manner in gal-9-KO and WT tumors, at an earlier stage of the serial transplantation assay, possibly during cycles 2 or 3. A glimpse of these early events was given by quantitative assessment of the diversity of the stromal T-cell repertoire. Using total tumor c-DNA, the diversity of the TCR complementary determining region 3 (CDR3) was assessed by PCR amplification and high throughput sequencing (Fig. 4). This analysis resulted in clonotypes characterized by a unique sequence and a frequency of reads matching this sequence. Figure 4 and Supplementary Table S1 show a greater number of clonotypes in KO by comparison with WT tumors and at cycle 3 by comparison with cycle 2. In gal-9-KO tumors, a substantial number of emerging clonotypes were of average size (between 100 and 1000 reads) therefore likely to be representative of functional T-cell clones. In summary, these observations suggested that the T-cell repertoire had a tendency to increase its diversity from cycle 2 to cycle 3 while being, in both cases, more diverse in KO than in WT tumors. In other words, it was suggested that long before intra-nodular T-cell infiltration, as early as the second cycle of tumor growth, changes in T-cell distribution and behavior were taking place preferentially in gal-9-KO tumors.

### Gal-9 ablation enhances transcription of genes related to interferon- $\gamma$ response.

To further investigate biological events occurring prior to T-cell infiltration and blockade of tumor growth, we performed a comparative transcriptome analysis of gal-9-KO and WT tumors through the successive cycles of the serial tumor transplantation assay (Fig. 5A). Our aim was to find correlations between the dynamics of transcriptional changes and the progressive inhibition of gal-9-KO tumor growth. RNAseq data from 30 samples were subjected to various types of comparative bioinformatics analyses. Unsupervised clustering as well as supervised comparisons did not achieve separation of gal-9-KO from WT tumors or early from late passages while there was a trend towards clusterization of tumors derived from the same MB49 clones (Supplementary Figure S8). It seems that biological characteristics related to the progressive immune response were, to a large extent, relegated



◀**Figure 3.** In gal-9-KO tumors, late stages of tumor growth reduction are associated with an increase in T-cells infiltrating tumor nodules. (A) Low magnification of CD45 staining on sections of WT and gal-9-KO tumors at cycles 2, 3 and 4 (tumors derived from clones # 116 and 345, respectively). At cycle 2, CD45 staining was detected almost exclusively in peri-nodular septa. However, for gal-9-KO tumors, at cycle 3 and even more at cycle 4, CD45 was becoming more and more abundant inside the tumor nodules. (B) High magnification of CD45, Ki-67, CD4 and CD8 staining on serial sections of a WT-Ctrl tumor (#116) and a gal-9-KO tumor (#345) at cycle 4. (C) Quantitative assessment of CD45, CD4 and CD8 staining on serial sections of tumors collected at cycles 2, 3 and 4 of tumor growth. Digitalization was performed in large Regions of Interest (ROIs) covering in as much as possible the whole tumor sections and excluding areas with absence or very low levels of Ki-67 staining, including peri-nodular septa. Therefore these ROIs were covering mainly the internal parts of the tumor nodules. Ratios of CD45, CD4 or CD8 to Ki-67 staining densities were acquired in these ROIs and plotted for each tumor growth cycles. Comparisons of mean ratios obtained for WT and KO tumors were subjected to Mann–Whitney tests for assessment of statistical significance.

to the background by other clonal private characteristics. We reasoned that it was not sufficient to compare the whole set of WT tumors with the whole set of KO tumors. We thought that it was possible to gain sensitivity by focusing the comparison on the subset of KO-tumors taken at the late stages of the serial transplantations, especially at the last cycles preceding the collapse or quasi-collapse of tumor growth, hereafter named “pre-terminal cycles” (Fig. 5A). Our bet was that it would be easier to find transcriptional characteristics consistent with the enhancement of the immune response in this subset of “pre-terminal” tumors. Reciprocally, these characteristics were expected to be absent or less visible in the rest of the KO tumors, non-pre-terminal tumors thereafter called “aggressive” KO tumors (Fig. 5A). Combining the RUVseq package<sup>25</sup> with the DESeq2 software we generated a list of differentially expressed (DE) genes resulting from the comparison of “pre-terminal” KO vs all WT tumors. This list of 344 genes resulted in effective separation of “pre-terminal” gal-9-KO from WT tumors as shown by the heat map in Fig. 5B. This same list was subjected to enrichment analysis using the package ClusterProfiler<sup>26</sup>. The greater enrichment scores were obtained for the following general functions: cell response to interferon- $\gamma$ , allograft rejection and inflammatory response (Fig. 5C). One gene related to these 3 general functions—*CCL5* (also called *Rantes*)—appeared to be strongly expressed in “pre-terminal” gal-9-KO tumors. Seeking confirmation of the enhancement of interferon- $\gamma$  response in “pre-terminal” KO tumors, we investigated by q-RT-PCR the abundance of interferon- $\gamma$  m-RNA along with mRNAs encoding 3 chemokines (*CCL5*, *CXCL9* and *CXCL10*) and two components of the MHC II complex (*CD274* and the  $\alpha$ -chain). The expression of these transcripts is known to be often enhanced by interferon- $\gamma$ . For each of them, we found a greater abundance in pre-terminal KO tumors than in WT tumors. The differences were statistically significant for interferon- $\gamma$ , *CXCL9* and *CXCL10* (Fig. 5D).

**Progressive increase in the concentrations of CXCL10 in gal-9-KO tumors.** In order to better understand the immune mechanisms of the progressive growth inhibition of gal-9-KO tumors, we used a multiplex ELISA assay to investigate the expression of a panel of 31 cytokines in the tumor cells and their micro-environment. This assay was carried on whole proteins extracted from WT and KO tumor fragments collected at cycle 2 and 3 of tumor growth. Cytokine concentrations were compared between these 3 sets of tumors: WT, aggressive gal-9-KO and “pre-terminal” gal-9-KO tumors (Fig. 6A). Significant differences between “pre-terminal” KO tumors and WT tumors were found for 2 cytokines—IL-1  $\alpha$  and  $\beta$ —which were more abundant in “pre-terminal” KO tumors than in WT tumors. The concentrations of *CXCL9* and *CXCL10* were also increased in “pre-terminal” KO tumors, although the differences with WT tumor did not reach statistical significance. Nevertheless, we retain this observation for our subsequent investigations for two reasons. First, as shown in Fig. 5D, *CXCL9* and *CXCL10* mRNAs were more abundant in pre-terminal than in WT tumors with statistical significance. Next, we were struck by the facts that, even at baseline (WT tumors), the concentrations of *CXCL9* and *CXCL10* in tumor extracts were greater than those of other cytokines by one or two orders of magnitude. This suggested that these two cytokines were produced, at least to a large extent, by malignant cells. To confirm this assumption we performed detection of their transcripts on tissue sections using the RNAscope technology. As shown in Fig. 6B, signals related to *CXCL9* and *CXCL10* mRNAs were mainly observed in malignant epithelial cells. In an attempt to connect results based on protein detection and RNAscope with the data resulting from transcriptome profiling, we investigated a potential correlation between the abundance of the transcripts encoding the four cytokines overexpressed in “pre-terminal” KO tumors and the mRNAs encoding interferon- $\gamma$ . As shown in Fig. 6C, for these four cytokines, there was a strong positive linear correlation of their expression with interferon- $\gamma$  expression in KO and WT tumors. The highest levels of concomitant expression for interferon- $\gamma$  on the one hand and IL-1  $\alpha$  or  $\beta$ , *CXCL-9* or *10* on the other hand, were recorded for “pre-terminal” tumors. This was one additional observation suggesting a critical role of interferon- $\gamma$  in the progressive deployment of the anti-tumor immune response.

**Gal-9 gene ablation in MB49 cells enhances in vitro CXCL10 induction in response to recombinant interferon- $\gamma$ .** In order to confirm the hypothesis of a greater sensitivity of MB49 cells to their stimulation by interferon- $\gamma$  in the absence of gal-9, we performed the following experiment in vitro. Gal-9-KO and WT cells were subjected to a 72 h treatment with increasing concentrations of recombinant interferon- $\gamma$  (from 2 to 25 ng/ml). Then, the concentration of *CXCL10* was assayed in the conditioned medium. As shown in Fig. 7A, *CXCL10* production was completely absent at baseline. It was induced in a dose-dependent manner by interferon- $\gamma$ . This induction was much stronger for gal-9-KO clones than for WT clones or MB49 parental

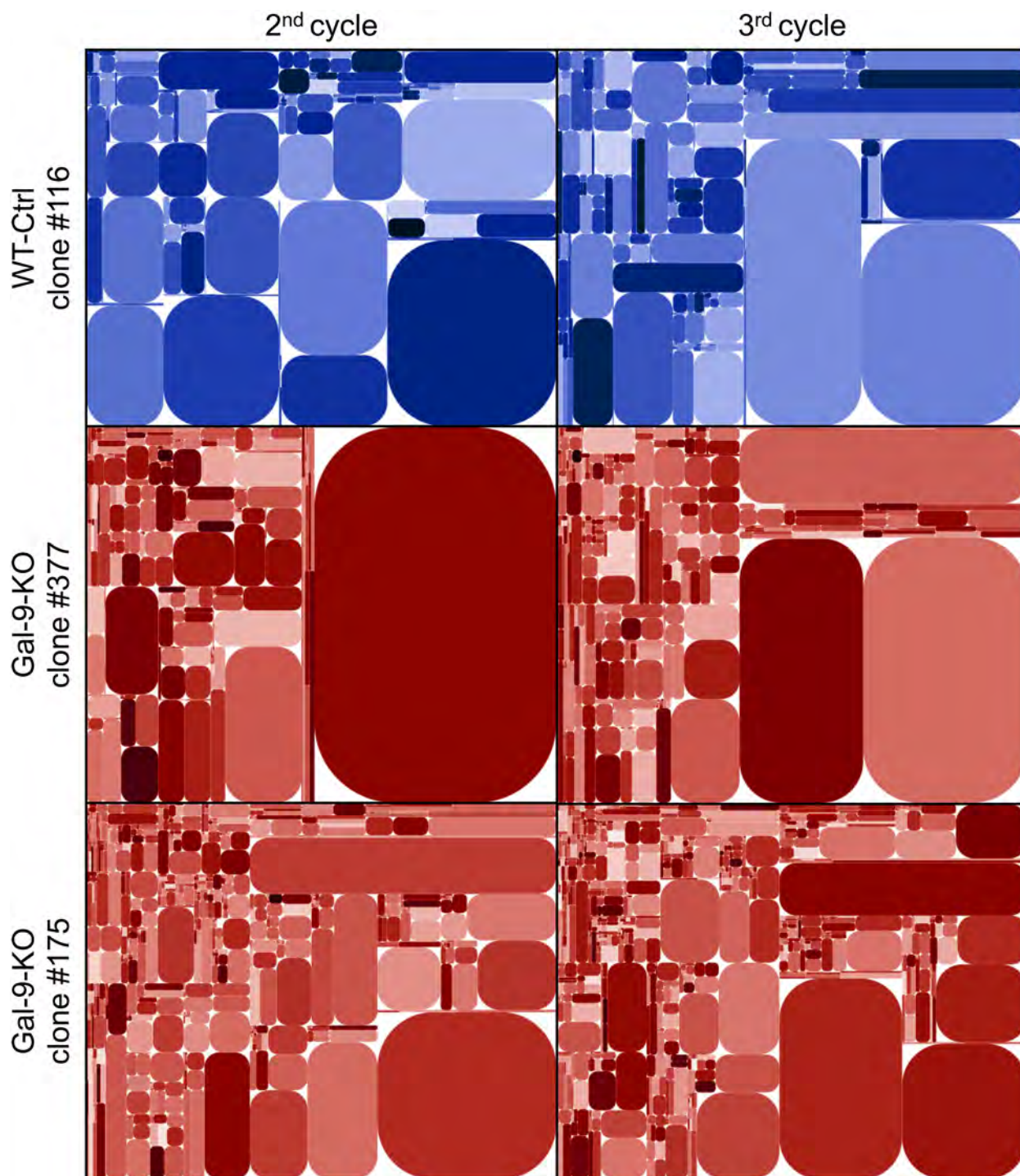


**Figure 4.** Modifications of T-cell clonotype profile at an early stage of tumor growth reduction in gal-9-KO tumors. The diversity of the CDR3 segment of the TCR  $\beta$ -chain was investigated using total tumor RNA subjected to reverse transcription, selective PCR amplification of the CDR3 coding region and deep sequencing. Here are shown tree maps of the clonotypes identified in one WT-Ctrl (#116) and two gal-9-KO (#175 and 377) tumors at the 2nd and 3rd cycles of tumor growth. These tree maps were generated as follows: the entire plot area was divided into sub-areas according to V-usage, then subdivided according to J-usage and again according to unique CDR3 sequences resulting from somatic hypermutations. Each clonotype is characterized by its unique sequence and the frequency of the reads matching this sequence. Those with a sufficient frequency of reads are represented by a rounded rectangle whose size is proportional to this frequency. At cycle 2, the number of clonotypes of average size (small rectangles) was greater in tumors derived from KO (#377 and #175) than from WT (#116) clones. This number was increasing from cycle 2 to cycle 3 but still with a greater abundance in tumors derived from gal-9-KO clones. Simultaneously, there was a relative size reduction of very large pre-existing clonotypes (represented by big rectangles). These tree map characteristics are in favor of a greater TCR diversity at cycle 3 compared to cycle 2 and in both cases for KO compared to WT tumors. For the precise numbers of unique sequences in the various experimental conditions, see Supplementary Table S1.

cells. This was a confirmation of the greater sensitivity of MB49 cells to their stimulation by interferon- $\gamma$  in the absence of gal-9.

## Discussion

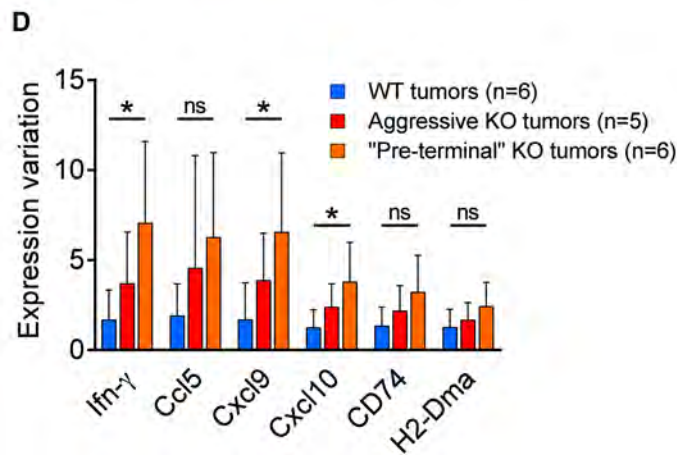
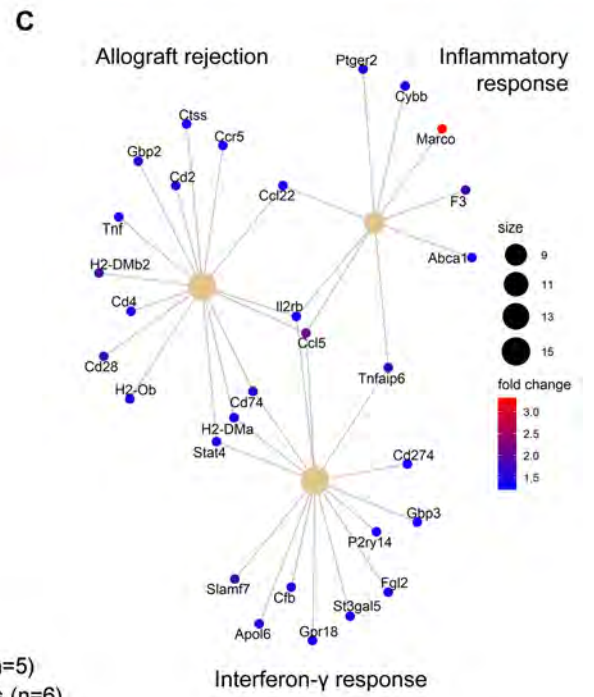
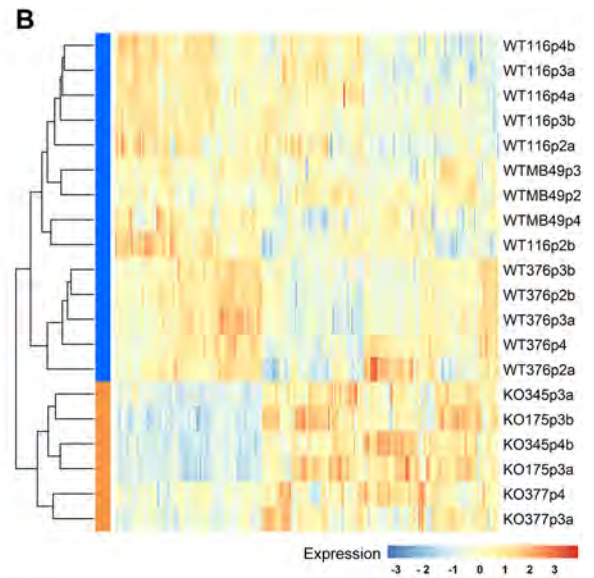
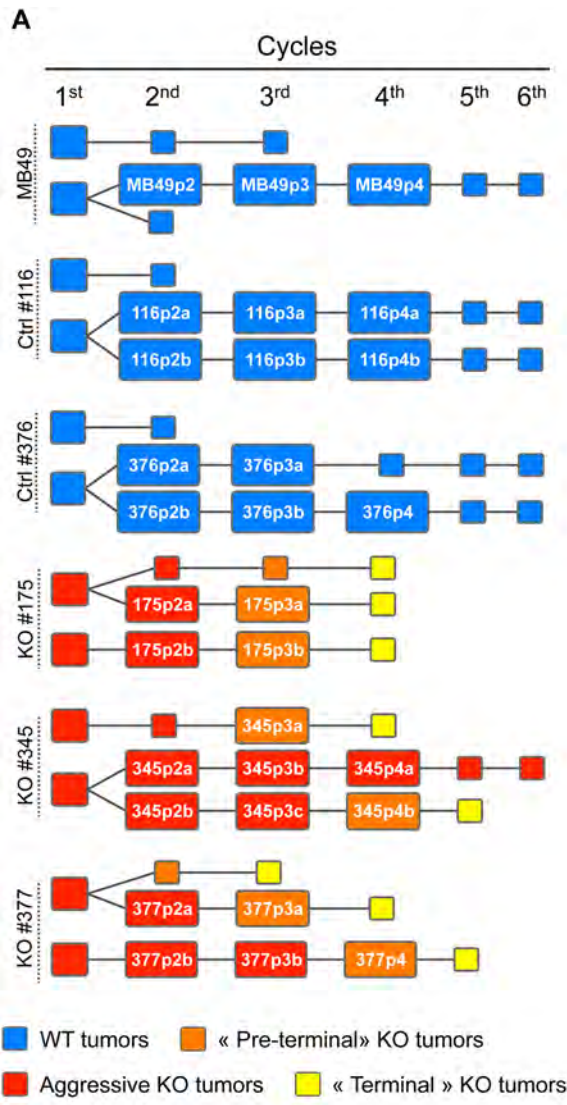
The aim of this study was to build a murine tumor model designed to investigate the role of gal-9 in host-tumor relationships in the context of immunocompetent syngeneic animals. Our approach was based on the production of MB49 isogenic clones with or without gal-9 expression. These clones were generated by the CRISPR/Cas9 method of gene editing. One major advantage of this approach was to guarantee that the silencing of the gal-9 gene would be irreversible. One disadvantage was the possibility of off-target genetic lesions that could randomly affect the phenotype of edited clones in a way which had nothing to do with gal-9 biology. Another source of heterogeneity was the cloning step taking place after transfection of the editing material. In order to minimize the influence of unwanted clonal heterogeneity, we have compared the gal-9-KO clones with control clones subjected to the same editing process but having retained gal-9 expression. They were used in addition to the parental MB49 cells through the whole study. No differences in terms of tumor growth were apparent when gal-9-KO or WT-Ctrl cells were injected subcutaneously. However serial transplantations of tumor fragments unmasked a completely different pattern of growth for gal-9-KO and Ctrl-cells. Gal-9-KO tumors were affected by a progressive inhibition of tumor growth resulting in minute, “exhausted” tumors at the third or fourth cycles of growth. This reduction of tumor growth was dependent on the immune response and involved T-cells since it was not observed when the serial transplantations were made into nude mice.

Our investigations based on IHC, RNAseq and cytokine profiling have confirmed the progressive enhancement of the immune response through 2 or 3 cycles of tumor growth. T-cell infiltration in the tumor nodules was only detected in terminal “exhausted” tumors. However, this change of histological pattern concomitant of growth termination was preceded by transcriptional changes in the micro-environment of “pre-terminal” tumors i.e. tumors taken at the last cycle of growth prior to the exhaustion. A fraction of these changes was highly suggestive of the emergence of an immune response. Enrichment analysis of genes differentially expressed between pre-terminal KO and WT tumors have highlighted three main processes related to the immune response: cell response to interferon- $\gamma$ , allograft rejection and inflammatory response. The *CCL5* mRNA was standing at the intersection of the three sets of genes highlighted by the enrichment analysis. This is consistent with a recent publication reporting the crucial role of *CCL5* produced by malignant cells to stimulate the penetration of tumor infiltrating lymphocytes in human malignancies and murine tumor models<sup>27</sup>.

Profiling of the T-cell repertoire by deep sequencing has unveiled critical events in host-tumor interactions which were taking place in KO-tumors upstream of pre-terminal tumors as early as the second cycle of tumor growth. Indeed, already at this stage, the repertoire of T-cell clonotypes was more diverse for gal-9-KO tumors. Thanks to our data obtained by IHC, we know that, at this stage, the overwhelming majority of T-cells are contained in perinodular margins. Therefore our observations on the T-cell repertoire suggest a mobilization of T-cells in these margins taking place before nodular invasion.

Overall, our data show that for tumors derived from gal-9-KO clones, the deployment of the immune response leading to tumor growth arrest requires 2 simultaneous conditions: (1) absence of gal-9 produced by tumor cells; (2) serial transplantation for 2 or 3 cycles of tumor growth. We now have to discuss by which mechanisms these two conditions are suspected to contribute to the anti-tumor immune response.

The contribution of gal-9 ablation to the enhancement of the immune response against MB49 tumors is consistent with several inhibitory effects of extra-cellular gal-9 on immune effectors cells which have been well documented in the murine context. These effects are mainly death of CD4<sup>+</sup> Th1 cells, expansion of MDSCs and functional impairment of natural killer cells<sup>4,11,12</sup>. Independently of these cell non-autonomous mechanisms, our investigations based on serial MB49 tumor transplantations has pointed to potential mechanisms of immune escape intrinsic to malignant cells. First, transcriptional studies have suggested a better response to interferon- $\gamma$  in tumors resulting from gal-9-KO cells. This was confirmed by additional investigations focused on cytokines. Cytokine profiling on tumor protein extracts showed a substantial increase in the expression of IL-1 $\alpha$  and  $\beta$ , CXCL9 and CXCL10 in pre-terminal gal-9-KO tumors by comparison with WT and aggressive gal-9-KO tumors. In addition, going back to the transcriptional level, we found remarkable correlations between the abundance of interferon- $\gamma$  transcripts and those of the above-mentioned cytokines including CXCL9 and CXCL10 which were shown to be produced by malignant cells (Fig. 6B,C). Finally, we obtained direct evidence of the influence of gal-9 expression on tumor cell response to interferon- $\gamma$  by in vitro comparative stimulation of gal-9-KO and WT MB49 clones. All these cells responded to recombinant interferon- $\gamma$  by a de novo, dose-dependent release of CXCL10. However, this release was much more abundant for gal-9-KO clones than for WT-Ctrl clones or parental cells. This suggests that gal-9 impairs MB49 cell response to interferon- $\gamma$ . So far, we do not know whether it exerts this effect when it is trafficking inside the cells or when it is bound to their surface and/or released in the extra-cellular medium. Although the mechanism of this alteration is not known, we can speculate that gal-9 slows down a feed-forward loop involving CD4<sup>+</sup> Th1 + T-cells, interferon- $\gamma$ , malignant cells and CXCL10 as explained in the cartoon on Fig. 7B. Our data showing that gal-9 produced by MB49 cells impairs the anti-tumor immune response probably by both cell-autonomous and cell-intrinsic mechanisms seems to contradict reports of a better prognosis for a category of human malignancies—especially breast carcinomas—with abundant expression of gal-9<sup>18</sup>. To cope with this paradox, one has to keep in mind that some biomolecules can have both pro- and anti-tumor effects. Intra-cellular gal-9 is suspected to decrease the metastatic potential of malignant cells but this might be achieved at the cost of some immunosuppressive effects<sup>18</sup>. In the future, concomitant detections of interferon- $\gamma$  and CXCL10 in tumor tissue sections and maybe in plasma samples might help to assess the immunosuppressive effects of gal-9 in various tumor contexts.



◀ **Figure 5.** RNAseq analysis of WT and gal-9-KO tumors at different cycles of in vivo tumor growth. (A) Cartoon depicting the serial tumor transplantation assay with emphasis on the tumor “lineages” and their changes in growth and aggressiveness: WT tumors are represented in blue, “aggressive” (WT-like) KO tumors in red, “terminal” (infiltrated by T-cells and exhausted) KO tumors in yellow and the “pre-terminal” KO tumors in orange. The annotated rectangles represent tumors used for RNA and/or protein analyses. Other tumors are represented by squares without annotations. The complete set of investigations performed on each tumor of this assay is shown in Supplementary Figure S6. (B) Heatmap representing the expression profile of the 344 most differentially expressed genes between WT and “pre-terminal” KO tumors, based on RUVseq ( $k=3$ ) and DESeq2 analysis (fold change  $>2$ , adjusted  $p$  value  $<0.05$ ). (C) Enrichment analysis of the differentially expressed genes within the “hallmark” gene sets defined in the clusterProfiler package (Bioconductor): 15 up-regulated genes in the “pre-terminal” KO tumors are associated with the “allograft rejection”, 9 with the “inflammatory response” and 15 with the “interferon- $\gamma$  response”. (D) RT-qPCR for quantitation of mRNAs transcribed from the *interferon- $\gamma$*  gene and 5 genes whose expression is known to be often stimulated by interferon- $\gamma$  (encoding the CCL5, CXCL9 and CXCL10 chemokines and the MHC class II components CD74 and H2-DMA). Comparative assessment was made in WT ( $n=6$ ), “aggressive” KO ( $n=5$ ) and “pre-terminal” KO tumors ( $n=6$ ). Interferon- $\gamma$ , CXCL9 and CXCL10 m-RNAs are significantly more abundant in “pre-terminal” gal-9-KO than in WT tumors (Kruskal–Wallis test followed by Dunn’s multiple comparisons test).

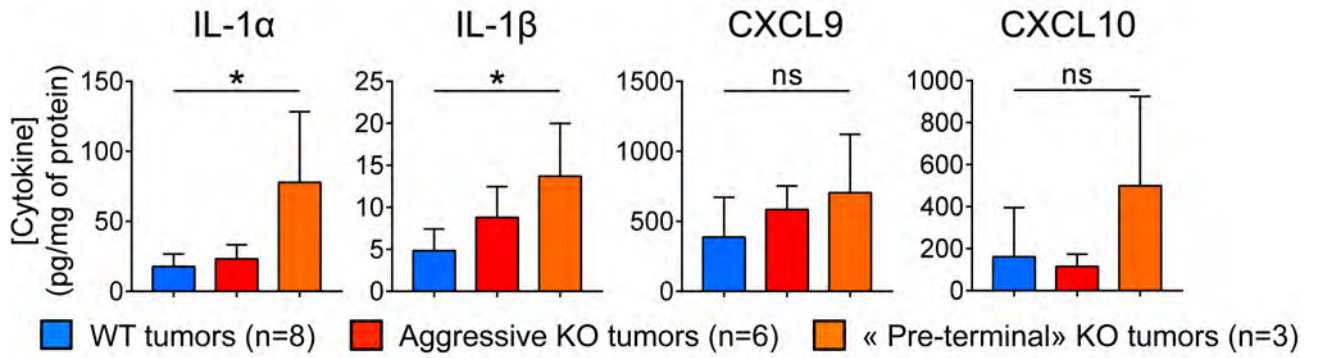
Serial transplantations are common in experimental hematology and onco-hematology, especially in studies dealing with stem cells or tumor initiating cells<sup>28,29</sup>. In contrast, to our knowledge, this method has not been previously reported for solid tumors grafted in syngeneic mice. It was introduced in our experimental system partly by chance while we were seeking better conditions of tumor growth which were achieved by transplantation of tumor fragments instead of cells expanded in vitro. Then, we realized that serial transplantations were required to unmask the greater vulnerability of gal-9-KO tumors to the immune response. On the side of malignant cells, it is difficult to consider a type of immune-editing that would result in the selection of cells with greater sensitivity to the immune response. In fact, it would be the contradiction of the concept of immuno-editing. On the other hand, tumor fragments used for serial transplantation are the only possible “vectors” going from one mouse to another with the capacity to increase the efficiency of the immune response. Since transplanted tumor fragments contain infiltrating leucocytes, their implantation in the recipient mice may result in the adoptive transfer of immune cells which may facilitate and accelerate the onset of the immune response in the recipient mice. This effect might be enhanced by concomitant mechanical factors: (1) the mincing of small tumor fragments may increase their immunogenicity; (2) the sub-cutaneous insertion of these fragments undergoing partial necrosis is likely to increase local inflammation in the tumor niche. Investigating the role of immune cells contained in tumor fragments and passively transferred from one mouse to another is conceivable but would require a dedicated project. However, on the basis of our data, we can already consider serial transplantation in syngeneic mice as a possible approach to refine the exploration of some mechanisms of tumor immune tolerance or rejection. It seems that it might help to investigate the maturation of host-tumor relationships through a greater period of time than what is possible when working with transplantation in a single mouse. Indeed, except for tumor models growing very slowly, it is usually difficult to extend for more than 3 to 4 weeks the investigations made on tumors grafted on a single animal, without breaking practical and/or ethical limits. Therefore, serial transplantation might prove useful to better mimic the evolution of host-tumor relationships as it takes place in the patients where tumor history usually spans several months or even several years.

## Material and methods

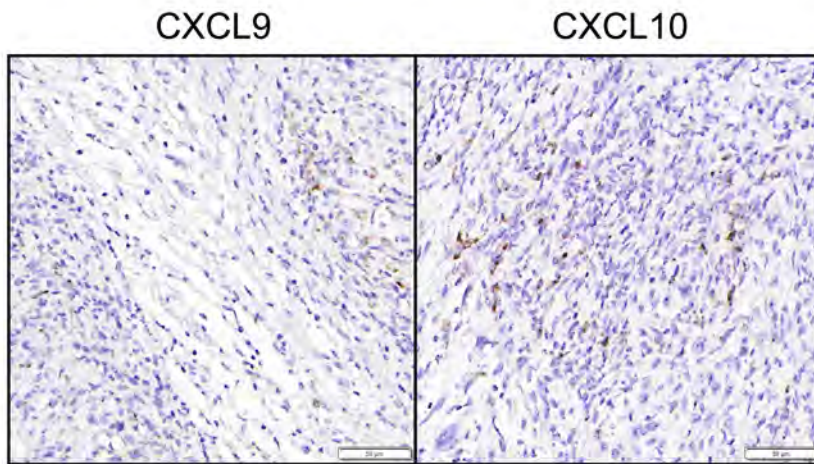
**MB49 cell line.** MB49 is a murine bladder carcinoma cell line derived from the C57BL/6 mouse strain which was purchased from Merck Inc (Millipore Cat# SCC148, RRID:CVCL\_7076). Cells were grown in DMEM medium (Gibco, Life Technologies) supplemented with 5% fetal calf serum, 2 mM glutamine and 5  $\mu$ g/mL gentamycin.

**Ablation of the gal-9 gene in the MB49 cells.** Our strategy to invalidate the gal-9 gene was to make a deletion framing the start codon by concomitant transfection of 2 guide RNAs. The sequences of these guide RNAs were designed in silico using the CRISPOR tools<sup>30</sup>. They were matching a sequence in the first exon and first intron of the gal-9 gene, respectively. The DNA inserts encoding the upstream and downstream guide RNAs were generated from two pairs of single strand oligonucleotides, respectively (F: 5'-CACCGCTGTCGTCCACCATCGAGTG-3'; R: 5'-AAACCACTCGATGGTGGACGACAGC-3') and (F: 5'-CACCGAGTGCCTGTGTGTGCAGGT-3'; R: 5'-AAACACCTGCACACACGGCGACTC-3'). These two pairs of oligonucleotides were annealed by denaturation and slow renaturation prior to vector insertion. These inserts were ligated to a backbone Lenti-CRISPR-V2puro plasmid (RRID:Addgene\_52961) to co-express the guide RNA sequences with *Streptococcus pyogenes* Cas9 linked either to the GFP or mCherry sequence by a P2A sequence encoding a self-cleaving peptide. These plasmids were digested by *BsmBI* and ligated with the annealed guide RNA sequences. Cell lines were transfected with both GFP and mCherry plasmids, using the TurboFect (Thermo Scientific) reagent according to the manufacturer’s instructions. They were harvested, 48 h after transfection, sorted according to their double GFP/mCherry positive expression and automatically seeded at one cell/well in a 96 well cloning plate (BD Influx). After 2 weeks, emerging clones were tested for their gal-9 expression by intracellular staining using rat anti-mouse gal-9 antibody clone 108A2 conjugated with allophycocyanin (APC) (BioLegend Cat# 137,911, RRID:AB\_2750154); they were analysed with an Accuri C6 flow cytometer (BD Biosciences). After sequencing analysis confirming their knock-out status, 3 of them were selected for the study (KO # 175, 345 and

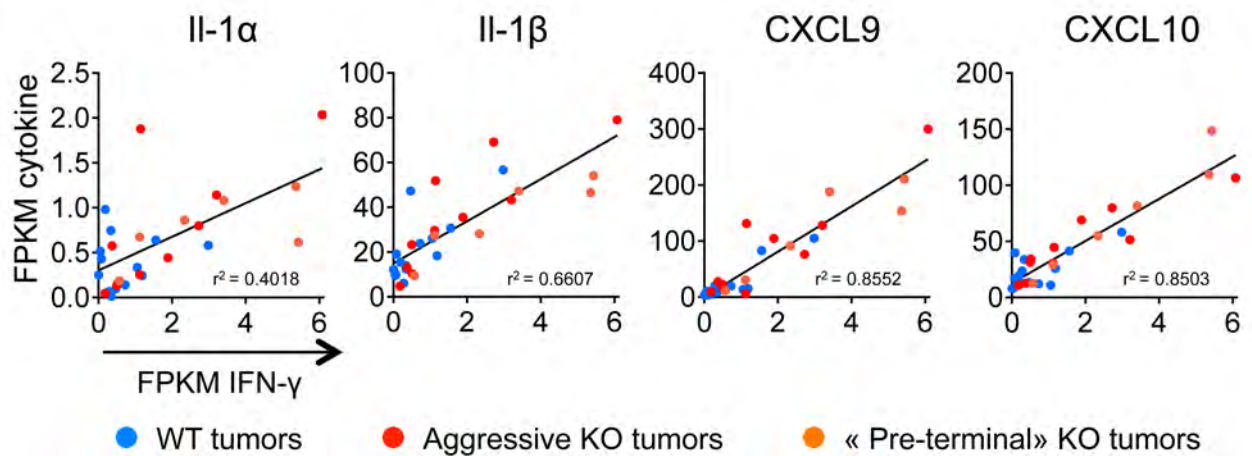
**A**



**B**



**C**





◀**Figure 6.** Cytokine status in gal-9-KO and WT tumors. (A) Concentrations of four cytokines resulting from a multiplex ELISA performed on 31 cytokines detected in tumor protein extracts at various cycles of tumor growth (8 WT tumors, 6 aggressive KO tumors and 3 “pre-terminal” KO tumors). For IL-1  $\alpha$  and  $\beta$ , there was a significant increase in their concentrations in the extracts of “pre-terminal” KO tumors compared to the WT. CXCL9 and CXCL10 concentrations were also greater in “pre-terminal” KO tumors, although the differences were not statistically significant. However, these observations are worth to mention because the concentrations of CXCL9 and CXCL10 in tumor extracts were greater than those of other cytokines by 2 orders of magnitude even at baseline (WT tumors). (B) RNAscope detection of CXCL9 and CXCL10 transcripts in “pre-terminal” KO tumors. Signals related to CXCL9 and CXCL10 mRNAs are mainly detected in malignant epithelial cells which often have a basal-like appearance, often located at the periphery of tumor nodules (this is best illustrated for CXCL9 in the left panel). (C) Abundance of the messenger RNAs of the above-mentioned cytokines (FPKM values from RNAseq data) as a function of the amount of IFN- $\gamma$  transcripts. For the four cytokines mentioned in (A), there is a strong positive linear correlation between their level of expression and that of interferon- $\gamma$ . This correlation is observed in KO as well as in WT tumors. However, tumors combining highest expressions of interferon- $\gamma$  combined with highest expressions of IL-1  $\alpha$  or IL-1  $\beta$ , CXCL9 or CXCL10 were “pre-terminal” tumors.

377). In addition, we selected 2 clones having undergone the same transfection treatment, sorting and clonal selection, but having preserved an intact gene sequence at the sites targeted by the guides and still strongly expressing gal-9 (Ctrl # 116 and 376). Furthermore, we generated a list of the most probable off-targets by in silico analysis (Supplementary Table S2 and Supplementary Figure S4) and compared the FPKM values of these transcripts in KO clones with the controls and parental lines. No differences went outside this analysis. Exome sequencing has been performed for authentication of MB49 parental cells and derived clones (3 gal-9-KO and 2 control clones). The corresponding data are publicly available on the ArrayExpress database of the European Bioinformatics Institute (<http://www.ebi.ac.uk/arrayexpress>) with the following accession number: MTAB-9836.

**Genomic DNA extraction, PCR and sequencing analysis.** Cells were lysed in Tri-reagent (MRC) and genomic DNA isolated according to the manufacturer’s instructions, using chloroform for the phase separation. DNA quality was assessed by spectrophotometry (Thermo Scientific Nanodrop 2000 microvolume spectrophotometer, RRID:SCR\_018042). PCR tests were performed (F: 5'-CCGTGCTAGATCAGGCTCTG-3'; R: 5'-TGGCCATGTGACTGGTTCTC-3') to amplify the region targeted by the guide RNAs, with a high-fidelity DNA polymerase Q5 (New England BioLabs) (amplicon size = 1360 bp for the WT). After migration on a 1.5% agarose gel, PCR products were extracted with DNA/RNA extraction/purification kit (SmartPure Gel kit, Eurogentec). After quality assessment, samples were sequenced by Sanger sequencing (Eurofins) using both forward and reverse primers. Sequencing results were analysed using FinchTV software.

**Protein extraction and western blotting.** Experiments were performed as previously described in Lhuillier et al.<sup>31</sup>. The following primary antibodies were used: polyclonal goat anti-mouse gal-1 (R&D Systems Cat# AF1245, RRID:AB\_354693), mouse anti-human/murine gal-3 clone B2C10 (Santa Cruz Biotechnology Cat# sc-32790, RRID:AB\_627657), polyclonal rabbit anti-human/murine gal-8 (#MBS828618, MyBioSource), rat anti-mouse galectin-9 clone 108A2 (BioLegend Cat# 137,901, RRID:AB\_10568691); mouse anti- $\beta$ -actin clone AC-74 (Sigma-Aldrich Cat# A2228, RRID:AB\_476697).

**Cell proliferation assay.** MB49 cells (WT and KO) were seeded in a 96-well plate at the rate of 2000 cells/well. The proliferation rate in 24 h was determined by measuring the ATP concentration in the wells at 24 and 48 h (ATPlite Luminescence Assay System, PerkinElmer).

**RNAseq analyses.** RNAseq analyses were performed in 2 distinct stages for in vitro cultured cells and tumor cells transplanted on syngeneic mice.

In vitro cultured cells were lysed in Tri-reagent (MRC) and total RNA isolated according to the manufacturer’s instructions, using chloroform for the phase separation. RNA quality was assessed by spectrophotometry (Thermo Scientific Nanodrop 2000 microvolume spectrophotometer, RRID:SCR\_018042). RNA sequencing and analysis were performed by IntegraGen (Evry, France). The raw data (bam files) are available on ArrayExpress under the following accession number: E-MTAB-9570. The quality of reads was assessed for each sample using FastQC. Fastq files were aligned to the reference Mouse genome mm10 with STAR (STAR, RRID:SCR\_015899). Reads mapping to multiple locations were removed. Gene expression was quantified using the full Gencode vM18 annotation. STAR was also used to obtain the number of reads associated to each gene in the Gencode (GENCODE, RRID:SCR\_014966) vM18 database (restricted to protein-coding genes, antisense and lincRNAs). Bioconductor DESeq package was used to generate the count matrix. After normalizing for library size, the count matrix was normalized by the coding length of genes to compute FPKM scores (number of fragments per kilobase of exon model and millions of mapped reads) (internal IntegraGen document and Anders et al. and Wang et al.<sup>32,33</sup>).

When dealing with tumors carried by syngeneic mice, RNA was extracted from frozen tumor fragments (30 mg) using the RNeasy kit (Qiagen) according to the manufacturer’s instructions. During the cell lysis step, tumor fragments were crushed with TissueRuptor (Qiagen) in RLT buffer supplemented with 40 mM dithiothreitol (DTT). RNA concentration and quality were assessed with a Bioanalyzer instrument (Agilent). RNA sequencing and analysis were performed by Novogene (Cambridge, UK). The raw data (bam files) are available

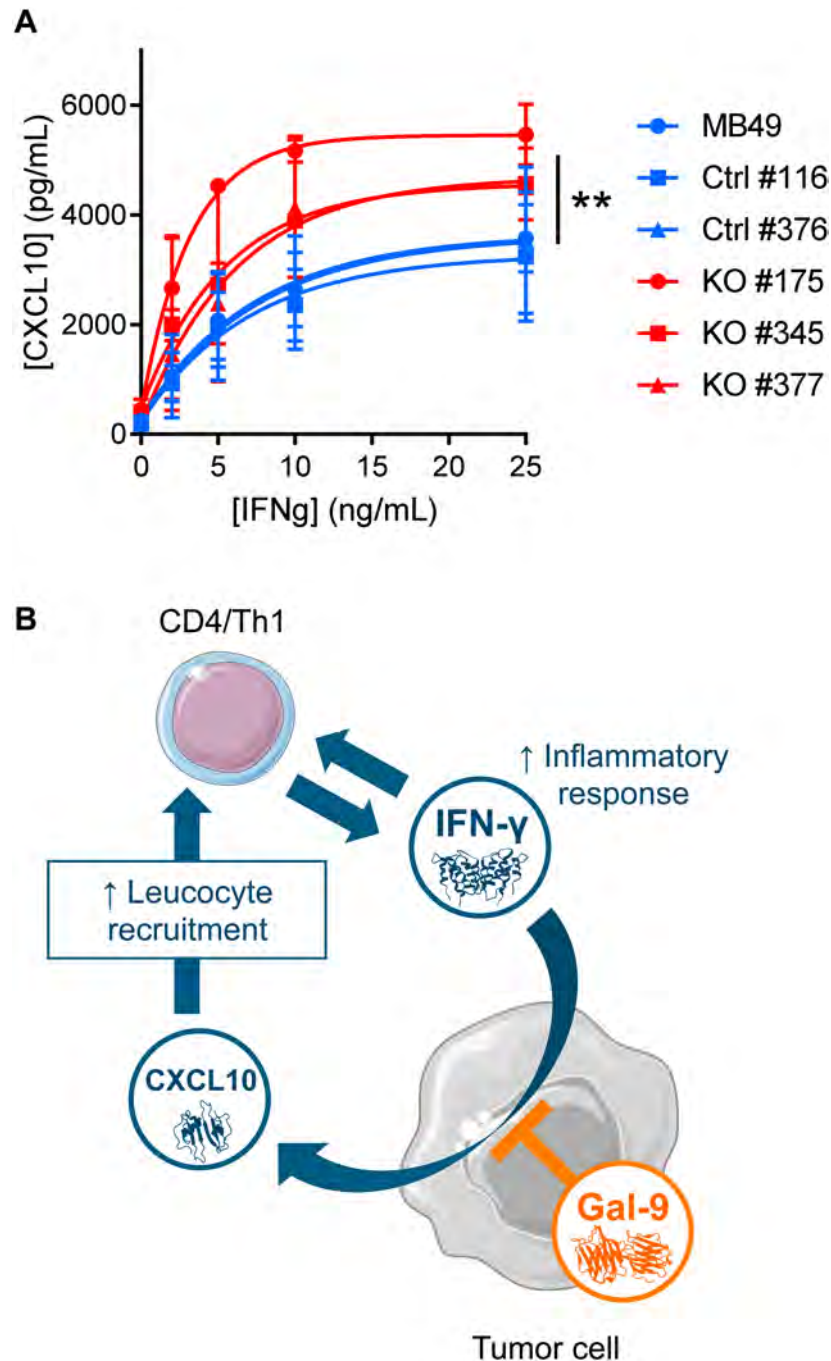


**Figure 7.** Gal-9 expressed by malignant epithelial cells inhibits CXCL10 induction resulting from stimulation by interferon- $\gamma$ . (A) Comparative assessment of CXCL10 production by gal-9-KO and WT MB49 cells stimulated *in vitro* by recombinant interferon- $\gamma$ . Conditioned media were collected after 72 h of stimulation with increasing concentrations of interferon- $\gamma$  and subjected to CXCL10 ELISA assay. At 25 ng/mL of interferon- $\gamma$  there was a significant difference of CXCL10 concentration in the medium between KO [KO#175 (n=2); KO#345 (n=2); KO#377 (n=2)] and WT cells [MB49 (n=2); Ctrl#116 (n=2); Ctrl#376 (n=2)] (Mann-Whitney test). (B) Proposed model of gal-9 attenuation of the amplification loop involving interferon- $\gamma$  and CXCL10. We assume that in the tumor microenvironment *in vivo*, interferon- $\gamma$  released by activated T-cells stimulates the production of CXCL10 by MB49 cells. In turn, CXCL10 stimulates T-cell infiltration, therefore boosting the anti-tumor immune response. However, the expression of gal-9 by malignant cells reduces their sensitivity to interferon- $\gamma$  therefore slowing down the amplification loop finally making the immune response weaker. So far, we do not know whether this inhibition is due to intra-cellular gal-9, gal-9 bound to the cell-surface and/or gal-9 released in the extra-cellular medium. Therefore, in our cartoon, the symbol of gal-9 is positioned with partial overlap of the intra-cellular structures, plasma membrane and extracellular medium.

on ArrayExpress under the following accession number: E-MTAB-9220. Sequencing libraries were generated using the NEBNext Ultra RNA Library Prep Kit for Illumina (NEB, USA). Index-coding was done by ligation of sequencing adaptors. Following PCR enrichment, index-coded samples were clustered using a cBot Cluster Generation System with the PE Cluster Kit cBot-HS (Illumina). Then libraries were sequenced on an Illumina platform and paired-end reads were generated. Raw data of FASTQ format were first filtered to remove reads with adaptor contamination and reads with low quality. The Q20, Q30 and GC content of the clean data were calculated. Downstream analyses were based on the paired-end clean reads which were aligned to the reference genome using the STAR software (*Mus musculus* GRCm38). The HTSeq software (HTSeq, RRID:SCR\_005514) was used to count the read numbers mapped of each gene. Then FPKM (Fragments Per Kilobase of transcript sequence per Million base pairs sequence) was calculated for each gene; it takes in account gene lengths in addition to mapped reads counts.

Differential expression was performed on raw counts of RNAseq, by applying the DESeq2<sup>25</sup> package, version 1.26.0, combined with the RUVseq (RUVSeq, RRID:SCR\_006263) package<sup>34</sup>, version 1.20.0 (both in R language). We identified genes with absolute value of fold change > 2 and FDR adjusted p value of F test < 0.05 as differentially expressed (DE). Heatmaps of DE genes were generated with Pheatmap (pheatmap, RRID:SCR\_016418) R package, version 1.0.12, after a transformation of raw counts using the function of variance stabilizing transformation of DESeq2.

Gene ontology was explored using the Bioconductor ClusterProfiler package<sup>26</sup> version 3.14.3, with DE genes identified from DESeq2 analysis. Over-representation and gene set enrichment analysis were done against MSigDb (Molecular Signatures Database, RRID:SCR\_016863) gene sets, which were loaded through the MSigDb package version 7.1.1, and genome wide annotation for Mouse, sourced from org.Mm.eg.db package version 3.10.0 (available at [www.bioconductor.org](http://www.bioconductor.org)). Enrichment analyses were later visualized by enrichplot (R package, version 1.6.1) ([www.bioconductor.org](http://www.bioconductor.org)).

**M-RNA quantification by RT-qPCR.** Following total RNA extraction, reverse transcription was made using the “High capacity cDNA reverse transcription kit” (#4368814, LifeTechnologies), q-PCR was done using TaqMan Real-Time PCR assays from Thermo Scientific according to the manufacturer instructions. Four house-keeping genes were used for normalization (*GUSB*, *GAPDH*, *PPIA*, *RPLP0*).

**Animal care and tumor growth assays.** Animal procedures were performed according to protocols approved by the Ethics Committee for animal experimentation n°26 certified by the French ministry of agriculture (“Comité d’Ethique en Expérimentation Animale n°26”) (project number n°20171108124492). Female C57BL/6 N were purchased from Janvier Labs (France) and housed in the Gustave Roussy animal facility. Mice were used between 8 and 12 weeks of age. Overall, 200 mice were used for this study. Animal care was done as previously described<sup>35</sup>: mice were housed in pathogen-free conditions in filter cap cages holding a maximum of 5 animals with irradiated aspen chip bedding and cotton fiber nesting material. They were maintained on a 12/12 light/dark cycle, with ad libitum UV-treated water and RM1 rodent diet. The animals were monitored every day for signs of pain, such as immobility or restlessness, reduction of drinking and food intake. The persistence of abnormal behaviors for more than one day led to the euthanasia of animals with suffering presumption. Prior to tumor collection, mice were sacrificed by cervical elongation. Otherwise, mice were euthanized by carbon dioxide asphyxiation. Body weight and tumor volume of all mice were measured at least twice a week. In any event, the animals were euthanized, when their tumor size had reached the limit of 1.7 cm<sup>3</sup>. Before and during tumor transplantations, mice were anesthetized with a 2L/min continuous flow of 2% isoflurane/oxygen mixture, using a rodent anesthesia work station (Anesteo, France). For initial tumor inoculation, in vitro expanded cells were injected subcutaneously (5.10<sup>5</sup> cells suspended in 100 µL of PBS). After 10 to 20 days of sub-cutaneous growth and mouse euthanasia, tumors were collected, weighted and cut in small fragments (70 or 100 mg) which were then subcutaneously engrafted on recipient mice. Tumor dimensions were measured every day using a digital caliper, starting from day 4 or 5 post-graft, and volumes were calculated based on the formula: width<sup>2</sup> × length/2. In addition, tumors collected at the time of sacrifice were weighed. A part of them was fixed in 4% paraformaldehyde in order to carry out IHC and/or RNAscope analysis, and the rest was frozen for RNA/protein extractions. Overall, our animal studies were conducted according to the ARRIVE guidelines (Animal Research: Reporting of In Vivo Experiments). Particularly, physical randomization of recipient mice based on ear tag numbers was done prior to tumor transplantation. Partial blinding was applied to outcome assessment: tumor measurements were made in a random order by a person not aware of the tumor status (gal-9-KO or wild-type). Statistical methods are described in a later part of the Material and methods section and in the figure legends.

Statement: As the corresponding author, on behalf of all authors, Dr Pierre Busson certifies that all experiments performed on mice were done according to the relevant guidelines and regulations of the French ministry of agriculture with the assistance and under the supervision of the Gustave Roussy committee for animal welfare.

**Histology and immunohistochemistry.** After fixation of tumors in 4% PFA, paraffin-embedded tumors were cut into 4 µm thick sections. At least one section per tumor was stained with hematoxylin–eosin–safranin (HES) for quality control. For Ki-67 and CD8 detection, slides were incubated with rabbit monoclonal antibodies specific of Ki-67 (1:500) (Cell Signaling Technology Cat# 12202, RRID:AB\_2620142) and CD8 (1:200) (Cell Signaling Technology Cat# 98941, RRID:AB\_2756376). Primary antibody binding was revealed with the Rabbit PowerVision Kit (UltraVision Technologies) and the DAB PowerVision kit (ImmunoVisionTechnologies Co.). For detection of CD45 and CD4, slides were incubated with rat monoclonal antibodies specific of CD45 (#10051.05, 1:100, Histopathology) and CD4 (1:100) (Thermo Scientific Cat# MA1-146, RRID:AB\_2536856).

Primary antibody binding was revealed with Polink 2 plus rat HRP kit (GBI Labs). All antibody applications were performed with a Bond RX automated Leica Slide Stainer. Image acquisition was performed with a Virtual Slide microscope VS120-SL (Olympus, Tokyo, Japan), 20X air objective (0.75 NA, 345 nm/pixel). Quantification of immunostaining was done using the Definiens Tissue Studio software (Definiens AG, Munich, Germany). For all markers, staining densities were expressed as a number of stained cells—equivalent to stained nuclei—per mm<sup>2</sup> of analyzed tissue. For Ki-67 which is concentrated in the nuclei, we used an algorithm performing automatic detection of nuclei stained with DAB according to their spectral properties. Positive and negative nuclei were counted in a manually selected Region of Interest (ROI) (excluding areas of necrosis, preparation artifacts, etc.). For CD45<sup>+</sup>, CD4<sup>+</sup> and CD8<sup>+</sup> staining, positive cells were detected using another algorithm performing detection of stained “objects” with a high probability of being single cells.

**In situ hybridization of mRNAs in tissue sections.** The detection of mRNAs in tumor sections was made by in situ hybridization using the RNAscope technology (ACD and Biotechne). Fixed (4% PFA) and paraffin-embedded tumors were cut into 5 +/− 1 μm sections using a microtome. The paraffin ribbons were mounted on Superfrost Plus slides and deparaffinized before starting the RNAscope workflow. This was performed following the manufacturer’s instructions. Gal-9 mRNA probe was specifically designed by BioTechne’s team and we validated it on our samples making parallel staining with a positive (Mm-Ppib) and negative control (DapB) probe. Probes for CXCL9 and CXCL10 were catalog probes. After the signal detection step, slides were counterstained with 50% hematoxylin staining solution and dehydrated with 70% ethanol. After mounting slides, images were acquired with a Virtual Slide microscope VS120-SL (Olympus, Tokyo, Japan), 20X air objective (0.75 NA, 345 nm/pixel).

**Deep profiling of the expressed TCR beta repertoire.** RNAs extracted from tumor fragments (as explained above) were used to profile the TCR beta repertoire of tumor lymphocytes. Wet lab and bioinformatics analyses were performed by iRepertoire Inc. (Alabama, USA). Sequencing libraries were generated using their proprietary “dimer avoiding multiplex” (dam)-PCR technology which uses iterative rounds of amplification and amplicon recovery to selectively amplify the TCR beta chains (all possible murine VDJ combinations in one single reaction). Libraries were then sequenced on an Illumina MiSeq platform and paired-end reads were generated. Data analysis and “tree map” illustrations were performed by iRepertoire Inc.

**Cytokines profiling.** Protein extraction was performed from 30 mg of frozen tumor fragments by crushing them with TissueRuptor (Qiagen) in low detergent lysis buffer (20 mM Tris-HCl pH 7.5, 0.5% tween20, 150 mM NaCl) supplemented with the cOmplete Protease Inhibitor Cocktail (Roche Applied Science). Extracts were then clarified and protein concentrations were determined by the Bradford method using protein assay (Bio-Rad) and a microplate reader (Tecan Infinity F200 Pro). Undiluted samples from 1.23 to 5.38 mg/mL were used to perform the mouse cytokine array/chemokine array 31-Plex (MD31, Evetechnologies) (Eotaxin, G-CSF, GM-CSF, IFN-γ, IL-1α, IL-1β, IL-2, IL-3, IL-4, IL-5, IL-6, IL-7, IL-9, IL-10, IL-12 (p40), IL-12 (p70), IL-13, IL-15, IL-17A, IP-10, KC, LIF, MCP-1, M-CSF, MIG, MIP-1α, MIP-1β, MIP-2, RANTES, TNFα, VEGF). The cytokine concentrations were then normalized to protein concentrations.

**CXCL10 ELISA assay.** WT (MB49, Ctrl # 116 and 376) and KO (KO # 175, 345 and 377) cells were cultured in normal media supplemented or not with recombinant murine IFN-γ (#315-05, PeproTech): 0, 2, 5, 10 and 25 ng/mL. After 72 h of IFN-γ treatment, supernatants were collected and secreted CXCL10 was assayed with mouse CXCL10 ELISA kit (#DY466-05, #DY008, R&D Systems) according to the manufacturer’s instructions.

**Statistical analysis.** Except for RNAseq data, statistical tests were performed using GraphPad Prism version 7.00 (GraphPad Prism, RRID:SCR\_002798). Kaplan–Meier survival curves were generated and analyzed using the log-rank, Mantel-cox test. Significant differences when comparing two groups were determined by two-tails Mann–Whitney test. Significant differences when comparing three groups were determined by Krustal–Wallis test followed by Dunn’s multiple comparisons test. *P* value < 0.05 was considered as significant.

Received: 24 September 2020; Accepted: 15 February 2021

Published online: 04 March 2021

## References

- Johannes, L., Jacob, R. & Leffler, H. Galectins at a glance. *J. Cell Sci.* **131**(9), jcs208884 (2018).
- John, S. & Mishra, R. Galectin-9: from cell biology to complex disease dynamics. *J. Biosci.* **41**(3), 507–534 (2016).
- Daley, D. *et al.* Dectin 1 activation on macrophages by galectin 9 promotes pancreatic carcinoma and peritumoral immune tolerance. *Nat. Med.* **23**(5), 556–567 (2017).
- Zhu, C. *et al.* The Tim-3 ligand galectin-9 negatively regulates T helper type 1 immunity. *Nat Immunol.* **6**(12), 1245–1252 (2005).
- Klibi, J. *et al.* Blood diffusion and Th1-suppressive effects of galectin-9-containing exosomes released by Epstein–Barr virus-infected nasopharyngeal carcinoma cells. *Blood* **113**(9), 1957–1966 (2009).
- Enninga, E. A. L., Nevala, W. K., Holtan, S. G., Leontovich, A. A. & Markovic, S. N. Galectin-9 modulates immunity by promoting Th2/M2 differentiation and impacts survival in patients with metastatic melanoma. *Melanoma Res.* **26** (5), 429–441 (2016).
- Enninga, E. A. L. *et al.* CD206-positive myeloid cells bind galectin-9 and promote a tumor-supportive microenvironment: galectin-9/CD206 binding. *J. Pathol.* **245**(4), 468–477 (2018).

8. Gonçalves Silva, I. *et al.* The Tim-3-galectin-9 secretory pathway is involved in the immune escape of human acute myeloid leukemia cells. *EBioMedicine*. **22**, 44–57 (2017).
9. Ohue, Y. *et al.* Survival of lung adenocarcinoma patients predicted from expression of PD-L1, galectin-9, and XAGE1 (GAGED2a) on tumor cells and tumor-infiltrating T cells. *Cancer Immunol. Res.* **4**(12), 1049–1060 (2016).
10. Anderson, A. C. *et al.* Promotion of tissue inflammation by the immune receptor Tim-3 expressed on innate immune cells. *Science* **318**(5853), 1141–1143 (2007).
11. Golden-Mason, L. *et al.* Galectin-9 functionally impairs natural killer cells in humans and mice. *J. Virol.* **87**(9), 4835–4845 (2013).
12. Dardalhon, V. *et al.* Tim-3/galectin-9 pathway: regulation of Th1 immunity through promotion of CD11b<sup>+</sup> Ly-6G<sup>+</sup> myeloid cells. *J. Immunol.* **185**(3), 1383–1392 (2010).
13. Zhang, C.-X. *et al.* Galectin-9 promotes a suppressive microenvironment in human cancer by enhancing STING degradation. *Oncogenesis*. **9**(7), 65 (2020).
14. Zhou, Q. *et al.* Coexpression of Tim-3 and PD-1 identifies a CD8<sup>+</sup> T-cell exhaustion phenotype in mice with disseminated acute myelogenous leukemia. *Blood* **117**(17), 4501–4510 (2011).
15. Oomizu, S. *et al.* Galectin-9 suppresses Th17 cell development in an IL-2-dependent but Tim-3-independent manner. *Clin. Immunol.* **143**(1), 51–58 (2012).
16. Wu, C. *et al.* Galectin-9-CD44 interaction enhances stability and function of adaptive regulatory T cells. *Immunity* **41**(2), 270–282 (2014).
17. Oomizu, S., Arikawa, T., Niki, T., Kadowaki, T., Ueno, M., Nishi, N. *et al.* Cell surface galectin-9 expressing Th cells regulate Th17 and Foxp3<sup>+</sup> Treg development by galectin-9 secretion. *PLoS One* **7** (11), e48574 (2012).
18. Irie, A. Galectin-9 as a prognostic factor with antimetastatic potential in breast cancer. *Clin. Cancer Res.* **11**(8), 2962–2968 (2005).
19. Fu, H. *et al.* Galectin-9 predicts postoperative recurrence and survival of patients with clear-cell renal cell carcinoma. *Tumor Biol.* **36**(8), 5791–5799 (2015).
20. Tavares, L. B. *et al.* Patients with pancreatic ductal adenocarcinoma have high serum galectin-9 levels: a sweet molecule to keep an eye on. *Pancreas* **47**(9), e59–e60 (2018).
21. Daley, D. *et al.*  $\gamma\delta$  T cells support pancreatic oncogenesis by restraining  $\alpha\beta$  T cell activation. *Cell* **166**(6), 1485–1499.e15 (2016).
22. El Behi, M. *et al.* An essential role for decorin in bladder cancer invasiveness. *EMBO Mol. Med.* **5**(12), 1835–1851 (2013).
23. Melchionda, F. *et al.* Adjuvant IL-7 or IL-15 overcomes immunodominance and improves survival of the CD8<sup>+</sup> memory cell pool. *J. Clin. Invest.* **115**(5), 1177–1187 (2005).
24. Perez-Diez, A. *et al.* CD4 cells can be more efficient at tumor rejection than CD8 cells. *Blood* **109**(12), 5346–5354 (2007).
25. Love, M. I., Huber, W. & Anders, S. Moderated estimation of fold change and dispersion for RNA-seq data with DESeq2. *Genome Biol.* **15**(12), 550 (2014).
26. Yu, G., Wang, L. -G., Han, Y., He, Q. -Y. clusterProfiler: an R package for comparing biological themes among gene clusters. *OMICS J. Integr. Biol.* **16** (5), 284–287 (2012).
27. Dangaj, D., Bruand, M., Grimm, A. J., Ronet, C., Barras, D., Duttagupta, P. A. *et al.* Cooperation between constitutive and inducible chemokines enables T cell engraftment and immune attack in solid tumors. *Cancer Cell.* **35** (6), 885–900.e10 (2019).
28. Ganuza, M. *et al.* The global clonal complexity of the murine blood system declines throughout life and after serial transplantation. *Blood* **133**(18), 1927–1942 (2019).
29. Wegner, C. S. *et al.* Increasing aggressiveness of patient-derived xenograft models of cervix carcinoma during serial transplantation. *Oncotarget.* **9**(30), 21036–21051 (2018).
30. Haeussler, M. *et al.* Evaluation of off-target and on-target scoring algorithms and integration into the guide RNA selection tool CRISPOR. *Genome Biol.* **17**(1), 148 (2016).
31. Lhuillier, C. *et al.* Impact of exogenous galectin-9 on human T cells: contribution of the T cell receptor complex to antigen-independent activation but not to apoptosis induction. *J Biol Chem.* **290**(27), 16797–16811 (2015).
32. Anders, S. & Huber, W. Differential expression analysis for sequence count data. *Genome Biol.* **11**(10), R106 (2010).
33. Wang, L., Wang, S. & Li, W. RSeQC: quality control of RNA-seq experiments. *Bioinformatics* **28**(16), 2184–2185 (2012).
34. Risso, D., Ngai, J., Speed, T. P. & Dudoit, S. Normalization of RNA-seq data using factor analysis of control genes or samples. *Nat. Biotechnol.* **32**(9), 896–902 (2014).
35. Lhuillier, C. *et al.* Characterization of neutralizing antibodies reacting with the 213–224 amino-acid segment of human galectin-9. *PLoS ONE* **13**(9), e0202512 (2018).

## Acknowledgements

This work was supported by the Bristol-Myers-Squibb Foundation for Research on Immuno-Oncology (Grant Number: 1709-04-040) and the French Institut National du Cancer (INCa, Grant No. 2017-031). VB was the recipient of a fellowship from the French Ministry of Research. We thank Lionel Apetoh, Nikiforos Kapetanakis and Aurélien Marabelle for helpful discussions.

## Author contributions

V.B.: conceptualization, investigation, preparation of the original draft manuscript; J.R.: resources, investigation; T.B.T.T.: formal analysis; A.G.: resources, investigation, administration; O.B.: investigation, visualization; N.S.: visualization; M.K.D.: formal analysis; P.D.: formal analysis; S.B.: conceptualization, funding acquisition; M.D.: conceptualization, review and editing; P.B.: conceptualization, funding acquisition, supervision, preparation of the original draft manuscript.

## Competing interests

PB, MD, AG and VB are members of a collaborative project about monoclonal antibodies neutralizing extracellular galectin-9. This project involves P. Busson's team and HiFiBiO-Therapeutics. Otherwise, the authors declare no potential conflicts of interest.

## Additional information

**Supplementary Information** The online version contains supplementary material available at <https://doi.org/10.1038/s41598-021-84270-1>.

**Correspondence** and requests for materials should be addressed to P.B.

**Reprints and permissions information** is available at [www.nature.com/reprints](http://www.nature.com/reprints).

**Publisher's note** Springer Nature remains neutral with regard to jurisdictional claims in published maps and institutional affiliations.



**Open Access** This article is licensed under a Creative Commons Attribution 4.0 International License, which permits use, sharing, adaptation, distribution and reproduction in any medium or format, as long as you give appropriate credit to the original author(s) and the source, provide a link to the Creative Commons licence, and indicate if changes were made. The images or other third party material in this article are included in the article's Creative Commons licence, unless indicated otherwise in a credit line to the material. If material is not included in the article's Creative Commons licence and your intended use is not permitted by statutory regulation or exceeds the permitted use, you will need to obtain permission directly from the copyright holder. To view a copy of this licence, visit <http://creativecommons.org/licenses/by/4.0/>.

© The Author(s) 2021

## Résumé

---

### **Caractéristiques immunomodulatrices de la galectine-9: études expérimentales et translationnelles**

Les galectines sont des lectines animales capables d'interagir avec des polysaccharides comportant des liaisons  $\beta$ 1-3 ou  $\beta$ 1-4 galactosides. Certaines galectines, notamment la galectine-9 (gal-9) peuvent être libérées dans le milieu extracellulaire où elles se comportent comme des cytokines en se liant à des protéines partenaires à la surface des cellules cibles. Tim-3 et Dectine-1 font partie des récepteurs membranaires de la gal-9 extra-cellulaire. Globalement les effets immunomodulateurs de la gal-9 qui sont très variés vont plutôt dans le sens de l'immunosuppression. Elle exerce un effet inhibiteur sur la plupart des cellules de l'immunité adaptative notamment les T CD8<sup>+</sup> et d'autre part elle favorise une polarisation M2 des macrophages. La gal-9 est souvent impliquée dans les résistances primaires ou secondaires aux agents de l'immunothérapie classique.

L'axe principal de ma thèse concernait la caractérisation des cellules T qui possèdent une résistance à l'effet apoptotique induit par la galectine-9. Une étude précédente dans notre équipe, qui a été réalisée par Claire Lhuillier, a montré que sur les cellules Jurkat ainsi que sur les cellules T isolées, galectine-9 provoquait deux effets en parallèles. Alors qu'une grande partie de la population (jusqu'à 80%) subissait l'apoptose sous l'effet de la galectine-9 extracellulaire, il se passait aussi une libération de calcium dans le cytoplasme des cellules Jurkat. Cette mobilisation était annulée dans les lignées Jurkat ayant les défauts dans les gènes de TCR $\beta$ , CD3 $\zeta$ , ou Lck qui touchaient directement l'intégralité de la signalisation TCR. Cependant, le flux de calcium revenait quand l'expression de TCR $\beta$ , CD3 $\zeta$ , ou Lck était rétablie dans ces lignées mutantes, ce qui montre que la galectine-9 stimule les cellules Jurkat par la voie de signalisation TCR. Les effets identiques ont été obtenus sur les cellules T isolées des PBMCs. Pour ces raisons, notre équipe s'intéresse

aux cellules qui sont sujettes à la stimulation par TCR et qui survivent au traitement par la galectine-9 extracellulaires.

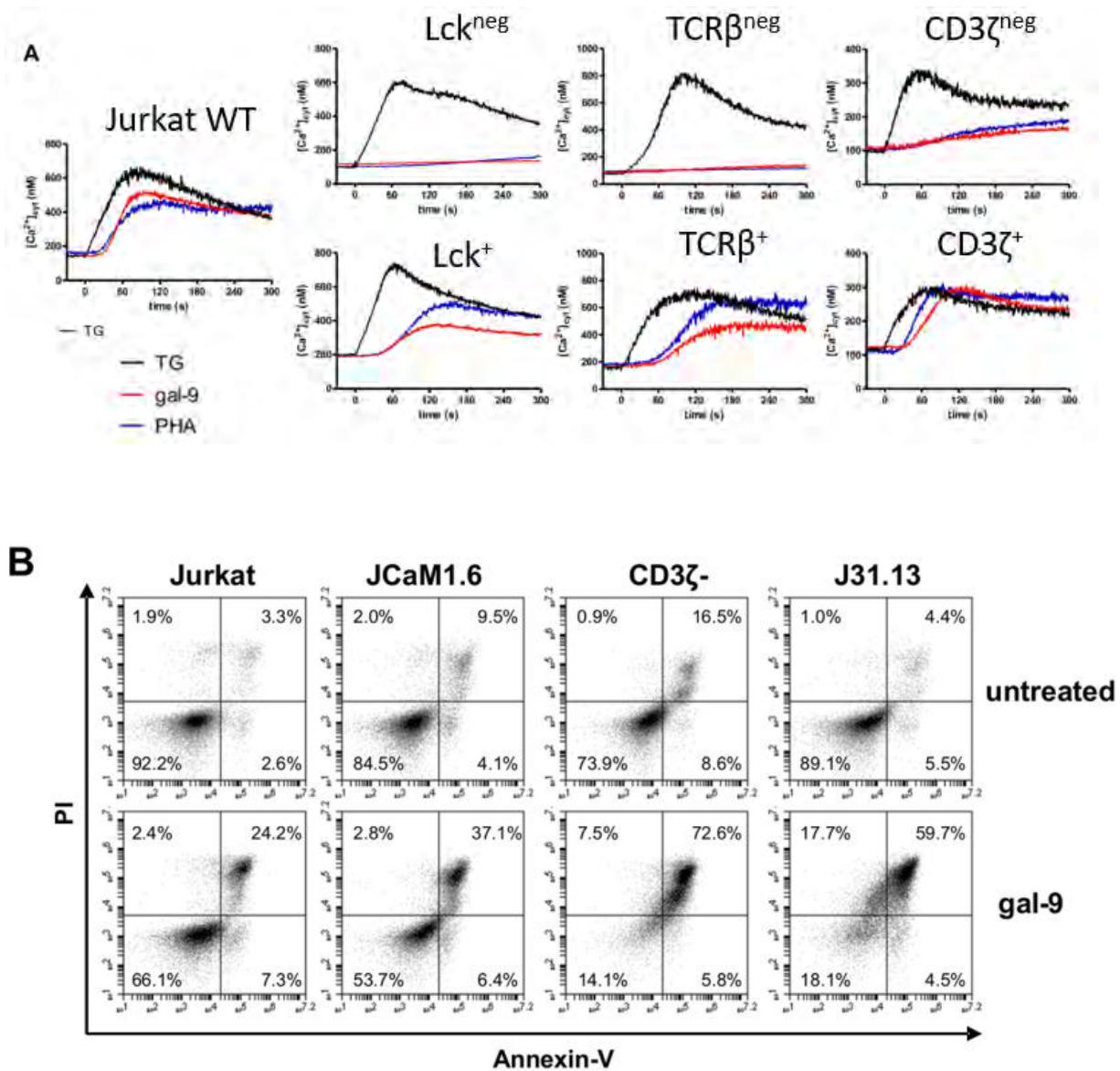


Fig. 22 **La galectine-9 provoque 2 effets en parallèle.** A) Dans la lignée sauvage de Jurkat, la gal-9 stimule un flux de calcium dans le cytoplasme, ce qui est abrogé dans les lignées mutantes. B) Ce flux revient dans les lignées avec Lck, TCRβ ou CD3ζ restauré.

Pour étudier cette question, j'ai établi un protocole expérimental où les PBMC récoltées des donneurs sains ont été cultivées en absence ou en présence de la galectine-9 à 45 nM, dans le milieu complété avec l'anti-CD3 et l'anti-CD28. Au bout de 7 jours, les cellules ont été passées



à une colonne magnétique qui permet d'isoler les cellules T dans la population. Ces lymphocytes T ont été caractérisées ensuite à plusieurs niveaux, pour explorer les modifications du phénotype des cellules T périphériques humaines. Celles exposées à la galectine-9 sont définies comme G9Expo-T cells et celles qui ne sont jamais exposées sont considérées comme G9Naive-T cells. Dans certaines étapes de caractérisation, une deuxième exposition à la galectine-9 a été effectuée sur chacun des types de cellules T (G9Expo et G9Naive) en parallèle avec la culture en milieu contrôlé. Cette exposition a donné comme résultat 4 types de cellules T : G9Expo-unstimulated (GEU), G9Expo-stimulated (GES), G9Naive-unstimulated (GNU) and G9Naive-stimulated (GNS).

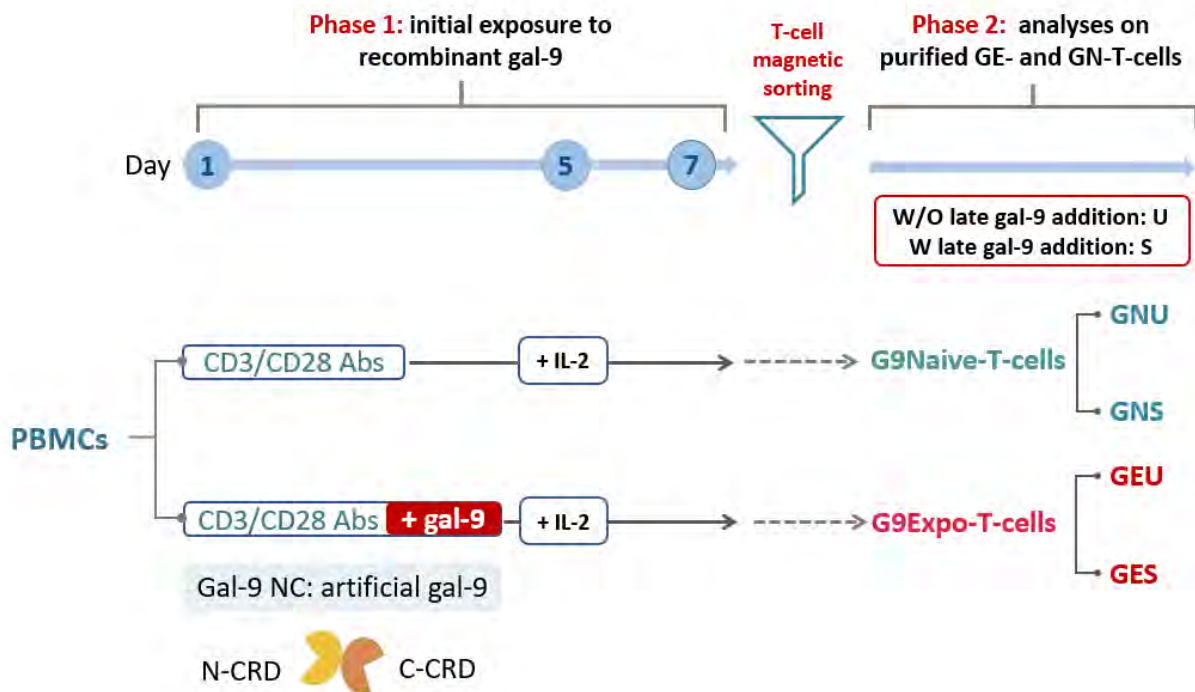


Fig. 23 **Schéma de la procédure expérimentale.** La galectine-9 utilisée dans cette étude se compose d'un N-terminal CRD (N-CRD) attaché directement à un C-terminal CRD, sans passer par le peptide linker. Cette gal-9 est une forme artificielle qui permet une meilleure stabilité que des formes naturelles et est appelée gal-9 NC due à sa structure. Dans certaines étapes de caractérisation, la gal-9 de l'isoforme M ayant une forme naturelle est utilisée.

Nous avons commencé la caractérisation par mesurer la capacité de prolifération des cellules T G9Naive et G9Expo et évaluer leur résistance à la galectine-9. Nous avons observé une nette prolifération dans le cas des cellules T G9Expo, démontrée par la dilution du marquage de prolifération Cell Trace et par l'incorporation de l'EdU, qui mesure la néosynthèse de l'ADN (5-éthynyl-2'-déoxyuridine), après 4 jours de culture supplémentaire à partir de l'isolation magnétique des cellules T. De l'autre côté, la résistance des cellules contre l'effet apoptotique de la galectine-9 a été évaluée par la mise en culture des cellules T isolées avec la gal-9. Le marquage

a été fait à 24 heures après l'exposition sur des cellules T qui n'avaient jamais été exposé à la gal-9 et celles qui avaient enduré 7 jours de traitement avec la gal-9. Dans le cas du traitement par la gal-9 NC ainsi que celui par la gal-9 M, les cellules T résistaient mieux à l'effet apoptotique quand elles avaient eu antérieurement une exposition à la gal-9. Ces résultats ont montré que les lymphocytes T G9Expo avaient un phénotype héritable et la plupart de cette population conservait la résistance à l'apoptose induite par la gal-9.

Au niveau transcriptomique, les cellules T G9Naive et G9Expo ont montrés des profils distincts. Par le séquençage d'ARN total sur les échantillons de 3 différents donneurs, j'ai obtenu une liste des gènes différentiellement exprimés qui ont séparé les cellules T G9Expo des cellules G9Naive; ces gènes ont été identifiés par DESeq2. Par contre, pour identifier un phénotype spécifique, une deuxième analyse a été faite sur une liste qui focalisait aux gènes typiques de chaque sous-population de lymphocytes T, notamment les gènes de lignée (par exemple CD4, CD8), de facteurs de transcriptions, récepteurs membranaires, et cytokines. Les échantillons de même type ont été bien regroupé selon leur modalité d'exposition à la galectin-9, ce qui a reconfirmé la distinction entre des cellules T G9Expo et G9Naive au niveau de leur transcriptome. En plus, grâce à cette liste de gène inspirée de l'étude de ..., nous avons identifié une augmentation des transcrits des gènes liés au phénotype de lymphocyte T folliculaire, notamment CXCR5, CD40L et IL-21, dans les lymphocytes T G9Expo. Ces résultats ont donné une indication qu'il y avait probablement une expansion de la sous-population de lymphocytes T folliculaires.

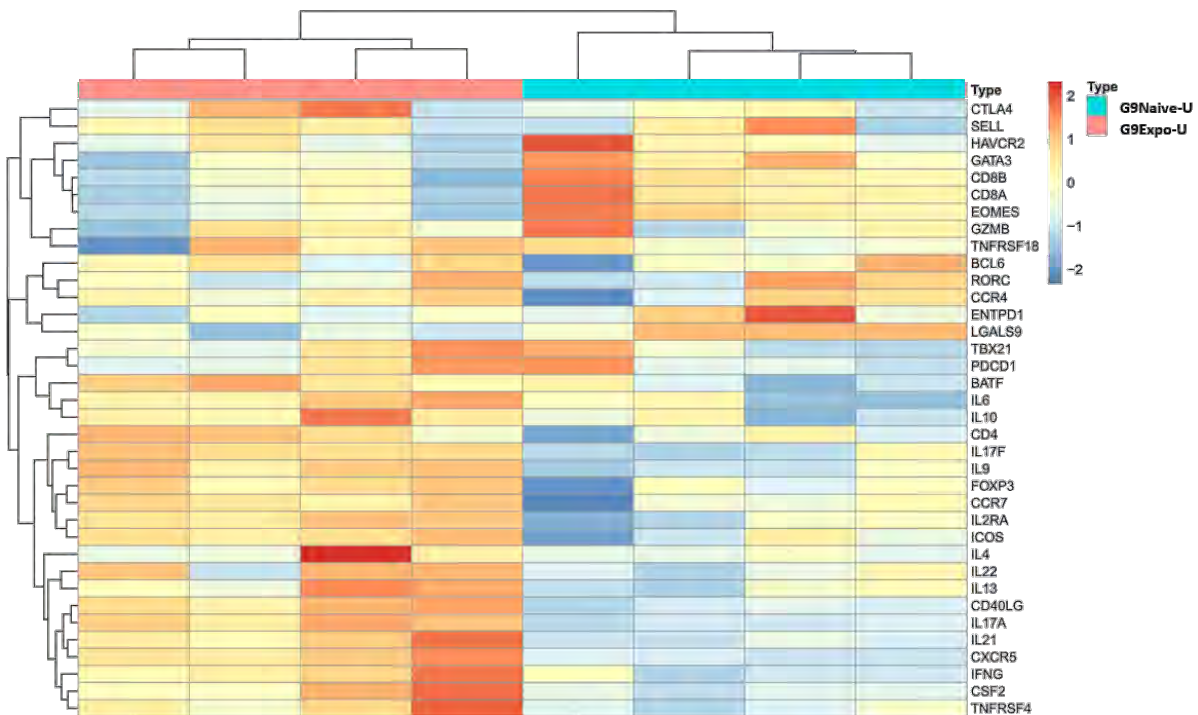


Fig. 24 **Regroupement des échantillons basé une liste de gène définie par la publication de Wong *et al.* (2015).** Cette liste focalise sur les gènes phénotypiques des sous-population de lymphocyte T.

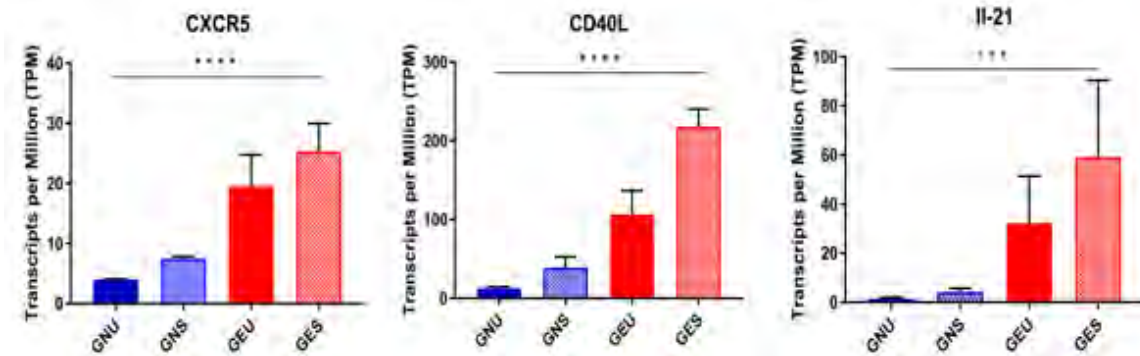


Fig. 25 **Analyse statistique de quelques gènes présents dans la liste à la figure 24**

Par la suite, j'ai vérifié cette accumulation au niveau protéique, en faisant une analyse de cytométrie de masse avec un panel de 21 marqueurs, y compris des facteurs de transcriptions et des protéines membranaires. Pour analyser l'expression des 21 marqueurs sur chaque cellule, il nécessite une réduction dimensionnelle, qui aide à représenter plusieurs dimensions sur une surface de 2 dimensions. Dans le cas de CyTOF, le profil de chaque cellule est représenté par un point sur une surface ; plus 2 cellules sont identiques, plus elles se retrouvent l'une à côté de l'autre sur un graphe qui s'appelle viSNE. L'expression de chaque marqueur est alors visualisée par un code couleur qui varie du bleu au rouge, le bleu étant une expression faible. En observant la variation de chaque cluster à travers des graphes viSNE, nous avons constaté un cluster apparaitre dans la population des lymphocytes T G9Expo, qui correspondait à une sous-population de T CD4, avec une expression plus forte de CXCR5, Bcl-6 et FoxP3. Certaines cellules dans ce cluster avaient en plus une forte expression de CD40L, ICOS, PD-1 et CCR4. Une étape de vérification par la cytométrie conventionnelle a été faite avec un panel composant de CD4, CXCR5, CD40L et FoxP3 sur les cellules de 3 donneurs. Comme attendu, l'expression de CXCR5, CD40L et FoxP3 étaient significativement plus forte dans les lymphocytes T G9Expo en termes de pourcentage de cellule positive et de la médiane de l'intensité fluorescente (MFI). Ces observations nous ont permis de confirmer l'induction d'expression de CXCR5 sur les lymphocytes T par l'exposition à la galectine-9.

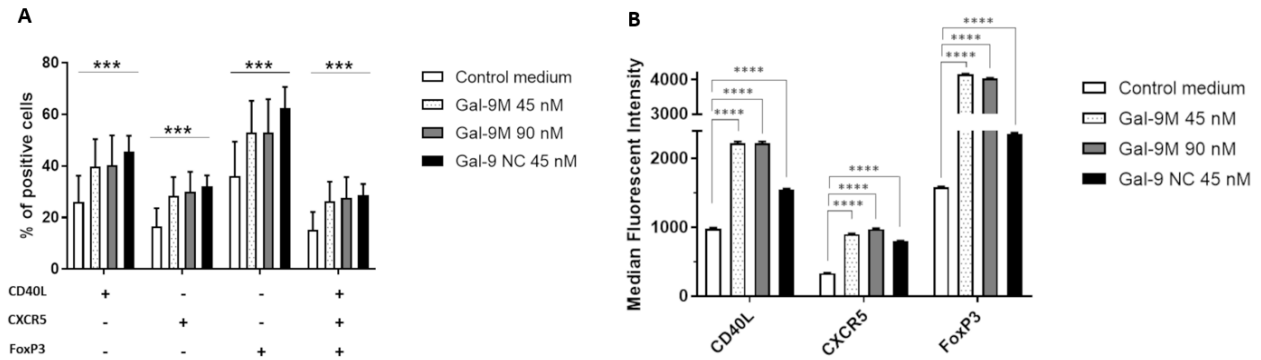


Fig. 26 **Analyse par cytométrie en flux sur l'expression de CXCR5, CD40 et FoxP3 des lymphocytes T traitées par la gal-9 NC ou la gal-9 M.** A) Pourcentage des cellules T CD4<sup>+</sup> qui expriment CXCR5, CD40L, FoxP3 ou co-expriment les 3 marqueurs. B) Médiane de l'intensité fluorescente mesurée dans chacune des populations.

Les dernières parties de cette étude consiste des observations *in vivo* et une première tentative de mettre en évidence la fonction de la population G9Expo. En examinant l'expression de CXCR5 et CD40L dans l'ensemble des splénocytes des souris sauvages et souris KO-gal-9, nous avons remarqué une baisse d'expression de CXCR5 en termes de pourcentage de positivité dans les souris KO-gal-9, par rapport aux sauvages. Quant au ligand de CD40, des sections histologiques ont montré aussi une expression plus abondante dans la rate sauvage, en particulier la zone périphérique des centres germinatifs. Dans le contexte physiologique normal, la galectine-9 se trouve plus abondante à la périphérie et à la zone sombre du centre germinatif. L'expression de CD40L observée dans ces sections histologiques ont mis en valeur le lien entre la production de la galectine-9 et l'expression de CD40L. Concernant la fonctionnalité de cellules T G9Expo, nous avons posé une hypothèse selon laquelle l'augmentation de CD40L induite par la galectine-9 pourrait protéger ou favoriser la survie des lymphocytes B en risque d'apoptose. Dans la première tentative, nous avons observé qu'il y avait moins de cellules B qui sont entrées en apoptose dans les co-culture avec des lymphos T G9Expos, dans un milieu avec ou sans galectine-9. Au regard de ces résultats, nous avons mis en avant une hypothèse que dans le contexte des structures lymphoïdes secondaires, la production en abondance de la galectin-9 par les lymphocytes B naïves effectuait une induction du phénotype folliculaire sur les lymphocytes T. Ces dernières expriment alors une augmentation de CXCR5 et du ligand de CD40, qui permet un sauvetage aux lymphocytes B en risque d'apoptose à travers l'interaction entre CD40 et son ligand sur les T folliculaires. Nous avons prévu d'améliorer des conditions d'étudier la fonction des lymphocytes T G9Expo en utilisant des cellules B autologues et les stimuler avec anti-IgM. Concernant les observations *in vivo*, nous voulons examiner les souris sauvages et KO-Gal-9 littermates pour

vérifier si nous pourrions retrouver les mêmes motifs d'expression de CXCR5 et du ligand de CD40. Ces résultats feront partie d'un article qui devrait arriver à maturité dans quelques mois.

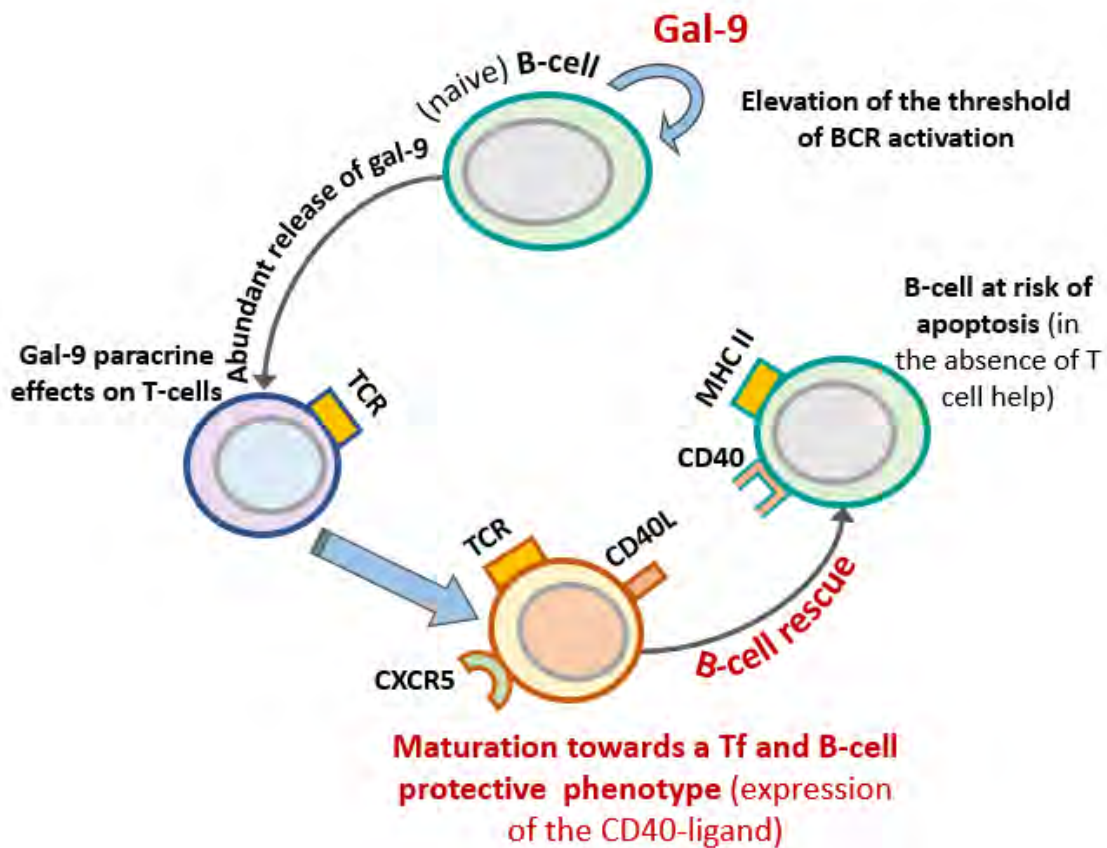


Fig. 27 **Modèle d'interaction entre lymphocytes B et T sous l'effet de la galectine-9, dans le contexte du microenvironnement des follicules secondaires.**

Le deuxième volet de ma thèse consiste à étudier le statut de la galectine-9 plasmatique dans les carcinomes épidermoïdes de la tête et du cou, dans le cadre du projet de recherche translationnelle TopNivo. Une série de 90 patients sont pris en charge pour des carcinomes des voies aérodigestives supérieures en rechute. En utilisant des systèmes d'ELISA, nous avons mis en évidence des concentrations plasmatiques de gal-9 plus élevées dans deux sous-groupes de patients : ceux dont la tumeur primitive dérivait de l'hypopharynx et ceux présentant plusieurs sites métastatiques. Les analyses plus approfondies sur la corrélation entre la galectine-9 et CXCL9, ou sur le profil métabolomique de ces patients sont prévues et feront partie d'un article en préparation.

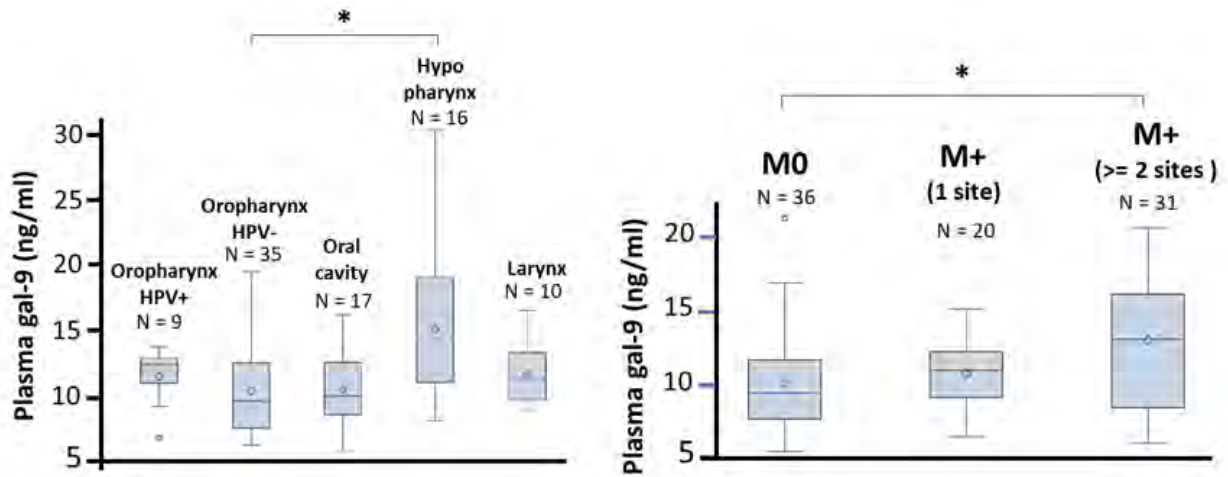


Fig. 28 **Distribution de la concentration de la galectine-9 plasmatique selon les sites de la tumeur primaire (à gauche) ou le nombre de sites métastatiques (à droite).**

## Bibliography

---

1. CRICK F. Central Dogma of Molecular Biology. *Nature*. 1970 Aug 1;227(5258):561–3.
2. Gabius H-J, Roth J. An introduction to the sugar code. *Histochem Cell Biol*. 2017 Feb 1;147(2):111–7.
3. Harry Schachter. Foreword. In: *The Sugar Code: Fundamentals of Glycosciences* | Wiley [Internet]. Wiley-Blackwell; 2009 [cited 2021 Mar 23]. Available from: <https://www.wiley.com/en-us/The+Sugar+Code%3A+Fundamentals+of+Glycosciences-p-9783527320899>
4. Hans-Joachim Gabius. *The Sugar Code: Fundamentals of Glycosciences* | Wiley [Internet]. Wiley-Blackwell; 2009 [cited 2021 Mar 23]. Available from: <https://www.wiley.com/en-us/The+Sugar+Code%3A+Fundamentals+of+Glycosciences-p-9783527320899>
5. Hans-Joachim Gabius. The Biochemical Basis and Coding Capacity of the Sugar Code. In: *The Sugar Code: Fundamentals of Glycosciences* | Wiley [Internet]. Wiley-Blackwell; 2009 [cited 2021 Mar 23]. Available from: <https://www.wiley.com/en-us/The+Sugar+Code%3A+Fundamentals+of+Glycosciences-p-9783527320899>
6. Hart GW. Glycosylation. *Curr Opin Cell Biol*. 1992 Dec 1;4(6):1017–23.
7. Cook GM. Glycobiology of the cell surface: the emergence of sugars as an important feature of the cell periphery. *Glycobiology*. 1995 Jul;5(5):449–58.
8. Seeberger PH. Monosaccharide Diversity. In: Varki A, Cummings RD, Esko JD, Stanley P, Hart GW, Aebi M, et al., editors. *Essentials of Glycobiology* [Internet]. 3rd ed. Cold Spring Harbor (NY): Cold Spring Harbor Laboratory Press; 2015 [cited 2021 Mar 23]. Available from: <http://www.ncbi.nlm.nih.gov/books/NBK453086/>
9. BeMiller JN. Occurrence and Significance. In: Fraser-Reid BO, Tatsuta K, Thiem J, editors. *Glycoscience: Chemistry and Chemical Biology I–III* [Internet]. Berlin, Heidelberg: Springer; 2001 [cited 2021 Mar 23]. p. 877–84. Available from: [https://doi.org/10.1007/978-3-642-56874-9\\_25](https://doi.org/10.1007/978-3-642-56874-9_25)
10. Varki A, Cummings RD, Aebi M, Packer NH, Seeberger PH, Esko JD, et al. Symbol Nomenclature for Graphical Representations of Glycans. *Glycobiology*. 2015 Dec;25(12):1323–4.
11. Neelamegham S, Aoki-Kinoshita K, Bolton E, Frank M, Lisacek F, Lütteke T, et al. Updates to the Symbol Nomenclature for Glycans guidelines. *Glycobiology*. 2019 Aug 20;29(9):620–4.
12. Suzuki T. Free Oligosaccharides (High Mannose-Type Free Glycans Found in Mammals and Yeast). In: Taniguchi N, Endo T, Hart GW, Seeberger PH, Wong C-H, editors.

Glycoscience: Biology and Medicine [Internet]. Tokyo: Springer Japan; 2015. p. 907–11. Available from: [https://doi.org/10.1007/978-4-431-54841-6\\_155](https://doi.org/10.1007/978-4-431-54841-6_155)

13. Harada Y, Buser R, Ngwa EM, Hirayama H, Aebi M, Suzuki T. Eukaryotic Oligosaccharyltransferase Generates Free Oligosaccharides during N-Glycosylation. *J Biol Chem*. 2013 Nov 8;288(45):32673–84.
14. Chantret I, Moore SEH. Free oligosaccharide regulation during mammalian protein N-glycosylation. *Glycobiology*. 2008 Mar 1;18(3):210–24.
15. Yanagida K, Natsuka S, Hase S. Structural diversity of cytosolic free oligosaccharides in the human hepatoma cell line, HepG2. *Glycobiology*. 2006 Apr 1;16(4):294–304.
16. Verbert A, Cacan R. Cell Surface Glycoconjugates. In: eLS [Internet]. American Cancer Society; 2001 [cited 2021 Mar 23]. Available from: <https://onlinelibrary.wiley.com/doi/abs/10.1038/npg.els.0000707>
17. Spiro RG. Protein glycosylation: nature, distribution, enzymatic formation, and disease implications of glycopeptide bonds. *Glycobiology*. 2002 Apr 1;12(4):43R–56R.
18. Gagneux P, Varki A. Evolutionary considerations in relating oligosaccharide diversity to biological function. *Glycobiology*. 1999 Aug;9(8):747–55.
19. Reily C, Stewart TJ, Renfrow MB, Novak J. Glycosylation in health and disease. *Nat Rev Nephrol*. 2019 Jun;15(6):346–66.
20. Stanley P, Taniguchi N, Aebi M. N-Glycans. In: Varki A, Cummings RD, Esko JD, Stanley P, Hart GW, Aebi M, et al., editors. *Essentials of Glycobiology* [Internet]. 3rd ed. Cold Spring Harbor (NY): Cold Spring Harbor Laboratory Press; 2015 [cited 2021 Mar 23]. Available from: <http://www.ncbi.nlm.nih.gov/books/NBK453020/>
21. Reily C, Stewart TJ, Renfrow MB, Novak J. Glycosylation in health and disease. *Nat Rev Nephrol*. 2019 Jun 1;15(6):346–66.
22. Varki A, Cummings R, Esko J, Freeze H, Hart G, Marth J. O-Glycans [Internet]. *Essentials of Glycobiology*. Cold Spring Harbor Laboratory Press; 1999 [cited 2021 Mar 23]. Available from: <https://www.ncbi.nlm.nih.gov/books/NBK20721/>
23. Zachara N, Akimoto Y, Hart GW. The O-GlcNAc Modification. In: Varki A, Cummings RD, Esko JD, Stanley P, Hart GW, Aebi M, et al., editors. *Essentials of Glycobiology* [Internet]. 3rd ed. Cold Spring Harbor (NY): Cold Spring Harbor Laboratory Press; 2015 [cited 2021 Mar 23]. Available from: <http://www.ncbi.nlm.nih.gov/books/NBK453063/>
24. van der Laarse SAM, Leney AC, Heck AJR. Crosstalk between phosphorylation and O-GlcNAcylation: friend or foe. *FEBS J*. 2018 Sep;285(17):3152–67.
25. Iozzo RV, Schaefer L. Proteoglycan form and function: A comprehensive nomenclature of proteoglycans. *Matrix Biol J Int Soc Matrix Biol*. 2015 Mar;42:11–55.



26. Lindahl U, Couchman J, Kimata K, Esko JD. Proteoglycans and Sulfated Glycosaminoglycans. In: Varki A, Cummings RD, Esko JD, Stanley P, Hart GW, Aebi M, et al., editors. *Essentials of Glycobiology* [Internet]. 3rd ed. Cold Spring Harbor (NY): Cold Spring Harbor Laboratory Press; 2015 [cited 2021 Mar 23]. Available from: <http://www.ncbi.nlm.nih.gov/books/NBK453033/>
27. Hans-Joachim Gabius. The history of lectinology. In: *The Sugar Code: Fundamentals of Glycosciences* | Wiley [Internet]. Wiley-Blackwell; 2009 [cited 2021 Mar 23]. Available from: <https://www.wiley.com/en-us/The+Sugar+Code%3A+Fundamentals+of+Glycosciences-p-9783527320899>
28. Manning JC, Romero A, Habermann FA, García Caballero G, Kaltner H, Gabius H-J. Lectins: a primer for histochemists and cell biologists. *Histochem Cell Biol.* 2017 Feb;147(2):199–222.
29. Gabius H. Breaking the Sugar Code : Six Levels of Affinity Regulation in Glycan-lectin Interaction [Internet]. 2012 [cited 2021 Mar 22]. Available from: </paper/Breaking-the-Sugar-Code-%3A-Six-Levels-of-Affinity-in-Gabius/7fdd87748346c17b9fc4a8267620c2c58a523f45>
30. Gready J, Zelensky AN. Routes in lectin evolution: case study of the C-type lectin-like domains. undefined [Internet]. 2009 [cited 2021 Mar 24]; Available from: </paper/Routes-in-lectin-evolution%3A-case-study-of-the-Gready-Zelensky/a671a9b6445f5cd7e4a0f041845638bc3228c794>
31. Apweiler R, Hermjakob H, Sharon N. On the frequency of protein glycosylation, as deduced from analysis of the SWISS-PROT database<sup>11</sup>Dedicated to Prof. Akira Kobata and Prof. Harry Schachter on the occasion of their 65th birthdays. *Biochim Biophys Acta BBA - Gen Subj.* 1999 Dec 17;1473(1):4–8.
32. Chang IJ, He M, Lam CT. Congenital disorders of glycosylation. *Ann Transl Med* [Internet]. 2018 Dec [cited 2021 Mar 24];6(24). Available from: <https://www.ncbi.nlm.nih.gov/pmc/articles/PMC6331365/>
33. Freeze HH, Schachter H, Kinoshita T. Genetic Disorders of Glycosylation. In: Varki A, Cummings RD, Esko JD, Stanley P, Hart GW, Aebi M, et al., editors. *Essentials of Glycobiology* [Internet]. 3rd ed. Cold Spring Harbor (NY): Cold Spring Harbor Laboratory Press; 2015 [cited 2021 Mar 24]. Available from: <http://www.ncbi.nlm.nih.gov/books/NBK453041/>
34. Witters P, Cassiman D, Morava E. Nutritional Therapies in Congenital Disorders of Glycosylation (CDG). *Nutrients.* 2017 Nov 7;9(11).
35. Brasil S, Pascoal C, Francisco R, Marques-da-Silva D, Andreotti G, Videira PA, et al. CDG Therapies: From Bench to Bedside. *Int J Mol Sci.* 2018 Apr 27;19(5).

36. Witters P, Honzik T, Bauchart E, Altassan R, Pascreau T, Bruneel A, et al. Long-term follow-up in PMM2-CDG: are we ready to start treatment trials? *Genet Med Off J Am Coll Med Genet*. 2019 May;21(5):1181–8.
37. Gámez A, Yuste-Checa P, Brasil S, Briso-Montiano Á, Desviat LR, Ugarte M, et al. Protein misfolding diseases: Prospects of pharmacological treatment. *Clin Genet*. 2018 Mar;93(3):450–8.
38. Meezan E, Wu HC, Black PH, Robbins PW. Comparative studies on the carbohydrate-containing membrane components of normal and virus-transformed mouse fibroblasts. II. Separation of glycoproteins and glycopeptides by sephadex chromatography. *Biochemistry*. 1969 Jun;8(6):2518–24.
39. Munkley J, Elliott DJ. Hallmarks of glycosylation in cancer. *Oncotarget*. 2016 Mar 17;7(23):35478–89.
40. Fuster MM, Esko JD. The sweet and sour of cancer: glycans as novel therapeutic targets. *Nat Rev Cancer*. 2005 Jul 1;5(7):526–42.
41. Pinho SS, Reis CA. Glycosylation in cancer: mechanisms and clinical implications. *Nat Rev Cancer*. 2015 Sep 1;15(9):540–55.
42. Peixoto A, Relvas-Santos M, Azevedo R, Santos LL, Ferreira JA. Protein Glycosylation and Tumor Microenvironment Alterations Driving Cancer Hallmarks. *Front Oncol [Internet]*. 2019 May 14 [cited 2021 Mar 21];9. Available from: <https://www.ncbi.nlm.nih.gov/pmc/articles/PMC6530332/>
43. Charpin C, Bhan AK, Zurawski VR, Scully RE. Carcinoembryonic antigen (CEA) and carbohydrate determinant 19-9 (CA 19-9) localization in 121 primary and metastatic ovarian tumors: an immunohistochemical study with the use of monoclonal antibodies. *Int J Gynecol Pathol Off J Int Soc Gynecol Pathol*. 1982;1(3):231–45.
44. Frenette PS, Thirlwell MP, Trudeau M, Thomson DM, Joseph L, Shuster JS. The diagnostic value of CA 27-29, CA 15-3, mucin-like carcinoma antigen, carcinoembryonic antigen and CA 19-9 in breast and gastrointestinal malignancies. *Tumour Biol J Int Soc Oncodevelopmental Biol Med*. 1994;15(5):247–54.
45. Brockhausen I, Yang JM, Burchell J, Whitehouse C, Taylor-Papadimitriou J. Mechanisms underlying aberrant glycosylation of MUC1 mucin in breast cancer cells. *Eur J Biochem*. 1995 Oct 15;233(2):607–17.
46. Gilgunn S, Conroy PJ, Saldova R, Rudd PM, O’Kennedy RJ. Aberrant PSA glycosylation--a sweet predictor of prostate cancer. *Nat Rev Urol*. 2013 Feb;10(2):99–107.
47. Narimatsu H, Iwasaki H, Nakayama F, Ikehara Y, Kudo T, Nishihara S, et al. Lewis and secretor gene dosages affect CA19-9 and DU-PAN-2 serum levels in normal individuals and colorectal cancer patients. *Cancer Res*. 1998 Feb 1;58(3):512–8.

48. Park J-J, Lee M. Increasing the  $\alpha$  2, 6 sialylation of glycoproteins may contribute to metastatic spread and therapeutic resistance in colorectal cancer. *Gut Liver*. 2013 Nov;7(6):629–41.
49. Chakraborty A, Dorsett KA, Trummell HQ, Yang ES, Oliver PG, Bonner JA, et al. ST6Gal-I sialyltransferase promotes chemoresistance in pancreatic ductal adenocarcinoma by abrogating gemcitabine-mediated DNA damage. *J Biol Chem*. 2018 Jan 19;293(3):984–94.
50. Schultz MJ, Swindall AF, Wright JW, Sztul ES, Landen CN, Bellis SL. ST6Gal-I sialyltransferase confers cisplatin resistance in ovarian tumor cells. *J Ovarian Res*. 2013 Apr 11;6(1):25.
51. Bos PD, Zhang XH-F, Nadal C, Shu W, Gomis RR, Nguyen DX, et al. Genes that mediate breast cancer metastasis to the brain. *Nature*. 2009 Jun;459(7249):1005–9.
52. Pereira MS, Alves I, Vicente M, Campar A, Silva MC, Padrão NA, et al. Glycans as Key Checkpoints of T Cell Activity and Function. *Front Immunol* [Internet]. 2018 [cited 2021 Mar 22];9. Available from: <https://www.frontiersin.org/articles/10.3389/fimmu.2018.02754/full>
53. Araujo L, Khim P, Mkhikian H, Mortales C-L, Demetriou M. Glycolysis and glutaminolysis cooperatively control T cell function by limiting metabolite supply to N-glycosylation. Paulson J, editor. *eLife*. 2017 Jan 6;6:e21330.
54. Demetriou M, Granovsky M, Quaggin S, Dennis JW. Negative regulation of T-cell activation and autoimmunity by Mgat5 N-glycosylation. *Nature*. 2001 Feb;409(6821):733–9.
55. Dias AM, Pereira MS, Padrão NA, Alves I, Marcos-Pinto R, Lago P, et al. Glycans as critical regulators of gut immunity in homeostasis and disease. *Cell Immunol*. 2018 Nov 1;333:9–18.
56. Swamy M, Pathak S, Grzes KM, Damerow S, Sinclair LV, van Aalten DMF, et al. Glucose and glutamine fuel protein O-GlcNAcylation to control T cell self-renewal and malignancy. *Nat Immunol*. 2016 Jun;17(6):712–20.
57. Dennis JW, Lau KS, Demetriou M, Nabi IR. Adaptive Regulation at the Cell Surface by N-Glycosylation. *Traffic*. 2009;10(11):1569–78.
58. Mkhikian H, Grigorian A, Li CF, Chen H-L, Newton B, Zhou RW, et al. Genetics and the environment converge to dysregulate N-glycosylation in multiple sclerosis. *Nat Commun*. 2011 May 31;2(1):334.
59. Cabral J, Hanley SA, Gerlach JQ, O'Leary N, Cunningham S, Ritter T, et al. Distinctive Surface Glycosylation Patterns Associated With Mouse and Human CD4+ Regulatory T Cells and Their Suppressive Function. *Front Immunol* [Internet]. 2017 [cited 2021 Mar 24];8. Available from: <https://www.frontiersin.org/articles/10.3389/fimmu.2017.00987/full>

60. Houzelstein D, Gonçalves IR, Fadden AJ, Sidhu SS, Cooper DNW, Drickamer K, et al. Phylogenetic analysis of the vertebrate galectin family. *Mol Biol Evol.* 2004 Jul;21(7):1177–87.
61. Meynier C, Feracci M, Espeli M, Chaspoul F, Gallice P, Schiff C, et al. NMR and MD investigations of human galectin-1/oligosaccharide complexes. *Biophys J.* 2009 Dec 16;97(12):3168–77.
62. Hirabayashi J, Hashidate T, Arata Y, Nishi N, Nakamura T, Hirashima M, et al. Oligosaccharide specificity of galectins: a search by frontal affinity chromatography. *Biochim Biophys Acta.* 2002 Sep 19;1572(2–3):232–54.
63. Kim B-W, Hong SB, Kim JH, Kwon DH, Song HK. Structural basis for recognition of autophagic receptor NDP52 by the sugar receptor galectin-8. *Nat Commun.* 2013;4:1613.
64. Elantak L, Espeli M, Boned A, Bornet O, Bonzi J, Gauthier L, et al. Structural basis for galectin-1-dependent pre-B cell receptor (pre-BCR) activation. *J Biol Chem.* 2012 Dec 28;287(53):44703–13.
65. Daley D, Mani VR, Mohan N, Akkad N, Ochi A, Heindel DW, et al. Dectin 1 activation on macrophages by galectin 9 promotes pancreatic carcinoma and peritumoral immune tolerance. *Nat Med.* 2017 May;23(5):556–67.
66. Teichberg VI, Silman I, Beitsch DD, Resheff G. A beta-D-galactoside binding protein from electric organ tissue of *Electrophorus electricus*. *Proc Natl Acad Sci U S A.* 1975 Apr;72(4):1383–7.
67. Barondes SH, Castronovo V, Cooper DN, Cummings RD, Drickamer K, Feizi T, et al. Galectins: a family of animal beta-galactoside-binding lectins. *Cell.* 1994 Feb 25;76(4):597–8.
68. Arthur CM, Baruffi MD, Cummings RD, Stowell SR. Evolving mechanistic insights into galectin functions. *Methods Mol Biol Clifton NJ.* 2015;1207:1–35.
69. Hirabayashi J, Kasai K. The family of metazoan metal-independent beta-galactoside-binding lectins: structure, function and molecular evolution. *Glycobiology.* 1993 Aug;3(4):297–304.
70. Earl LA, Bi S, Baum LG. Galectin multimerization and lattice formation are regulated by linker region structure. *Glycobiology.* 2011 Jan;21(1):6–12.
71. Nio-Kobayashi J. Tissue- and cell-specific localization of galectins,  $\beta$ -galactose-binding animal lectins, and their potential functions in health and disease. *Anat Sci Int.* 2017 Jan;92(1):25–36.
72. Poirier F, Timmons PM, Chan CT, Guénet JL, Rigby PW. Expression of the L14 lectin during mouse embryogenesis suggests multiple roles during pre- and post-implantation development. *Dev Camb Engl.* 1992 May;115(1):143–55.

73. Hsu DK, Liu F-T. Regulation of cellular homeostasis by galectins. *Glycoconj J*. 2002;19(7–9):507–15.
74. Than NG, Romero R, Balogh A, Karpati E, Mastrolia SA, Staretz-Chacham O, et al. Galectins: Double-edged Swords in the Cross-roads of Pregnancy Complications and Female Reproductive Tract Inflammation and Neoplasia. *J Pathol Transl Med*. 2015 May;49(3):181–208.
75. Sahraravand M, Järvelä IY, Laitinen P, Tekay AH, Ryyänen M. The secretion of PAPP-A, ADAM12, and PP13 correlates with the size of the placenta for the first month of pregnancy. *Placenta*. 2011 Dec;32(12):999–1003.
76. Niki T, Fujita K, Rosen H, Hirashima M, Masaki T, Hattori T, et al. Plasma Galectin-9 Concentrations in Normal and Diseased Condition. *Cell Physiol Biochem Int J Exp Cell Physiol Biochem Pharmacol*. 2018;50(5):1856–68.
77. Barrow H, Guo X, Wandall HH, Pedersen JW, Fu B, Zhao Q, et al. Serum galectin-2, -4, and -8 are greatly increased in colon and breast cancer patients and promote cancer cell adhesion to blood vascular endothelium. *Clin Cancer Res Off J Am Assoc Cancer Res*. 2011 Nov 15;17(22):7035–46.
78. Vinnai JR, Cumming RC, Thompson GJ, Timoshenko AV. The association between oxidative stress-induced galectins and differentiation of human promyelocytic HL-60 cells. *Exp Cell Res*. 2017 Jun 15;355(2):113–23.
79. Rhodes DH, Pini M, Castellanos KJ, Montero-Melendez T, Cooper D, Perretti M, et al. Adipose tissue-specific modulation of galectin expression in lean and obese mice: evidence for regulatory function. *Obes Silver Spring Md*. 2013 Feb;21(2):310–9.
80. Imaizumi T, Kumagai M, Sasaki N, Kurotaki H, Mori F, Seki M, et al. Interferon-gamma stimulates the expression of galectin-9 in cultured human endothelial cells. *J Leukoc Biol*. 2002 Sep;72(3):486–91.
81. Gauthier S, Pelletier I, Ouellet M, Vargas A, Tremblay MJ, Sato S, et al. Induction of galectin-1 expression by HTLV-I Tax and its impact on HTLV-I infectivity. *Retrovirology*. 2008 Nov 25;5:105.
82. Georgiadis V, Stewart HJS, Pollard HJ, Tavsanoglu Y, Prasad R, Horwood J, et al. Lack of galectin-1 results in defects in myoblast fusion and muscle regeneration. *Dev Dyn Off Publ Am Assoc Anat*. 2007 Apr;236(4):1014–24.
83. Gendronneau G, Sidhu SS, Delacour D, Dang T, Calonne C, Houzelstein D, et al. Galectin-7 in the control of epidermal homeostasis after injury. *Mol Biol Cell*. 2008 Dec;19(12):5541–9.
84. Delacour D, Koch A, Ackermann W, Eude-Le Parco I, Elsässer H-P, Poirier F, et al. Loss of galectin-3 impairs membrane polarisation of mouse enterocytes in vivo. *J Cell Sci*. 2008 Feb 15;121(Pt 4):458–65.

85. Vasta GR, Ahmed H, Nita-Lazar M, Banerjee A, Pasek M, Shridhar S, et al. Galectins as self/non-self recognition receptors in innate and adaptive immunity: an unresolved paradox. *Front Immunol.* 2012;3:199.
86. Popa SJ, Stewart SE, Moreau K. Unconventional secretion of annexins and galectins. *Semin Cell Dev Biol.* 2018 Nov;83:42–50.
87. Lukyanov P, Furtak V, Ochieng J. Galectin-3 interacts with membrane lipids and penetrates the lipid bilayer. *Biochem Biophys Res Commun.* 2005 Dec 16;338(2):1031–6.
88. Stewart SE, Menzies SA, Popa SJ, Savinykh N, Petrunkina Harrison A, Lehner PJ, et al. A genome-wide CRISPR screen reconciles the role of N-linked glycosylation in galectin-3 transport to the cell surface. *J Cell Sci.* 2017 Oct 1;130(19):3234–47.
89. Cooper DN, Barondes SH. Evidence for export of a muscle lectin from cytosol to extracellular matrix and for a novel secretory mechanism. *J Cell Biol.* 1990 May;110(5):1681–91.
90. Aits S, Krickler J, Liu B, Ellegaard A-M, Hämälistö S, Tvingsholm S, et al. Sensitive detection of lysosomal membrane permeabilization by lysosomal galectin puncta assay. *Autophagy.* 2015;11(8):1408–24.
91. Keryer-Bibens C, Pioche-Durieu C, Villemant C, Souquère S, Nishi N, Hirashima M, et al. Exosomes released by EBV-infected nasopharyngeal carcinoma cells convey the viral latent membrane protein 1 and the immunomodulatory protein galectin 9. *BMC Cancer.* 2006 Dec 8;6:283.
92. Klibi J, Niki T, Riedel A, Pioche-Durieu C, Souquere S, Rubinstein E, et al. Blood diffusion and Th1-suppressive effects of galectin-9-containing exosomes released by Epstein-Barr virus-infected nasopharyngeal carcinoma cells. *Blood.* 2009 Feb 26;113(9):1957–66.
93. Bänfer S, Schneider D, Dewes J, Strauss MT, Freibert S-A, Heimerl T, et al. Molecular mechanism to recruit galectin-3 into multivesicular bodies for polarized exosomal secretion. *Proc Natl Acad Sci U S A.* 2018 May 8;115(19):E4396–405.
94. Shalom-Feuerstein R, Plowman SJ, Rotblat B, Ariotti N, Tian T, Hancock JF, et al. K-ras nanoclustering is subverted by overexpression of the scaffold protein galectin-3. *Cancer Res.* 2008 Aug 15;68(16):6608–16.
95. Elad-Sfadia G, Haklai R, Balan E, Kloog Y. Galectin-3 augments K-Ras activation and triggers a Ras signal that attenuates ERK but not phosphoinositide 3-kinase activity. *J Biol Chem.* 2004 Aug 13;279(33):34922–30.
96. Paz I, Sachse M, Dupont N, Mounier J, Cederfur C, Enninga J, et al. Galectin-3, a marker for vacuole lysis by invasive pathogens. *Cell Microbiol.* 2010 Apr 1;12(4):530–44.
97. Cheng Y-L, Wu Y-W, Kuo C-F, Lu S-L, Liu F-T, Anderson R, et al. Galectin-3 Inhibits Galectin-8/Parkin-Mediated Ubiquitination of Group A Streptococcus. *mBio.* 2017 Jul 25;8(4).

98. Nakahara S, Hogan V, Inohara H, Raz A. Importin-mediated nuclear translocation of galectin-3. *J Biol Chem*. 2006 Dec 22;281(51):39649–59.
99. Dagher SF, Wang JL, Patterson RJ. Identification of galectin-3 as a factor in pre-mRNA splicing. *Proc Natl Acad Sci U S A*. 1995 Feb 14;92(4):1213–7.
100. Thurston TLM, Wandel MP, von Muhlinen N, Foeglein A, Randow F. Galectin 8 targets damaged vesicles for autophagy to defend cells against bacterial invasion. *Nature*. 2012 Jan 15;482(7385):414–8.
101. Flavin WP, Bousset L, Green ZC, Chu Y, Skarpathiotis S, Chaney MJ, et al. Endocytic vesicle rupture is a conserved mechanism of cellular invasion by amyloid proteins. *Acta Neuropathol (Berl)*. 2017 Oct;134(4):629–53.
102. Garner OB, Baum LG. Galectin–glycan lattices regulate cell-surface glycoprotein organization and signalling. *Biochem Soc Trans*. 2008 Dec;36(Pt 6):1472–7.
103. Johannes L, Wunder C, Shafaq-Zadah M. Glycolipids and Lectins in Endocytic Uptake Processes. *J Mol Biol*. 2016 Oct 27;
104. Johannes L, Billet A. Glycosylation and raft endocytosis in cancer. *Cancer Metastasis Rev*. 2020 Jun;39(2):375–96.
105. Elola MT, Blidner AG, Ferragut F, Bracalente C, Rabinovich GA. Assembly, organization and regulation of cell-surface receptors by lectin-glycan complexes. *Biochem J*. 2015 Jul 1;469(1):1–16.
106. Mosmann TR, Coffman RL. TH1 and TH2 cells: different patterns of lymphokine secretion lead to different functional properties. *Annu Rev Immunol*. 1989;7:145–73.
107. Mosmann TR, Cherwinski H, Bond MW, Giedlin MA, Coffman RL. Two types of murine helper T cell clone. I. Definition according to profiles of lymphokine activities and secreted proteins. *J Immunol Baltim Md 1950*. 1986 Apr 1;136(7):2348–57.
108. Zhu J, Paul WE. Peripheral CD4+ T-cell differentiation regulated by networks of cytokines and transcription factors. *Immunol Rev*. 2010 Nov;238(1):247–62.
109. Eagar TN, Miller SD. 16 - Helper T-Cell Subsets and Control of the Inflammatory Response. In: Rich RR, Fleisher TA, Shearer WT, Schroeder HW, Frew AJ, Weyand CM, editors. *Clinical Immunology (Fifth Edition)* [Internet]. London: Elsevier; 2019 [cited 2021 Apr 5]. p. 235-245.e1. Available from: <https://www.sciencedirect.com/science/article/pii/B9780702068966000168>
110. Paul WE, Zhu J. How are T(H)2-type immune responses initiated and amplified? *Nat Rev Immunol*. 2010 Apr;10(4):225–35.
111. Muñoz M, Hegazy AN, Brunner TM, Holeccka V, Marek RM, Fröhlich A, et al. Th2 cells lacking T-bet suppress naive and memory T cell responses via IL-10. *Proc Natl Acad Sci*

[Internet]. 2021 Feb 9 [cited 2021 Apr 5];118(6). Available from: <https://www.pnas.org/content/118/6/e2002787118>

112. Hültner L, Druetz C, Moeller J, Uyttenhove C, Schmitt E, Rude E, et al. Mast cell growth-enhancing activity (MEA) is structurally related and functionally identical to the novel mouse T cell growth factor P40/TCGFIII (interleukin 9). *Eur J Immunol*. 1990 Jun;20(6):1413–6.
113. Harrington LE, Hatton RD, Mangan PR, Turner H, Murphy TL, Murphy KM, et al. Interleukin 17–producing CD4 + effector T cells develop via a lineage distinct from the T helper type 1 and 2 lineages. *Nat Immunol*. 2005 Nov;6(11):1123–32.
114. Zhou L, Lopes JE, Chong MMW, Ivanov II, Min R, Victora GD, et al. TGF-beta-induced Foxp3 inhibits T(H)17 cell differentiation by antagonizing RORgamma function. *Nature*. 2008 May 8;453(7192):236–40.
115. Ivanov II, Zhou L, Littman DR. Transcriptional Regulation of Th17 Cell Differentiation. *Semin Immunol*. 2007 Dec;19(6):409–17.
116. Veldhoen M, Uyttenhove C, van Snick J, Helmby H, Westendorf A, Buer J, et al. Transforming growth factor-beta “reprograms” the differentiation of T helper 2 cells and promotes an interleukin 9-producing subset. *Nat Immunol*. 2008 Dec;9(12):1341–6.
117. Dardalhon V, Awasthi A, Kwon H, Galileos G, Gao W, Sobel RA, et al. IL-4 inhibits TGF-beta-induced Foxp3+ T cells and, together with TGF-beta, generates IL-9+ IL-10+ Foxp3(-) effector T cells. *Nat Immunol*. 2008 Dec;9(12):1347–55.
118. Wang A, Pan D, Lee Y-H, Martinez GJ, Feng X-H, Dong C. Cutting edge: Smad2 and Smad4 regulate TGF-β-mediated IL9 gene expression via EZH2 displacement. *J Immunol Baltim Md* 1950. 2013 Nov 15;191(10):4908–12.
119. Ramming A, Druzd D, Leipe J, Schulze-Koops H, Skapenko A. Maturation-related histone modifications in the PU.1 promoter regulate Th9-cell development. *Blood*. 2012 May 17;119(20):4665–74.
120. Li P, Spolski R, Liao W, Leonard WJ. Complex interactions of transcription factors in mediating cytokine biology in T cells. *Immunol Rev*. 2014 Sep;261(1):141–56.
121. Goswami R, Jabeen R, Yagi R, Pham D, Zhu J, Goenka S, et al. STAT6-dependent regulation of Th9 development. *J Immunol Baltim Md* 1950. 2012 Feb 1;188(3):968–75.
122. Chen J, Guan L, Tang L, Liu S, Zhou Y, Chen C, et al. T Helper 9 Cells: A New Player in Immune-Related Diseases. *DNA Cell Biol*. 2019 Oct 1;38(10):1040–7.
123. Yang L, Anderson DE, Baecher-Allan C, Hastings WD, Bettelli E, Oukka M, et al. IL-21 and TGF-beta are required for differentiation of human T(H)17 cells. *Nature*. 2008 Jul 17;454(7202):350–2.



124. Trifari S, Kaplan CD, Tran EH, Crellin NK, Spits H. Identification of a human helper T cell population that has abundant production of interleukin 22 and is distinct from T(H)-17, T(H)1 and T(H)2 cells. *Nat Immunol*. 2009 Aug;10(8):864–71.
125. Boniface K, Bernard F-X, Garcia M, Gurney AL, Lecron J-C, Morel F. IL-22 inhibits epidermal differentiation and induces proinflammatory gene expression and migration of human keratinocytes. *J Immunol Baltim Md 1950*. 2005 Mar 15;174(6):3695–702.
126. Aujla SJ, Chan YR, Zheng M, Fei M, Askew DJ, Pociask DA, et al. IL-22 mediates mucosal host defense against Gram-negative bacterial pneumonia. *Nat Med*. 2008 Mar;14(3):275–81.
127. In Vivo-Activated Cd4 T Cells Upregulate Cxc Chemokine Receptor 5 and Reprogram Their Response to Lymphoid Chemokines | *Journal of Experimental Medicine* | Rockefeller University Press [Internet]. [cited 2021 Apr 6]. Available from: <https://rupress.org/jem/article/190/8/1123/7959/In-Vivo-Activated-Cd4-T-Cells-Upregulate-Cxc>
128. Crotty S. T follicular helper cell differentiation, function, and roles in disease. *Immunity*. 2014 Oct 16;41(4):529–42.
129. Baumjohann D, Okada T, Ansel KM. Cutting Edge: Distinct Waves of BCL6 Expression during T Follicular Helper Cell Development. *J Immunol*. 2011 Sep 1;187(5):2089–92.
130. Hao H, Nakayamada S, Tanaka Y. Differentiation, functions, and roles of T follicular regulatory cells in autoimmune diseases. *Inflamm Regen* [Internet]. 2021 May 3 [cited 2021 May 20];41. Available from: <https://www.ncbi.nlm.nih.gov/pmc/articles/PMC8088831/>
131. Chung Y, Tanaka S, Chu F, Nurieva RI, Martinez GJ, Rawal S, et al. Follicular regulatory T cells expressing Foxp3 and BCL6 suppress germinal center reactions. *Nat Med*. 2011 Jul 24;17(8):983–8.
132. Linterman MA, Pierson W, Lee SK, Kallies A, Kawamoto S, Rayner TF, et al. Foxp3+ follicular regulatory T cells control the germinal center response. *Nat Med*. 2011 Jul 24;17(8):975–82.
133. Xie MM, Chen Q, Liu H, Yang K, Koh B, Wu H, et al. T follicular regulatory cells and IL-10 promote food antigen-specific IgE. *J Clin Invest*. 2020 Jul 1;130(7):3820–32.
134. Laidlaw BJ, Lu Y, Amezquita RA, Weinstein JS, Vander Heiden JA, Gupta NT, et al. Interleukin-10 from CD4+ follicular regulatory T cells promotes the germinal center response. *Sci Immunol*. 2017 Oct 20;2(16).
135. Noble A, Giorgini A, Leggat JA. Cytokine-induced IL-10-secreting CD8 T cells represent a phenotypically distinct suppressor T-cell lineage. *Blood*. 2006 Jun 1;107(11):4475–83.
136. Ostroukhova M, Ray A. CD25+ T cells and regulation of allergen-induced responses. *Curr Allergy Asthma Rep*. 2005 Jan;5(1):35–41.

137. Kretschmer K, Apostolou I, Hawiger D, Khazaie K, Nussenzweig MC, von Boehmer H. Inducing and expanding regulatory T cell populations by foreign antigen. *Nat Immunol.* 2005 Dec;6(12):1219–27.
138. St Paul M, Ohashi PS. The Roles of CD8+ T Cell Subsets in Antitumor Immunity. *Trends Cell Biol.* 2020 Sep;30(9):695–704.
139. Ray A, Khare A, Krishnamoorthy N, Qi Z, Ray P. Regulatory T cells in many flavors control asthma. *Mucosal Immunol.* 2010 May;3(3):216–29.
140. Yu Y, Ma X, Gong R, Zhu J, Wei L, Yao J. Recent advances in CD8+ regulatory T cell research. *Oncol Lett.* 2018 Jun;15(6):8187–94.
141. Yu D, Ye L. A Portrait of CXCR5+ Follicular Cytotoxic CD8+ T cells. *Trends Immunol.* 2018 Dec 1;39(12):965–79.
142. Chan WL, Pejnovic N, Lee CA, Al-Ali NA. Human IL-18 Receptor and ST2L Are Stable and Selective Markers for the Respective Type 1 and Type 2 Circulating Lymphocytes. *J Immunol.* 2001 Aug 1;167(3):1238.
143. Croft M, Carter L, Swain SL, Dutton RW. Generation of polarized antigen-specific CD8 effector populations: reciprocal action of interleukin (IL)-4 and IL-12 in promoting type 2 versus type 1 cytokine profiles. *J Exp Med.* 1994 Nov 1;180(5):1715–28.
144. Mittrücker H-W, Visekruna A, Huber M. Heterogeneity in the Differentiation and Function of CD8+ T Cells. *Arch Immunol Ther Exp (Warsz).* 2014 Dec 1;62(6):449–58.
145. Kemp RA, Ronchese F. Tumor-Specific Tc1, But Not Tc2, Cells Deliver Protective Antitumor Immunity. *J Immunol.* 2001 Dec 1;167(11):6497.
146. Res PCM, Piskin G, Boer OJ de, Loos CM van der, Teeling P, Bos JD, et al. Overrepresentation of IL-17A and IL-22 Producing CD8 T Cells in Lesional Skin Suggests Their Involvement in the Pathogenesis of Psoriasis. *PLOS ONE.* 2010 Nov 24;5(11):e14108.
147. St. Paul M, Saibil SD, Lien SC, Han S, Sayad A, Mulder DT, et al. IL6 Induces an IL22+ CD8+ T-cell Subset with Potent Antitumor Function. *Cancer Immunol Res.* 2020 Mar 1;8(3):321.
148. Intlekofer AM, Banerjee A, Takemoto N, Gordon SM, DeJong CS, Shin H, et al. Anomalous Type 17 Response to Viral Infection by CD8+ T Cells Lacking T-bet and Eomesodermin. *Science.* 2008 Jul 18;321(5887):408.
149. Huber M, Heink S, Grothe H, Guralnik A, Reinhard K, Elflein K, et al. A Th17-like developmental process leads to CD8+ Tc17 cells with reduced cytotoxic activity. *Eur J Immunol.* 2009;39(7):1716–25.
150. Visekruna A, Ritter J, Scholz T, Campos L, Guralnik A, Poncette L, et al. Tc9 cells, a new subset of CD8+ T cells, support Th2-mediated airway inflammation. *Eur J Immunol.* 2013;43(3):606–18.

151. Boyton RJ, Altmann DM. Is selection for TCR affinity a factor in cytokine polarization? *Trends Immunol.* 2002 Nov 1;23(11):526–9.
152. Kanno Y, Vahedi G, Hirahara K, Singleton K, O’Shea JJ. Transcriptional and epigenetic control of T helper cell specification: molecular mechanisms underlying commitment and plasticity. *Annu Rev Immunol.* 2012;30:707–31.
153. Allan RS, Zueva E, Cammas F, Schreiber HA, Masson V, Belz GT, et al. An epigenetic silencing pathway controlling T helper 2 cell lineage commitment. *Nature.* 2012 Jul 12;487(7406):249–53.
154. Tumes DJ, Onodera A, Suzuki A, Shinoda K, Endo Y, Iwamura C, et al. The polycomb protein Ezh2 regulates differentiation and plasticity of CD4(+) T helper type 1 and type 2 cells. *Immunity.* 2013 Nov 14;39(5):819–32.
155. Geginat J, Paroni M, Maglie S, Alfen JS, Kastirr I, Gruarin P, et al. Plasticity of human CD4 T cell subsets. *Front Immunol.* 2014;5:630.
156. Messi M, Giacchetto I, Nagata K, Lanzavecchia A, Natoli G, Sallusto F. Memory and flexibility of cytokine gene expression as separable properties of human T(H)1 and T(H)2 lymphocytes. *Nat Immunol.* 2003 Jan;4(1):78–86.
157. Peine M, Rausch S, Helmstetter C, Fröhlich A, Hegazy AN, Köhl AA, et al. Stable T-bet+GATA-3+ Th1/Th2 Hybrid Cells Arise In Vivo, Can Develop Directly from Naive Precursors, and Limit Immunopathologic Inflammation. *PLoS Biol* [Internet]. 2013 Aug 20 [cited 2021 Apr 18];11(8). Available from: <https://www.ncbi.nlm.nih.gov/pmc/articles/PMC3747991/>
158. Giorgio Trinchieri FG. Interleukin-12 primes human CD4 and CD8 T cell clones for high production of both interferon-gamma and interleukin-10. *J Exp Med.* 1996 Jun 1;183(6):2559–69.
159. Häring B, Lozza L, Steckel B, Geginat J. Identification and characterization of IL-10/IFN- $\gamma$ -producing effector-like T cells with regulatory function in human blood. *J Exp Med.* 2009 May 11;206(5):1009–17.
160. Hegazy AN, Peine M, Helmstetter C, Panse I, Fröhlich A, Bergthaler A, et al. Interferons direct Th2 cell reprogramming to generate a stable GATA-3(+)T-bet(+) cell subset with combined Th2 and Th1 cell functions. *Immunity.* 2010 Jan 29;32(1):116–28.
161. Stumhofer JS, Laurence A, Wilson EH, Huang E, Tato CM, Johnson LM, et al. Interleukin 27 negatively regulates the development of interleukin 17-producing T helper cells during chronic inflammation of the central nervous system. *Nat Immunol.* 2006 Sep;7(9):937–45.
162. Lexberg MH, Taubner A, Förster A, Albrecht I, Richter A, Kamradt T, et al. Th memory for interleukin-17 expression is stable in vivo. *Eur J Immunol.* 2008 Oct;38(10):2654–64.

163. McGeachy MJ, Bak-Jensen KS, Chen Y, Tato CM, Blumenschein W, McClanahan T, et al. TGF-beta and IL-6 drive the production of IL-17 and IL-10 by T cells and restrain T(H)-17 cell-mediated pathology. *Nat Immunol.* 2007 Dec;8(12):1390–7.
164. Zhou L, Ivanov II, Spolski R, Min R, Shenderov K, Egawa T, et al. IL-6 programs T(H)-17 cell differentiation by promoting sequential engagement of the IL-21 and IL-23 pathways. *Nat Immunol.* 2007 Sep;8(9):967–74.
165. Voo KS, Wang Y-H, Santori FR, Boggiano C, Wang Y-H, Arima K, et al. Identification of IL-17-producing FOXP3+ regulatory T cells in humans. *Proc Natl Acad Sci U S A.* 2009 Mar 24;106(12):4793–8.
166. Kleinewietfeld M, Hafler DA. The plasticity of human Treg and Th17 cells and its role in autoimmunity. *Semin Immunol.* 2013 Nov 15;25(4):305–12.
167. Dominguez-Villar M, Baecher-Allan CM, Hafler DA. Identification of T helper type 1-like, Foxp3+ regulatory T cells in human autoimmune disease. *Nat Med.* 2011 Jun;17(6):673–5.
168. Boissonnas A, Scholer-Dahirel A, Simon-Blancal V, Pace L, Valet F, Kissenpfennig A, et al. Foxp3+ T cells induce perforin-dependent dendritic cell death in tumor-draining lymph nodes. *Immunity.* 2010 Feb 26;32(2):266–78.
169. Grossman WJ, Verbsky JW, Tollefsen BL, Kemper C, Atkinson JP, Ley TJ. Differential expression of granzymes A and B in human cytotoxic lymphocyte subsets and T regulatory cells. *Blood.* 2004 Nov 1;104(9):2840–8.
170. Cao X, Cai SF, Fehniger TA, Song J, Collins LI, Piwnicka-Worms DR, et al. Granzyme B and perforin are important for regulatory T cell-mediated suppression of tumor clearance. *Immunity.* 2007 Oct;27(4):635–46.
171. Tsuji M, Komatsu N, Kawamoto S, Suzuki K, Kanagawa O, Honjo T, et al. Preferential generation of follicular B helper T cells from Foxp3+ T cells in gut Peyer's patches. *Science.* 2009 Mar 13;323(5920):1488–92.
172. Zheng Y, Chaudhry A, Kas A, deRoos P, Kim JM, Chu T-T, et al. Regulatory T-cell suppressor program co-opts transcription factor IRF4 to control T(H)2 responses. *Nature.* 2009 Mar 19;458(7236):351–6.
173. Abbas AK, Lichtman AH, Pillai S, Baker DL, Baker A. Chapter 7: Antigen receptors and accessory molecules of T lymphocytes. In: *Cellular and molecular immunology.* 2018.
174. Abbas AK, Lichtman AH, Pillai S, Baker DL, Baker A. Chapter 9: Activation of T lymphocytes. In: *Cellular and molecular immunology.* 2018.
175. Abbas AK, Lichtman AH, Pillai S, Baker DL, Baker A. Chapter 5: The major histocompatibility complex. In: *Cellular and molecular immunology.* 2018.

176. Minguet S, Swamy M, Alarcón B, Luescher IF, Schamel WWA. Full activation of the T cell receptor requires both clustering and conformational changes at CD3. *Immunity*. 2007 Jan;26(1):43–54.
177. Gil D, Schamel WWA, Montoya M, Sánchez-Madrid F, Alarcón B. Recruitment of Nck by CD3 epsilon reveals a ligand-induced conformational change essential for T cell receptor signaling and synapse formation. *Cell*. 2002 Jun 28;109(7):901–12.
178. Lin J, Weiss A. T cell receptor signalling. *J Cell Sci*. 2001 Jan;114(Pt 2):243–4.
179. Huppa JB, Davis MM. T-cell-antigen recognition and the immunological synapse. *Nat Rev Immunol*. 2003 Dec;3(12):973–83.
180. Barda-Saad M, Braiman A, Titerence R, Bunnell SC, Barr VA, Samelson LE. Dynamic molecular interactions linking the T cell antigen receptor to the actin cytoskeleton. *Nat Immunol*. 2005 Jan;6(1):80–9.
181. Campi G, Varma R, Dustin ML. Actin and agonist MHC-peptide complex-dependent T cell receptor microclusters as scaffolds for signaling. *J Exp Med*. 2005 Oct 17;202(8):1031–6.
182. Gallego MD, Santamaría M, Peña J, Molina IJ. Defective actin reorganization and polymerization of Wiskott-Aldrich T cells in response to CD3-mediated stimulation. *Blood*. 1997 Oct 15;90(8):3089–97.
183. Dustin ML. The immunological synapse. *Cancer Immunol Res*. 2014 Nov;2(11):1023–33.
184. Valitutti S, Coombs D, Dupré L. The space and time frames of T cell activation at the immunological synapse. *FEBS Lett*. 2010 Dec 15;584(24):4851–7.
185. Bertrand F, Esquerré M, Petit A-E, Rodrigues M, Duchez S, Delon J, et al. Activation of the ancestral polarity regulator protein kinase C zeta at the immunological synapse drives polarization of Th cell secretory machinery toward APCs. *J Immunol Baltim Md 1950*. 2010 Sep 1;185(5):2887–94.
186. Kupfer H, Monks CR, Kupfer A. Small splenic B cells that bind to antigen-specific T helper (Th) cells and face the site of cytokine production in the Th cells selectively proliferate: immunofluorescence microscopic studies of Th-B antigen-presenting cell interactions. *J Exp Med*. 1994 May 1;179(5):1507–15.
187. Monks CR, Freiberg BA, Kupfer H, Sciaky N, Kupfer A. Three-dimensional segregation of supramolecular activation clusters in T cells. *Nature*. 1998 Sep 3;395(6697):82–6.
188. Stinchcombe JC, Bossi G, Booth S, Griffiths GM. The Immunological Synapse of CTL Contains a Secretory Domain and Membrane Bridges. *Immunity*. 2001 Nov 1;15(5):751–61.
189. Zinselmeyer BH, Heydari S, Sacristán C, Nayak D, Cammer M, Herz J, et al. PD-1 promotes immune exhaustion by inducing antiviral T cell motility paralysis. *J Exp Med*. 2013 Mar 25;210(4):757–74.

190. Brossard C, Feuillet V, Schmitt A, Randriamampita C, Romao M, Raposo G, et al. Multifocal structure of the T cell – dendritic cell synapse. *Eur J Immunol*. 2005;35(6):1741–53.
191. Zanin-Zhorov A, Ding Y, Kumari S, Attur M, Hippen KL, Brown M, et al. Protein Kinase C- $\theta$  Mediates Negative Feedback on Regulatory T Cell Function. *Science*. 2010 Apr 16;328(5976):372–6.
192. Kumari S, Colin-York H, Irvine DJ, Fritzsche M. Not All T Cell Synapses Are Built the Same Way. *Trends Immunol*. 2019 Nov 1;40(11):977–80.
193. Comrie WA, Burkhardt JK. Action and Traction: Cytoskeletal Control of Receptor Triggering at the Immunological Synapse. *Front Immunol* [Internet]. 2016 Mar 7 [cited 2021 Apr 9];7. Available from: <https://www.ncbi.nlm.nih.gov/pmc/articles/PMC4779853/>
194. Tan YX, Manz BN, Freedman TS, Zhang C, Shokat KM, Weiss A. Inhibition of the kinase Csk in thymocytes reveals a requirement for actin remodeling in the initiation of full TCR signaling. *Nat Immunol*. 2014 Feb;15(2):186–94.
195. Baker RG, Hsu CJ, Lee D, Jordan MS, Maltzman JS, Hammer DA, et al. The adapter protein SLP-76 mediates “outside-in” integrin signaling and function in T cells. *Mol Cell Biol*. 2009 Oct;29(20):5578–89.
196. Sánchez-Martín L, Sánchez-Sánchez N, Gutiérrez-López MD, Rojo AI, Vicente-Manzanares M, Pérez-Alvarez MJ, et al. Signaling through the leukocyte integrin LFA-1 in T cells induces a transient activation of Rac-1 that is regulated by Vav and PI3K/Akt-1. *J Biol Chem*. 2004 Apr 16;279(16):16194–205.
197. Kumar R, Ferez M, Swamy M, Arechaga I, Rejas MT, Valpuesta JM, et al. Increased sensitivity of antigen-experienced T cells through the enrichment of oligomeric T cell receptor complexes. *Immunity*. 2011 Sep 23;35(3):375–87.
198. Lillemeier BF, Mörtelmaier MA, Forstner MB, Huppa JB, Groves JT, Davis MM. TCR and Lat are expressed on separate protein islands on T cell membranes and concatenate during activation. *Nat Immunol*. 2010 Jan;11(1):90–6.
199. Lämmermann T, Bader BL, Monkley SJ, Worbs T, Wedlich-Söldner R, Hirsch K, et al. Rapid leukocyte migration by integrin-independent flowing and squeezing. *Nature*. 2008 May 1;453(7191):51–5.
200. Sánchez-Madrid F, Serrador JM. Bringing up the rear: defining the roles of the uropod. *Nat Rev Mol Cell Biol*. 2009 May;10(5):353–9.
201. Dustin ML. Hunter to gatherer and back: immunological synapses and kinapses as variations on the theme of amoeboid locomotion. *Annu Rev Cell Dev Biol*. 2008;24:577–96.
202. Varma R, Campi G, Yokosuka T, Saito T, Dustin ML. T cell receptor-proximal signals are sustained in peripheral microclusters and terminated in the central supramolecular activation cluster. *Immunity*. 2006 Jul;25(1):117–27.

203. Choudhuri K, Llodrá J, Roth EW, Tsai J, Gordo S, Wucherpennig KW, et al. Polarized release of T-cell-receptor-enriched microvesicles at the immunological synapse. *Nature*. 2014 Mar 6;507(7490):118–23.
204. Rudd PM, Wormald MR, Stanfield RL, Huang M, Mattsson N, Speir JA, et al. Roles for glycosylation of cell surface receptors involved in cellular immune recognition. *J Mol Biol*. 1999 Oct 22;293(2):351–66.
205. Kern P, Hussey RE, Spoerl R, Reinherz EL, Chang HC. Expression, purification, and functional analysis of murine ectodomain fragments of CD8 $\alpha$  $\alpha$  and CD8 $\alpha$  $\beta$  dimers. *J Biol Chem*. 1999 Sep 17;274(38):27237–43.
206. Van den Steen P, Rudd PM, Dwek RA, Opdenakker G. Concepts and principles of O-linked glycosylation. *Crit Rev Biochem Mol Biol*. 1998;33(3):151–208.
207. Grigorian A, Torossian S, Demetriou M. T-cell growth, cell surface organization, and the galectin-glycoprotein lattice. *Immunol Rev*. 2009 Jul;230(1):232–46.
208. Togayachi A, Kozono Y, Ishida H, Abe S, Suzuki N, Tsunoda Y, et al. Polylysosamine on glycoproteins influences basal levels of lymphocyte and macrophage activation. *Proc Natl Acad Sci U S A*. 2007 Oct 2;104(40):15829–34.
209. Kuball J, Hauptrock B, Malina V, Antunes E, Voss R-H, Wolfl M, et al. Increasing functional avidity of TCR-redirected T cells by removing defined N-glycosylation sites in the TCR constant domain. *J Exp Med*. 2009 Feb 16;206(2):463–75.
210. Chen I-J, Chen H-L, Demetriou M. Lateral compartmentalization of T cell receptor versus CD45 by galectin-N-glycan binding and microfilaments coordinate basal and activation signaling. *J Biol Chem*. 2007 Nov 30;282(48):35361–72.
211. Chen H-L, Li CF, Grigorian A, Tian W, Demetriou M. T cell receptor signaling co-regulates multiple Golgi genes to enhance N-glycan branching. *J Biol Chem*. 2009 Nov 20;284(47):32454–61.
212. Grigorian A, Araujo L, Naidu NN, Place DJ, Choudhury B, Demetriou M. N-acetylglucosamine inhibits T-helper 1 (Th1)/T-helper 17 (Th17) cell responses and treats experimental autoimmune encephalomyelitis. *J Biol Chem*. 2011 Nov 18;286(46):40133–41.
213. Rabinovich GA, Croci DO. Regulatory circuits mediated by lectin-glycan interactions in autoimmunity and cancer. *Immunity*. 2012 Mar 23;36(3):322–35.
214. Antonopoulos A, Demotte N, Stroobant V, Haslam SM, van der Bruggen P, Dell A. Loss of effector function of human cytolytic T lymphocytes is accompanied by major alterations in N- and O-glycosylation. *J Biol Chem*. 2012 Mar 30;287(14):11240–51.
215. Lau KS, Partridge EA, Grigorian A, Silvescu CI, Reinhold VN, Demetriou M, et al. Complex N-Glycan Number and Degree of Branching Cooperate to Regulate Cell Proliferation and Differentiation. *Cell*. 2007 Apr 6;129(1):123–34.

216. Chen H-Y, Fermin A, Vardhana S, Weng I-C, Lo KFR, Chang E-Y, et al. Galectin-3 negatively regulates TCR-mediated CD4<sup>+</sup> T-cell activation at the immunological synapse. *Proc Natl Acad Sci U S A*. 2009 Aug 25;106(34):14496–501.
217. Liu SD, Tomassian T, Bruhn KW, Miller JF, Poirier F, Miceli MC. Galectin-1 tunes TCR binding and signal transduction to regulate CD8 burst size. *J Immunol Baltim Md 1950*. 2009 May 1;182(9):5283–95.
218. Zajac AJ, Blattman JN, Murali-Krishna K, Sourdive DJD, Suresh M, Altman JD, et al. Viral Immune Evasion Due to Persistence of Activated T Cells Without Effector Function. *J Exp Med*. 1998 Dec 21;188(12):2205–13.
219. Wherry EJ, Ha S-J, Kaech SM, Haining WN, Sarkar S, Kalia V, et al. Molecular signature of CD8<sup>+</sup> T cell exhaustion during chronic viral infection. *Immunity*. 2007 Oct;27(4):670–84.
220. Blackburn SD, Shin H, Haining WN, Zou T, Workman CJ, Polley A, et al. Coregulation of CD8<sup>+</sup> T cell exhaustion by multiple inhibitory receptors during chronic viral infection. *Nat Immunol*. 2009 Jan;10(1):29–37.
221. Wherry EJ, Blattman JN, Murali-Krishna K, van der Most R, Ahmed R. Viral Persistence Alters CD8 T-Cell Immunodominance and Tissue Distribution and Results in Distinct Stages of Functional Impairment. *J Virol*. 2003 Apr;77(8):4911–27.
222. Richter K, Agnellini P, Oxenius A. On the role of the inhibitory receptor LAG-3 in acute and chronic LCMV infection. *Int Immunol*. 2010 Jan 1;22(1):13–23.
223. Sharpe AH, Wherry EJ, Ahmed R, Freeman GJ. The function of programmed cell death 1 and its ligands in regulating autoimmunity and infection. *Nat Immunol*. 2007 Mar;8(3):239–45.
224. Liu X, Mo W, Ye J, Li L, Zhang Y, Hsueh EC, et al. Regulatory T cells trigger effector T cell DNA damage and senescence caused by metabolic competition. *Nat Commun [Internet]*. 2018 Jan 16 [cited 2021 Apr 13];9. Available from: <https://www.ncbi.nlm.nih.gov/pmc/articles/PMC5770447/>
225. Ye J, Huang X, Hsueh EC, Zhang Q, Ma C, Zhang Y, et al. Human regulatory T cells induce T-lymphocyte senescence. *Blood*. 2012 Sep 6;120(10):2021–31.
226. Ye J, Ma C, Hsueh EC, Eickhoff CS, Zhang Y, Varvares MA, et al. Tumor-derived  $\gamma\delta$  regulatory T cells suppress innate and adaptive immunity through the induction of immunosenescence. *J Immunol Baltim Md 1950*. 2013 Mar 1;190(5):2403–14.
227. Ye J, Ma C, Hsueh EC, Dou J, Mo W, Liu S, et al. TLR8 signaling enhances tumor immunity by preventing tumor-induced T-cell senescence. *EMBO Mol Med*. 2014 Oct;6(10):1294–311.
228. Zhao Y, Shao Q, Peng G. Exhaustion and senescence: two crucial dysfunctional states of T cells in the tumor microenvironment. *Cell Mol Immunol*. 2020 Jan;17(1):27–35.



229. Martinez GJ, Pereira RM, Äijö T, Kim EY, Marangoni F, Pipkin ME, et al. The transcription factor NFAT promotes exhaustion of activated CD8+ T cells. *Immunity*. 2015 Feb 17;42(2):265–78.
230. Khan O, Giles JR, McDonald S, Manne S, Ngiow SF, Patel KP, et al. TOX transcriptionally and epigenetically programs CD8+ T cell exhaustion. *Nature*. 2019 Jul;571(7764):211–8.
231. Mognol GP, Spreafico R, Wong V, Scott-Browne JP, Togher S, Hoffmann A, et al. Exhaustion-associated regulatory regions in CD8+ tumor-infiltrating T cells. *Proc Natl Acad Sci U S A*. 2017 Mar 28;114(13):E2776–85.
232. Singer M, Wang C, Cong L, Marjanovic ND, Kowalczyk MS, Zhang H, et al. A distinct gene module for dysfunction uncoupled from activation in tumor-infiltrating T cells. *Cell*. 2016 Sep 8;166(6):1500–1511.e9.
233. Blackburn SD, Shin H, Freeman GJ, Wherry EJ. Selective expansion of a subset of exhausted CD8 T cells by alphaPD-L1 blockade. *Proc Natl Acad Sci U S A*. 2008 Sep 30;105(39):15016–21.
234. Paley MA, Kroy DC, Odorizzi PM, Johnnidis JB, Dolfi DV, Barnett BE, et al. Progenitor and terminal subsets of CD8+ T cells cooperate to contain chronic viral infection. *Science*. 2012 Nov 30;338(6111):1220–5.
235. Li H, Wu K, Tao K, Chen L, Zheng Q, Lu X, et al. Tim-3/galectin-9 signaling pathway mediates T-cell dysfunction and predicts poor prognosis in patients with hepatitis B virus-associated hepatocellular carcinoma. *Hepatology*. 2012 Oct;56(4):1342–51.
236. Heffner M, Fearon DT. Loss of T cell receptor-induced Bmi-1 in the KLRG1(+) senescent CD8(+) T lymphocyte. *Proc Natl Acad Sci U S A*. 2007 Aug 14;104(33):13414–9.
237. Fourcade J, Sun Z, Benallaoua M, Guillaume P, Luescher IF, Sander C, et al. Upregulation of Tim-3 and PD-1 expression is associated with tumor antigen-specific CD8+ T cell dysfunction in melanoma patients. *J Exp Med*. 2010 Sep 27;207(10):2175–86.
238. Yang OO, Lin H, Dagarag M, Ng HL, Effros RB, Uittenbogaart CH. Decreased perforin and granzyme B expression in senescent HIV-1-specific cytotoxic T lymphocytes. *Virology*. 2005 Feb 5;332(1):16–9.
239. Coppé J-P, Desprez P-Y, Krtolica A, Campisi J. The Senescence-Associated Secretory Phenotype: The Dark Side of Tumor Suppression. *Annu Rev Pathol*. 2010;5:99–118.
240. Gunasinghe SD, Peres NG, Goyette J, Gaus K. Biomechanics of T Cell Dysfunctions in Chronic Diseases. *Front Immunol* [Internet]. 2021 [cited 2021 Apr 14];12. Available from: <https://www.frontiersin.org/articles/10.3389/fimmu.2021.600829/full>
241. Ramsay AG, Johnson AJ, Lee AM, Gorgün G, Le Dieu R, Blum W, et al. Chronic lymphocytic leukemia T cells show impaired immunological synapse formation that can be reversed with an immunomodulating drug. *J Clin Invest*. 2008 Jul;118(7):2427–37.

242. Koneru M, Schaer D, Monu N, Ayala A, Frey AB. Defective proximal TCR signaling inhibits CD8+ tumor-infiltrating lymphocyte lytic function. *J Immunol Baltim Md 1950*. 2005 Feb 15;174(4):1830–40.
243. Yokosuka T, Takamatsu M, Kobayashi-Imanishi W, Hashimoto-Tane A, Azuma M, Saito T. Programmed cell death 1 forms negative costimulatory microclusters that directly inhibit T cell receptor signaling by recruiting phosphatase SHP2. *J Exp Med*. 2012 Jun 4;209(6):1201–17.
244. Borthwick NJ, Lowdell M, Salmon M, Akbar AN. Loss of CD28 expression on CD8(+) T cells is induced by IL-2 receptor gamma chain signalling cytokines and type I IFN, and increases susceptibility to activation-induced apoptosis. *Int Immunol*. 2000 Jul;12(7):1005–13.
245. Chiu WK, Fann M, Weng N. Generation and growth of CD28nullCD8+ memory T cells mediated by IL-15 and its induced cytokines. *J Immunol Baltim Md 1950*. 2006 Dec 1;177(11):7802–10.
246. Fletcher JM, Vukmanovic-Stejic M, Dunne PJ, Birch KE, Cook JE, Jackson SE, et al. Cytomegalovirus-specific CD4+ T cells in healthy carriers are continuously driven to replicative exhaustion. *J Immunol Baltim Md 1950*. 2005 Dec 15;175(12):8218–25.
247. Yokosuka T, Kobayashi W, Sakata-Sogawa K, Takamatsu M, Hashimoto-Tane A, Dustin ML, et al. Spatiotemporal regulation of T cell costimulation by TCR-CD28 microclusters and protein kinase C theta translocation. *Immunity*. 2008 Oct 17;29(4):589–601.
248. Céfaï D, Schneider H, Matangkasombut O, Kang H, Brody J, Rudd CE. CD28 receptor endocytosis is targeted by mutations that disrupt phosphatidylinositol 3-kinase binding and costimulation. *J Immunol Baltim Md 1950*. 1998 Mar 1;160(5):2223–30.
249. Weng N, Akbar AN, Goronzy J. CD28– T cells: their role in the age-associated decline of immune function. *Trends Immunol*. 2009 Jul;30(7):306–12.
250. Pagès F, Ragueneau M, Rottapel R, Truneh A, Nunes J, Imbert J, et al. Binding of phosphatidylinositol-3-OH kinase to CD28 is required for T-cell signalling. *Nature*. 1994 May 26;369(6478):327–9.
251. Brzostek J, Gascoigne NRJ, Rybakin V. Cell Type-Specific Regulation of Immunological Synapse Dynamics by B7 Ligand Recognition. *Front Immunol [Internet]*. 2016 Feb 4 [cited 2021 Apr 15];7. Available from: <https://www.ncbi.nlm.nih.gov/pmc/articles/PMC4740375/>
252. Nagae M, Nishi N, Nakamura-Tsuruta S, Hirabayashi J, Wakatsuki S, Kato R. Structural analysis of the human galectin-9 N-terminal carbohydrate recognition domain reveals unexpected properties that differ from the mouse orthologue. *J Mol Biol*. 2008 Jan 4;375(1):119–35.

253. Türeci Ö, Schmitt H, Fadle N, Pfreundschuh M, Sahin U. Molecular Definition of a Novel Human Galectin Which Is Immunogenic in Patients with Hodgkin's Disease \*. *J Biol Chem.* 1997 Mar 7;272(10):6416–22.
254. Wada J, Kanwar YS. Identification and Characterization of Galectin-9, a Novel  $\beta$ -Galactoside-binding Mammalian Lectin \*. *J Biol Chem.* 1997 Feb 28;272(9):6078–86.
255. Matsumoto R, Matsumoto H, Seki M, Hata M, Asano Y, Kanegasaki S, et al. Human Ecalectin, a Variant of Human Galectin-9, Is a Novel Eosinophil Chemoattractant Produced by T Lymphocytes \*. *J Biol Chem.* 1998 Jul 3;273(27):16976–84.
256. Yoshida H, Teraoka M, Nishi N, Nakakita S, Nakamura T, Hirashima M, et al. X-ray structures of human galectin-9 C-terminal domain in complexes with a biantennary oligosaccharide and sialyllactose. *J Biol Chem.* 2010 Nov 19;285(47):36969–76.
257. Nagae M, Nishi N, Murata T, Usui T, Nakamura T, Wakatsuki S, et al. Structural analysis of the recognition mechanism of poly-N-acetyllactosamine by the human galectin-9 N-terminal carbohydrate recognition domain. *Glycobiology.* 2009 Feb;19(2):112–7.
258. Hirashima M, Kashio Y, Nishi N, Yamauchi A, Imaizumi T, Kageshita T, et al. Galectin-9 in physiological and pathological conditions. *Glycoconj J.* 2004;19(7–9):593–600.
259. Nagae M, Nishi N, Murata T, Usui T, Nakamura T, Wakatsuki S, et al. Crystal structure of the galectin-9 N-terminal carbohydrate recognition domain from *Mus musculus* reveals the basic mechanism of carbohydrate recognition. *J Biol Chem.* 2006 Nov 24;281(47):35884–93.
260. Giovannone N, Liang J, Antonopoulos A, Geddes Sweeney J, King SL, Pochebit SM, et al. Galectin-9 suppresses B cell receptor signaling and is regulated by I-branching of N-glycans. *Nat Commun.* 2018 Aug 17;9(1):3287.
261. Chabot S, Kashio Y, Seki M, Shirato Y, Nakamura K, Nishi N, et al. Regulation of galectin-9 expression and release in Jurkat T cell line cells. *Glycobiology.* 2002 Feb;12(2):111–8.
262. Zhang F, Zheng M, Qu Y, Li J, Ji J, Feng B, et al. Different roles of galectin-9 isoforms in modulating E-selectin expression and adhesion function in LoVo colon carcinoma cells. *Mol Biol Rep.* 2009 May;36(5):823–30.
263. Bi S, Earl LA, Jacobs L, Baum LG. Structural features of galectin-9 and galectin-1 that determine distinct T cell death pathways. *J Biol Chem.* 2008 May 2;283(18):12248–58.
264. Nishi N, Itoh A, Fujiyama A, Yoshida N, Araya S, Hirashima M, et al. Development of highly stable galectins: truncation of the linker peptide confers protease-resistance on tandem-repeat type galectins. *FEBS Lett.* 2005 Apr 11;579(10):2058–64.
265. Padilla ST, Niki T, Furushima D, Bai G, Chagan-Yasutan H, Telan EF, et al. Plasma Levels of a Cleaved Form of Galectin-9 Are the Most Sensitive Biomarkers of Acquired Immune Deficiency Syndrome and Tuberculosis Coinfection. *Biomolecules.* 2020 Oct 30;10(11).

266. Spitzenberger F, Graessler J, Schroeder HE. Molecular and functional characterization of galectin 9 mRNA isoforms in porcine and human cells and tissues. *Biochimie*. 2001 Sep;83(9):851–62.
267. Heusschen R, Freitag N, Tirado-González I, Barrientos G, Moschansky P, Muñoz-Fernández R, et al. Profiling Lgals9 Splice Variant Expression at the Fetal-Maternal Interface: Implications in Normal and Pathological Human Pregnancy. *Biol Reprod*. 2012 Dec 12;88(1):Article 22, 1-10.
268. Lipkowitz MS, Leal-Pinto E, Cohen BE, Abramson RG. Galectin 9 is the sugar-regulated urate transporter/channel UAT. *Glycoconj J*. 2002;19(7–9):491–8.
269. Park S-S, Stankiewicz P, Bi W, Shaw C, Lehoczyk J, Dewar K, et al. Structure and Evolution of the Smith-Magenis Syndrome Repeat Gene Clusters, SMS-REPs. *Genome Res*. 2002 May;12(5):729–38.
270. Broséus J, Mourah S, Ramstein G, Bernard S, Mounier N, Cuccuini W, et al. VEGF121, is predictor for survival in activated B-cell-like diffuse large B-cell lymphoma and is related to an immune response gene signature conserved in cancers. *Oncotarget*. 2017 Jul 19;8(53):90808–24.
271. Asakura H, Kashio Y, Nakamura K, Seki M, Dai S, Shirato Y, et al. Selective Eosinophil Adhesion to Fibroblast Via IFN- $\gamma$ -Induced Galectin-9. *J Immunol*. 2002 Nov 15;169(10):5912–8.
272. Zhu C, Anderson AC, Schubart A, Xiong H, Imitola J, Khoury SJ, et al. The Tim-3 ligand galectin-9 negatively regulates T helper type 1 immunity. *Nat Immunol*. 2005 Dec;6(12):1245–52.
273. Mengshol JA, Golden-Mason L, Arikawa T, Smith M, Niki T, McWilliams R, et al. A crucial role for Kupffer cell-derived galectin-9 in regulation of T cell immunity in hepatitis C infection. *PloS One*. 2010 Mar 4;5(3):e9504.
274. Yang R, Sun L, Li C-F, Wang Y-H, Yao J, Li H, et al. Galectin-9 interacts with PD-1 and TIM-3 to regulate T cell death and is a target for cancer immunotherapy. *Nat Commun*. 2021 Feb 5;12(1):832.
275. Wu C, Thalhamer T, Franca RF, Xiao S, Wang C, Hotta C, et al. Galectin-9-CD44 interaction enhances stability and function of adaptive regulatory T cells. *Immunity*. 2014 Aug 21;41(2):270–82.
276. Imaizumi T, Yoshida H, Nishi N, Sashinami H, Nakamura T, Hirashima M, et al. Double-stranded RNA induces galectin-9 in vascular endothelial cells: involvement of TLR3, PI3K, and IRF3 pathway. *Glycobiology*. 2007 Jul 1;17(7):12C-15C.
277. Kasamatsu A, Uzawa K, Shimada K, Shiiba M, Otsuka Y, Seki N, et al. Elevation of galectin-9 as an inflammatory response in the periodontal ligament cells exposed to

- Porphyromonas gingivalis* lipopolysaccharide in vitro and in vivo. *Int J Biochem Cell Biol.* 2005 Feb 1;37(2):397–408.
278. John S, Mishra R. Galectin-9: From cell biology to complex disease dynamics. *J Biosci.* 2016 Sep;41(3):507–34.
279. Carter KL, Cahir-McFarland E, Kieff E. Epstein-barr virus-induced changes in B-lymphocyte gene expression. *J Virol.* 2002 Oct;76(20):10427–36.
280. Lai J-H, Luo S-F, Wang M-Y, Ho L-J. Translational Implication of Galectin-9 in the Pathogenesis and Treatment of Viral Infection. *Int J Mol Sci.* 2017 Oct 8;18(10).
281. Chiariotti L, Salvatore P, Frunzio R, Bruni CB. Galectin genes: regulation of expression. *Glycoconj J.* 2002;19(7–9):441–9.
282. Heusschen R, Griffioen AW, Thijssen VL. Galectin-9 in tumor biology: a jack of multiple trades. *Biochim Biophys Acta.* 2013 Aug;1836(1):177–85.
283. Schaefer K, Webb NE, Pang M, Hernandez-Davies JE, Lee KP, Gonzalez P, et al. Galectin-9 binds to O-glycans on protein disulfide isomerase. *Glycobiology.* 2017 Sep 1;27(9):878–87.
284. Mishra R, Grzybek M, Niki T, Hirashima M, Simons K. Galectin-9 trafficking regulates apical-basal polarity in Madin-Darby canine kidney epithelial cells. *Proc Natl Acad Sci U S A.* 2010 Oct 12;107(41):17633–8.
285. Barjon C, Niki T, Vérillaud B, Opolon P, Bedossa P, Hirashima M, et al. A novel monoclonal antibody for detection of galectin-9 in tissue sections: application to human tissues infected by oncogenic viruses. *Infect Agent Cancer.* 2012 Jul 17;7:16.
286. Pioche-Durieu C, Keryer C, Souquère S, Bosq J, Faigle W, Loew D, et al. In nasopharyngeal carcinoma cells, Epstein-Barr virus LMP1 interacts with galectin 9 in membrane raft elements resistant to simvastatin. *J Virol.* 2005 Nov;79(21):13326–37.
287. Oomizu S, Arikawa T, Niki T, Kadowaki T, Ueno M, Nishi N, et al. Cell surface galectin-9 expressing Th cells regulate Th17 and Foxp3+ Treg development by galectin-9 secretion. *PLoS One.* 2012;7(11):e48574.
288. Jia J, Bissa B, Brecht L, Allers L, Choi SW, Gu Y, et al. AMPK, a Regulator of Metabolism and Autophagy, Is Activated by Lysosomal Damage via a Novel Galectin-Directed Ubiquitin Signal Transduction System. *Mol Cell.* 2020 Mar 5;77(5):951–969.e9.
289. Jia J, Abudu YP, Claude-Taupin A, Gu Y, Kumar S, Choi SW, et al. Galectins Control mTOR in Response to Endomembrane Damage. *Mol Cell.* 2018 Apr 5;70(1):120–135.e8.
290. Querol Cano L, Tagit O, Dolen Y, van Duffelen A, Dieltjes S, Buschow SI, et al. Intracellular Galectin-9 Controls Dendritic Cell Function by Maintaining Plasma Membrane Rigidity. *iScience.* 2019 Dec 20;22:240–55.

291. Madireddi S, Eun S-Y, Lee S-W, Nemčovičová I, Mehta AK, Zajonc DM, et al. Galectin-9 controls the therapeutic activity of 4-1BB-targeting antibodies. *J Exp Med*. 2014 Jun 30;211(7):1433–48.
292. Madireddi S, Eun S-Y, Mehta AK, Birta A, Zajonc DM, Niki T, et al. Regulatory T Cell-Mediated Suppression of Inflammation Induced by DR3 Signaling Is Dependent on Galectin-9. *J Immunol Baltim Md 1950*. 2017 15;199(8):2721–8.
293. Sakuishi K, Ngiow SF, Sullivan JM, Teng MWL, Kuchroo VK, Smyth MJ, et al. TIM3+FOXP3+ regulatory T cells are tissue-specific promoters of T-cell dysfunction in cancer. *Oncoimmunology*. 2013 Apr 1;2(4):e23849.
294. Anderson AC, Anderson DE, Bregoli L, Hastings WD, Kassam N, Lei C, et al. Promotion of tissue inflammation by the immune receptor Tim-3 expressed on innate immune cells. *Science*. 2007 Nov 16;318(5853):1141–3.
295. Du W, Yang M, Turner A, Xu C, Ferris RL, Huang J, et al. TIM-3 as a Target for Cancer Immunotherapy and Mechanisms of Action. *Int J Mol Sci*. 2017 Mar 16;18(3).
296. Sabatos-Peyton CA, Nevin J, Brock A, Venable JD, Tan DJ, Kassam N, et al. Blockade of Tim-3 binding to phosphatidylserine and CEACAM1 is a shared feature of anti-Tim-3 antibodies that have functional efficacy. *Oncoimmunology*. 2018;7(2):e1385690.
297. Chiba S, Baghdadi M, Akiba H, Yoshiyama H, Kinoshita I, Dosaka-Akita H, et al. Tumor-infiltrating DCs suppress nucleic acid-mediated innate immune responses through interactions between the receptor TIM-3 and the alarmin HMGB1. *Nat Immunol*. 2012 Sep;13(9):832–42.
298. Cao E, Zang X, Ramagopal UA, Mukhopadhyaya A, Fedorov A, Fedorov E, et al. T cell immunoglobulin mucin-3 crystal structure reveals a galectin-9-independent ligand-binding surface. *Immunity*. 2007 Mar;26(3):311–21.
299. Acharya N, Sabatos-Peyton C, Anderson AC. Tim-3 finds its place in the cancer immunotherapy landscape. *J Immunother Cancer*. 2020 Jun;8(1).
300. Rangachari M, Zhu C, Sakuishi K, Xiao S, Karman J, Chen A, et al. Bat3 promotes T cell responses and autoimmunity by repressing Tim-3-mediated cell death and exhaustion. *Nat Med*. 2012 Sep;18(9):1394–400.
301. Clayton KL, Haaland MS, Douglas-Vail MB, Mujib S, Chew GM, Ndhlovu LC, et al. T cell Ig and mucin domain-containing protein 3 is recruited to the immune synapse, disrupts stable synapse formation, and associates with receptor phosphatases. *J Immunol Baltim Md 1950*. 2014 Jan 15;192(2):782–91.
302. Moritoki M, Kadowaki T, Niki T, Nakano D, Soma G, Mori H, et al. Galectin-9 ameliorates clinical severity of MRL/lpr lupus-prone mice by inducing plasma cell apoptosis independently of Tim-3. *PLoS One*. 2013;8(4):e60807.

303. Tanikawa R, Tanikawa T, Hirashima M, Yamauchi A, Tanaka Y. Galectin-9 induces osteoblast differentiation through the CD44/Smad signaling pathway. *Biochem Biophys Res Commun*. 2010 Apr 2;394(2):317–22.
304. Bi S, Hong PW, Lee B, Baum LG. Galectin-9 binding to cell surface protein disulfide isomerase regulates the redox environment to enhance T-cell migration and HIV entry. *Proc Natl Acad Sci U S A*. 2011 Jun 28;108(26):10650–5.
305. Wang F, He W, Zhou H, Yuan J, Wu K, Xu L, et al. The Tim-3 ligand galectin-9 negatively regulates CD8+ alloreactive T cell and prolongs survival of skin graft. *Cell Immunol*. 2007 Dec;250(1–2):68–74.
306. Reddy PBJ, Sehrawat S, Suryawanshi A, Rajasagi NK, Mulik S, Hirashima M, et al. Influence of galectin-9/Tim-3 interaction on herpes simplex virus-1 latency. *J Immunol Baltim Md 1950*. 2011 Dec 1;187(11):5745–55.
307. Sehrawat S, Reddy PBJ, Rajasagi N, Suryawanshi A, Hirashima M, Rouse BT. Galectin-9/TIM-3 interaction regulates virus-specific primary and memory CD8 T cell response. *PLoS Pathog*. 2010 May 6;6(5):e1000882.
308. Zhou Q, Munger ME, Veenstra RG, Weigel BJ, Hirashima M, Munn DH, et al. Coexpression of Tim-3 and PD-1 identifies a CD8+ T-cell exhaustion phenotype in mice with disseminated acute myelogenous leukemia. *Blood*. 2011 Apr 28;117(17):4501–10.
309. Nebbia G, Peppas D, Schurich A, Khanna P, Singh HD, Cheng Y, et al. Upregulation of the Tim-3/Galectin-9 Pathway of T Cell Exhaustion in Chronic Hepatitis B Virus Infection. *PLoS ONE* [Internet]. 2012 Oct 24 [cited 2021 Mar 25];7(10). Available from: <https://www.ncbi.nlm.nih.gov/pmc/articles/PMC3480425/>
310. Seki M, Oomizu S, Sakata K-M, Sakata A, Arikawa T, Watanabe K, et al. Galectin-9 suppresses the generation of Th17, promotes the induction of regulatory T cells, and regulates experimental autoimmune arthritis. *Clin Immunol Orlando Fla*. 2008 Apr;127(1):78–88.
311. Wang F, Wan L, Zhang C, Zheng X, Li J, Chen ZK. Tim-3-Galectin-9 pathway involves the suppression induced by CD4+CD25+ regulatory T cells. *Immunobiology*. 2009;214(5):342–9.
312. Ju Y, Shang X, Liu Z, Zhang J, Li Y, Shen Y, et al. The Tim-3/galectin-9 pathway involves in the homeostasis of hepatic Tregs in a mouse model of concanavalin A-induced hepatitis. *Mol Immunol*. 2014 Mar;58(1):85–91.
313. Ji XJ, Ma CJ, Wang JM, Wu XY, Niki T, Hirashima M, et al. HCV-infected hepatocytes drive CD4+ CD25+ Foxp3+ regulatory T-cell development through the Tim-3/Gal-9 pathway. *Eur J Immunol*. 2013 Feb;43(2):458–67.

314. Mrizak D, Martin N, Barjon C, Jimenez-Pailhes A-S, Mustapha R, Niki T, et al. Effect of nasopharyngeal carcinoma-derived exosomes on human regulatory T cells. *J Natl Cancer Inst.* 2015 Jan;107(1):363.
315. Lv K, Zhang Y, Zhang M, Zhong M, Suo Q. Galectin-9 promotes TGF- $\beta$ 1-dependent induction of regulatory T cells via the TGF- $\beta$ /Smad signaling pathway. *Mol Med Rep.* 2013 Jan;7(1):205–10.
316. Shan M, Carrillo J, Yeste A, Gutzeit C, Segura-Garzón D, Walland AC, et al. Secreted IgD Amplifies Humoral T Helper 2 Cell Responses by Binding Basophils via Galectin-9 and CD44. *Immunity.* 2018 Oct 16;49(4):709-724.e8.
317. Enninga EAL, Nevala WK, Holtan SG, Leontovich AA, Markovic SN. Galectin-9 modulates immunity by promoting Th2/M2 differentiation and impacts survival in patients with metastatic melanoma. *Melanoma Res.* 2016 Oct;26(5):429–41.
318. Gooden MJM, Wiersma VR, Samplonius DF, Gerssen J, van Ginkel RJ, Nijman HW, et al. Galectin-9 activates and expands human T-helper 1 cells. *PloS One.* 2013;8(5):e65616.
319. Lhuillier C, Barjon C, Niki T, Gelin A, Praz F, Morales O, et al. Impact of Exogenous Galectin-9 on Human T Cells. *J Biol Chem.* 2015 Jul 3;290(27):16797–811.
320. Vahl JC, Drees C, Heger K, Heink S, Fischer JC, Nedjic J, et al. Continuous T cell receptor signals maintain a functional regulatory T cell pool. *Immunity.* 2014 Nov 20;41(5):722–36.
321. Levine AG, Arvey A, Jin W, Rudensky AY. Continuous requirement for the TCR in regulatory T cell function. *Nat Immunol.* 2014 Nov;15(11):1070–8.
322. Colomb F, Giron LB, Premeaux TA, Mitchell BI, Niki T, Papasavvas E, et al. Galectin-9 Mediates HIV Transcription by Inducing TCR-Dependent ERK Signaling. *Front Immunol.* 2019;10:267.
323. Cao A, Alluqmani N, Buhari FHM, Wasim L, Smith LK, Quaile AT, et al. Galectin-9 binds IgM-BCR to regulate B cell signaling. *Nat Commun.* 2018 Aug 17;9(1):3288.
324. Orr SL, Le D, Long JM, Sobieszczuk P, Ma B, Tian H, et al. A phenotype survey of 36 mutant mouse strains with gene-targeted defects in glycosyltransferases or glycan-binding proteins. *Glycobiology.* 2013 Mar;23(3):363–80.
325. Chakraborty A, Staudinger C, King SL, Erickson FC, Lau LS, Bernasconi A, et al. Galectin-9 bridges human B cells to vascular endothelium while programming regulatory pathways. *J Autoimmun.* 2021 Feb;117:102575.
326. Matsumoto R, Hirashima M, Kita H, Gleich GJ. Biological activities of ecalectin: a novel eosinophil-activating factor. *J Immunol Baltim Md 1950.* 2002 Feb 15;168(4):1961–7.
327. Vega-Carrascal I, Bergin DA, McElvaney OJ, McCarthy C, Banville N, Pohl K, et al. Galectin-9 signaling through TIM-3 is involved in neutrophil-mediated Gram-negative bacterial



- killing: an effect abrogated within the cystic fibrosis lung. *J Immunol Baltim Md* 1950. 2014 Mar 1;192(5):2418–31.
328. Golden-Mason L, McMahan RH, Strong M, Reisdorph R, Mahaffey S, Palmer BE, et al. Galectin-9 functionally impairs natural killer cells in humans and mice. *J Virol*. 2013 May;87(9):4835–45.
329. Ndhlovu LC, Lopez-Vergès S, Barbour JD, Jones RB, Jha AR, Long BR, et al. Tim-3 marks human natural killer cell maturation and suppresses cell-mediated cytotoxicity. *Blood*. 2012 Apr 19;119(16):3734–43.
330. Li Y, Zhang J, Zhang D, Hong X, Tao Y, Wang S, et al. Tim-3 signaling in peripheral NK cells promotes maternal-fetal immune tolerance and alleviates pregnancy loss. *Sci Signal*. 2017 Sep 26;10(498).
331. Lajko A, Meggyes M, Polgar B, Szereday L. The immunological effect of Galectin-9/TIM-3 pathway after low dose Mifepristone treatment in mice at 14.5 day of pregnancy. *PloS One*. 2018;13(3):e0194870.
332. Wang Y, Sun J, Ma C, Gao W, Song B, Xue H, et al. Reduced Expression of Galectin-9 Contributes to a Poor Outcome in Colon Cancer by Inhibiting NK Cell Chemotaxis Partially through the Rho/ROCK1 Signaling Pathway. *PloS One*. 2016;11(3):e0152599.
333. Zhang W, Zhang Y, He Y, Wang X, Fang Q. Lipopolysaccharide mediates time-dependent macrophage M1/M2 polarization through the Tim-3/Galectin-9 signalling pathway. *Exp Cell Res*. 2019 Mar 15;376(2):124–32.
334. Enninga EAL, Chatzopoulos K, Butterfield JT, Sutor SL, Leontovich AA, Nevala WK, et al. CD206-positive myeloid cells bind galectin-9 and promote a tumor-supportive microenvironment. *J Pathol*. 2018 Aug;245(4):468–77.
335. de Kivit S, Kostadinova AI, Kerperien J, Morgan ME, Muruzabal VA, Hofman GA, et al. Dietary, nondigestible oligosaccharides and *Bifidobacterium breve* M-16V suppress allergic inflammation in intestine via targeting dendritic cell maturation. *J Leukoc Biol*. 2017 Jul;102(1):105–15.
336. de Kivit S, Kostadinova AI, Kerperien J, Ayechu Muruzabal V, Morgan ME, Knippels LMJ, et al. Galectin-9 Produced by Intestinal Epithelial Cells Enhances Aldehyde Dehydrogenase Activity in Dendritic Cells in a PI3K- and p38-Dependent Manner. *J Innate Immun*. 2017;9(6):609–20.
337. Dai S-Y, Nakagawa R, Itoh A, Murakami H, Kashio Y, Abe H, et al. Galectin-9 induces maturation of human monocyte-derived dendritic cells. *J Immunol Baltim Md* 1950. 2005 Sep 1;175(5):2974–81.
338. de Mingo Pulido Á, Gardner A, Hiebler S, Soliman H, Rugo HS, Krummel MF, et al. TIM-3 Regulates CD103+ Dendritic Cell Function and Response to Chemotherapy in Breast Cancer. *Cancer Cell*. 2018 08;33(1):60-74.e6.

339. Dardalhon V, Anderson AC, Karman J, Apetoh L, Chandwaskar R, Lee DH, et al. Tim-3/galectin-9 pathway: regulation of Th1 immunity through promotion of CD11b+Ly-6G+ myeloid cells. *J Immunol Baltim Md 1950*. 2010 Aug 1;185(3):1383–92.
340. Zhang Y, Zhang M, Li X, Tang Z, He L, Lv K. Expansion of CD11b+Ly-6C+ myeloid-derived suppressor cells (MDSCs) driven by galectin-9 attenuates CVB3-induced myocarditis. *Mol Immunol*. 2017 Mar;83:62–71.
341. Zhang C-X, Huang D-J, Baloche V, Zhang L, Xu J-X, Li B-W, et al. Galectin-9 promotes a suppressive microenvironment in human cancer by enhancing STING degradation. *Oncogenesis*. 2020 Jul 6;9(7):65.
342. Seki M, Sakata K, Oomizu S, Arikawa T, Sakata A, Ueno M, et al. Beneficial effect of galectin 9 on rheumatoid arthritis by induction of apoptosis of synovial fibroblasts. *Arthritis Rheum*. 2007 Dec;56(12):3968–76.
343. Arikawa T, Watanabe K, Seki M, Matsukawa A, Oomizu S, Sakata K, et al. Galectin-9 ameliorates immune complex-induced arthritis by regulating Fc gamma R expression on macrophages. *Clin Immunol Orlando Fla*. 2009 Dec;133(3):382–92.
344. Katoh S, Ishii N, Nobumoto A, Takeshita K, Dai S-Y, Shinonaga R, et al. Galectin-9 inhibits CD44-hyaluronan interaction and suppresses a murine model of allergic asthma. *Am J Respir Crit Care Med*. 2007 Jul 1;176(1):27–35.
345. Katoh S, Shimizu H, Obase Y, Oomizu S, Niki T, Ikeda M, et al. Preventive effect of galectin-9 on double-stranded RNA-induced airway hyperresponsiveness in an exacerbation model of mite antigen-induced asthma in mice. *Exp Lung Res*. 2013 Dec;39(10):453–62.
346. Ikeda M, Katoh S, Shimizu H, Hasegawa A, Ohashi-Doi K, Oka M. Beneficial effects of Galectin-9 on allergen-specific sublingual immunotherapy in a *Dermatophagoidea farinae*-induced mouse model of chronic asthma. *Allergol Int Off J Jpn Soc Allergol*. 2017 Jul;66(3):432–9.
347. Sziksz E, Kozma GT, Pállinger E, Komlósi ZI, Adori C, Kovács L, et al. Galectin-9 in allergic airway inflammation and hyper-responsiveness in mice. *Int Arch Allergy Immunol*. 2010;151(4):308–17.
348. Yamamoto H, Kashio Y, Shoji H, Shinonaga R, Yoshimura T, Nishi N, et al. Involvement of galectin-9 in guinea pig allergic airway inflammation. *Int Arch Allergy Immunol*. 2007;143 Suppl 1:95–105.
349. Sun J, Sui Y, Wang Y, Song L, Li D, Li G, et al. Galectin-9 expression correlates with therapeutic effect in rheumatoid arthritis. *Sci Rep*. 2021 Mar 10;11(1):5562.
350. Wang Y, Meng J, Wang X, Liu S, Shu Q, Gao L, et al. Expression of human TIM-1 and TIM-3 on lymphocytes from systemic lupus erythematosus patients. *Scand J Immunol*. 2008 Jan;67(1):63–70.

351. Jiao Q, Qian Q, Zhao Z, Fang F, Hu X, An J, et al. Expression of human T cell immunoglobulin domain and mucin-3 (TIM-3) and TIM-3 ligands in peripheral blood from patients with systemic lupus erythematosus. *Arch Dermatol Res*. 2016 Oct;308(8):553–61.
352. Nakajima R, Miyagaki T, Oka T, Nakao M, Kawaguchi M, Suga H, et al. Elevated serum galectin-9 levels in patients with atopic dermatitis. *J Dermatol*. 2015 Jul;42(7):723–6.
353. Nofal E, Eldesoky F, Nofal A, Abdelshafy A, Zedan A. Serum galectin-9 levels in atopic dermatitis, psoriasis and allergic contact dermatitis: A cross-sectional study. *Indian J Dermatol Venereol Leprol*. 2019 Apr;85(2):195–6.
354. Stone KD, Prussin C, Metcalfe DD. IgE, mast cells, basophils, and eosinophils. *J Allergy Clin Immunol*. 2010 Feb;125(2 Suppl 2):S73-80.
355. Wiersma VR, Clarke A, Pouwels SD, Perry E, Abdullah TM, Kelly C, et al. Galectin-9 Is a Possible Promoter of Immunopathology in Rheumatoid Arthritis by Activation of Peptidyl Arginine Deiminase 4 (PAD-4) in Granulocytes. *Int J Mol Sci*. 2019 Aug 19;20(16).
356. Harwood NMK, Golden-Mason L, Cheng L, Rosen HR, Mengshol JA. HCV-infected cells and differentiation increase monocyte immunoregulatory galectin-9 production. *J Leukoc Biol*. 2016 Mar;99(3):495–503.
357. Zhuo Y, Zhang Y-F, Wu H-J, Qin L, Wang Y-P, Liu A-M, et al. Interaction between Galectin-9/TIM-3 pathway and follicular helper CD4+ T cells contributes to viral persistence in chronic hepatitis C. *Biomed Pharmacother Biomedecine Pharmacother*. 2017 Oct;94:386–93.
358. Kared H, Fabre T, Bédard N, Bruneau J, Shoukry NH. Galectin-9 and IL-21 mediate cross-regulation between Th17 and Treg cells during acute hepatitis C. *PLoS Pathog*. 2013;9(6):e1003422.
359. Tandon R, Chew GM, Byron MM, Borrow P, Niki T, Hirashima M, et al. Galectin-9 is rapidly released during acute HIV-1 infection and remains sustained at high levels despite viral suppression even in elite controllers. *AIDS Res Hum Retroviruses*. 2014 Jul;30(7):654–64.
360. Liu T, Khanna KM, Chen X, Fink DJ, Hendricks RL. CD8(+) T cells can block herpes simplex virus type 1 (HSV-1) reactivation from latency in sensory neurons. *J Exp Med*. 2000 May 1;191(9):1459–66.
361. Abdel-Mohsen M, Chavez L, Tandon R, Chew GM, Deng X, Danesh A, et al. Human Galectin-9 Is a Potent Mediator of HIV Transcription and Reactivation. *PLoS Pathog*. 2016 Jun;12(6):e1005677.
362. Katoh S, Ikeda M, Shimizu H, Mouri K, Obase Y, Kobashi Y, et al. Increased Levels of Plasma Galectin-9 in Patients with Influenza Virus Infection. *Tohoku J Exp Med*. 2014;232(4):263–7.

363. Sharma S, Sundararajan A, Suryawanshi A, Kumar N, Veiga-Parga T, Kuchroo VK, et al. T cell immunoglobulin and mucin protein-3 (Tim-3)/Galectin-9 interaction regulates influenza A virus-specific humoral and CD8 T-cell responses. *Proc Natl Acad Sci U S A*. 2011 Nov 22;108(47):19001–6.
364. Shete A, Bichare S, Pujari V, Virkar R, Thakar M, Ghate M, et al. Elevated Levels of Galectin-9 but Not Osteopontin in HIV and Tuberculosis Infections Indicate Their Roles in Detecting MTB Infection in HIV Infected Individuals. *Front Microbiol*. 2020;11:1685.
365. Kageshita T, Kashio Y, Yamauchi A, Seki M, Abedin MJ, Nishi N, et al. Possible role of galectin-9 in cell aggregation and apoptosis of human melanoma cell lines and its clinical significance. *Int J Cancer*. 2002 Jun 20;99(6):809–16.
366. Wiersma VR, de Bruyn M, van Ginkel RJ, Sigar E, Hirashima M, Niki T, et al. The glycan-binding protein galectin-9 has direct apoptotic activity toward melanoma cells. *J Invest Dermatol*. 2012 Sep;132(9):2302–5.
367. Zhou X, Sun L, Jing D, Xu G, Zhang J, Lin L, et al. Galectin-9 Expression Predicts Favorable Clinical Outcome in Solid Tumors: A Systematic Review and Meta-Analysis. *Front Physiol*. 2018;9:452.
368. Liang M, Ueno M, Oomizu S, Arikawa T, Shinonaga R, Zhang S, et al. Galectin-9 expression links to malignant potential of cervical squamous cell carcinoma. *J Cancer Res Clin Oncol*. 2008 Aug;134(8):899–907.
369. Fík Z, Valach J, Chovanec M, Mazánek J, Kodet R, Kodet O, et al. Loss of adhesion/growth-regulatory galectin-9 from squamous cell epithelium in head and neck carcinomas. *J Oral Pathol Med Off Publ Int Assoc Oral Pathol Am Acad Oral Pathol*. 2013 Feb;42(2):166–73.
370. Chan SW, Kallarakkal TG, Abraham MT. Changed expression of E-cadherin and galectin-9 in oral squamous cell carcinomas but lack of potential as prognostic markers. *Asian Pac J Cancer Prev APJCP*. 2014;15(5):2145–52.
371. Irie A, Yamauchi A, Kontani K, Kihara M, Liu D, Shirato Y, et al. Galectin-9 as a prognostic factor with antimetastatic potential in breast cancer. *Clin Cancer Res Off J Am Assoc Cancer Res*. 2005 Apr 15;11(8):2962–8.
372. de Mingo Pulido Á, Gardner A, Hiebler S, Soliman H, Rugo HS, Krummel MF, et al. TIM-3 Regulates CD103+ Dendritic Cell Function and Response to Chemotherapy in Breast Cancer. *Cancer Cell*. 2018 Jan 8;33(1):60–74.e6.
373. Nobumoto A, Nagahara K, Oomizu S, Katoh S, Nishi N, Takeshita K, et al. Galectin-9 suppresses tumor metastasis by blocking adhesion to endothelium and extracellular matrices. *Glycobiology*. 2008 Sep;18(9):735–44.
374. Melief SM, Visconti VV, Visser M, van Diepen M, Kapiteijn EHW, van den Berg JH, et al. Long-term Survival and Clinical Benefit from Adoptive T-cell Transfer in Stage IV

- Melanoma Patients Is Determined by a Four-Parameter Tumor Immune Signature. *Cancer Immunol Res.* 2017 Feb;5(2):170–9.
375. He Y, Jia K, Dziadziuszko R, Zhao S, Zhang X, Deng J, et al. Galectin-9 in non-small cell lung cancer. *Lung Cancer Amst Neth.* 2019 Oct;136:80–5.
376. Seifert AM, Reiche C, Heiduk M, Tannert A, Meinecke A-C, Baier S, et al. Detection of pancreatic ductal adenocarcinoma with galectin-9 serum levels. *Oncogene.* 2020 Apr;39(15):3102–13.
377. Wiersma VR, de Bruyn M, Wei Y, van Ginkel RJ, Hirashima M, Niki T, et al. The epithelial polarity regulator LGALS9/galectin-9 induces fatal frustrated autophagy in KRAS mutant colon carcinoma that depends on elevated basal autophagic flux. *Autophagy.* 2015;11(8):1373–88.
378. Bertino P, Premeaux TA, Fujita T, Haun BK, Marciel MP, Hoffmann FW, et al. Targeting the C-terminus of galectin-9 induces mesothelioma apoptosis and M2 macrophage depletion. *Oncoimmunology.* 2019;8(8):1601482.
379. Daley D, Zambirinis CP, Seifert L, Akkad N, Mohan N, Werba G, et al.  $\gamma\delta$  T Cells Support Pancreatic Oncogenesis by Restraining  $\alpha\beta$  T Cell Activation. *Cell.* 2016 Sep 8;166(6):1485–1499.e15.
380. Fu H, Liu Y, Xu L, Liu W, Fu Q, Liu H, et al. Galectin-9 predicts postoperative recurrence and survival of patients with clear-cell renal cell carcinoma. *Tumour Biol J Int Soc Oncodevelopmental Biol Med.* 2015 Aug;36(8):5791–9.
381. Ohue Y, Kurose K, Nozawa R, Isobe M, Nishio Y, Tanaka T, et al. Survival of Lung Adenocarcinoma Patients Predicted from Expression of PD-L1, Galectin-9, and XAGE1 (GAGED2a) on Tumor Cells and Tumor-Infiltrating T Cells. *Cancer Immunol Res.* 2016 Dec;4(12):1049–60.
382. Gao J, Qiu X, Li X, Fan H, Zhang F, Lv T, et al. Expression profiles and clinical value of plasma exosomal Tim-3 and Galectin-9 in non-small cell lung cancer. *Biochem Biophys Res Commun.* 2018 Apr 6;498(3):409–15.
383. Liu Z, Han H, He X, Li S, Wu C, Yu C, et al. Expression of the galectin-9-Tim-3 pathway in glioma tissues is associated with the clinical manifestations of glioma. *Oncol Lett.* 2016 Mar;11(3):1829–34.
384. Liang T, Wang X, Wang F, Feng E, You G. Galectin-9: A Predictive Biomarker Negatively Regulating Immune Response in Glioma Patients. *World Neurosurg.* 2019 Dec;132:e455–62.
385. Yuan F, Ming H, Wang Y, Yang Y, Yi L, Li T, et al. Molecular and clinical characterization of Galectin-9 in glioma through 1,027 samples. *J Cell Physiol.* 2020 May;235(5):4326–34.
386. Dong J, Cheng L, Zhao M, Pan X, Feng Z, Wang D. Tim-3-expressing macrophages are functionally suppressed and expanded in oral squamous cell carcinoma due to virus-

- induced Gal-9 expression. *Tumour Biol J Int Soc Oncodevelopmental Biol Med*. 2017 May;39(5):1010428317701651.
387. Dama P, Tang M, Fulton N, Kline J, Liu H. Gal9/Tim-3 expression level is higher in AML patients who fail chemotherapy. *J Immunother Cancer*. 2019 Jul 10;7(1):175.
388. Kikushige Y, Miyamoto T, Yuda J, Jabbarzadeh-Tabrizi S, Shima T, Takayanagi S, et al. A TIM-3/Gal-9 Autocrine Stimulatory Loop Drives Self-Renewal of Human Myeloid Leukemia Stem Cells and Leukemic Progression. *Cell Stem Cell*. 2015 Sep 3;17(3):341–52.
389. Yoon HK, Kim TH, Park S, Jung H, Quan X, Park SJ, et al. Effect of anthracycline and taxane on the expression of programmed cell death ligand-1 and galectin-9 in triple-negative breast cancer. *Pathol Res Pract*. 2018 Oct;214(10):1626–31.
390. Jabbari N, Kenerson HL, Lausted C, Yan X, Meng C, Sullivan KM, et al. Modulation of Immune Checkpoints by Chemotherapy in Human Colorectal Liver Metastases. *Cell Rep Med*. 2020 Dec 22;1(9):100160.
391. Koyama S, Akbay EA, Li YY, Herter-Sprue GS, Buczkowski KA, Richards WG, et al. Adaptive resistance to therapeutic PD-1 blockade is associated with upregulation of alternative immune checkpoints. *Nat Commun*. 2016 Feb 17;7:10501.
392. Limagne E, Richard C, Thibaudin M, Fumet J-D, Truntzer C, Lagrange A, et al. Tim-3/galectin-9 pathway and mMDSC control primary and secondary resistances to PD-1 blockade in lung cancer patients. *Oncoimmunology*. 2019;8(4):e1564505.
393. Yazdanifar M, Zhou R, Grover P, Williams C, Bose M, Moore LJ, et al. Overcoming Immunological Resistance Enhances the Efficacy of A Novel Anti-tMUC1-CAR T Cell Treatment against Pancreatic Ductal Adenocarcinoma. *Cells*. 2019 Sep 11;8(9).
394. Vilar K de M, Pereira MC, Tavares Dantas A, de Melo Rêgo MJB, Pitta I da R, Pinto Duarte ÂLB, et al. Galectin-9 gene (LGALS9) polymorphisms are associated with rheumatoid arthritis in Brazilian patients. *PloS One*. 2019;14(10):e0223191.
395. Holderried TAW, de Vos L, Bawden EG, Vogt TJ, Dietrich J, Zarbl R, et al. Molecular and immune correlates of TIM-3 (HAVCR2) and galectin 9 (LGALS9) mRNA expression and DNA methylation in melanoma. *Clin Epigenetics*. 2019 Nov 20;11(1):161.
396. Sasidharan Nair V, Toor SM, Taha RZ, Shaath H, Elkord E. DNA methylation and repressive histones in the promoters of PD-1, CTLA-4, TIM-3, LAG-3, TIGIT, PD-L1, and galectin-9 genes in human colorectal cancer. *Clin Epigenetics*. 2018 Aug 6;10(1):104.
397. Yang Q, Hou C, Huang D, Zhuang C, Jiang W, Geng Z, et al. miR-455-5p functions as a potential oncogene by targeting galectin-9 in colon cancer. *Oncol Lett*. 2017 Mar;13(3):1958–64.
398. Yang Q, Jiang W, Zhuang C, Geng Z, Hou C, Huang D, et al. microRNA-22 downregulation of galectin-9 influences lymphocyte apoptosis and tumor cell proliferation in liver cancer. *Oncol Rep*. 2015 Oct;34(4):1771–8.

399. Gupta R, Leon F, Rauth S, Batra SK, Ponnusamy MP. A Systematic Review on the Implications of O-linked Glycan Branching and Truncating Enzymes on Cancer Progression and Metastasis. *Cells*. 2020 Feb 14;9(2).
400. Nakagawa R, Calado DP. Positive Selection in the Light Zone of Germinal Centers. *Front Immunol*. 2021;12:661678.
401. Stebegg M, Kumar SD, Silva-Cayetano A, Fonseca VR, Linterman MA, Graca L. Regulation of the Germinal Center Response. *Front Immunol*. 2018;9:2469.
402. Ramiscal RR, Vinuesa CG. T-cell subsets in the germinal center. *Immunol Rev*. 2013 Mar;252(1):146–55.
403. Lederman S, Yellin MJ, Cleary AM, Pernis A, Inghirami G, Cohn LE, et al. T-BAM/CD40-L on helper T lymphocytes augments lymphokine-induced B cell Ig isotype switch recombination and rescues B cells from programmed cell death. *J Immunol Baltim Md* 1950. 1994 Mar 1;152(5):2163–71.
404. Monteiro C, Kasahara T, Sacramento PM, Dias A, Leite S, Silva VG, et al. Human pregnancy levels of estrogen and progesterone contribute to humoral immunity by activating TFH /B cell axis. *Eur J Immunol*. 2021 Jan;51(1):167–79.
405. Lee B-H, Park Y, Kim J-H, Kang K-W, Lee S-J, Kim SJ, et al. Prognostic Value of Galectin-9 Relates to Programmed Death-Ligand 1 in Patients With Multiple Myeloma. *Front Oncol*. 2021;11:669817.

**Titre :** Caractéristiques immunomodulatrices de la galectine-9: études expérimentales et translationnelles

**Mots clés :** galectine-9, immunomodulation, lymphocyte T folliculaire,

**Résumé :** Les galectines sont des lectines animales capables d'interagir avec des polysaccharides comportant des liaisons  $\beta$ 1-3 ou  $\beta$ 1-4 galactosides. Certaines galectines, notamment la galectine-9 (gal-9), peuvent être libérées dans le milieu extracellulaire où elles se comportent comme des cytokines en se liant à des protéines partenaires à la surface des cellules cibles. Tim-3 et Dectine-1 font partie des récepteurs membranaires de la gal-9 extra-cellulaire. Globalement les effets immunomodulateurs de la gal-9 qui sont très variés vont plutôt dans le sens de l'immunosuppression. Elle exerce un effet inhibiteur sur la plupart des cellules de l'immunité adaptative notamment les T CD8<sup>+</sup> et d'autre part elle favorise une polarisation M2 des macrophages. La gal-9 est souvent impliquée dans les résistances primaires ou secondaires aux agents de l'immunothérapie classique. Le premier volet de mon travail de thèse se situait dans le cadre de la recherche cognitive et visait à explorer les modifications du phénotype des cellules T périphériques humaines activées in vitro et exposées pendant plusieurs jours à

une concentration élevée de gal-9 extra-cellulaire. J'ai pu montrer qu'il en résulte une quasi-disparition des T CD8<sup>+</sup> et un biais d'expansion des T CD4<sup>+</sup> au bénéfice d'une sous-population ayant un phénotype proche de celui des T folliculaires avec une forte expression du ligand de CD40. Ces résultats font l'objet d'un manuscrit proche de la soumission. Le deuxième volet de ma thèse se situait dans le cadre d'un projet de recherche translationnelle et visait à déterminer le statut de la gal-9 plasmatique dans une série de 80 patients pris en charge pour des carcinomes des voies aérodigestives supérieures en rechute. Nous avons mis en évidence des concentrations plasmatiques de gal-9 plus élevées dans deux sous-groupes de patients : ceux dont la tumeur primitive dérivait de l'hypopharynx et ceux présentant plusieurs sites métastatiques. Un second manuscrit devant aussi intégrer des données sur les concentrations plasmatiques de gal-1 et gal-3 est en cours d'élaboration et devrait arriver à maturité au cours de l'été.

**Title:** Immunomodulatory properties of galectin-9 : experimental and translational investigations

**Keywords:** galectine-9, immunomodulation, follicular T cells

**Abstract:** Galectins are animal lectins with the ability to bind polysaccharides containing  $\beta$ 1-3 or  $\beta$ 1-4 galactoside bonds. Certain galectins, notably galectin-9 (gal-9), can be released into the extracellular medium where they behave like cytokines by binding to partner proteins on the surface of target cells. Tim-3 and Dectin-1 are examples of membrane receptors for extracellular gal-9. Overall, the immunomodulatory effects of gal-9, which are quite diverse, tend to result in immunosuppression. Gal-9 exerts an inhibitory effect on most cells of the adaptive immunity, in particular CD8<sup>+</sup> T cells, and on the other hand, it promotes M2 polarization of macrophages. Gal-9 is often implicated in primary or secondary resistance to classical immunotherapy agents. The first part of my thesis work was in the context of cognitive research and aimed to explore the modifications of the phenotype of human peripheral T cells activated in vitro and exposed for several days to a

high concentration of extracellular gal-9. I was able to show that the result is a virtual disappearance of CD8<sup>+</sup> T and expansion of CD4<sup>+</sup> T-cells with a bias in favor of a subpopulation with a phenotype similar to that of follicular T cells with a strong expression of the CD40 ligand. These results are the subject of a manuscript close to submission. The second part of my thesis was part of a translational research project and aimed to determine the status of plasma gal-9 in a series of 80 patients treated for relapsed Head and Neck carcinomas. We found higher plasma gal-9 concentrations in two subgroups of patients: those whose primary tumor was derived from the hypopharynx and those with multiple metastatic sites. We intend to also include data on plasma concentrations of gal-1 and gal-3 in a second manuscript which is under development and is expected to mature during the summer.